Hashemite Kingdom of Jordan

Jordan Journal of Biological Sciences

An International Peer-Reviewed Scientific Journal

Financed by the Scientific Research and Innovation Support Fund

This title is indexed in Scopus

http://jjbs.hu.edu.jo/

المجلة الأردنية للعلوم الحياتية
Jordan Journal of Biological Sciences (JJBS)
http://jjbs.hu.edu.jo

Jordan Journal of Biological Sciences (JJBS) (ISSN: 1995–6673 (Print); 2307-7166 (Online)): An International Peer- Reviewed Open Access Research Journal financed by the Scientific Research and Innovation Support Fund, Ministry of Higher Education and Scientific Research, Jordan and published quarterly by the Deanship of Scientific Research , The Hashemite University, Jordan.

Submission Address

Professor Atoum, Manar F

The Hashemite Universit y
P.O. Box 330127, Zarqa, 13115, Jordan
Phone: +962-5-3903333 ext.4147
E-Mail: jjbs@hu.edu.jo

المجلة الاردنية للعلوم الحياتية
Jordan Journal of Biological Sciences (JJBS)
http://jjbs.hu.edu.jo

International Advisory Board (Arranged alphabetically)

Instructions to Authors

Scopes

Study areas include cell biology, genomics, microbiology, immunology, molecular biology, biochemistry, embryology, immunogenetics, cell and tissue culture, molecular ecology, genetic engineering and biological engineering, bioremediation and biodegradation, bioinformatics, biotechnology regulations, gene therapy, organismal biology, microbial and environmental biotechnology, marine sciences. The JJBS welcomes the submission of manuscript that meets the general criteria of significance and academic excellence. All articles published in JJBS are peer-reviewed. Papers will be published approximately one to two months after acceptance.

Type of Papers

The journal publishes high-quality original scientific papers, short communications, correspondence and case studies. Review articles are usually by invitation only. However, Review articles of current interest and high standard will be considered.

Submission of Manuscript

Manuscript, or the essence of their content, must be previously unpublished and should not be under simultaneous consideration by another journal. The authors should also declare if any similar work has been submitted to or published by another journal. They should also declare that it has not been submitted/ published elsewhere in the same form, in English or in any other language, without the written consent of the Publisher. The authors should also declare that the paper is the original work of the author(s) and not copied (in whole or in part) from any other work. All papers will be automatically checked for duplicate publication and plagiarism. If detected, appropriate action will be taken in accordance with International Ethical Guideline. By virtue of the submitted manuscript, the corresponding author acknowledges that all the co-authors have seen and approved the final version of the manuscript. The corresponding author should provide all co-authors with information regarding the manuscript, and obtain their approval before submitting any revisions. Electronic submission of manuscripts is strongly recommended, provided that the text, tables and figures are included in a single Microsoft Word file. Submit manuscript as e-mail attachment to the Editorial Office at: JJBS@hu.edu.jo. After submission, a manuscript number will be communicated to the corresponding author within 48 hours.

Peer-review Process

It is requested to submit, with the manuscript, the names, addresses and e-mail addresses of at least 4 potential reviewers. It is the sole right of the editor to decide whether or not the suggested reviewers to be used. The reviewers' comments will be sent to authors within 6-8 weeks after submission.
Manuscripts and figures for review will not be returned to authors whether the editorial decision is to accept, revise, or reject. All Case Reports and Short Communication must include at least one table and/ or one figure.

Preparation of Manuscript

The manuscript should be written in English with simple lay out. The text should be prepared in single column format. Bold face, italics, subscripts, superscripts etc. can be used. Pages should be numbered consecutively, beginning with the title page and continuing through the last page of typewritten material.

The text can be divided into numbered sections with brief headings. Starting from introduction with section 1. Subsections should be numbered (for example 2.1 (then 2.1.1, 2.1.2, 2.2, etc.), up to three levels. Manuscripts in general should be organized in the following manner:

Title Page

The title page should contain a brief title, correct first name, middle initial and family name of each author and name and address of the department(s) and institution(s) from where the research was carried out for each author. The title should be without any abbreviations and it should enlighten the contents of the paper. All affiliations should be provided with a lower-case superscript number just after the author's name and in front of the appropriate address.
The name of the corresponding author should be indicated along with telephone and fax numbers (with country and area code) along with full postal address and e-mail address.

Abstract

The abstract should be concise and informative. It should not exceed **350 words** in length for full manuscript and Review article and **150 words** in case of Case Report and/ or Short Communication. It should briefly describe the purpose of the work, techniques and methods used, major findings with important data and conclusions. No references should be cited in this part. Generally non-standard abbreviations should not be used, if necessary they should be clearly defined in the abstract, at first use.

Keywords

Immediately after the abstract, **about 4-8 keywords** should be given. Use of abbreviations should be avoided, only standard abbreviations, well known in the established area may be used, if appropriate. These keywords will be used for indexing.

Abbreviations

Non-standard abbreviations should be listed and full form of each abbreviation should be given in parentheses at first use in the text.

Introduction

Provide a factual background, clearly defined problem, proposed solution, a brief literature survey and the scope and justification of the work done.

Materials and Methods

Give adequate information to allow the experiment to be reproduced. Already published methods should be mentioned with references. Significant modifications of published methods and new methods should be described in detail. Capitalize trade names and include the manufacturer's name and address. Subheading should be used.

Results

Results should be clearly described in a concise manner. Results for different parameters should be described under subheadings or in separate paragraph. Results should be explained, but largely without referring to the literature. Table or figure numbers should be mentioned in parentheses for better understanding.

Discussion

The discussion should not repeat the results, but provide detailed interpretation of data. This should interpret the significance of the findings of the work. Citations should be given in support of the findings. The results and discussion part can also be described as separate, if appropriate. The Results and Discussion sections can include subheadings, and when appropriate, both sections can be combined

Conclusions

This should briefly state the major findings of the study.

Acknowledgment

A brief acknowledgment section may be given after the conclusion section just before the references. The acknowledgment of people who provided assistance in manuscript preparation, funding for research, etc. should be listed in this section.

Tables and Figures

Tables and figures should be presented as per their appearance in the text. It is suggested that the discussion about the tables and figures should appear in the text before the appearance of the respective tables and figures. No tables or figures should be given without discussion or reference inside the text.

Tables should be explanatory enough to be understandable without any text reference. Double spacing should be maintained throughout the table, including table headings and footnotes. Table headings should be placed above the table. Footnotes should be placed below the table with superscript lowercase letters. Each table should be on a separate page, numbered consecutively in Arabic numerals.

Each figure should have a caption. The caption should be concise and typed separately, not on the figure area. Figures should be self-explanatory. Information presented in the figure should not be repeated in the table. All symbols and abbreviations used in the illustrations should be defined clearly. Figure legends should be given below the figures.

References

References should be listed alphabetically at the end of the manuscript. Every reference referred in the text must be also present in the reference list and vice versa. In the text, a reference identified by means of an author's name should be followed by the year of publication in parentheses (e.g.(Brown,2009)). For two authors, both authors' names followed by the year of publication (e.g.(Nelson and Brown, 2007)). When there are more than two authors, only the first author's name followed by "*et al*." and the year of publication (e.g. (Abu-Elteen *et al*., 2010)). When two or more works of an author has been published during the same year, the reference should be identified by the letters "a", "b", "c", etc., placed after the year of publication. This should be followed both in the text and reference list. e.g., Hilly, (2002a, 2002b); Hilly, and Nelson, (2004). Articles in preparation or submitted for publication, unpublished observations, personal communications, etc. should not be included in the reference list but should only be mentioned in the article text (e.g., Shtyawy,A., University of Jordan, personal communication). Journal titles should be abbreviated according to the system adopted in Biological Abstract and Index Medicus, if not included in Biological Abstract or Index Medicus journal title should be given in full. The author is responsible for the sccuracy and completeness of the references and for their correct textual citation. Failure to do so may result in the paper being withdraw from the evaluation process. Example of correct reference form is given as follows:-

Reference to a journal publication:

Bloch BK. 2002. Econazole nitrate in the treatment of *Candida vaginitis*. *S Afr Med J.* , **58**:314-323.

Ogunseitan OA and Ndoye IL. 2006. Protein method for investigating mercuric reductase gene expression in aquatic environments. *Appl Environ Microbiol*., **64**: 695-702.

Hilly MO, Adams MN and Nelson SC. 2009. Potential fly-ash utilization in agriculture. *Progress in Natural Sci.*, **19**: 1173-1186.

Reference to a book:

Brown WY and White SR.1985. **The Elements of Style**, third ed. MacMillan, New York.

Reference to a chapter in an edited book:

Mettam GR and Adams LB. 2010. How to prepare an electronic version of your article. In: Jones BS and Smith RZ (Eds.), **Introduction to the Electronic Age**. Kluwer Academic Publishers, Netherlands, pp. 281–304.

Conferences and Meetings:

Embabi NS. 1990. Environmental aspects of distribution of mangrove in the United Arab Emirates. Proceedings of the First ASWAS Conference. University of the United Arab Emirates. Al-Ain, United Arab Emirates.

Theses and Dissertations:

El-Labadi SN. 2002. Intestinal digenetic trematodes of some marine fishes from the Gulf of Aqaba. MSc dissertation, The Hashemite University, Zarqa, Jordan.

Nomenclature and Units

Internationally accepted rules and the international system of units (SI) should be used. If other units are mentioned, please give their equivalent in SI.

For biological nomenclature, the conventions of the *International Code of Botanical Nomenclature, the International Code of Nomenclature of Bacteria,* and the *International Code of Zoological Nomenclature* should be followed.
Scientific names of all biological creatures (crops, plants, insects, birds, mammals, etc.) should be mentioned in parentheses at first use of their English term.

Chemical nomenclature, as laid down in the *International Union of Pure and Applied Chemistry* and the official recommendations of the *IUPAC-IUB Combined Commission on Biochemical Nomenclature* should be followed. All biocides and other organic compounds must be identified by their Geneva names when first used in the text. Active ingredients of all formulations should be likewise identified.

Math formulae

All equations referred to in the text should be numbered serially at the right-hand side in parentheses. Meaning of all symbols should be given immediately after the equation at first use. Instead of root signs fractional powers should be used. Subscripts and superscripts should be presented clearly. Variables should be presented in italics. Greek letters and non-Roman symbols should be described in the margin at their first use.

To avoid any misunderstanding zero (0) and the letter O, and one (1) and the letter l should be clearly differentiated. For simple fractions use of the solidus (/) instead of a horizontal line is recommended. Levels of statistical significance such as: $^{*}P < 0.05$, $^{**}P < 0.01$ and $^{***}P < 0.001$ do not require any further explanation.

Copyright

Submission of a manuscript clearly indicates that: the study has not been published before or is not under consideration for publication elsewhere (except as an abstract or as part of a published lecture or academic thesis); its publication is permitted by all authors and after accepted for publication it will not be submitted for publication anywhere else, in English or in any other language, without the written approval of the copyright-holder. The journal may consider manuscripts that are translations of articles originally published in another language. In this case, the consent of the journal in which the article was originally published must be obtained and the fact that the article has already been published must be made clear on submission and stated in the abstract. It is compulsory for the authors to ensure that no material submitted as part of a manuscript infringes existing copyrights, or the rights of a third party.

Ethical Consent

All manuscripts reporting the results of experimental investigation involving human subjects should include a statement confirming that each subject or subject's guardian obtains an informed consent, after the approval of the experimental protocol by a local human ethics committee or IRB. When reporting experiments on animals, authors should indicate whether the institutional and national guide for the care and use of laboratory animals was followed.

Plagiarism

The JJBS hold no responsibility for plagiarism. If a published paper is found later to be extensively plagiarized and is found to be a duplicate or redundant publication, a note of retraction will be published, and copies of the correspondence will be sent to the authors' head of institute.

Galley Proofs

The Editorial Office will send proofs of the manuscript to the corresponding author as an e-mail attachment for final proof reading and it will be the responsibility of the corresponding author to return the galley proof materials appropriately corrected within the stipulated time. Authors will be asked to check any typographical or minor clerical errors in the manuscript at this stage. No other major alteration in the manuscript is allowed. After publication authors can freely access the full text of the article as well as can download and print the PDF file.

Publication Charges

There are no page charges for publication in Jordan Journal of Biological Sciences, except for color illustrations,

Reprints

Ten (10) reprints are provided to corresponding author free of charge within two weeks after the printed journal date. For orders of more reprints, a reprint order form and prices will be sent with article proofs, which should be returned directly to the Editor for processing.

Disclaimer

Articles, communication, or editorials published by JJBS represent the sole opinions of the authors. The publisher shoulders no responsibility or liability what so ever for the use or misuse of the information published by JJBS.

Indexing

JJBS is indexed and abstracted by:

DOAJ (Directory of Open Access Journals)	CABI
Google Scholar	EBSCO
Journal Seek	CAS (Chemical Abstract Service)
HINARI	ETH- Citations
Index Copernicus	Open J-Gat
NDL Japanese Periodicals Index	SCImago
SCIRUS	Clarivate Analytics (Zoological Abstract)
OAJSE	Scopus
ISC (Islamic World Science Citation Center)	AGORA (United Nation's FAO database)
Directory of Research Journal Indexing (DRJI)	SHERPA/RoMEO (UK)
Ulrich's	

المجلة الأردنية للعلوم الحياتية
Jordan Journal of Biological Sciences (JJBS)
ISSN 1995- 6673 (Print), 2307- 7166 (Online)
http://jjbs.hu.edu.jo

The Hashemite University

Deanship of Scientific Research

TRANSFER OF COPYRIGHT AGREEMENT

Journal publishers and authors share a common interest in the protection of copyright: authors principally because they want their creative works to be protected from plagiarism and other unlawful uses, publishers because they need to protect their work and investment in the production, marketing and distribution of the published version of the article. In order to do so effectively, publishers request a formal written transfer of copyright from the author(s) for each article published. Publishers and authors are also concerned that the integrity of the official record of publication of an article (once refereed and published) be maintained, and in order to protect that reference value and validation process, we ask that authors recognize that distribution (including through the Internet/WWW or other on-line means) of the authoritative version of the article as published is best administered by the Publisher.

To avoid any delay in the publication of your article, please read the terms of this agreement, sign in the space provided and return the complete form to us at the address below as quickly as possible.

Article entitled:----------

Corresponding author: ----------

To be published in the journal: Jordan Journal of Biological Sciences (JJBS)

I hereby assign to the Hashemite University the copyright in the manuscript identified above and any supplemental tables, illustrations or other information submitted therewith (the "article") in all forms and media (whether now known or hereafter developed), throughout the world, in all languages, for the full term of copyright and all extensions and renewals thereof, effective when and if the article is accepted for publication. This transfer includes the right to adapt the presentation of the article for use in conjunction with computer systems and programs, including reproduction or publication in machine-readable form and incorporation in electronic retrieval systems.
Authors retain or are hereby granted (without the need to obtain further permission) rights to use the article for traditional scholarship communications, for teaching, and for distribution within their institution.

☐ **I am the sole author of the manuscript**

☐ **I am signing on behalf of all co-authors of the manuscript**

☐ **The article is a 'work made for hire' and I am signing as an authorized representative of the employing company/institution**

Please mark one or more of the above boxes (as appropriate) and then sign and date the document in black ink.

Signed:_____ **Name printed:** _____
Title and Company (if employer representative) : _____
Date: _____

Data Protection: By submitting this form you are consenting that the personal information provided herein may be used by the Hashemite University and its affiliated institutions worldwide to contact you concerning the publishing of your article.

Please return the completed and signed original of this form by mail or fax, or a scanned copy of the signed original by e-mail, retaining a copy for your files, to:

Hashemite University
Jordan Journal of Biological Sciences
Zarqa 13115 Jordan
Fax: +962 5 3903338
Email: jjbs@hu.edu.jo

EDITORIAL PREFACE

Jordan Journal of Biological Sciences (JJBS) is a refereed, quarterly international journal financed by the Scientific Research and Innovation Support Fund, Ministry of Higher Education and Scientific Research in cooperation with the Hashemite University, Jordan. JJBS celebrated its 12th commencement this past January, 2020. JJBS was founded in 2008 to create a peer-reviewed journal that publishes high-quality research articles, reviews and short communications on novel and innovative aspects of a wide variety of biological sciences such as cell biology, developmental biology, structural biology, microbiology, entomology, molecular biology, biochemistry, medical biotechnology, biodiversity, ecology, marine biology, plant and animal biology, plant and animal physiology, genomics and bioinformatics.

We have watched the growth and success of JJBS over the years. JJBS has published 11 volumes, 45 issues and 479 articles. JJBS has been indexed by SCOPUS, CABI's Full-Text Repository, EBSCO, Clarivate Analytics- Zoological Record and recently has been included in the UGC India approved journals. JJBS Cite Score has improved from 0.18 in 2015 to 0.58 in 2019 (Last updated on 16 March, 2020) and with Scimago Institution Ranking (SJR) 0.21 (Q3) in 2018.

A group of highly valuable scholars have agreed to serve on the editorial board and this places JJBS in a position of most authoritative on biological sciences. I am honored to have six eminent associate editors from various countries. I am also delighted with our group of international advisory board members coming from 15 countries worldwide for their continuous support of JJBS. With our editorial board's cumulative experience in various fields of biological sciences, this journal brings a substantial representation of biological sciences in different disciplines. Without the service and dedication of our editorial; associate editorial and international advisory board members, JJBS would have never existed.

In the coming year, we hope that JJBS will be indexed in Clarivate Analytics and MEDLINE (the U.S. National Library of Medicine database) and others. As you read throughout this volume of JJBS, I would like to remind you that the success of our journal depends on the number of quality articles submitted for review. Accordingly, I would like to request your participation and colleagues by submitting quality manuscripts for review. One of the great benefits we can provide to our prospective authors, regardless of acceptance of their manuscripts or not, is the feedback of our review process. JJBS provides authors with high quality, helpful reviews to improve their manuscripts.

Finally, JJBS would not have succeeded without the collaboration of authors and referees. Their work is greatly appreciated. Furthermore, my thanks are also extended to The Hashemite University and the Scientific Research and Innovation Support Fund, Ministry of Higher Education and Scientific Research for their continuous financial and administrative support to JJBS.

March, 2020

JJBS

Volume 13, Number 2,June 2020
ISSN 1995-6673

Jordan Journal of Biological Sciences

CONTENTS

Original Articles

Short Communication

JJBS

Volume 13, Number 2, June 2020
ISSN 1995-6673
Pages 127 - 132

Jordan Journal of Biological Sciences

Acute Effect of Cadmium Chloride on Chromosomal Abnormalities in the Nile Tilapia Fish *In Vivo*

Bundit Tengjaroenkul [1, 2] and Lamyai Neeratanaphan [1, 3*]

[1] *Research Group on Toxic Substances in Livestock and Aquatic Animals,* [2] *Faculty of Veterinary Medicine,* [3] *Division of Environmental Science, Faculty of Science, Khon Kaen University, Khon Kaen 40002, Thailand*

Received April 15, 2019; Revised June 6, 2019; Accepted June 25, 2019

Abstract

The cytotoxic potential of cadmium chloride ($CdCl_2$) in *Oreochromis niloticus* was conducted by assessment of chromosomal abnormalities (CA). Treatment fish were intraperitoneally injected with 5, 10, 20 and 30 mg/L $CdCl_2$ solution, and the CA effects were compared with those of control fish. After 48 h, muscles of the fish were analyzed for cadmium (Cd) concentration, and the kidneys were evaluated for CA. Cd concentrations in the fish from the control and treatments revealed as lower than detection limits, 0.04±0.02, 0.11±0.01, 0.20±0.06 and 0.17±0.04 mg/kg, respectively, whereas Cd was not detected in water samples. Eleven types of CA were demonstrated as single chromatid gap (SCG), sister chromatid gap, sister chromatid fragment, fragmentation, single chromatid breaks, deletion, dicentric, centromere separate, C-mitotic, centric fusion and pericentric invertion. The most CA in the treated fish was SCG. The percentages of CA cells in the control and treatments were 0, ٢٠.٦٦±6.80, 21.66±4.04, 25.00±5.29 and 37.66±2.08, respectively. The number of CA and the percentage of CA cells in the control and the treatments were statistically significant ($p<0.05$). The treatment fish injected with 30 mg/L was significant from the other treatments ($p<0.05$). This study demonstrates that acute toxicity with relatively low concentrations (5 mg/L) of $CdCl_2$ can induce CA in the Nile tilapia fish.

Keywords: Chromosomal abnormality, Cadmium chloride, Cytotoxicity, Fish, Tilapia.

1. Introduction

Aquatic ecosystem contamination by heavy metals from industrial, domestic and agriculture wastewater has been gaining increased attention. Heavy metals contamination can harm life of aquatic organisms after being absorbed through contaminated water, sediment and the food chain. Accumulation of heavy metals could produce adverse effects on structures and functions of cells and tissues of the exposed aquatic creatures. Cadmium (Cd) is one of nonessential metals in all living creatures (Besirovic *et al*., 2010); however, it is widely used in numerous industrial processes, including electroplating, smelting, making batteries and production of color as well as plastic (Waisberg *et al*., 2003). In case of leaching into aquatic ecosystem, Cd can be bioaccumulated, and cause detrimental consequences to various creatures along the aquatic food chain, including snail, shrimp and fish as well as to human as the top consumer in the food chain. Cd is generally accepted as one of hazardous agents to human health, and has been documented as teratogenic, apoptotic and genotoxic, hepatotoxic, pancreatotoxic, nephrotoxic and carcinogenic agent (Ahmed and Abdel-Wahhab, 2000; Horiguchi *et al*., 2000; Hovland *et al*., 2000; Shimada *et al*., 2000; Banerjee and Flores-Rozas, 2005; Kim *et al*., 2005; Mondal *et al*., 2005; Goodale *et al*., 2008). Cd exerts toxicological effects, mostly in the kidneys and liver (Stoeppler, 1991; Cai *et al*., 2001). Previous reports have shown that exposure to Cd at relatively high levels results in diseases, disorders and life threatening conditions (Othumpangat *et al*., 2005).

Presently, numerous research reports have revealed accumulation and toxicity of Cd in fish, including oxidative effects, morphology and physiology changes, osmoregulation and immune response and endocrine disruptions (Romeo *et al*., 2000; Dang and Wang, 2009; Garcia-Santos *et al*., 2011; Guardiola *et al*., 2013; Li *et al*., 2014). Fish, including the Nile tilapia, *Oreochromis niloticus*, are major aquatic creatures in the food chain of aquatic ecosystems, and are often used as biomarkers in toxicological studies. When they ingest organisms contaminated with heavy metals, deleterious health effects occur (Clearwater *et al*., 2002; Giusto *et al*., 2012; Mustafa *et al*., 2012; Al-Bairuty *et al*., 2013; Intamat *et al*., 2016). Among pollutants, Cd is one of hazardous toxicants to fish when absorbed via diet or the water medium (Kalman *et al*., 2010; Sriuttha *et al*., 2017). Currently, we have little knowledge of CA resulting from acute Cd exposure (Kamunde and MacPhail, 2011). The aim of this study was to investigate CA in *O. niloticus* resulting from acute Cd exposure (48 h) at four different concentrations.

* Corresponding author. e-mail: hlamya@kku.ac.th.

2. Materials and Methods

2.1. Experimental fish specimens

Oreochromis niloticus with weight 15-20 g received from a private fish farm in Khon Kaen city, Thailand, were bathed with $KMnO_4$ solution (0.05% v/v) to avoid skin infection (Pandey *et al*., 2011). They were acclimatized under experimental conditions for 10 days before the Cd toxicity study *in vivo*.

2.2. Exposure concentration of Cd

The acclimatized fish in the control were intraperitoneally injected with 0.8% sterilized normal saline, whereas the fish in four treatments were injected with 5, 10, 20 and 30 mg/L at a volume of 100 µL of cadmium chloride ($CdCl_2$). The experimental fish were kept for 48 h before the CA assessment.

2.3. Cd concentration in water

After 48 h, a 25-mL water sample was put in a glass container, and nitric acid (1.25 mL) was added. The container was set in water bath at 90±5°C, for 30 min. Deionized water was later added to the acid digested water sample to make a 25 mL final volume before being filtered using standard 11 µm filter paper. Cd in the water was evaluated by inductively coupled plasma optical emission spectrometry (ICP-OES) (Promsid *et al*., 2015).

2.4. Cd concentration in O. niloticus

The fish muscle weighed 1 g was homogenized, and mixed with 7 mL of nitric acid. After adding 1 mL of hydrogen peroxide, the samples were set in water bath at 90±5°C for 2 h. After cooling, deionized water samples were adjusted to make a suspended mixture of 25 mL. Then, the mixture was passed through an 11 µm cellulose filter paper. Cd concentration in fish muscle was measured using ICP-OES (Promsid *et al*., 2015) with a wavelength of 226.502 nm and a detection limit of 0.001 mg/L.

2.5. Quality assurance

Following standards of quality assurance, detection and measurement for Cd contamination were conducted at every tenth sample. The blank Cd concentrations were < 5% of the average of analyzed concentrations. Accuracy as well as precision of the analyses were confirmed by the replication of analyzed samples against Cd standard reference (APHA, 2005).

2.6. Chromosome preparation

The fish chromosomes were collected following conventional method (Srikacha *et al*., 2018; Tengjaroenkul *et al*., 2018). Each experimental fish was injected intramuscularly using 1 ml colchicine solution (0.05%) per 100 g fish weight, kept approximately 1 h, and anesthetized in ground ice. The kidneys were excised, made to small pieces and mixed with 0.075 M KCl. Sediment cells of 8 mL was incubated at 25°C for 30 min, before being fixed in cool methanol-acetic acid fixative at ratio 3:1. Later, the cells were centrifuged for 4 times at 1500 rpm for 10 min with 8 mL of the cool fixative. For chromosomal study, the cleaned sediment was added with 1 mL of the cool fixative, dropped to a glass slide, air dried and then stained with Giemsa solution (20%) for 30 min (Intamat *et al*., 2016).

One hundred with clear and well spread chromosomes in each treatment were photographed. Number of CA cells was recorded. All parameters as well as fundamental number (number of chromosome arms or NF) were used for karyotyping. Cytotoxicity was evaluated by determining the percentage of CA cells of the fish (Intamat *et al*., 2016).

2.7. Statistical analysis

Levels of Cd in water and *O. niloticus* muscles, as well as number and the percentage of CA cells were statistically analyzed using Analysis of Variance as well as Turkey's post hoc test (at 95% confidence).

3. Results

3.1. Cd concentration in water and O. niloticus

Cd in all experimental water samples was not detected. The Cd concentration in *O. niloticus* is demonstrated in Table 1. The highest Cd level in the fish muscle was shown in the treatment injected with 20 mg/L. Statistical results demonstrated that Cd concentrations of the fish in the control and the treatments revealed significant difference ($p<0.05$), and only the treatment received 5 mg/L was significantly different ($p<0.05$) from the other treatments.

Table 1. Cd concentration in *O. niloticus* samples.

$CdCl_2$ concentration (mg/L)	Cd concentration in fish muscle (mg/kg) experimental unit			Average Cd concentration
	1	2	3	(mg/kg)
Control	ND	ND	ND	ND
٥	0.02	0.04	0.06	0.04±0.02[a]
١٠	0.12	0.10	0.11	0.11±0.01[b]
٢٠	0.27	0.16	0.17	0.20±0.06[c]
٣٠	0.21	0.15	0.14	0.17±0.04[c]

ND: Not detected

[a, b, c] Values in the same column with different letters are significantly different ($p<0.05$).

3.2. Assessment of chromosomal abnormalities

The current study used a CA test to evaluate cytotoxic consequences on the Nile tilapia (*O. niloticus*) after acutely (48 h) injected with Cd. The diploid chromosome number (2*n)* of the Nile tilapia is 44. The karyotype of the tilapia fish consisted of two submetacentric, twelve acrocentric and thirty telocentric chromosomes (Figure 1). The different categories of CA found in the current study were single chromatid gap (SCG), single chromatid breaks (SCB), sister chromatid gap (SSCG), sister chromatid fragment (SSCF), fragmentation (F), deletion (D), dicentric (DC), centromere separate (CS), C-mitotic, centric fusion (CF) and pericentric invertion (PI) (Figure 2 and Table 2). The type of CA found in *O. niloticus* was different among levels of Cd concentrations. The control fish had no CA, whereas the treatment fish injected with Cd at 5 and 10 mg/L revealed nine types of CA (SCG, SSCG, F, D, DC, CS, C-mitotic, CF and PI). The treatment fish injected with Cd at 20 and 30 mg/L revealed eleven types of CA (SCG, SSCG, SCB, F, SSCF, D, DC, CS, C-mitotic, CF and PI).

The highest total number of CA was demonstrated in the treatment injected with 20 mg/L, while the highest number of cells with CA was demonstrated in the

treatment injected with 30 mg/L (Table 2). Statistical analyses indicated that there were significant differences in the number of CA and the number of CA cells between the control and the treatments ($p<0.05$), except for the fish treated with 5 mg/L. Among the numbers of CA cells in the treatments, there were significant differences between the fish treated with 30 mg/L and the other treatments ($p<0.05$) (Table 2).

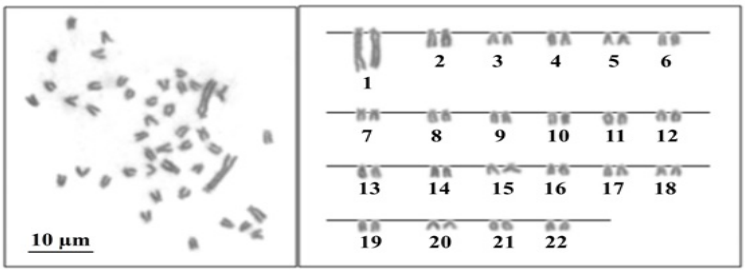

Figure 1. Karyotypes of diploid chromosome ($2n=44$) of the *O. niloticus* in the control.

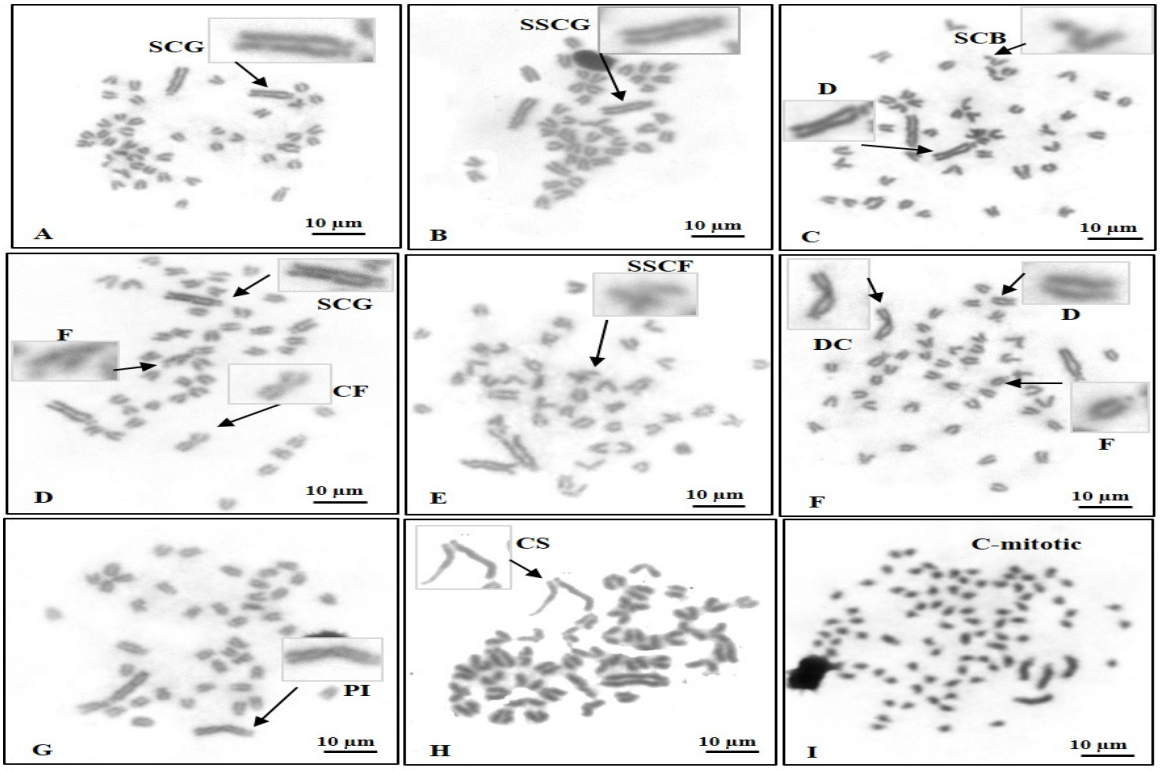

Figure 2. Examples of different chromosomal abnormalities in *O. niloticus* (*2n*=44): single chromatid gap (SCG), sister chromatid gap (SSCG), single chromatid breaks (SCB), centric fusion (CF), fragmentation (F), sister chromatid fragment (SSCF), deletion (D), dicentric (DC), pericentric invertion (PI), centromere separate (CS) and C-mitotic.

Table 2. Number and percentage of CA cells of *O. niloticus* in the control and the $CdCl_2$ treatments.

$CdCl_2$ concentrations	Number of CA											Total number of CA	Number of cells with CA	Percentage of cells with CA
	SCG	SSCG	SCB	SSCF	CF	F	D	PI	DC	CS	C-mitotic			
Control	0	0	0	0	0	0	0	0	0	0	0	0	0	0[a]
5	5	2	0	0	6	1	5	2	7	3	6	36	21	٢٠.٦٦±6.80[b]
10	9	4	0	0	2	2	2	2	7	1	3	33	21	21.66±4.04[b]
20	9	5	1	1	5	2	4	3	7	4	7	48	25	25.00±5.29[b]
30	7	3	1	1	7	2	4	4	7	4	7	47	32	37.66±2.08[c]

[a, b, c] Values in the same column with different letters are significantly different ($p<0.05$).

4. Discussion

The Cd concentration in water samples was not detected. This result could be due to the distribution and elimination of toxicants in fish. As Cd elimination in fish is low, resulting in Cd accumulation in liver, gill and muscle of various fish species (Jayakumar and Paul, 2006; Cyrille *et al*., 2012). Fish muscle, a valuable edible protein source, was selected as a target organ to detect low levels of Cd deposition. Previous studies have reported that the main target organs for Cd accumulation in fish samples are

the kidneys, liver, gills and skin. A potential reason that the muscle accumulated Cd as the lowest level is that it is not directly contact to the water medium. Another probable reason is that muscle has no function related to detoxification of xenobiotics, and consequently, accumulation of Cd in the muscle as compared with the liver and kidney is less likely to occur (Jayakumar and Paul, 2006). In addition, an accumulation of Cd in fish could be long in their life time; this is supported by Agency for Toxic Substances Disease Registry (1999) who reported half-life of Cd in the liver approximately 4-19 years.

The diploid chromosome number of *O. niloticus* is similar to previous studies (Vervoort, 1980; Sofy *et al*., 2008; Intamat, 2016; Sriuttha *et al*., 2017). This result implies that numerical of chromosome is not changed after acutely injected with Cd in the Nile tilapia fish.

The results using CA assessment revealed that *O. niloticus* injected with Cd had greater in both of the number of CA cells and the percentage of CA cells as the Cd concentration increased. Eleven types of CA indicate that Cd, particularly at higher levels is more effective on changing chromosome structures. The results of this study were different from other findings. For example, Intamat (2016) studied cytotoxic effects of sodium arsenite on *O. niloticus* on an experimental scale, and found five types of CA, including SCG, SCB, CG, F and D. Sriuttha *et al*. (2017) demonstrated that heavy metals of *O. niloticus* in domestic wastewater canals could induce six types of CA, including SCG, SCB, CG, F, D and DC. This variable CA information could imply that the CA may correlate to types, toxicities as well as the contact time of the exposed heavy metals. Several heavy metals have adverse effects on genetic materials (Achanzar *et al*., 2002; Asmuss *et al*., 2000; Hartwig and schwerstle, 2002; Fatur *et al*., 2003; Jin *et al*., 2003; Potts *et al*., 2003; Waisberg *et al*., 2003). Our results revealed that the different levels of Cd concentrations were associated with different types of CA. The most abnormality of chromosome from the tilapia kidney cells was SCG (Table 2). This result is similar to previous studies. Intamat *et al*. (2016) and Sriuttha *et al*. (2017) reported that SCG was the most found CA in kidney cells of the tilapia fish collected from both laboratory experiments and heavy metal contaminated areas. SCG has been demonstrated probably due to a lack of folding of the metaphase chromosome fiber into a chromatid. Palitti (2004) mentioned that SCG could occur as results of protein or DNA damages.

Cd compounds can cause breaking of DNA strand and CA that demonstrate less mutagenic in mammalian cells (Waalkes, 2003). Ashmawy *et al*. (2015) demonstrated that micronuclei formation was lower at low concentrations and shorter exposure times of Cd than at higher concentrations and longer exposure times. Toxic effects of heavy metal are generally produced at high exposure concentrations. In contrast, Cd exhibits both acute and chronic toxicity at very low exposure levels (NCM-WHO, 2003). In this study, Cd could demonstrate acute toxicity in term of CA at relatively low concentrations (5 mg/L) in the Nile tilapia fish. Similarly, Parveen and Shadab (2012) found that 5 mg/L of $CdCl_2$ caused genotoxicity as CA in *Channa punctatus* specimen. This provided evidence that duration of exposure of treatment can affect the genomic system of *O. niloticus* exposed to Cd at several concentrations (16, 18, 20 and 22 mg/L) and at different time periods (1, 7, 14, 21 and 28 days). Similarly, Jindal and Verma (2015) reported that a comet assay showed a greater value of mean percentage of DNA collected from the tail of the freshwater fish, *Labeo rohita*, after contacted to 0.37 and 0.62 mg/L $CdCl_2$ for 100 days. The genotoxicity of Cd has been described by indirect mechanisms involving in cell proliferation, free radical reactivity, tumor-suppression functions and DNA-repairing processes (Stohs *et al*., 2001; Pagliuca *et al*., 2003; Lutzen *et al*., 2004; Youn *et al*., 2005; Valko *et al*., 2006). Furthermore, Cd inhibited DNA repair mechanisms, including excision of nucleotide, default of nuclotide repair and deletion of the DNA precursor (Asmuss *et al*., 2000; Achanzar *et al*., 2002; Hartwig and schwerstle, 2002; Fatur *et al*., 2003; Jin *et al*., 2003; Potts *et al*., 2003). Cd reacted to signal transduction pathways, mainly with mitogenic signaling. Submicromolar levels of Cd have induced DNA synthesis and caused cell divisions of myoblast and macrophage (Misra *et al*., 2002). In addition, on an experimental scale, Cd stimulates a release of the secondary messenger of calcium, mitogenic kinases, factors related to transcription and translation, and oncogene expression (Waisberg *et al*., 2003). These mechanisms could be the major roles in the CA formation in tilapia fish cells.

5. Conclusion

Acute exposure at different concentrations of $CdCl_2$ causes significant difference in the numbers of cells with CA and the percentages of cell with CA between *O. niloticus* in the control and the treatments. The CA could be as potential indicator of acute Cd cytotoxicity in the tilapia fish. Further investigations coping with cytotoxic effects of $CdCl_2$ at various exposure times and at more variable concentrations are required.

References

Achanzar WE, Brabila EM, Diwan BA, Webber MM and Waalkes MP. 2002. Inorganic arsenite-induced malignant transformation of human prostate epithelial cells. *J Natl Cancer Inst*, **94**:1888-1891.

Agency for Toxic Substances Disease Registry. 1999. Toxicological profile for cadmium. Department of Health and Human Services, Atlanta.

Ahmed HH and Abdel-Wahhab MA. 2000. Protection against cadmium-induced toxicity in the rats: potential for hidden risks. *J Egypt Soc Toxicol*, **22**:51-57.

Al-Bairuty GA, Shaw BJ, Handy RD and Henry TB. 2013. Histopathological effects of waterborne copper nanoparticles and copper sulphate on the organs of rainbow trout (*Oncorhynchus mykiss*). *Aquat Toxicol*, **126**:104-115.

American Public Health Association (APHA). 2005. Standard Methods for the Examination of Water and Wastewater. American Public Health Association, Washington DC.

Ashmawy AA, Rashed MA, Atta AH, Ibranhim AG and Abdel-Gawad FH. 2015. Genotoxic effect of cadmium on nile tilapia (*Oreochromis niloticus*). *Int J Sci Eng Res*, **6**:971-980.

Asmuss M, Mullenders LH, Eker A and Hartwig A. 2000. Differential effects of toxic metal compounds on the activities of Fpg and XPA, two zinc finger proteins involved in DNA repair. *Carcinogenesis*, **21**:2097-104.

Banerjee S and Flores-Rozas H. 2005. Cadmium in hibits mismatch repair by blocking the ATP ase activity of the MSH2–MMSH6 complex. *Nucl Acids Res*, **33**:1410-1419.

Besirovic H, Alic A, Prasovic S and Drommer W. 2010. Histopathological effects of chronic exposure to cadmium and zinc on kidneys and gills of brown trout (*Salmotrutta m. fario*). *Turk J Fish Aquat Sci*, **10**:255-262.

Cai Y, Aoshima K, Katoh T, Teranishi H and Kasuya M. 2001. Renal tubular dysfunction in malein habitants of a cadmium-polluted area in Toyama, Japan- an eleven-yearfollow-upstudy. *J Epidemiol*, **11**:180-189.

Clearwater SJ, Farag AM and Meyer JS. 2002. Bioavailability and toxicity of diet borne copper and zinc to fish. *Comp Biochem Phys*, **132C**:269-313.

Cyrille YDA, Victor K, Sanogo TA, Boukary S and Joseph W. 2012. Cadmium accumulation in tissues of *Sarotherodon melanotheron* (Ruppel, 1852) from the Aby lagoon system in Cote d'Ivoire. *Int J Environ Res Public Health*, **9**:821-830.

Dang F and Wang WW. 2009. Assessment of tissue-specific accumulation and effects of cadmium in a marine fish fed contaminated commercially produced diet. *Aquat Toxicol*, **95**:248-255.

Fatur T, Lah TT and Filipic M. 2003. Cadmium inhibits repair of UV-methyl methanesulfonate- and N-methyl-N-nitrosourea-induced DNA damage in Chinese hamster ovary cells. *Mutat Res*, **529**:109-16.

Garcia-Santos S, Vargas-Chacoff L, Ruiz-Jarabo I, Varela JL, Mancera JM, Fontainhas-Fernandes A and Wilson JM. 2011. Metabolic and osmoregulatory changes and cell proliferation in gilthead sea bream (*Sparus aurata*) exposed to cadmium. *Ecotoxicol Environ Saf*, **74**:270-278.

Giusto A, Somma LA and Ferrari L. 2012. Cadmium toxicity assessment in juveniles of the Austral South America amphipod *Hyalella curvispina*. *Ecotoxicol Environ Saf*, **79**:163-169.

Goodale BC, Waiter R, Pelsue SR, Thompson WD, Wise SS, Winn RN, Mitani H and Wise JP. 2008. The cytotoxicity and genotoxicity of hexavalent chromium in medaka (*Oryzias latipes*) cells. *Aquat Toxicol*, **87**:60-67.

Guardiola FA, Cuesta A, Meseguer J, Martínez S, Martinez-Sanchez MJ, Perez-Sirvent C and Esteban MA. 2013. Accumulation, histopathology and immunotoxicological effects of waterborne cadmium on gilthead seabream (*Sparus aurata*). *Fish Shellfish Immunol*, **35**:792-800.

Hartwig A and Schwerdtle T. 2002. Interactions by carcinogenic metal compounds with DNA repair processes: toxicological implications. *Toxicol Lett*, **127**:47-54.

Horiguchi H, Harada A, Oguma E, Sato M, Homma Y, Kayama F, Fukushima M and Matsushima K. 2000. Cadmium-induced acute hepatic injury is exacerbated in human interleukin-8 transgenic mice. *Toxicol Appl Pharmacol*, **163**:231-239.

Hovland JDN, Cantor RM, Lee GS, Machado AF and Collins MD. 2000. Identifi-cation of amurine locus conveying susceptibility to cadmium induced for elimb malformations. *Genomics*, **63**:193-201.

Intamat S, Phoonaploy U, Sriuttha M, Tengjaroenkul B and Neeratanaphan L. 2016. Heavy metal accumulation in aquatic animals around the gold mine area of Loei province, Thailand. *Human Ecologi Risk Assess: An Internat J*, **22**:1418-1432.

Jayakumar P and Paul VI. 2006. Pattern of cadmium accumulation in selected tissues of the catfish *Clarias batrachus* (Linn.) exposed to sub-lethal concentration of cadmium chloride. *Veterinarski Arhiv*, **76**:167-177.

Jin YH, Clark AB, Slebos RJ, Al-Refai H, Taylor JA, Kunkel TA, Resnick MA and Gordenin DA. 2003. Cadmium is a mutagen that acts by inhibiting mismatch repair. *Nat Genet*, **34**:326-329.

Jindal R and Verma S. 2015. In vivo genotoxicity and cytotoxicity assessment of cadmium chloride in peripheral erythrocytes of *Labeo rohita* (Hamilton). *Ecotoxicol Environ Saf*, **118**:1-10.

Kalman J, Riba I, DelValls TA and Blasco J. 2010. Comparative toxicity of cadmium in the commercial fish species *Sparus aurata* and *Solea senegalensis*. *Ecotoxicol Environ Saf*, **73**:306-311.

Kamunde C and MacPhail R. 2011. Metal-metal interactions of dietary cadmium, copper and zinc in rainbow trout, *Oncorhynchus mykiss*. *Ecotoxicol Environ Saf*, **74**:658-667.

Kim SD, Moon CK, Eun SY, Ryu PD and Jo SA. 2005. Identification of ASK1, MKK4, JNK, c-Jun, and caspase-3 asasign aling cascade involved in cadmium induced neuronal cell apoptosis. *Biochem Biophys Res Commun*, **328**:326-334.

Li ZH, Chen L, Wu YH, Li P, Li YF and Ni ZH. 2014. Effects of waterborne cadmium on thyroid hormone levels and related gene expression in Chinese rare minnow larvae. *Comp Biochem Physiol*, **161**:53-57.

Lutzen A, Liberti SE and Rasmussen LJ. 2004. Cadmium inhibits human DNA mismatch repair in vivo. *Biochem Biophys Res Commun*, **321**:21-25.

Misra UK, Gawdi G, Akabani G and Pizzo SV. 2002. Cadmium-induced DNA synthesis and cell proliferation in macrophages: the role of intracellular calcium and signal transduction mechanisms. *Cell Signal*, **14**:327-340.

Mondal TK, Li D, Swami K, Dean JK, Hauer C and Lawrence DA. 2005. Mercury impairment of mouse thymocyte survival invitro: involvement of cellular thiols. *J Toxicol Environ Health*, **68**:535-556.

Mustafa SA, Davies SJ, and Jha AN. 2012. Determination of hypoxia and dietary copper mediated sub-lethal toxicity in carp, *Cyprinus carpio*, at different levels of biological organization. *Chemosphere*, **87**:413-422.

NCM-WHO. 2003. Cadmium Review. NMR Report 1; Nordic Council of Ministers-World Health Organization, 23 pp.

Othumpangat S, Kashon M and Joseph P. 2005. Eukaryotic translation initiation factor 4E is a cellular target for toxicity and death due to exposure to cadmium chloride. *J Biol Chem*, **280**: 162-169.

Pandey AK, Nagpure NS, Trivedi SP, Kumar R and Kushwaha B. 2011. Profenofos induced DNA damage in freshwater fish, *Channa punctatus* (Bloch) using alkaline single cell gel electrophoresis. *Mutat Res*, **726**:209-214.

Pagliuca MG, Lerose R, Cigliano S and Leone A. 2003. Regulation by heavy metals and temperature of the human BAG-3 gene, a modulator of Hsp70 activity. *FEBS Lett*, **541**:11-15.

Palitti F. 2004. Mechanism of formation of chromosomal aberrations: insights from studies with DNA repair-deficient cells. *Cytogenet Genome Res*, **104**:95-99.

Parveen N and Shadab GG. 2012. Cytogenetic evaluation of cadmium chloride on *Channa punctatus*. *J Environ Biol*, **33(3)**:663-666.

Potts RJ, Watkin RD and Hart BA. 2003. Cadmium exposure down-regulates 8-oxoguanine DNA glycosylase expression in rat lung and alveolar epithelial cells. *Toxicol*, **184**:189-2020.

Promsid P, Neeratanaphan L, Supiwong W, Sriuttha M and Tanomtong A. 2015. Chromosomal aberration of snakehead fish (*Channa striata*) in affected reservoir by leachate with lead and mercury contamination. *Internat J Environ Res*, **9**:897-906.

Roméo M, Bennani N, Gnassia-Barelli M, Lafaurie M and Girard JP. 2000. Cadmium and copper display different responses

towards oxidative stress in the kidney of the sea bass *Dicentrarchus labrax*. *Aquat Toxicol*, **48**:185-194.

Shimada H, Funakoshi T and Waalkes MP. 2000. Acute, non-toxic cadmium exposure inhibits pancreatic protease activities in the mouse. *Toxicol Sci*, **53**:474-480.

Srikacha N, Neeratanaphan L, Jongyotha S, Tengjaroensakul U and Tengjaroenkul B. 2018. Acute cytotoxicity of the young Nile tilapia (*Oreochromis niloticus*) injected by aflatoxin B_1. *Livestock Res Rural Dev*, **30(8)**:1-8.

Sofy HI, Layla AM and Iman MKA. 2008. Karyotypic of some tilapia species. *Nat Sci*, **6**:19-27.

Sriuttha M, Khammanichanh A, Patawang I, Tanomtong A, Tengjaroenkul B and Neeratanaphan L. 2017. Cytotoxic assessment of nile tilapia (*Oreochromis niloticus*) from a domestic wastewater canal with heavy metal contamination. *Cytologia*, **82**:41-50.

Stoeppler M. 1991. Cadmium. In: Merian, E. (Ed.), Metals and Their Compounds in the Environment. VCH, New York, pp. 803-851.

Stohs SJ, Bagchi D, Hassoun E and Bagchi M. 2001. Oxidative mechanisms in the toxicity of chromium and cadmium ions. *J Environ Pathol Toxicol Oncol*, **20**:77-88.

Tengjaroenkul B, Intamat S, Thanomsangad P, Phoonaploy U and Neeratanaphan L. 2018. Cytotoxic effect of sodium arsenite on Nile tilapia (*Oreochromis niloticus*) *in vivo*. *Int J Environ Stu*, **75(4)**:580-591.

Valko M, Rhodes CJ, Moncol J, Izakovic M and Mazur M. 2006. Free radicals, metals and antioxidants in oxidative stress-induced cancer. *Chem Biol Interact*, **160**:1-40.

Vervoort A. 1980. The karyotypes of seven species of tilapia (Teleostei: Cichlidae). *Cytologia*, **45**:651-656.

Waalkes MP. 2003. Cadmium carcinogenesis. *Mutat Res*, **533**:107-120.

Waisberg M, Joseph P, Hale B and Beyersmann D. 2003. Molecular and cellular mechanisms of cadmium carcinogenesis. *Toxicology*, **192**:95-117.

Youn CK, Kim SH, Lee do Y, Song SH, Chang IY, Hyun JW, Chung MH and You HJ. 2005. Cadmium down-regulates human OGG1 through suppression of Sp1 activity. *J Biol Chem*, **280**:25185-25195.

JJBS

Volume 13, Number 2, June 2020
ISSN 1995-6673
Pages 133 - 138

Jordan Journal of Biological Sciences

Effects of *Trigona* honey on the Gene Expression Profile of *Pseudomonas aeruginosa* ATCC 10145 and *Streptococcus pyogenes* ATCC 19615

Mohammad Abdulraheem Al-kafaween[1*], Abu Bakar Mohd Hilmi[1*], Norzawani Jaffar[1], Hamid Ali Nagi Al-Jamal[1], Mohd Khairi Zahri[1], Malik Amonov[2], Bouacha Mabrouka[3] and Nour A.Elsahoryi[4]

[1]Faculty of Health Sciences; [2]Faculty of Medicine, Universiti Sultan Zainal Abidin, Terengganu, Malaysia; [3]Laboratory of Biochemistry and Microbiology, Department of Biochemistry, Faculty of Sciences, University of Badji Mokhtar, 23000 Annaba, Algeria; [4]Department of Nutrition, Faculty of Pharmacy and Medical Sciences, University of Petra, Amman/Jordan

Received May 10, 2019; Revised May 22, 2019; Accepted June 25, 2019

Abstract

Honey is a broad-spectrum antimicrobial agent that seems to affect different bacteria in many different ways. The aim of this study was to evaluate the antibacterial activities of *Trigona* honey against *P. aeruginosa* and *S. pyogenes*. The effect of *Trigona* honey on *P. aeruginosa* and *S. pyogenes* was investigated using growth kinetics curve and real-time PCR. The growth kinetics of *P. aeruginosa* and *S. pyogenes* with 20% (w/v)(MIC) *Trigona* honey inhibited the growth cells number of *P. aeruginosa* and *S. pyogenes* compared with cells grown without honey. Treatment with 10% (w/v) (half-MIC) showed slightly decreased number of cells of *P. aeruginosa* and *S. pyogenes* over a period of 24 hours. Conversely, treatment with 5% (w/v) (quarter-MIC) was observed to have a similar untreated samples of *P. aeruginosa* and *S. pyogenes*. The RT-qPCR results showed that the expression of *Sof* and *Sfbl* decreased 7.82-fold and 9.23-fold respectively after exposure to 20% concentration of *Trigona* honey, whereas the expression of *algD* and *oprF* decreased 6.28-fold and 11.11-fold respectively after exposure to 20% concentration of *Trigona* honey. *Trigona* honey demonstrated the highest antibacterial activity against *P. aeruginosa* and *S. pyogenes in vitro*. Our results indicate that *Trigona* honey has the potential to be an effective inhibitor on virulence genes of *P. aeruginosa* and *S. pyogenes*.

Keywords: Pseudomonas aeruginosa, Streptococcus pyogenes, Trigona honey, Growth kinetics, RT-qPCR.

1. Introduction

Pseudomonas aeruginosa is a pathogen of plants, animals and humans with colonies as diverse as the site of isolation and is able to cause devastating infections because of the strong attachment potential with pili (Lyczak *et al*., 2000; Van Delden and Iglewski, 1998) and production multiple virulence genes such as *oprF* and *algD* (van Delden, 2004; Wendt *et al*., 2017). *oprF* is a general outer membrane porin of *P.aeruginosa* allowing nonspecific diffusion of ionic species and small polar nutrients, including polysaccharides (Nestorovich *et al*., 2006). *oprF* is described as a structural protein, anchoring the outer membrane to the peptidoglycan layer (Rawling *et al*., 1998; Woodruff and Hancock, 1989). The structure and positioning of *oprF* provides structural stability, forming an anchor point between the outer membrane and peptidoglycan layer (Bouffartigues *et al*., 2015; Chevalier *et al*., 2017; Fito-Boncompte *et al*., 2011; Rosay *et al*., 2015; Sugawara *et al*., 2006). The reduced expression of this gene not only could result in the disruption of diffusion, but may also compromise cellular integrity; the latter supports the scanning microscopy data, which showed a loss and disruption of extracellular components and abnormal cell structure observed in previous studies (Henriques *et al*., 2011; Al-Kafaween *et al*., 2019). Currently, *oprF* has been shown to play a role in the growth and biofilm formation (Bouffartigues *et al*., 2015; Chevalier *et al*., 2017; Fito-Boncompte *et al*., 2011; Rosay *et al*., 2015; Sugawara *et al*., 2006) of *P.aeruginosa* (Bjarnsholt *et al*., 2008; James *et al*., 2008; Yoon *et al*., 2002). The mucoid phenotype of *P.aeruginosa* is caused by excessive alginate production and has long been associated with prolonged infection of the pulmonary cavity, particularly in those suffering from cystic fibrosis (Jones *et al*., 2013; McIntyre *et al*., 2010; Wozniak *et al*., 2003). Recent studies (Wood and Ohman, 2012) have shown that alginate genes are under the regulation of sigma factor (s22) and are upregulated as part of an extra cytoplasmic stress response to cell wall stress. Of the many genes regulated, 11 are directly involved in cell envelope homeostasis. The *algD* (GDP-mannose dehydrogenase), which is essential for the production of alginate (*algB*, alg*C*, *algE*, *algR*, *algG* and *algT*) and as a virulence factor (Leid *et al*., 2005; May *et al*., 1991). Additionally, *algD* is

* Corresponding author e-mail: mhilmiab@unisza.edu.my, mohammadalkafaween25@yahoo.com..

a key enzyme of the alginate biosynthetic pathway (Manzo et al., 2011;Jones *et al*., 2013; McIntyre *et al*., 2010; Wozniak *et al*., 2003). *S. pyogenes* produces a wide range of virulence factors, and the cell wall associated M protein is a major virulence factor of *S. pyogenes*, which can bind directly to the extracellular matrix components (e.g. fibrinogen)(Cole *et al*., 2007; Yamaguchi *et al*., 2013). Fibronectin (Fn) is a high-molecular weight glycoprotein that circulates free as a dimer in the soluble form in blood plasma or as a fibrillar form is assembled by cells as major component of the extracellular matrix. So far, fibronectin binding proteins are the best studied adhesions of *S. pyogenes* and currently 11 different such adhesions have been identified (Yamaguchi *et al*., 2013), divided in two types. First type proteins are SfbI, PrtF2, Sof, SfbX, Fbp54, FbaA, and FbaB and they all contain Fn-binding repeats. Second type proteins are M1, Shr, Scl1, and GAPDH and they do not contain these repeats. It is estimated that 60% of initial attachment to cells is realized by streptococcal lipoteichoic acid. Fibronectin binding proteins are the most important in the irreversible stage of adherence. Binding of these adhesions to Fn could result in irreversible attachment to the cell or biofilm production in tissue or bacterial internalization. Expression of Fn-binding proteins is regulated as response to the environmental conditions in which streptococci survive and multiply. Protein F/SfbI, which allows binding to cells of the dermis and Langerhans cells, shows increased expression on bacterial surface with increasing pressure of oxygen. Similarly as in protein F1/SfbI, F2 activity is also response to the environmental oxygen pressure (Jaffe *et al*., 1996). Previous studies showed that the expression of *oprF* and *algD* of *P. aeruginosa* and *Sof* and *Sfbl* of *S. pyogenes* were suppressed after treated with Manuka honey (Maddocks *et al*., 2012; Roberts *et al*., 2012). Honey is a natural product and for many centuries was held in high regard due to its antibacterial properties (Crane, 2001; Rao *et al*., 2016). Such effects have been observed against more than 80 bacterial species, including both Gram-positive and Gram-negative bacteria, and multidrug-resistant pathogens (Cooper *et al*., 2009; Molan, 1992). The inherent antibacterial properties of honey are partly conferred by sugars, which account for 80% of its weight, resulting in a high osmolarity and low water activity (Abu Baker *et al*., 2018; Jibril *et al*., 2019). This study was undertaken to determine the effect of *Trigona* honey on the level of gene expression of *P. aeruginosa* and *S. pyogenes*.

2. Materials And Methods

2.1. Bacterial strains and culture conditions

Pseudomonas aeruginosa ATCC 10145 and *Streptococcus pyogenes* (ATCC 19615) were used throughout the study. One to five colonies of test organism were inoculated into 20 ml nutrient broth (Oxoid, UK) and incubated at 37ºC for 24 hours. After incubation time, the turbidity of the suspension was adjusted to achieve 0.5 McFarland with the absorbance range of 0.08 to 0.1 by using spectrophotometer at wave length of 600 nm (Bouacha *et al*., 2018; Zainol *et al*., 2013).

2.2. Honey Samples

Trigona honey samples were obtained from farm in Kelantan state in East Coast of Peninsula Malaysia. The samples were kept in the dark (Bouacha *et al*., 2018; Garedew *et al*., 2003; Ng *et al*., 2017). The MIC of this *Trigona* honey for the test organisms is 20% (w/v) as described by AL-kafaween *et al*., (2020)

2.3. Growth Kinetics

To determine the effects of *Trigona* honey on the growth of *P. aeruginosa* and *S. pyogenes* cells were grown and treated in 96-well plate with MIC 20% (w/v), half-MIC 10% (w/v) and quarter-MIC 5% (w/v) concentration of honey. Initially, column number 1 was filled 200 µl of final volume of 20%, column number 2 was filled 200 µl of final volume of 10% and column number 3 was filled 200 µl of final volume of 5%. The plate was incubated at 37ºC for 24 hours. At 60 min intervals, the plate was measured at 570nm using a microplate reader (Tecan Infinite 200 PRO, Austria). The experiments were performed in triplicate (Bouacha *et al*., 2018; Maddocks *et al*., 2012; Roberts *et al*., 2012; Zainol *et al*., 2013).

2.4. RNA extraction from P.aeruginosa and S.pyogenes

P. aeruginosa and *S.pyogenes* cells were grown in duplicate in 10 ml of Mueller Hinton broth for 24 hours at 37°C. The total RNA from untreated and treated *P.aeruginosa* and *S.pyogenes* was extracted using the SV Total RNA Isolation System (Promega, UK)(França *et al*., 2011; Goldsworthy, 2008; Maddocks *et al*., 2012; Roberts *et al*., 2012; Wasfi *et al*., 2016; Yadav *et al*., 2012). Total RNA concentrations from untreated and treated of *P.aeruginosa* and *S.pyogenes* were examined by using Implen NanoPhotometer® NP80. RNA purity levels were assessed using the 260/280 absorbance ratio, with only sample ratios between 1.8 and 2.1 being accepted for conversion to cDNA. The experiments were performed in triplicate.

2.5. Conversion of RNA to cDNA

Reverse transcription of RNA was performed with Oligo $(dT)_{15}$ primers and Random Primers. Total RNA samples were converted to cDNA using a high capacity RNA to cDNA conversion kit (Promega, UK). Samples were diluted to 100 ng/µl using ultra pure water. Mastermix 1 was prepared for RNA samples extracted from cells treated and untreated as per the manufacturer's instructions (Promega, UK). For each reaction, 4 µl of (100 ng/µl) RNA, 1 µl of Oligo (dT)15, 2 µl of random primers and nuclease-free water was added to get 10 µl. Mastermix 1 was incubated in PCR thermal cycler at 70°C for 5 minutes to denature the secondary structures of RNA that potentially formed in samples, before was chilled on ice for 5 minutes. While matermix 1 was being incubated, mastermix 2 for each reaction was prepared as following 4 µl 5X Reaction Buffer, 2 µl MgCl2, 1 µl PCR nucleotide mix, 0.5 µl ribonuclease inhibitor, 1 µl reverse transcriptase primers and topped up with nuclease-free water to a final volume of 10 µl. Negative controls were created by substituting total RNA with ultra pure water. The mixture of Mastermix 1 and Mastermix 2 was incubated at 5 minutes at 25ºC, 60 minutes at 42ºC and a final hold at 70ºC for 15 minutes by using a thermal cycler. Following conversion to cDNA, samples were

stored at -20ºC until ready to use (Maddocks et al., 2012; Roberts et al., 2012; Yadav et al., 2012).

2.6. Reverse Transcriptase Quantitative Polymerase Chain Reaction (RT-qPCR)

Primers of *P. aeruginosa* and *S. pyogenes* were retrieved from previous studies as shown in Table 1. Lyophilised and desalted oligonucleotides were reconstituted using sterile ultra-pure water following the manufacturer's instructions. Stock solutions were stored at -20ºC. The RT-qPCR mastermix for each reaction was prepared by following the manufacturer's instructions (Promega, UK), 10µl of qPCR Master Mix, 1µl of forward primer, 1µl of reverse primer, 2µl of cDNA template, 0.2µl CXR Reference dye and topped up with nuclease-free water to 20µl. Wells were closed with strip caps, centrifuged and placed into PCR instrument. The following PCR protocol was used: denaturation at 95°C for 2 minutes one cycle, amplification at 95°C for 15 seconds 40 cycles and a final elongation annealing: at 60 °C for 1 min 40 cycles. The positive control for the reaction was provided by the manufacturer (Promega), and nano-pure water was used to exclude the possibility of contamination. Also, negative control primers were used for both bacteria. Densitometry was performed by using the Applied Biosystems StepOne Software v2.3. The experiments were performed in triplicate to determine the level of relative gene expression in samples, a modified 2-ΔΔ Ct method was used (Livak and Schmittgen, 2001; Maddocks *et al*., 2012; Roberts *et al*., 2012; Schmittgen and Livak, 2008; Wasfi *et al*., 2016; Yadav *et al*., 2012).

Table 1. Primers used for the RT-qPCR analysis of *P.aeruginosa* and *S.pyogenes*

Gene of name	Amplicon Size (bp)	GC content	Annealing temp (C°)	Number of cycles	Direction	Primer sequence (5' → 3')
1. *algD*	144	42.5 % 42.9%	56	41	Forward Reverse	CGCCGAGATGATCAAGTACA AGGTTGAGCTTGTGGTCCTG
2. *oprF*	101	41.2% 42%	54	41	Forward Reverse	CTGGACGCCATCTACCACTT CTGTCGCTGTTGATGTTGGT
3. *rpoD**	146	42.3% 42.6%	53	41	Forward Reverse	GCGACGGTATTCGAACTTGT CGAAGAAGGAAATGGTCGAG
4. *Sof*	873	36.4 % 42.9 %	57	41	Forward Reverse	ACTTAGAAAGTTATCTGTAGGG TCTCTCGAGCTTTATGGATAG
5. *SfbI*	960	42.9 % 52.6 %	55	41	Forward Reverse	AACTGCTTTAGGAACAGCTTC CCACCATAGCCACAATGCT
6. *glr**	797	42.9 % 47.6 %	54	41	Forward Reverse	ATGGATACAAGACCAATTGG TCATAAGGTGACATGCTCCAC

**rpoD* was used as a reference gene for *P.aeruginosa* and **glr* was used as a reference gene for *S.pyogenes*

2.7. Statistical Analysis

Data was expressed as mean ± standard error of means, one way analysis of variance and graphing was performed using SPSS program, version 20.For each data set, three replicates were performed.

3. Results

3.1. Growth kinetic curves

As shown in Figure 1 and 2, results showed *P.aeruginosa* and *S.pyogenes* could not be recovered after 24 h incubation with MIC (20% (w/v) and prevented the growth of *P.aeruginosa* and *S.pyogenes*. *P. aeruginosa* and *S.pyogenes* treated with half-MIC (10% w/v) have resulted a decreased optical density and decreased lag phase and exponential phase compared to untreated sample. Conversely, *P.aeruginosa* and *S.pyogenes* treated with quarter-MIC concentrations (5 %, w/v) had no inhibition in growth compared with untreated cells. The data obtained from growth kinetics supporting the MIC of *Trigona* honey as mentioned in previous study by Al-kafaween et al., (2020)

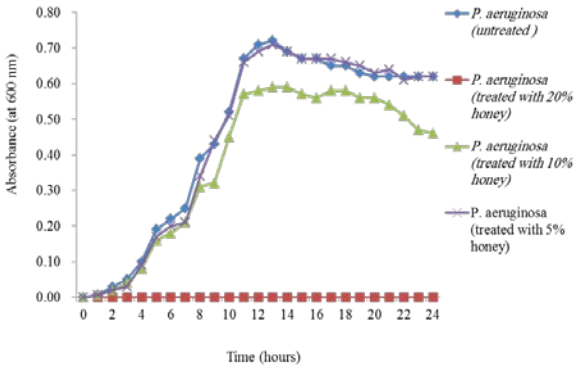

Figure 1. Growth curves of *P.aeruginosa* cells grown with and without *Trigona* honey.

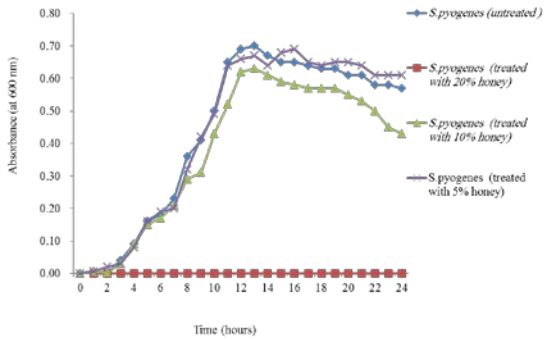

Figure 2. Growth kinetics curve of *S.pyogenes* cells grown with and without *Trigona* honey.

3.2. RT-qPCR of genes expression of P.aeruginosa and S.pyogenes

Two genes *oprF* and *algD* of *P.aeruginosa* and two genes *Sof* and *Sfbl* of *S.pyogenes* showed a statistically significant reduction in gene expression after being treated with 20% (w/v) of *Trigona* honey. As shown in Table 2 and Figure 3, results showed all genes were downregulated and different degrees of downregulation were observed. The RT-qPCR results demonstrated that the expressions of *oprF* and *algD* genes of *P. aeruginosa* were decreased 11.11-fold and 6.28-fold respectively after treated with 20% (MIC) *Trigona* honey. Whereas *Sof* and *Sfbl* of *S. pyogenes* were decreased 7.82-fold and 9.23-fold respectively after treated with 20% (MIC) *Trigona* honey.

Table 2. Effect of *Trigona* honey on the expression of *P.aeruginosa* and *S.pyogenes* detected by RT-qPCR (Schmittgen & Livak, 2008).

Gene name	Average ΔΔCt	Expression Fold Change (2^-ΔΔCt)	Expression Fold Change	*P*-value	SD
1. *oprF*	3.47	0.09	-11.11	0.04*	1.0
2. *algD*	2.65	0.16	-6.28	0.04*	1.5
3. *Sof*	2.97	0.13	-7.82	0.03*	1.3
4. *Sfbl*	3.21	0.11	-9.23	0.03*	1.5

If the delta-delta Ct has a negative value, the gene of interest is upregulated, because the fold change will be larger than 1. On the other hand, if the delta-delta Ct has a positive value, the gene is down regulated and the fold change is <1. *Statistically significant change in the level expression (P<0.05).

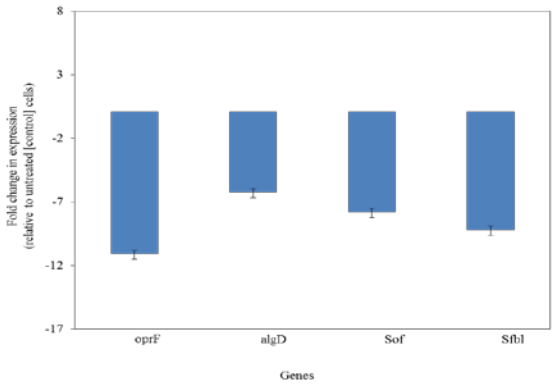

Figure 3. Alterations in gene expression profiles associated with exposure of *P.aeruginosa* and *S.pyogenes* to *Trigona* honey as determined by RT-qPCR. Mean values of fold changes (±SD) are shown in relation to untreated (control).Error bars denote standard error of the mean from three biological samples.

4. Discussion

This study describes the first systematic analysis of the effect of *Trigona* honey on level of gene expression of *P.aeruginosa* and *S. pyogenes*. Total viable cell decreased after exposure to 20% (w/v) and 10% (w/v) of *Trigona* honey. Studies by (Zainol et al., 2013) reported that *Trigona* honey inhibited growth of *P.aeruginosa* at 20% concentration of honey. Studies by (Maddocks et al., 2012; Roberts et al., 2012) showed that the number of cells of *S.pyogenes* were decreased after treated with 20% concentration of Manuka honey. Previous studies showed that the growth kinetics of *P.aeruginosa* and *S.epidermidis* was gradually declined after exposure to 40% (w/v) concentration of Indian honey (Chakraborti *et al*., 2014). Recently, honey has been documented to reduce growth rate of Gram-positive and Gram-negative bacteria (Nassar *et al*., 2011). RT-qPCR was used to determine the level of gene expression of *P.aeruginosa* and *S.pyogenes* after treated with Trigona honey. Reduced expression was noticeable with a different level of expression in both bacteria. The expression of *Sof* and *SfbI* of *S.pyogenes* decreased 7.82-fold and 9.23-fold respectively after treated with 20% (MIC) of *Trigona* honey. Whereas *oprF* and *algD* of *P.aeruginosa* decreased 11.11-fold and 6.28-fold respectively after treated with 20% (MIC) of *Trigona* honey. In previous study *oprF* has been shown to play a role in the anaerobic growth of *P.aeruginosa*(Yoon *et al*., 2002) and subsequent biofilm formation, concurrent with chronic wound infection (Bjarnsholt *et al*., 2008; James *et al*., 2008). The observed reduction of *oprF* in *P.aeruginosa* following treatment with *Trigona* honey may therefore, in part, account for the observed ability of honey-treated *P.aeruginosa* to form microcolonies. GDP-mannose dehydrogenase is essential for the production of *algD* (Leid *et al*., 2005; May *et al*., 1991). It is, therefore, possible that the observed decrease in *algD* and oprF causes instability of the cell envelope, making *P.aeruginosa* susceptible to the osmotic action of *Trigona* honey, which results in the decreased expression of *algD* as the extra cytoplasmic stress response system is activated. Sfbl is regarded as one of the major adhesions of *S.pyogenes* (Medina *et al*., 2000) and Sof is regarded as a major virulence factor that is known to contribute to pathogenesis of streptococcal infection in animal models (Courtney and Pownall, 2010). The *Sof* gene was first sequenced over 15 years ago (Rakonjac *et al*., 1995) and its product was found to be a surface bound protein of over 100 kDa, with a C-terminal domain comprised of numerous repeating peptides that bound to both fibronectin and fibrinogen (Courtney *et al*., 2003; Courtney and Pownall, 2010). It is a possibility that the reduction in fibronectin binding was a combination of reduced expression and specific physical disruption of binding or stearic hindrance by components of the *Trigona* honey.

A study by (Roberts *et al*., 2012) showed that *algD* of *P.aeruginosa* increased 16-fold in the expression whereas *oprF* decreased 10-fold after treated with 12% (MIC) of Manuka honey. A previous study showed that the *Sof* and *Sfbl* proteins decreased in the expression of *S. pyogenes* after treated with 20% (MIC) of Manuka honey (Maddocks *et al*., 2012). A study by (Roberts *et al*., 2014) showed that six genes (*fliA, fliC, flhF, fleN, fleQ* and *fleR*) of *P. aeruginosa* were reduced in gene expression after exposure to 24% (MIC) of Manuka honey. A previous study showed that *tnaA* and *yjfO* (*bsmA*) genes were down-regulated in expression of *E.coli* in the range of 12.5–16.2-fold after treated with 25% (MIC) of Egyptian honey (Wasfi *et al*., 2016). A study by (Wasfi *et al*., 2016) reported that *ycfR* (*BhsA*) and *evgA* genes of *E.coli* were upregulated in expression in the range of 2.2–4.19-fold and 1.09-fold respectively after treated with 25% (MIC) of Egyptian honey. Honey is a complex substance estimated to be comprised of between 200 and 600 components,

including fructose (~38.2 %), glucose (~31.3 %), sucrose (1 %) and 'other sugars' (9 %) (Bogdanov et al., 2008). Additional minor constituents include acids (0.57 %), proteins (0.266 %), amino acids (0.1 %), nitrogen (0.41 %), minerals (0.17 %) The antibacterial action of Trigona honey is attributed to its high osmolarity, low water activity, viscosity, low PH and the presence of hydrogen peroxide; it is the combination of these factors that is thought to provide an unsuitable environment for bacterial growth (Cooper, 2008; Adams et al., 2009). It is evident that Trigona honey is effective at inhibiting the growth of *P. aeruginosa* and *S. pyogenes*, causing abnormal cell by reducing structural integrity to the point of cell lysis as mentioned in previous study by (Al-kafaween et al., 2019). The data presented here supports previous findings and describes the effects of *Trigona* honey on *P. aeruginosa* and *S. pyogenes* at a genetic level. These effects may be compounded by the high osmolarity of *Trigona* honey. Whether these are the only targets remains to be determined, and the global effect of *Trigona* honey on *P. aeruginosa* and *S. pyogenes* will be the subject of future research.

5. Conclusion

This is the first comprehensive study of the level of gene expression of *P. aeruginosa* and *S. pyogenes* after exposure to Malaysian *Trigona* honey. Taken together, our results revealed that the tested Trigona honey has the potential to be effective inhibitors of *S.pyogenes*. Differential gene expression in response to honey exposure exhibited down-regulation of two genes involved in microcolonies and biofilm formation in *P. aeruginosa* and *S. pyogenes.* The obtained results indicate that the honey under study may represent promising antibacterial, antibiofilm and anti-virulence agents for treatment and modulation of infections caused by *P.aeruginosa* and *S.pyogenes*. Future clinical evidence pertaining to the efficacy of the tested *Trigona* honey in the prevention and treatment of *P. aeruginosa* and *S. pyogenes* induced infections at various tissue/cell types might be required.

Acknowledgments

This work was supported by grant: UniSZA/2017/DPU/37 R0018-R341. We thank all the staff members of the Faculty of Health Sciences and Microbiology Laboratory, Universiti Sultan Zainal Abidin for their support and commitment.

References

Al-kafaween MA, Hilmi ABM, Jaffar N, Al-Jamal HAN, Zahri MK, Jibril FI. 2020. Antibacterial and Antibiofilm activities of Malaysian Trigona honey against Pseudomonas aeruginosa ATCC 10145 and Streptococcus pyogenes ATCC 19615. *Jordan Journal of Biological Sciences.*, **13(1)**:69 –76.

Abu Baker, M H, Jibril, FI, Manivannan,L. 2018.Physicochemical Characteristics of Malaysian Stingless Bee Honey from Trigona Species. *International Medical Journal Malaysia,* **17(1)**:187-191.

Bjarnsholt T, Kirketerp-Møller K, Jensen PØ, Madsen KG, Phipps R, Krogfelt K, Høiby N, Givskov M. 2008. Why chronic wounds will not heal: a novel hypothesis. *Wound repair and regeneration.,* **16(1)**: 2-10.

Bouacha M, Ayed H., Grara N. 2018. Honey Bee as Alternative Medicine to Treat Eleven Multidrug-Resistant Bacteria Causing Urinary Tract Infection during Pregnancy. *Scientia pharmaceutica.,* **86(2)**: 14.

Bouffartigues E, Moscoso J A, Duchesne R, Rosay T, Fito-Boncompte L, Gicquel G, Lesouhaitier O. 2015. The absence of the Pseudomonas aeruginosa OprF protein leads to increased biofilm formation through variation in c-di-GMP level. *Frontiers in microbiology.,* **6**: 630.

Chakraborti T, Barman S, Mandal NC, Bhattacharya K. 2014. Evaluation of antibacterial potential of some Indian honey samples against throat and skin infective pathogens. *Int. J. Curr. Microbiol. App Sci.,* **3**: 362-369.

Cooper R, Molan P, White R. 2009. *Honey in modern wound management*: Wounds UK., **7(1)**:101.

Courtney HS, Pownall HJ.. 2010. The structure and function of serum opacity factor: a unique streptococcal virulence determinant that targets high-density lipoproteins. *BioMed Research International.,* 56-71

Fito-Boncompte L, Chapalain A, Bouffartigues E, Chaker H, Lesouhaitier O, Gicquel G, Bazire A, Madi A, Connil N, Véron W, Taupin L. 2011. Full virulence of Pseudomonas aeruginosa requires OprF. *Infection and immunity.,* **79(3)**: 1176-1186.

Garedew A, Schmolz E, Lamprecht I. 2003. The antimicrobial activity of honey of the stingless bee Trigona spp. *Journal of Apicultural Science.,* **47(1)**: 37-40.

Goldsworthy MJH. 2008. Gene expression of Pseudomonas aeruginosa and MRSA within a catheter-associated urinary tract infection biofilm model. *Bioscience Horizons.,* **1(1)**: 28-37.

Henriques AF, Jenkins RE, Burton NF, Cooper RA. 2011. The effect of manuka honey on the structure of Pseudomonas aeruginosa. *European journal of clinical microbiology & infectious diseases.,* **30**: 167-171.

Jaffar N, Miyazaki T, Maeda T. 2016. Biofilm formation of periodontal pathogens on hydroxyapatite surfaces: Implications for periodontium damage. *Journal of Biomedical Materials Research Part A.,* **104**: 2873-2880.

Jaffe J, Natanson S, Caparon MG, Hanski E. 1996. Protein F2, a novel fibronectin-binding protein from Streptococcus pyogenes, possesses two binding domains. *Molecular microbiology.,* **21**: 373-384.

James GA, Swogger E, Wolcott R, Pulcini, ED, Secor P, Sestrich J, Costerton JW, Stewart PS. 2008. Biofilms in chronic wounds. *Wound Repair and regeneration.,* **16(1)**: 37-44.

Jibril FI, Hilmi AB, Manivannan L. 2019. Isolation and characterization of polyphenols in natural honey for the treatment of human diseases. *Bulletin of the National Research Centre.,* **43(1)**:4.

Jones CJ, Ryder CR, Mann EE, Wozniak DJ. 2013. AmrZ modulates Pseudomonas aeruginosa biofilm architecture by directly repressing transcription of the psl operon. *Journal of bacteriology,* **195**:1637-1644.

Leid JG, Willson CJ, Shirtliff ME, Hassett DJ, Parsek MR, Jeffers AK. 2005. The exopolysaccharide alginate protects Pseudomonas aeruginosa biofilm bacteria from IFN-γ-mediated macrophage killing. *The Journal of Immunology.,* **175**: 7512-7518.

Livak KJ and Schmittgen TD.. 2001. Analysis of relative gene expression data using real-time quantitative PCR and the $2^{-\Delta\Delta CT}$ method. *methods.,* **25**: 402-408.

Lyczak JB, Cannon CL, Pier GB. 2000. Establishment of Pseudomonas aeruginosa infection: lessons from a versatile opportunist1. *Microbes and infection.,* **2**: 1051-1060.

Maddocks SE and Jenkins RE. 2013. Honey: a sweet solution to the growing problem of antimicrobial resistance. *Future microbiology.,* **8**: 1419-1429.

Maddocks SE, Lopez MS, Rowlands RS, Cooper RA. 2012. Manuka honey inhibits the development of Streptococcus pyogenes biofilms and causes reduced expression of two fibronectin binding proteins. *Microbiology.,* **158**: 781-790.

Maddocks SE, Wright CJ, Nobbs AH, Brittan JL, Franklin L, Strömberg N, Kadioglu A, Jepson MA, Jenkinson HF. 2011. Streptococcus pyogenes antigen I/II-family polypeptide AspA shows differential ligand-binding properties and mediates biofilm formation. *Molecular microbiology.,* **81**: 1034-1049.

May TB, Shinabarger D, Maharaj RO, Kato J, Chu L, DeVault JD, Roychoudhury SI, Zielinski NA, Berry A, Rothmel RK. 1991. Alginate synthesis by Pseudomonas aeruginosa: a key pathogenic factor in chronic pulmonary infections of cystic fibrosis patients. *Clinical microbiology reviews.,* **4(2)**: 191-206.

McIntyre-Smith A, Schneiderman J, Zhou K. 2010. Alginate does not appear to be essential for biofilm production by PAO1 Pseudomonas aeruginosa. *J. Exp. Microbiol. Immunol.,* **14**: 63-68.

Medina E, Schulze K, Chhatwal GS, Guzmán CA. 2000. Nonimmune Interaction of the SfbI Protein of Streptococcus pyogenes with the Immunoglobulin GF (ab′) 2Fragment. *Infection and immunity.,* **68**: 4786-4788.

Molan, PC. 1992. The antibacterial activity of honey: 1. The nature of the antibacterial activity. *Bee world.,***73(1)**: 5-28.

Nassar HM, Li M, Gregory RL. 2011. Effect of honey on Streptococcus mutans growth and biofilm formation. *Applied and environmental microbiology,* AEM., **78(2)**:36-40..

Nestorovich EM, Sugawara E, Nikaido H, Bezrukov SM. 2006. Pseudomonas aeruginosa porin OprF properties of the channel. *Journal of Biological Chemistry.,* **16(24)**:230-237.

Ng WJ, Chan YJ, Lau ZK, Lye PY, Ee KY. 2017. Antioxidant properties and inhibitory effects of trigona honey against Staphylococcus aureus planktonic and biofilm cultures. *International Journal.,* **12(37)**: 28-33.

Rakonjac JV, Robbins JC, Fischetti VA. 1995. DNA sequence of the serum opacity factor of group A streptococci: identification of a fibronectin-binding repeat domain. *Infection and immunity.,* **63(2)**: 622-631.

Rao PV, Krishnan KT, Salleh N, Gan SH. 2016. Biological and therapeutic effects of honey produced by honey bees and stingless bees: a comparative review. *Revista Brasileira deFarmacognosia.,* **26(5)**: 657-664.

Rawling EG, Brinkman FS, Hancock RE. 1998. Roles of the carboxy-terminal half of Pseudomonas aeruginosa major outer membrane protein OprF in cell shape, growth in low-osmolarity medium, and peptidoglycan association. *Journal of bacteriology.,* **180(14)**:56-62.

Roberts AE, Maddocks SE, Cooper RA. 2012. Manuka honey is bactericidal against Pseudomonas aeruginosa and results in differential expression of oprF and algD. *Microbiology.,* **158(12)**:5-13

Roberts AE, Maddocks SE, Cooper RA. 2014. Manuka honey reduces the motility of Pseudomonas aeruginosa by suppression of flagella-associated genes. *Journal of Antimicrobial Chemotherapy.,* **70(3)**:716-725.

Rosay T, Bazire A, Diaz S, Clamens T, Blier AS, Mijouin L, Hoffmann B, Sergent JA, Bouffartigues E, Boireau W, Vieillard J. 2015. Pseudomonas aeruginosa expresses a functional human natriuretic peptide receptor ortholog: involvement in biofilm formation. *MBio.,* **6(4)**:3-15.

Schmittgen TD, Livak KJ. 2008. Analyzing real-time PCR data by the comparative C T method. *Nature protocols.*,3(6): 1101.

Sugawara E, Nestorovich EM, Bezrukov SM, Nikaido H. 2006. Pseudomonas aeruginosa porin OprF exists in two different conformations. *Journal of Biological Chemistry.,* **281(24)**: 16220-16229.

Van Delden C. 2004. Virulence factors in Pseudomonas aeruginosa. *Virulence and Gene Regulation*., 3-45

Van Delden C and Iglewski BH. 1998. Cell-to-cell signaling and Pseudomonas aeruginosa infections. *Emerging infectious diseases.,* **4(4)**: 551.

Wasfi R, Elkhatib WF, Khairalla AS. 2016. Effects of selected Egyptian honeys on the cellular ultrastructure and the gene expression profile of Escherichia coli. *PloS one.,* **11(3)**: 0150984.

Wendt M, De Silva BC, Heo GJ. 2017. Research Article Virulence Factors and Antimicrobial Resistance of Pseudomonas aeruginosa Isolated from Pet Turtles. *Asian J Anim Vet Adv*., **12(4)**:5-11

Wood LF and Ohman DE. 2012. Identification of genes in the σ22 regulon of Pseudomonas aeruginosa required for cell envelope homeostasis in either the planktonic or the sessile mode of growth. *MBio*., **3(3)**:4-12.

Woodruff WA and Hancock RE. 1989. Pseudomonas aeruginosa outer membrane protein F: structural role and relationship to the Escherichia coli OmpA protein. *Journal of Bacteriology*., **171(6)**:4-9.

Wozniak DJ, Wyckoff TJ, Starkey M, Keyser R, Azadi P, O'Toole GA, Parsek MR. 2003. Alginate is not a significant component of the extracellular polysaccharide matrix of PA14 and PAO1 Pseudomonas aeruginosa biofilms. *Proceedings of the National Academy of Sciences.,* **100(13)**:7-12

Yadav MK, Kwon SK, Cho CG, Park SW, Chae SW, Song JJ. 2012. Gene expression profile of early in vitro biofilms of Streptococcus pneumoniae. *Microbiology and immunology.,* **56(9)**: 621-629.

Yamaguchi M, Terao Y, Kawabata S. 2013. Pleiotropic virulence factor–S treptococcus pyogenes fibronectin-binding proteins. *Cellular microbiology.,* **15(4)**: 503-511.

Yoon SS, Hennigan RF, Hilliard GM, Ochsner UA, Parvatiyar K, Kamani MC, Allen HL, DeKievit TR, Gardner PR, Schwab U, Rowe JJ. 2002. Pseudomonas aeruginosa anaerobic respiration in biofilms: relationships to cystic fibrosis pathogenesis. *Developmental cell.,* **3(4)**:593-603.

Zainol MI, Yusoff KM, Yusof MY. 2013. Antibacterial activity of selected Malaysian honey. *BMC Complementary and Alternative Medicine.,* **13(1)**: 129.

JJBS
Jordan Journal of Biological Sciences

Volume 13, Number 2, June 2020
ISSN 1995-6673
Pages 139 - 144

Molecular Divergence of *Staphylococcus aureus* Isolated from Dogs and Cats

Mona A. Elshabrawy*, Hussien A. Abouelhag, Eman A. Khairy , Hanan Sh. Marie and Ashraf S. Hakim

Microbiology and Immunology, National Research Centre, 33 Bohouth st., Dokki, Cairo, Postal code 12622, Egypt

Received May 8, 2019; Revised June 19, 2019; Accepted June 30, 2019

Abstract

Coagulase positive staphylococci particularly *Staphylococcus aureus* are responsible for a variety of illnesses in humans and animals and commonly identified and discriminated by certain virulence factor coagulase (*coa*) genes. A total of 85 nasal discharge and wound samples were collected from 55 dogs and 30 cats. The samples were cultured and examined for detection of *Staphylococcus aureus* and then checked using PCR for the presence of *nuc* and *coa* virulence genes. The positive *coa* bands were subjected to restriction fragment length polymorphism analysis (RFLP) using *AluI* enzyme and sequenced. The results confirmed 10 isolates as *Staphylococcus aureus.* All ten isolates harbored *nuc* and *coa* genes. The RFLP analysis demonstrated five different patterns, and the genetic lineage of recovered isolates was related to a human origin strain sharing 75% homology. This alerts for the potential public health hazard of companion pets.

Keywords: *Staphylococcus aureus*- pets- *coa* gene– *nuc* gene– RFLP

1. Introduction

Staphylococcus aureus could be addressed as an opportunistic pathogen for both humans and animals which is part of the normal microbiota and acts as a pathogen in particular circumstances. Although the bacteria are detected in clinically healthy bodies, they can induce a wide range of infections when the immune system becomes compromised or select conditions are associated (Bierowiec *et al*., 2016). The microbiota on an organism depends on the species, feed, and environment and population density. However, *S. aureus* is the most frequently recovered coagulase positive *Staphylococcus* from the anterior nares and temporarily from the skin of humans (Otto, 2010). Similarly, for dogs and cats; *S. aureus* is also noticed as the major species in this tissue and mucosa's natural microbiota. Investigation of the nasal carriage is used in epidemiology, as an indicator of *S. aureus* exposure with rising risk of infection in humans; among others skin diseases, wound colonization or respiratory tract infections. Also, in pet animals, colonization of the nares with *S. aureus* is commonly used to estimate human exposition to livestock or pet related *S. aureus.* The circulation of *S. aureus* clones varies among hosts, environments and countries (Bierowiec *et al*., 2016).

For a long time, *S. aureus* has been associated with skin, soft tissue infections and foreign body infections. One of the essential virulence figures of *S. aureus* is the unique ability to induce clotting. *S. aureus* secretes two coagulases, an extracellular staphylocoagulase and a cell wall associated von Willebrand factor binding protein that both activate prothrombin to generate fibrin (Peetermans *et al*., 2015). It is clear that coagulase subtyping is useful in *S. aureus* strains discrimination, phylogeny and source tracking through many molecular based techniques. PCR-restriction fragment length polymorphism (RFLP) typing of the coagulase gene (*coa*) can be used to discriminate *S. aureus* strains on the basis of sequence variation within the 3' end coding region of the gene (Ishino *et al*., 2007).

Another virulence factor present in *S. aureus* is the ability of the pathogen to produce nuclease enzyme, which plays an important role in immune evasion by *S. aureus*. It degrades neutrophil extracellular traps, facilitating bacteria to avoid killing and eliminate macrophages from abscesses. Moreover, this enzyme is essential for biofilm, where it is thought to facilitate detachment and dispersal of the biofilm, allowing the bacteria to spread to additional sites (Richard *et al*., 2017).

The companion animals (including cats, dogs) are geographically wide spread and generally not associated with occupational activities. To know the *Staphylococcus* divergence in companion animals is a continuing issue to understand the human – "pets' infection cycle" (Haenni *et al*., 2017).

As these pet species are in frequent and close contact with humans, the epidemiology of *S. aureus* is of public health importance. A better grasp of the molecular mechanisms of *S. aureus* virulence should be a target of promising objective for novel diagnostic and therapeutic strategies. Consequently, this study aimed to the virulence and divergence characterization of *S. aureus* isolated from clinically ill dogs and cats.

* Corresponding author e-mail: migris410@yahoo.com.

2. Materials and methods

2.1. Sampling and isolation of Staphylococci coagulase positive

A total of 85; 25 nasal and 60 wound swabs were collected from clinically ill dogs (55) and cats (30) in Cairo pet clinics during October 2017- March 2018. The samples were transferred to the microbiology laboratory in National Research Centre, Giza in chilled, insulated containers under aseptic condition. The swabs were incubated in nutrient broth at 37°C for 24 h. Then the samples were subcultured on manitol salt agar (Difco) and incubated at 37°C for 24-48 h, and presumptive coagulase-positive *staphylococci* produce colonies surrounded by bright yellow zones. The presumptive colonies were identified by Gram stain, catalase, coagulase (both the slide and tube) and DNase tests. The isolates were subjected to further testing using API STAPH IDENT 32 Staph (Biomerieux, Marcy l'Etoile, France) (Soriano *et al*., 2000).

2.2. Antimicrobial Susceptibility Testing

Staphylococcus aureus were tested for antimicrobial susceptibility by disc diffusion method in Muller-Hinton agar (Difco) according to CLSI (2015). The following antibiotic discs (Sigma) were used; amoxicillin/clavulinic acid (20/10µg), bacitracin (10µg), gentamycin (10µg), vancomycin (3µg), neomycin (30µg) and polymyxin (10µg).

Susceptibility categorization was carried out according to performance standards for antimicrobial disk susceptibility tests (CLSI 2018).

2.3. Genomic DNA extraction and PCR assay

2.3.1. DNA extraction

The standard *S. aureus* strain (ATCC 25923) was obtained from the reference laboratory of the Cairo Microbiological Resources Center (Cairo MIRCEN), Faculty of Agriculture, Ain-Shams University.

DNA was extracted from *S. aureus* isolates and the standard strain using the QIAamp DNA Mini kit (Qiagen, Germany, GmbH) with modifications from the manufacturer's recommendations. Briefly, 200 µl of the sample suspension was incubated with 10 µl of proteinase K and 200 µl of lysis buffer at 56°C for 10 min. After incubation, 200 µl of 100% ethanol was added to the lysate. The sample was then washed and centrifuged following the manufacturer's recommendations. Nucleic acid was eluted with 100 µl of elution buffer provided in the kit.

2.3.2. PCR detection of nuc gene and coa gene

For either *nuc* or *coa* uniplex PCRs were carried out in a 25 µl reaction containing 12.5 µl of EmeraldAmp Max PCR Master Mix (Takara, Japan), 1 µl of each primer of 20 pmol concentration, 4.5 µl of water, and 6 µl of DNA template. The *coa* gene was amplified using two sequences of primers: 5′-CGAGACCAAGATTCAACAAG-3′ and 5′-AAAGAAAACCACTCACATCA-3′. For the amplification of *nuc* gene were used the following primers: R: 5′ GTTTTTGGCTGCTTCTCTTG-3′ and F: 5′-ATATGTATGGCAATCGTTTCAAT-3′. The primers used were supplied from Metabion (Germany). Amplification was conducted in thermal cycler (Biometra, Germany), which was adjusted for *coa* gene amplification as follows (Aslantaş *et al*., 2007): an initial denaturation at 94˚C for 3 min, 30 cycles of denaturation at 94˚C for 1 min, annealing at 55˚C for 1 min, and extension at 72˚C for 1 min and a final extension at 72˚C for 5 min. For amplification of *nuc* gene the program consisted of an initial denaturation at 94˚C for 4 min, 30 cycles of denaturation at 94˚C for 30 sec, annealing at 50˚C for 30 sec, and extension at 72˚C for 1 min and a final extension at 72˚C for 4 min (Gao *et al*., 2011). The amplification of *coa* and *nuc* genes generated amplicons of 970 bp and 270 bp respectively.

The PCR reaction mixtures were analyzed by electrophoresis on a 1.5% (w/v) agarose gel in the presence of 100- bp DNA ladder (Fermentas Life Science, EU) according to (Sambrook *et al*., 1989).

2.4. Coagulase gene typing by RFLP method

S. aureus strains positive for *coa* gene were subjected to restriction fragment length polymorphism. PCR amplified *coa* gene products were digested with *AluI* enzyme (Aslantaş *et al*., 2007). Restriction master mix was prepared according to Promega instruction kit, accurate fragment size analysis based on the electrophoretic mobility and was determined by using DNA size TOTALAB 1D analysis software. For sequencing of PCRs' products each amplicon was purified using the ExoSAP-IT PCR Product Cleanup kit (Affymetrix, USA) according to the manufacturer's instructions. Sequencing reactions were performed with the ABI PRISM®BigDyedye™ terminator cycle sequencing kit with AmpliTaq® DNA polymerase on an MJ Research PTC-225 Peltier Thermal Cycler (Applied Biosystems, USA) as described by the manufacturer. Each sequencing reaction was repeated at least 3 times in both directions before being accepted for analysis. Then sequences of each PCR product were aligned with homologous GenBank records (http://www.ncb i.nlm.nih.gov) by multiple sequence alignment using the Clustal®W program46.

3. Results

The conventional cultural, staining methods showed an isolation of a total number of 18 *staphylococci* (table 1). Fourteen (23.3%) were isolated from wound swabs (8 from dog samples and 6 from cats) and the rest 4 (16%) were isolated from nasal swabs (3 from dogs while the last one from cat source).

Table 1. Number of *Staphylococci* isolated from dog and cat samples.

Isolation origin	No. of *Staphylococci* isolates / wound swabs	%	No. of *Staphylococci* isolates / nasal swabs	%	Total No. of isolates / total No. of swabs	%
Dog	8 / 35	22.8	3 / 20	15	11/ 55	20
Cat	6 / 25	20.8	1/ 5	16.6	7 / 30	22.2
Total	14 / 60	23.3	4 / 25	16	18 / 85	21.2

Considering the coagulase production species specific API identification, 10 isolates were confirmed as *S. aureus* (table 2). Seven were from dog samples (5 from wounds and 2 from nasal swabs) while the other three of feline source (2 from wounds and the last one from nasal swabs).

Table 2. Number of confirmed *S. aureus* isolates.

No. of confirmed *S. aureus* isolates	wound swabs	nasal swabs	Total
Dog	5	2	7
Cat	2	1	3
Total	7	3	10

The susceptibility of the isolates to six antibiotics was achieved using the disc diffusion method. According to this technique *S. aureus* isolates were resistant to bacitracin, gentamycin and neomycin 100% and more sensitive to amoxicillin/clavulinic acid and vancomycin 94, and 88% respectively.

All *S. aureus* isolates showed positive *nuc* gene amplification using specific primer and produced amplicons of average molecular size 270 bp (figure 1). In the same way, all *S. aureus* isolates showed positive *coa* gene amplification and produced the amplicons of 970 bp (figure 2).

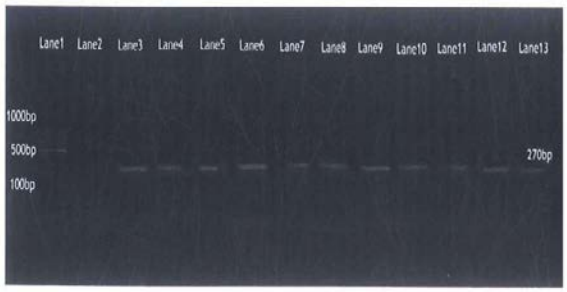

Figure 1: Amplified PCR product of *nuc* gene Lane 1: 100bp ladder. Lane 2: negative control. Lane 3: positive control. Lanes 4-13: represented *S. aureus* isolates, the *nuc* gene PCR products of 10 confirmed *S. aureus* produced same sized fragments 270 bp.

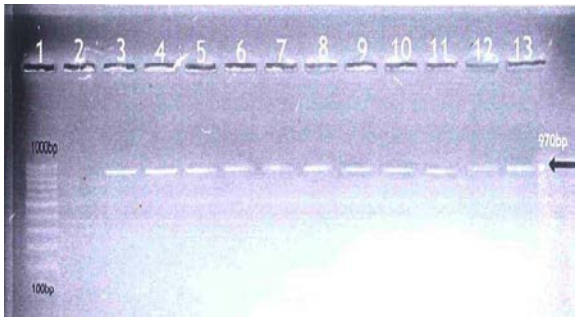

Figure 2: Amplified PCR product of *coa* gene Lane 1: 100bp ladder. Lane 2: negative control. Lane 3: positive control. Lanes 4-13: represented *S. aureus* isolates, the *coa* gene PCR products of 10 confirmed *S. aureus* produced same sized fragments 970 bp.

The *coa* gene PCR products (970 bp) were exposed to restriction digestion using RFLP with *AluI* enzyme. The fragment size was accurately analyzed by using DNA size TOTALAB 1D analysis software. According to figures 3 and 4, and table 3, a total of 5 different electrophoretic patterns of the confirmed 10 isolates were obtained (I, II, III, IV and V), with predomination of pattern III in 3 dog wound samples, and the patterns tend to be specific.

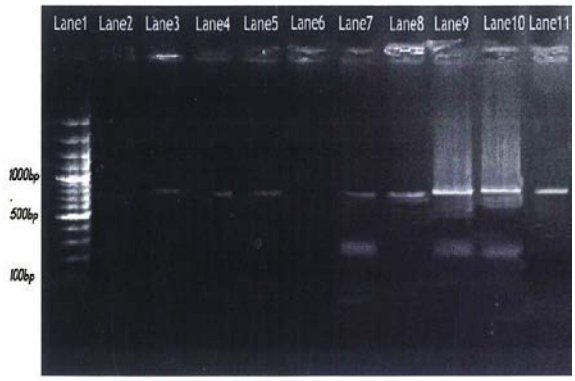

Figure 3. Restricted fragments of *coa* gene by *AluI* enzyme; Lane 1: 100bp ladder. Lanes2,3: represented dog nasal samples isolates. Lanes (4-8) represented dog wound samples isolates, Lanes (9,10) represented cat wound samples isolates. Lane 11represented cat nasal sample isolate. The results of *coa* gene typing of *S. aureus* isolates by RFLP were mentioned in the table (4).

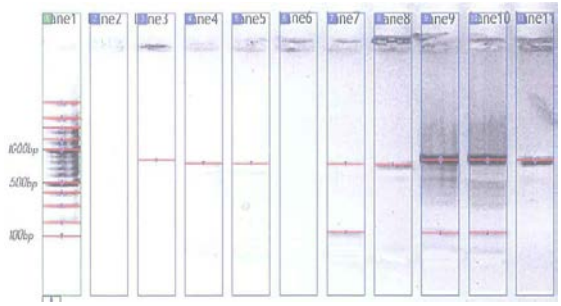

Figure 4: ID software analysis of *coa* gene restriction products.

Table 3. Restricted fragment size of *coa* gene, genotypes and sample sources.

Sample no	Source	Restricted fragments (bp)	Genotype
1(lane 2)	Dog nasal	-	I
2 (lane 3)	Dog nasal	825	II
3 (lane 4)	Dog wound	795	III
4 (lane 5)	Dog wound	795	III
5 (lane 6)	Dog wound	-	I
6 (lane 7)	Dog wound	105, 795	IV
7 (lane 8)	Dog wound	795	III
8 (lane 9)	Cat wound	105, 825	V
9 (lane 10)	Cat wound	105, 825	V
10 (lane 11)	Cat nasal	825	II

Sequences of the amplified *coa* gene exhibited a (99-100%) consistency when matched with those obtainable in GenBank using gapped BLASTN software. Identification to the species and subspecies levels was considered for segments with sequences identities >97%. BLASTN analysis of the ranged sequences of the isolates showed 96-99% identity with the similar genes sequence of *S. aureus* subsp. *aureus* strain M013 (accession No. CP003166).

4. Discussion

Staphylococcus genus includes up to 58 valid species, and subspecies, as two species *S. argenteus* and *S. schweitzeri* were identified (Tong *et al*., 2015), and another new coagulase negative species; *S. edaphicus* has been recovered from Antarctica (Pantůček *et al*., 2017).

Coagulase positive *Staphylococcus* (CPS) such as *S. aureus* includes both human and animal pathogens and is considered the major player associated with outbreaks of food intoxication worldwide (Argudin *et al.*, 2010; Hennekinne *et al*., 2012). In Egypt, many studies highlighted the role of CPS as animal pathogens. The frequent isolation of CPS from mastitic milk of cows and buffaloes were encountered (El-Jakee, 2008; El Seedy *et al.*, 2012).

Moreover, the isolation of CPS from septic wound and infected respiratory tract has drawn the attention to the risk of this pathogenic bacteria to human beings and consequently to pet animals, who are in a continuous contact with humans and act as reservoir of coagulase positive *Staphylococcus* (Robinson, 2004). It has been shown previously that *S. aureus* colonization of the nose increases the risk for developing a *S. aureus* infection (Wertheim *et al.*, 2005). Bacteremia is more common in the severe cases of skin infections but even the mild superficial cases carry a risk of systemic spread. Therefore, skin and soft tissue infections are the most commonly reported sources of systemic bacteremia (Wilson *et al*. 2011). All such aspects support that the identification of *S.aureus* is crucial for proper management of skin infection abscesses, septicemia/bacteremia or respiratory infections of pet animals which in contact to humans gain public health importance (Jurate and Jurate 2015).

In the present study, the data obtained (table 2) demonstrated the isolation of 18 *staphylococcus* with an average incidence of 20-23%. The confirmed *S. aureus* isolates constituted little more the half number 10 as the wounds showed 7 isolates (5 from dogs and 2 from cats) while nasal swabs exhibited 3 isolates (2 from dogs and one from cats). The nearly same incidences were reported in other studies, 24.58% (Abraham *et al.*, 2007) and 22.9% (Jang *et al.*, 2014). Higher incidences also were detected 36.3% (Drougka *et al.*, 2016; Han *et al*., 2016). The high rate of *staphylococci* recovery is of particular zoonotic importance, as such pet animals can constitute a dangerous source of infection to pet owners (Bierowiec *et al*. 2014).

The susceptibility of *S. aureus* to antimicrobials was tested by agar diffusion method. The results showed that the isolates were resistant to bacitracin, gentamycin and neomycin and more sensitive to amoxicillin/clavulinic acid and vancomycin. Similar findings were obtained by Hakim *et al*. (2016) and Conner *et al*. (2018), however in another study *S. aureus* was susceptible to bacitracin (89.3%) and gentamicin (86.1%) (Chang *et al*., 2015).

Thermonuclease (*nuc*) gene is used as primary molecular target for rapid identification of *S. aureus* as an important characteristic virulence factor of the pathogen (Thomas *et al.*, 2007). The results obtained (figure 1) showed that all examined isolates produced amplicons of same average size 270 bp. The same results were mentioned in many studies; Balbutskaya *et al*., (2017) confirmed 100% of 117 *S. aureus* isolates for *nuc* molecular analysis. Also, Jiang *et al*., (2019) detected *nuc* gene in all *S. aureus* investigated isolates. Hoegh *et al*. (2014) also mentioned that the occurrence of *nuc*-negative *S. aureus* isolates is extremely rare, representing less than 1% of all *S. aureus* isolates.

Production of coagulase is an important phenotypic feature, used worldwide to identify *S. aureus*. Several studies have implemented the molecular analysis of the coagulase gene as an accurate defined test (Tiwari *et al.* 2008).

In our study, all examined *S. aureus* isolates amplified *coa* gene, producing an amplicon of 970 bp. An uniform amplicon of 500bp was mentioned by another study among *S. aureus* subclinical mastitis strains in Nigeria (Suleiman *et al*., 2012).

This result may be unusual; as commonly, the *coa* gene encoding coagulase protein is highly polymorphic because of the inconstant sequences (81 bp tandem repeats) at its 3' end (Janwithayanuchit *et al*., 2006). There is a great variability in size of a *coa* gene on cited articles in that topic as many authors studied variation of the obtained PCR product for *coa* gene by using the same primer (Salasia *et al.*, 2004; Kalorey *et al.*, 2007; Reinoso *et al.*, 2008; Hakim *et al.*, 2017).The *coa* gene polymorphism allows differentiation of *S. aureus* species. Depending on this phenomenon, it has been considered a technically simple method of good reproducibility and discriminatory power for typing *S. aureus* strains (Javid *et al*., 2018).

The cause for this polymorphism among *S. aureus* isolates is indistinct, but it seems to be due to deletion or insertion of many nucleotides at 3' end region. This results in mutations and a consequent change of the *coa* gene size and perhaps antigenic properties of the coagulase enzyme (Saei *et al.*, 2009). This antigenic variation of coagulase is supposed to be essential for the pathogen escape from inhibitory effect of anticoagulase components. Some reports have suggested that antibody and non-antibody agents can neutralize the coagulase activity and therefore increase resistance against staphylococcal infections (Engelmann and Massberg 2013).

According to figures 3 and 4, a total of 5 different electrophoretic patterns (I, II, III, IV and V) from the 10 confirmed *S. aureus* isolates were observed. The patterns tend to be specific with predominance of pattern III in 3 dog wound samples, followed by pattern I and II. The pattern V was present in 2 cats wound samples while the pattern IV was observed in one dog wound sample.

Although many genotypes were detected, only a few prevailed. This perception was frequently observed; in an earlier survey performed in Brazil, the 64 *S. aureus* isolates were categorized into 49 types for *coa* gene RFLP with the 10 most observed representing 39% of the isolates (da Silva and da Silva, 2005). In other studies, PCR-RFLP of *coa* gene differentiated the isolates into 15 genotypic patterns, of which 4 patterns only were predominant (Sharma *et al.*, 2017).

Sequencing of staphylococcal *coa* genes obtained from the ten *S. aureus* isolates was performed during this study. Gene sequences exhibited a high level of inter-individual correspondence (99-100%) confirming that the amplified products were really identical to the *coa* gene. The *coa* gene is a target for phylogenetic analysis of staphylococci and differentiation of staphylococcal isolates at the species level. Canine and feline isolates came in one clade and

shared homology by 75% with the strain obtained in 2002 from a wound specimen of a pediatric outpatient in Taiwan (Huang *et al*., 2012).

5. Conclusion

The analysis of the *coa* gene supplied a useful typing tool for *S. aureus* from various pet animals. Additionally, the obtained data showed that the studied cases harbored *S. aureus* isolates and that more than one coagulase genotype was detected, although only one or two forms dominated. However, further studies using a large collection of strains from different areas and animals are needed so that the obtained information improves the efficiency of staphylococcal infection control measures. Moreover, these results assume the probability of the transmission of some strains of coagulase positive staphylococci in between human and companion pets.

References

Abraham JL, Morris DO, Griffeth GC, Shofer FS and Rankin SC. 2007. Surveillance of healthy cats and cats with inflammatory skin disease for colonization of the skin by methicillin-resistant coagulase positive staphylococci and *Staphylococcus schleiferi* spp. *schleiferi*. *Vet Dermatol*, **18**: 252-259.

Argudin MA, Mendoza MC and Rodicio MR. 2010. Food poisoning and *Staphylococcus aureus* enterotoxins. *Toxins*, **2**: 1751–1773.

Aslantas O, Demir C, Turutoglu H, Cantekin Z, Ergun Y and Dogruer G. 2007. Coagulase gene polymorphism of *Staphylococcus aureus* isolated from subclinical bovine mastitis. *Turk J Vet Anim Sci*, **31**:253-257.

Balbutskaya AA, Dmitrenko OA and Skvortsov VN. 2017. The modern characteristics of species identification of coagulase-positive bacteria of *Staphylococcus* genus**.** *Klin Lab Diagn*, **62**(8):497-502.

Bierowiec K, Płoneczka-Janeczko K and Rypuła K. 2016. Is the Colonization of *Staphylococcus aureus* in Pets Associated with Their Close Contact with Owners? *PLoS One*, **11**(5):e0156052.

Bierowiec K, Płoneczka-Janeczko K and Rypuła K. 2014. Cats and dogs as a reservoir for *Staphylococcus aureus*. *Postepy Hig Med Dosw* (Online), **68**:992-7.

Chang VS, Dhaliwal DK, Raju L and Kowalski RP. 2015. Antibiotic Resistance in the Treatment of *Staphylococcus aureus* Keratitis: a 20-Year Review**.** *Cornea*, **34**(6):698-703.

Clinical Laboratory Standards Institute 2015. Performance Standards for Antimicrobial Disk Suscebility Tests; Approved Standards - Twelfth Edition, M02-A12.

Clinical Laboratory Standards Institute 2018. Performance Standards for Antimicrobial Suscebility Testing – 28th Edition, M100 –S28.

Conner JG, Smith J, Erol E, Locke S, Phillips E, Carter CN and Odoi A. 2018. Temporal trends and predictors of antimicrobial resistance among *Staphylococcus* spp. isolated from canine specimens submitted to a diagnostic laboratory**.** *PLoS One*, **13**(8):e0200719.

da Silva ER and da Silva N. 2005. Coagulase gene typing of *Staphylococcus aureus* isolated from cows with mastitis in southeastern Brazil. *Can J Vet Res*, 69(4): 260–264**.**

Drougka E, Foka A, Koutinas CK, Jelastopulu E, Giormezis N, Farmaki O, Sarrou S, Anastassiou ED, Petinaki E and Spiliopoulou I. 2016. Interspecies spread of *Staphylococcus aureus* clones among companion animals and human close contacts in a veterinary teaching hospital. A cross-sectional study in Greece**.** *Prev Vet Med*, **1**:126:190-8.

El-Jakee J, Nagwa AS, Bakry M, Sahar AZ, Elgabry E and Gad El-Said WA. 2008. Characteristics of *Staphylococcus aureus* Strains Isolated from Human and Animal Sources American-Eurasian *J Agric Environ Sci*, **4** (2): 221-229.

El-Seedy FR, El-Shabrawy M, Hakim AS, Syame SF and Osman NM. 2012. Advanced techniques used for isolation and characterization of *Staphylococcus aureus* isolated from mastitic buffaloes. *Global Veterinaria*, **8** (2): 144-152.

Engelmann B and Massberg S. 2013. Thrombosis as an intravascular effector of innate immunity. *Nat Rev Immunol*, **13**(1): 34–45.

Gao J, Ferreri M, Liu XQ, Chen LB, Su JL and Han B. 2011. Development of multiplex polymerase chain reaction assay for rapid detection of *Staphylococcus aureus* and selected antibiotic resistance genes in bovine mastitic milk samples. *J Vet Diagn Invest*, **23**(5):894-901.

Haenni M, Châtre P, Dupieux-Chabert C, Métayer V, Bes M, Madec JY and Laurent F. 2017. Molecular Epidemiology of Methicillin-Resistant *Staphylococcus aureus* in Horses, Cats, and Dogs Over a 5-Year Period in France**.** *Front Microbiol*, **13**(8):2493.

Hakim AS, Samy AA, Sohad MD, Shimaa TO, and Elgabry EA. 2017. Molecular Divergence of *Staphylococcus Aureus* Isolated from Pork Byproducts Based on Coagulase Gene Polymorphism and The Presence of Enterotoxigenic genes. *IOSR Journal of Agriculture and Veterinary Science (IOSR-JAVS)* **10**: (5) 34-39.

Hakim AS, Shimaa TO, Elgabry EA and Bakry MA. 2016. Molecular Screening of Clumping Factor and Some Antibiotic Resistance Genes In Staphylococcal Isolates Obtained from Retail Pork Byproducts in Egyptian Markets. *International Journal of ChemTech Research*, **9**(8):37-42.

Han JI, Yang CH and Park HM. 2016. Prevalence and risk factors of Staphylococcus spp. carriage among dogs and their owners: A cross-sectional study**.** *Vet J*, **212**:15-21.

Hennekinne JA, de Buyser M and Dragacci L. 2012. *Staphylococcus aureus* and its food poisoning toxins: Characterization and outbreak investigation. *FEMS Microbiol Rev*, **36**: 815–836.

Hoegh SV, Skov MN, Boye K, Worning P, Jensen TG and Kemp M. 2014. Variations in the *Staphylococcus aureus*-specific *nuc* gene can potentially lead to misidentification of meticillin-susceptible and -resistant *S. aureus***.** *J Med Microbiol*, **63**(7):1020-2.

Huang TW, Chen FJ, Miu WC, Liao TL, Lin AC, Huang IW, Wu KM, Tsai SF, Chen YT and Lauderdale TL. 2012. Complete genome sequence of *Staphylococcus aureus* M013, a pvl-positive, ST59-SCCmec type V strain isolated in Taiwan**.** *J Bacteriol*, **194**(5):1256-7.

Ishino K, Tsuchizaki N, Ishikawa J and Hotta K**.** 2007. Usefulness of PCR-restriction fragment length polymorphism typing of the coagulase gene to discriminate arbekacin-resistant methicillin-resistant *Staphylococcus aureus* strains**.** *J Clin Microbiol*, **45**(2):607-9.

Jang Y, Bae DH, Cho JK, Bahk GJ, Lim SK and Lee YJ. 2014. Characterization of methicillin-resistant *Staphylococcus* spp. isolated from dogs in Korea**.** *Jpn J Vet Res*, **62**(4):163-70**.**

Janwithayanuchit I, Somying N, Porntip P and Watcharin R. 2006. Epidemiologic Study of methicillin-resistant *Staphylococcus aureus* by Coagulase Gene Polymorphism. *Science Asia*, **32**: 127-132.

Javid F, Taku A, Bhat MA, Badroo GA, Mudasir M, Sofi TA. 2018. Molecular typing of *Staphylococcus aureus* based on coagulase gene**.** *Vet World*, **11**(4):423-430.

Jiang R, Zhu J, Wenig X and Kong H. 2019. Investigation of Virulence Genes and Resistance Genes in a Group of *Staphylococcus aureus* Isolated in Yuhang, China**.** *Clin Lab*, **65**(3):180737**.**

Jurate S and Jurate S. 2015. Distribution of coagulase-positive staphylococci in humans and dogs *Acta Vet. Brno*, **84**: 313–320.

Kalorey DR, Shanmugam Y, Kurkure NV, Chousalkar KK, Barbuddhe SB. 2007. PCR-based detection of genes encoding virulence determinants in *Staphylococcus aureus* from bovine subclinical mastitis cases**.** *J Vet Sci*, **8**(2):151-4**.**

Mauriello G, Casaburi A, Blaiotta G and Villani F. 2004. Isolation and technological properties of coagulase negative staphylococci from fermented sausages of Southern Italy. *Meat Science*, **67**: 149–158.

National Committee for Clinical Laboratory Standards 2004. Global consensus standardization for health standardization for health technology Atlanta, GA.

Otto M. 2010. *Staphylococcus* colonization of the skin and antimicrobial peptides. *Expert Rev Dermatol*, **5**(2):183–195.

Pantůček R, Sedláček I, Indráková A, Vrbovská V, Mašlaňová I, Kovařovic V, Švec P, Králová S, Krištofová L, Kekláková J, Petráš P, and Doškař J. 2017. "*mec* C gene and genomic islands with suspected role in adaptation to extreme environment". *Applied and Environmental Microbiology*, **84** (2): e01746–17.

Peetermans M, Verhamme P and Vanassche T. 2015. Coagulase Activity by *Staphylococcus aureus*: A Potential Target for Therapy? *Semin Thromb Hemost*, **41**(4):433-44.

Reinoso, EB, El-Sayed A, Lämmler C, Bogni C and Zschöck M. 2008. Genotyping of *S. aureus* isolated from bovine clinical mastitis in Argentina. *Microbial*. *Res*, **163**(3): 314-322.

Richard E, Wiemels A, Stephanie M, Cech A, Nikki M and Ronan K. 2017. An Intracellular Peptidyl-Prolyl cis/trans Isomerase Is Required for Folding and Activity of the *Staphylococcus aureus* Secreted Virulence Factor Nuclease. *J Bacteriol*, **199**(1): e00453-16**.**

Robinson JMD. 2004. Colonization and infection of the respiratory tract: What do we know? *Paediatr Child Health*, **9**(1): 21–24**.**

Saei HD, Ahmadi M, Mardani K and Batavani RA. 2009. Molecular typing of *Staphylococcus aureus* isolated from bovine mastitis based on polymorphism of the coagulase gene in the north west of Iran**.** *Vet Microbiol*, **137**(1-2):202-6.

Salasia, SIO, Khusnan, Z, Lämmler, C, Zschöck, M. 2004. Comparative studies on pheno- and genotypic properties of *Staphylococcus aureus*, isolated from bovine subclinical mastitis in Central Java in Indonesia and Hesse in Germany. *J. Vet. Sci*, **5**:103–109.

Sambrook J, Fritsch EF and Maniatis T. 1989. Purification of closed circular DNA by equilibrium centrifugation in Cs-Clethidium bromide gradients. In: **Molecular Cloning: A Laboratory Manual**, New York, CSH Laboratory.

Sharma V, Sanjita Sharma S, Dinesh K D, Aarif K, Manisha M, and Aayushi S. 2017. Coagulase gene polymorphism, enterotoxigenecity, biofilm production, and antibiotic resistance in *Staphylococcus aureus* isolated from bovine raw milk in North West India. *Ann Clin Microbiol Antimicrob*, **16**: 65**.**

Soriano JM, Rico H, Moltó JC and Manes J. 2000. Microbial evaluation of Spanish potato omelette and cooked meat samples in University restaurants. *Journal Food Protection*, **63**: 1273-1276**.**

Suleiman AB, Kwaga JKP, Umoh VJ, Okolocha EC, Muhammed M, Lammler C, Shaibu SJ, Akineden O, and Weiss R. 2012. Macro-restriction analysis of *Staphylococcus aureus* isolated from subclinical bovine mastitis in Nigeria. *African Journal of Microbiology Research*, **6**(33): 6270-6274.

Thomas LC, Gidding HF, Ginn AN, Olma T and Iredell J. 2007. Development of a real-time *Staphylococcus aureus* and MRSA (SAM-) PCR for routine blood culture. *J Microbiol Methods*, **68**: 296—302.

Tiwari HK, Sapkota D and Sen MR. 2008. Evaluation of different tests for detection of *Staphylococcus aureus* using coagulase (*coa*) gene PCR as the gold standard**.** *Nepal Med Coll J*, **10**(2):129-31**.**

Tong SY, Schaumburg F, Ellington MJ, Corander J, Pichon B, Leendertz F, Bentley SD, Parkhill J, Holt DC, Peters G, and Giffard PM. 2015. Novel staphylococcal species that form part of a *Staphylococcus aureus*-related complex: the non-pigmented *Staphylococcus argenteus* sp. *nov*. and the non-human primate-associated *Staphylococcus schweitzeri* sp. *nov*. *International Journal of Systematic and Evolutionary Microbiology*, **65** (1): 15–22.

Werthiem HF, Melles DC, Vos MC, Van leeuwen W, van belkum A, Verbrugh, HA and Nouwen JL.2005. The role of nasal carriage in *Staphylococcus aureus* infections. *Lancet Infect. Dis*, **5**:751-62.

Wilson J. 2011. Trends in sources of meticillin-resistant *Staphylococcus aureus* (MRSA) bacteraemia: data from the national mandatory surveillance of MRSA bacteraemia in England, 2006-2009. *J Hosp Infect*, **79**(3): 211-7.

JJBS

Volume 13, Number 2, June 2020
ISSN 1995-6673
Pages 145 - 151

Jordan Journal of Biological Sciences

Development of SCAR Marker Linked to *Begomovirus* Resistance in Melon (*Cucumis melo* L.)

Yasir Sidiq[1], Aprilia Sufi Subiastuti[2], Wiko Arif Wibowo[2] and Budi Setiadi Daryono[2*]

[1] *Graduate student Alumny of Faculty of Biology, Universitas Gadjah Mada,* [2] *Department of Tropical Biology, Faculty of Biology, Universitas Gadjah Mada, Yogyakarta, Indonesia.*

Received May 7, 2019; Revised June 12, 2019; Accepted June 30, 2019

Abstract

Begomovirus is one of the most devastating diseases of melon causing high economic losses for farmers. The most eco-friendly strategy to overcome *Begomovirus* infection is to develop resistant or tolerant cultivar. However, this strategy is time consuming, expensive and complex, especially for hybrid selection process. A pair of Sequence Characterized Amplified Region (SCAR) marker was successfully developed from OPA-4 Random Amplified Polymorphisms DNA (RAPD) marker to discriminate potential *Begomovirus* resistant genotypes from the susceptible ones. Leaf samples were amplified using OPA-4 primer and produced specific band at 1198 bp. The band was purified from gel then sequenced. The sequence was analyzed and extended until 20 bp so it becomes a more specific SCAR marker. BLAST analysis showed that amplified sequence had 95.8% identity with *Cucumis melo* L. mitochondrial DNA. To ensure the consistency of marker, SCAR marker was applied in bulk F_2 plants. The results showed that the marker was consistent amplified same DNA fragment only in *Begomovirus*-uninfected samples. Chi-square test determined that the F_2 bulk segregated following 3:1 pattern for resistant. It was likely indicated that *Begomovirus* resistance trait was possibly controlled by single dominant genes. Furthermore, this marker has been validated using eight different melon cultivars and confirmed not to be affected by environmental conditions.

Keywords: *Begomovirus*; PCR; *Cucumis melo*, L.; SCAR; RAPD

1. Introduction

Melon (*Cucumis melo* L.) is a fruit that has a high economical value. In Indonesia, melon export volume has increased every year since 2008. It also has high nutrition value such as ascorbic acid, beta-caroten, folate acid, and potassium (Park and Crosby, 2004). However, virus infection is a serious threat in melon production either in Indonesia or in the world. *Begomovirus* is one of the most devastating diseases of melon causing high economic losses for the farmer. It was transmitted by *Bemisia tabaci* and caused yellowing leaves, curling leaves, and stunted growth of plants and fruit (Chang *et al*. 2010). Julijantono *et al.* (2010) reported that *Begomovirus* infected melon in East Java and Yogyakarta at 2008 with the infection ranged between 5-100% in the first and 14.3-100% in the second cultivation. The infection causes significant quality and yield loss when high temperature and humidity increased vector population (Alemandri *et al*., 2012; Khrisnareddy, 2013).

Begomovirus control management that is widely used in Indonesia is still dependent on intensive use of insecticides. Some farmers have used greenhouses to reduce the incidence of *Begomovirus* infections, but the development of *Begomovirus*-resistant melon cultivars has not been intensified. The development of resistant or tolerant cultivar is the most eco-friendly and efficient strategy to overcome *Begomovirus* infection, especially for farmers with limited resources (Seal *et al*., 2006, Meija *et al*., 2005). Some melon accession has been confirmed resistant to *Begomovirus*, such as Sudan Accession HSD 2445-005, African accession PI 282448, three Indian accession; 90625, PI 124112, and PI 414723, and Wm-7 (Yousif *et al*, 2007; Saez *et al.*, 2017) but no one reported from Indonesia.

However, the development of resistant cultivar through conventional breeding is time consuming, expensive and complex. Field screening is necessary to select the hybrids that have resistance to *Begomovirus* from some big populations based on visual symptoms. The results also must be confirmed many years at least using two generations (Eathington *et al*., 2007; Nevame *et al*, 2018). The advance of molecular markers is very helpful in accelerating hybrid selection process. The marker helps to distinguish a character among hybrids in early stages, so it can also minimize the costs (Hayward *et al*, 2015).

Molecular marker can be divided into non-PCR based techniques (Restriction Fragment Length Polymorphisms (RFLP)) and PCR-based techniques (RAPD, Amplified Fragment Length Polymorphims (AFLP), Simple Sequence Repeat (SSR), Single Nucleotide Polymorphisms (SNP), etc.). Each method has its advantages and disadvantages (Kumar *et al*., 2009). This study focused on RAPD and SCAR. RAPD is a random method using a short primer to find the molecular marker, whereas SCAR is developed by extending primer based on a specific sequence of DNA. The main advantage of

* Corresponding author e-mail: bs_daryono@mail.ugm.ac.id.

RAPD is easy and fast to determine. But it has low reproducibility, which is its main drawback (Bhagyawant, 2016). A marker resulted from SCAR is relatively more stable than those from RAPD. One significant advantage of SCAR compared to RAPD is more specific and reproducible (Lu *et al*., 2010; Yadav *et al*., 2012, Bhagyawant, 2016). Development of SCAR marker linked to plant resistance gene has been widely reported previously such as, powdery mildew in melon (Daryono *et al*., 2011; Daryono *et al*., 2009), powdery mildew in pea (Srivasthava *et al*., 2012), *Fusarium oxysporum* in Banana (Cunha *et al*., 2015), *Puccinia psidii* in *Eucalyptus grandis* (Laia *et al*, 2015), Mungbean yellow mosaic virus in mungbean (Dhole and Reddy, 2012), and *Begomovirus* in tomato (Garcia-Andrez *et al*., 2007). However, no SCAR marker linked to *Begomovirus* resistance in melon has been reported.

MG3 cultivar was used as sample in this study. MG3 was resulted from crossing Melodi Gama-1 (MG1) and Lad-3 cultivar. MG1 was the result of crossing cultivars, the Andes and PI 414723. PI 414723 has been confirmed to be resistant to *Begomovirus* (Yousif *et al*., 2007). Hence, genetically, MG3 may inherit the resistance characters of PI 414723. T Considering the urgency of development *Begomovirus* resistant melon cultivars, this study was conducted to develop SCAR marker linked to *Begomovirus* resistant based on RAPD marker and to reveal inheritance pattern of bulk F_2 through the application of SCAR marker in the population. Furthermore, SCAR marker was also applied to 8 othercultivars for further validation.

2. Materials And Methods

2.1. Plant materials and symptoms observation

A total of 1000 ‘MG3’ melon plants was observed in the university field located in Berbah, Sleman, Yogyakarta. The incidence of *Begomovirus* in this location has been reported by Julijantono *et al.*, (2010) and Subiastuti *et al.*, (2019). *Begomovirus* infection occurred naturally in the field. The symptoms observation was conducted according to Lopez *et al* (2015). For bulk segregation analysis, 100 ‘MG3’ melon plants were planted in open field where *Begomovirus* infections were naturally found. Additionally, 8 cultivars were used for validation developed SCAR marker. *Begomovirus* symptoms were also evaluated under natural conditions.

2.2. DNA extraction

A total of 21 of the 1000 plants observed were used for DNA extraction, consisting of 10 uninfected samples and 11 infected samples. As much as 0.3- 0.5 g of melon leaves was used for DNA extraction using Phytopure (Healthcare) according to Daryono and Natsuaki (2002) with little modification on samples weight and the volume of some reagent. We used 0.3 g leaf samples and 25 µL resin. Then extracted DNAs were analyzed quantitatively using Nanovue Plus Nanodrop spectrophotometer at absorbance 260/280 nm.

2.3. DNA Amplification using CP Primer and RAPD Marker

Molecular detection of *Begomovirus* particle was done to confirm the result of symptoms evaluation. This method was to ensure whether DNA *Begomovirus* in plants or not. A total of 11 DNA melon samples were amplified using CP primer according to Julijantono *et al.* (2010). The reaction was carried out in Bio-Rad T 100TM Thermal Cycler PCR which began with 95 ˚C for 5 minutes, followed by 35 cycles of 95 ˚C for 1 minutes, 52.5 ˚C for 1 minutes, and 72 ˚C for 1 minutes, then ended with 72 ˚C for 3 minutes. Infected samples were marked with 770 bp DNA band.s Amplified DNA were sequenced and analyzed using BLAST. PCR reaction was also conducted using RAPD marker. In this study, OPA-4 primer (5’-AATCGGGCTG-3’) was used to identify specific band correlated with *Begomovirus* resistance in ‘MG3’ melon (Julijantono*et al*., 2012). A total of 25 microliters of PCR mixture containing 12.5 µL PCR kit ready mix (Fastart), 3 µL of 70µg/ml DNA template, 2.2 µL of 3 pmol OPA-4 primers, and 7.3 µL distilled water (ddH_2O) were prepared for PCR. The PCR was done with the following programs: an initial denaturation at 94 ˚C for 3 minutes, 45 cycles of denaturation at 94 ˚C for 3 minutes, annealing at 36 ˚C for 3 minutes and elongation at 72 ˚C for 2 minutes, followed by final extension at 72 ˚C for 5 minutes. PCR results were confirmed by electrophoresis on 1 % agarose gel at 50 V for 60 minutes. The gel was stained using etidium bromide for 30 minutes. A 100 bp DNA ladder (Vivantiz) was used as standar for estimation of DNA band size. After 60 minutes, the gels were visualized using UV transilluminator then analyzed.

2.4. Markers Screening and Sequence Analysis of Polymorphic Fragments

Markers screening was done by selecting bands showing polymorphism between infected and non-infected samples. Those bands were excised from gels and purified according to Daryono *et al*., (2011) using Agarose Gel Extraction Kit (Roche). The purified DNA samples then sent for sequencing that was performed using ABI PRISM 3730xl Genetic Analyzer (Applied Biosystems, USA) and BigDye® Terminator v3.1 sequencing kit.

2.5. Development SCAR Markers

SCAR primer design was initiated by aligned sequence of selected DNA fragment to identify the locations of OPA-4 primer sequences. SCAR markers were developed by extending forward and reverse primer up to 20 bp. Each primer consisted of first 10 bases of OPA-4 primer. Subsequently, both were tested using the primer Oligo calculator to determine the temperature of melting (Tm) of primers, GC content, and the possibility of a hairpin loop.

2.6. Linkage analysis and validation of SCAR Markers

Linkage analysis was performed to analyze segregation pattern of the SCAR marker linked to resistance to *Begomovirus* in the F_2 progenies of ‘MG3’ melon. A total of 100 plants were analyzed using chi square test. Meanwhile, validation of SCAR marker was performed on 9 different cultivars (Tacapa GB’, ‘Tacapa Silver’, ‘Tacapa Gold’, ‘Hikapel’, ‘Meloni’, ‘Melona’, ‘Gracia’, ‘Luna’, and ‘Madesta’). A total of 13 melon samples, consisted of uninfected samples from all cultivars and 4 infected samples from cultivars ‘Tacapa GB’, ‘Tacapa Silver’, ‘Hikapel’, and ‘Meloni’, were used. DNA samples were amplified using designed SCAR marker in 25 µL PCR reaction consisting of 12.5 µL PCR kit ready mix (Fastart), 3 µL of 250 µg/ml DNA template, 2.5 µL of 100 nM of

each SCAR primer, and 4.5 µL distilled water (ddH_2O). The PCR was performed on 5 minutes initial denaturation at 95 ˚C followed by 35 cycles of 1 minute at 95 ˚C, 1 minutes at 60 ˚C, and 2 minutes at 72 ˚C, then followed with a final extension for 10 minutes at 72 ˚C. PCR products were separated by electrophoresis on 1.5% agarose gel stained with ethidium bromide. Electrophoresis was carried out at 50 V for 45 minutes. Then gels were visualized using UV trans-illuminator.

3. Results

3.1. Begomovirus Infection Assesment

Disease assessment was conducted by visual observations and PCR detection. Visual observations revealed that 10 from 1000 observed plants exhibit common *Begomovirus* symptoms i.e. mosaic, leaf curling, and stunting (Fig.1). *Bemisia tabaci* populations, vector of *Begomovirus*, were also found in bottom surface of melon leaf. Furthermore, all infected leaves and one uninfected leaf (as control) were tested using PCR. Infected samples amplified ~770 bp DNA fragment which not found in uninfected samples (Sawangjit *et al*., 2004). Three out from 10 infected samples did not show targeted DNA band (Fig.2) but amplified untargeted band at 550 bp. However, untargeted band was found either at infected samples or uninfected samples.

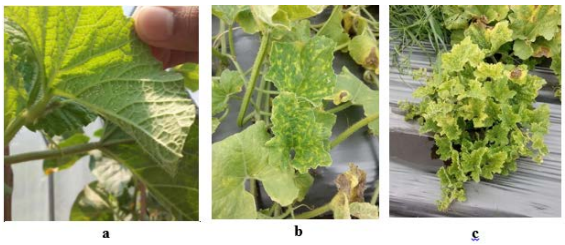

Figure1.*Begomovirus* infected melon leaves with observed *Begomovirus* symptoms, *Bemisia* tabaci population found in bottom surface of the leaf (a), mosaic and leaf curling (b), and stunting growth (c).

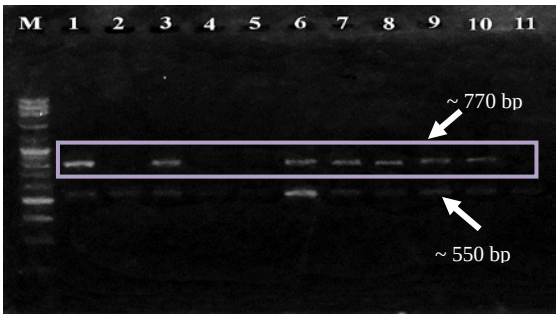

Figure 2. PCR assessment of *Begomovirus* infected melon using CPA2 and CPA5 primer. Infected samples showed targeted band at 770 bp (M: Marker; 1-10: Infected melon samples; 11: Uninfected sample).

3.2. Development of SCAR Markers linked to Begomovirus resistance

'MG3', a hybrid from 'MG1' and 'La-3', were used to detect polymorphisms by RAPD Markers. A total of 13 samples consisting of 9 uninfected plants and 4 *Begomovirus* infected plants were used to detect specific markers linked to *Begomovirus* resistance. OPA-4 primer generated 7 bands consisting of 6 monomorphic bands and 1 polymorphic band (Fig.3). An approximately 1198 bp was consistently present in uninfected plants while absent in infected plants. To construct SCAR marker, the specific band was excised from the gels, purified, and then sequenced. The obtained sequence matched with the amplified band size (i.e. 1198 bp) and showed 95.88 % identity with *Cucumis melo* subsp. melo mitochondrial sequence (Gene Bank Accession No:JF412792). Based on this sequence, a set of SCAR primer, named SCOPA4-1 (5'-TCTCGGGCTGCTAACTGCAG-3') and SCOPA4-2 (5'-TACGAGAACCGTCAGGCCTG-3') were designed containing 60% GC content. Each primer was overlapped with 6-8 first base of OPA-4 primer sequence in both ends (Fig 4). The annealing temperature (Tm) of developed SCAR primer was 55.9 ˚C, calculated by the program OligoCalc-Oligonucleotide Properties Calculator (Kibbe, 2007). However, an optimum temperature for obtained clear bands was 49.7 ˚C.

3.3. Segregation Analysis and Marker Validation

To confirm the linkage of newly developed SCAR marker with *Begomovirus* resistance, 100 F_2 progenies were tested. Phenotypic evaluation revealed that 70 plants showed *Begomovirus* symptoms while 30 do not showed. Then DNA of observed plants was amplified using developed SCAR marker. Each plant was scored for the presence of specific amplicon. An 1198 bp specific band was consistently amplified in 82 uninfected plants (Fig. 5). The segregation pattern of marker locus was expected as Mendelian segregation ratio of 3 (resistant): 1 (susceptible) and confirmed using Chi square test. The results confirmed that segregation pattern was equivalent with expected ratio either on phenotypic evaluation or PCR validation (X^2= 2,25; df=1; P= 0.05). Meanwhile, developed SCAR markers are known to differentiate individuals which potentially resistance to *Begomovirus* in a population. However, further analysis is needed to determine the accuracy of this primer in other cultivars. Nine cultivars from different breeding lines, named 'Tacapa GB', 'Tacapa Silver', 'Tacapa Gold', 'Hikapel', 'Meloni', 'Melona', 'Gracia', and 'Madesta', were used for this analysis. Gracia and Madesta were commercial cultivars that were confirmed as resistant cultivars. There were 9 unifected samples from each cultivar and 4 infected samples which have confirmed by PCR using CP gene primer for *Begomovirus*. SCOPA4-1 and SCOPA4-2 were consistently amplified 1198 bp band only in uninfected samples for all cultivars (Fig 6). This result was in agreement with symptom observation data and PCR identification. So, it can be confirmed that newly developed marker was consistent and reliable.

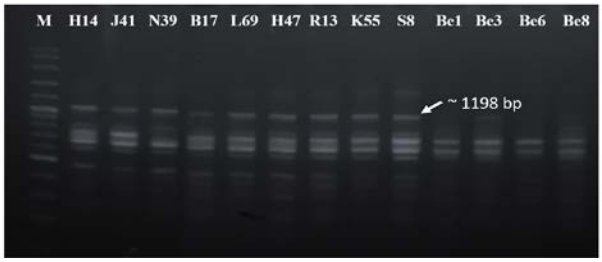

Figure 3. Identification of RAPD DNA fragment related to *Begomovirus* resistance was performed with DNA from 9 unifected samples (from H-14 to S8) and 4 infected samples (from Bel to Be8) Arrow indicates the band that discriminated infected and uninfected melon. (M= 100 bp molecular weight DNA marker (Vivantiz)

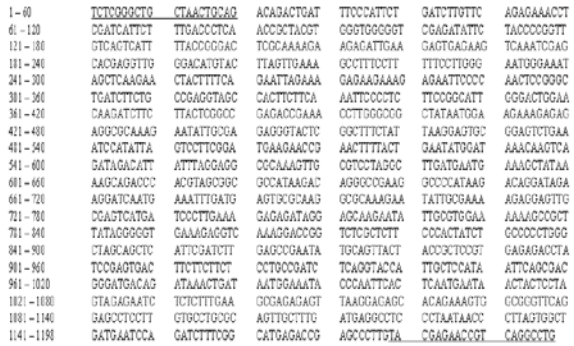

Figure 4. The complete sequence of RAPD fragment related to *Begomovirus* resistance (1198 bp). Underlined sequences indicate sequences of newly developed SCAR primers.

4. Discussion

Begomovirus is one of the most devastating diseases in melon crops. *Begomovirus* infected melon was initially reported in America in 1981 while in Indonesia in the early 2010 (Cohen*et al*., 1983; Julijantono *et al*., 2010). After almost a decade, Begomovirus in Indonesia has developed rapidly. There were three *Begomovirus* species that have been reported to infect melon plants, namely PepYLCIV, ToLCNDV, and TYLCV (Subiastuti et al., 2019). In order to overcome *Begomovirus* outbreaks, development resistant cultivar is a promising solution. However, the selection of *Begomovirus*-resistant genotypes will be very tricky if it only relies on symptom observation. This method is often ambiguous in discriminating tolerant and susceptible genotypes because appearing symptoms usually look similar (Maiti *et al*., 2010, Nevame *et al*., 2018). Sometimes, *Begomovirus-infected* plant yield as good as uninfected plants and showed different level of symptoms. This may be due to virus strain, time of infection, plant of genotype, biotype of vector, and environmental factor (Polston and Anderson, 1997; Delatte *et al*., 2006; Azizi *et al*., 2008).

Another method that might be used is molecular detection using universal CP gene primers to detect viral genomes in plants. This method was accurate, less time-consuming, and only required little amount of leaf tissue (Sharma *et al*., 2005). PCR based detection has been successfully used to detect *Begomovirus* in tomato (Yang *et al*., 2011), cucurbit (Mizutani *et al*., 2011), okra (Venkataravanappa *et al*., 2013), sweetpotato (Wasswa *et al*., 2011), legume (Tsai *et al*., 2013), melon (Subiastuti *et al*., 2019), chili and eggplant (Maruthi *et al*. 2007). But this method has a disadvantage if the viral DNA concentration in plants is low, the obtained DNA bands will be not clear (Swanson *et al*., 1992; Ghosh *et al*., 2009). Moreover, this method also cannot be used to identify whether an individual was resistant or susceptible. Since the concentration of *Begomovirus* genome in plants was found to be very low, rapid detection by amplifying plant genome was more promising for early identification of resistant genotype as well as *Begomovirus* infection.

As *Begomovirus* resistance gene in melon has to be found yet, many studies try to develop molecular markers linked to resistance against *Begomovirus* (Diaz-Pendon *et al*., 2004; Saez *et al*., 2017). This study developed a SCAR marker from RAPD for early identification of *Begomovirus*-resistant individuals in a population as a resistant genotype source in breeding melon resistant cultivar. This method provides an alternative screening method to avoid long-term phenotypic and to characterize genetic resources with potential role in resistant plant development. Several reports explicated that RAPD is often used to distinguish individuals resistant to disease among susceptible individuals. Luongo *et al*., (2012) managed to identify RAPD, with OP-F15 primer, which is able to recognize melon cultivars resistant to *Fusarium oxiporum* infection. The OP-F15 primer is able to bring the base length of polymorphic band of 420 bp and has been developed into a SCAR marker. In addition, primers OPE - 14 and APB-05 are capable of distinguishing between melon cultivars resistant and susceptible to Cucumber mosaic virus (CMV) (Daryono *et al*., 2009). Similar to this RAPD, pUBC411 has been proven to be able to distinguish the melon cultivars resistant to powdery mildew by generating the 1061 bp polymorphic band (Daryono *et al*., 2011). By using MG3 melon DNA, the SCAR marker developed was able to distinguish resistant/tolerant individuals from susceptible ones. Primer OPA-4 was used to develop SCAR marker in this study because it had reported could differentiate between infected and uninfected samples in melon populations infected by *Begomovirus* (Julijantono *et al*., 2012). However, it is relatively unstable and influenced by the conditions of PCR reaction. SCOPA4-1 and SCOPA4-2, newly developed SCAR marker constructed from OPA-4 primer, were able to distinguish uninfected and infected individuals of 9 Indonesian melon cultivars through the appearance of 1198 bp DNA band. SCAR marker was codominant marker, more accurate, and more reliable as marker linked-trait than RAPD. Converting RAPD to SCAR marker by adding nucleotide of primer sequence will increase primer specificity to targeted locus. Even though, SCAR marker construction was not easy because it is still possible to produced non-targeted fragment (Ardiel *et al*., 2002; Bhagyawant, 2016).

Furthermore, similarity analysis using BLAST revealed that amplified sequence matched relatively with DNA mitochondria sequence of melon. Mitochondria was cellular organelles of eukaryotic cells and has important role in provide energy for cells, apoptosis, regulation of cell metabolisms, antiviral responses, signal transduction, stress responses, and cell-cycle control (Anand and Tikoo, 2013). Some study reported that mitochondria has important roles in biotic stress, including in viral infection. Virus infection triggered reactive oxygen species (ROS) accumulation and induces alternative oxidase (AOX) in plants. The induction of AOX would increase plant resistance against virus as reported in *Arabidopsis thaliana* and *Solanum tuberosum* infected by Tobacco Mosaic Virus (TMV) (Amirsagedhi *et al*., 2007; Fu *et al*., 2010). These results informed that developed SCAR marker was related with plant resistance trait yet further study was needed to analyze the distance between developed SCAR marker with resistance gene locus. It usually happened in development of linked-trait marker, some advance studies were needed to improve previous results. However, molecular marker linked to *Begomovirus* resistance was first reported in melons. Andersen and Lubberstedt (2003) showed that functional gene markers are polymorphic DNA sequences that are likely to be involved in phenotypic variation, in this case discriminating *Begomovirus*-infected and uninfected individuals.

Furthermore, segregation analysis showed that newly developed SCAR marker was segregated to F_2 progeny with ratio 3:1 for resistant. This indicated that *Begomovirus* resistance trait was regulated by single dominant gene. Many studies revealed that molecular marker linked to disease resistance trait segregated in ratio 3:1, such as Daryono *et al*.,(2010) reported that SCAR Marker linked to CMV-B2 resistance gene in melon also segregated in expected ratio 3:1. Other studies in different plant also reported that SCAR marker linked to *Xca1Bo* conferring resistance to black rot disease in cauliflower and SCAR marker linked to *Rpf1* gene that control resistance to red stele disease also segregated with ratio 3:1 (Kalia *et al*., 2017; Ruguenius *et al*., 2006). Furthermore, such studies which have contributed to identification of resistance gene explained that resistance gene for plant viruses appear to be predominantly inherited as monogenic dominant characters (Diaz-Pendon *et al*., 2004).

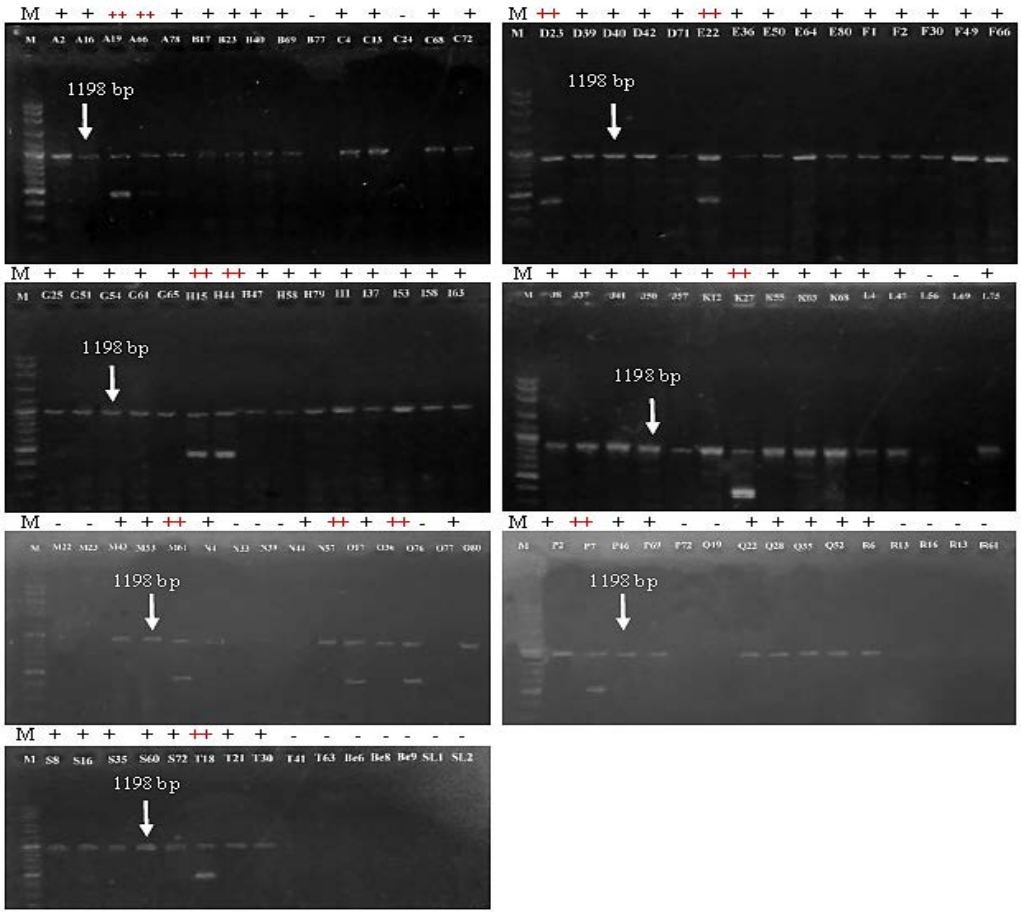

Figure 5. Validation of SCOPA4-1 and SCOPA4-2 primers in F_2 genotypes.

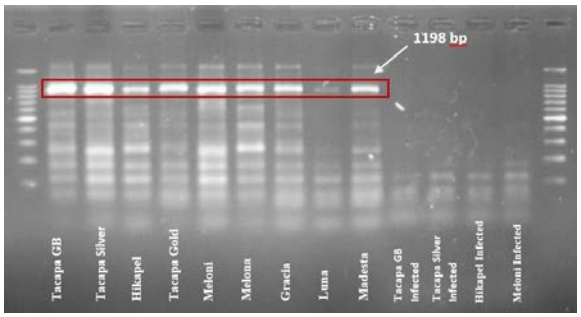

Figure 6. Validation of developed SCAR Marker in 9 melon cultivars. Amplified bands discriminated *Begomovirus* infected samples from uninfected one (M= 100 bp molecular weight DNA marker (Promega).

One of essential properties for molecular marker is havinghigh repeatability and independence from any environmental conditions (Kesawat and Das, 2009). It means the molecular marker can not only be used in certain object of the study but also apply to other objects in similar studies. In the present study, obtained SCAR marker was validated in different genetic backgrounds. An eight different melon cultivars was tested and revealed that this marker was reproducible and able to be used in other melon species. Because of limited information about *Begomovirus*-resistant genotype in melon, this marker only discriminate *Begomovirus* infected and uninfected individuals. The results also indicated that this marker was neutral from any genetic background with any doubt.

Development of SCAR marker linked to *Begomovirus* resistance to identify potential resistant melons genotype was firstly reported. An 1198 bp band was confirmed can consistently differentiate resistant and susceptible melon hybrid against *Begomovirus* infection. There was still limited report about molecular marker linked to *Begomovirus* resistant in melon. Therefore, this marker make a potential contribution for melon resistant breeding programs by reducing the time, labor, and production cost as well as increasing the efficiency of plant screening. Furthermore, this study only uses melons that develop in the tropics, especially Indonesia. Validation of non-tropical cultivars needs to be done to further confirm this

primary reliability. Moreover, experimental investigations are required, particularly to find out the specific gene that has a role to play in plant resistance mechanisms against *Begomovirus*.

Acknowledgments

The authors would like to express special thanks to Ministry of Research, Technology and Higher Education for financial support through MP3EI (Masterplan, Expansion, and Acceleration Indonesian Economic Development) (LPPT-UGM/1259/LIT/2014), PMDSU (4543/UN1-P.III/LT/DIT-LIT/2016), and PKPI-Sandwich (2018) programs. The research was also supported by Final Project Recognition programs 2019 from Gadjah Mada University (2990/UN1/DITLIT/DIT-LIT/LT/2019).

References

Alemandri, V., Pardina PR, Izaurralde J, Medina SG, Caro EA, Mattio MF, Dumon A, Rodriguez, SM, and Truol G. 2012. Incidence of *Begomoviruses* and climatic characterisation of Bemisia tabaci- geminivirus complex in soybean and bean in Argentina. *Agriscientia*., Xxix: 31-39.

Anand SK and Tikoo SK. 2013. Viruses as modulators of mitochondrial functions. *Adv Virol.,* **2**: 1-17.

Azizi A, Hashjin JM and Shams-Bakhsh. 2008. Phenotypic and molecular screening of tomato germplasm for resistance to Tomato yellow leaf curl virus. *Iran J Biotechnol.,* **6**:199-207.

Bhagyawant SS. 2016. RAPD-SCAR markers: An interface tool for authentication of traits. *J Biosci Med.,* **4**: 1-9.

Chang H, Ku H and Tsai W. 2010. Identification and characterization of a mechanical transmissible *Begomovirus* causing leaf curl on oriental melon. *Eur J Plant Pathol.,* **127(2):** 219–228.

Lu C, Zhang W, Peng X, Gu G, Chen M and Tang Z. 2010. Development of Randomly Amplified Polymorphic DNA-Sequence Characterized Amplified Region Marker for Identification of *Apocynum venetum* LINN. from A . *pictum* S CHRENK. *Biol Pharm Bull.,* **33(3)**: 522–526.

Cohen S, Duffus JE, Larsen RC, Liu HY and Flock RA. 1983. Purification , serology, and vector relationship of *Squash lef curl virus* a whitefly transmitted geminivirus. *Phytopathol.,* **3**: 1669-1673.

Cunha CMS, Hinz RH, Preira A, Tcacenco FA, Paulino EC and Stadnik MJ. 2015. A SCAR marker for identifying susceptibility to *Fusarium oxysporum* f. sp. *cubense* in banana. *Sci Hort.,* **191**:108-112.

Daryono BS, Aristya GR and Kasiamdari RS. 2011. Development of Random Amplified Polymorphism DNA Markers Linked to Powdery Mildew Resistance Gene in Melon. *I J Biotech.,* **16(I)**: 76–82.

Daryono BS and Natsuaki KT. 2002. Application of random amplified DNA markers for detection of resistant cultivars of melon (*Cucumis melo* L.) against cucurbit virus. *Acta Hort.,* **588**: 321-329.

Daryono BS, Wakui K and Natsuaki KT. 2009. Development of Random Amplified Polymorphism DNA Markers Linked to CMV-B2 Resistance Gene in Melon. *Hayati.,* **16(4)**: 142–146.

Daryono BS, Wakui K and Natsuaki K. 2010. Linkage analysis and mapping of SCAR markers linked to CMV-B2 resistance gene in melon. *Sabrao J Breed Genet*., **42**: 35-45.

Delatte H, Holota H, Reynand B and Dintinger J. 2006. Characterization of a quantitative resistance to vector transmission of Tomato yellow leaf curl virus in *Lycopersion pimpinellifolium. Europ J Plant Pathol.,* **114**: 245-253.

Diaz-Pendon JA, Truniger V, Nieto C, Garcia-Mas J, Bendahmane A and Aranda MA. 2004. Advances in understanding recessive resistance to plant viruses. *Mol Plant Pathol.* **5**: 222-232.

Dhole VJ and Reddy KS. 2012. Genetic analysis of resistance to mungbean yellow mosaic virus in mungbean (*Vigna radiata). Plant Breed.* **131**: 1-4.

Eathington SR, Crosbie TM, Edwards MD, Seiter RS and Bull JK. 2007. Molecular markers in a commercial breeding programs. *Crop Sci.,* **47**: 154-163.

Fu L, Shi K, Gu M, Zhou Y, Song D, Liang W, Song F and Yu J. 2010. Systemic induction and role of mitochondrial alternative oxidase and nitric oxide in a compatible tomato- *Tobacco mosaic virus* infection. *Mol Plant Microbe Interact.,* **23**: 39-48.

Garcia-Andrez S, Acotto GP, Navas-Castillo J and Moriones E. 2007. Founder effect, plant host, and recombination shape the emergent population of *Begomovirus*es that cause the tomato yellow leaf curl disease in the Meditteranean basin. *Virology.,* **359**: 302-312.

Ghosh R, Paul S, Ghosh SK and Roy A. 2009. An improved method of DNA isolation suitable for PCR-based detection of *Begomovirus*es from jute and other mucilaginous plants. *J Virol Methods.,* **159**: 34-39.

Hayward AC, Tollenaere R, Dalton-Morgan and Batley J. 2015. Molecular marker applications in plants. In: Batley J (Ed). Plant Genotyping: Methods in Molecular Biology. Springer Science-Bussiness Media, New York, pp: 13-27.

Julijantono I. 2012. Identifikasi Penyebab Penyakit, Vektor, dan Marka Molekular Terpaut Gen Ketahanan Melon terhadap *Begomovirus*. Ph.D Dissertation. Universitas Gadjah Mada, Yogyakarta, Indonesia.

Julijantono I, Somowiyarjo, Susamto, Trisyono YA and Daryono BS. 2010. Disease incidence of melon leaf curl in east java. *Jurnal Perlindungan Tanaman Indonesia*, **16(2)**:76–81.

Kalia P, Saha P and Ray S. 2017. Development of RAPD and ISSR derived SCAR markers linked to *Xca1Bo* gene conferring resistance to black rot disease in cauliflower *(Brassica oleracea* var. *botrytis* L.). *Euphytica.* **213**: 231-224.

Kesawat MS and Das RK. 2009. Molecular markers: It's application in crop improvement. *J Crop Sci Biotech.,* **12**: 168-178.

Khrisnareddy M. 2013. Impact of climate change on insect vectors and vector-borne plant viruses and phytoplasma. In: Singh HCP, Shivashankara KS, and Rao NKS (Eds.), Climate-Resilient Horticulture: Adaptation and Mitigation Strategies**.** Springer. India, pp. 255-278.

Kumar P, Gupta VK, Misra AK, Modi DR and Pandey BK. 2009. Potential of Molecular Markers in Plant Biotechnology. *Plant Omics.,* **2(4)**: 141–162.

Laia ML, Alfenas AC, Brommonschenkel S, Oda S, de Melo EJ, Silva IMDA, Goncalves JF and Marques A. 2015. Cloning and characterization of gene-resistant analogs (RGAs) involved in rust (*Puccinia psidii)* resistance in *Eucalyptus grandis. Afr J Agric Res.,* **10**:1957-1964.

Maiti S, Basak J, Kundagrami S, Kundu A and Pal A. 2011. Molecular marker-assistes genotyping of *Mungbean yellow mosaic India virus* resistant in germplasm of mingbean and urdbean. *Mol Biotechnol*., **47**: 95-104.

Maruthi MN, Rekha AR, Mirza RS, Alam SN and Colvin J. 2007. PCR-based detection and partial genome sequencing indicate high genetic diversity in Bangladeshi *Begomovirus*es and their whitefly vector, *Bemisia tabaci*. *Virus Genes.*, **34**: 373-385.

Meija L, Teni RE, Vidavski F, Czoznek H, Lapidot M, Nakhla M and Maxwell D. 2005 Evaluation of tomato germplasm and selection of breeding lines for resistance to *Begomovirus*es in Guatemala. *Acta Hort.*, **695**: 1-5.

Mizutani T, Daryono BS, Ikegami M and Natsuaki K. 2011. First Report of Tomato leaf curl New Delhi virus Iinfecting Cucumber in Central Java, Indonesia. *Plant Dis.*, **95**:1485.

Nevame AYM, Xia L, Nchongboh CG, Hasan MM, Alam MA, Yongbo L, Wenting Z, Yafei H, Emon RM, Ismail MR, Efisue A, Gang S, Wenhu L and Longting S. 2018. Development of a new molecular marker for the resistance to Tomato yellow leaf curl virus. Biomed Res Int., **1**: 1-10.

Park SO and Crosby KM. 2004. Development of RAPD marker linked to the male-sterile *ms-3* Gene in Melon. *Acta Hort.*, **637**: 243-249.

Polston JE and Anderson PK. 1997. The emergence of whitefly-transmitted geminiviruses in tomato in the western hemisphere. *Plant Dis.*, **81**: 1358-1369.

Ruguenius R, Siksnianas T, Stanys V and Bendokas V. 2006. Use of RAPD and SCAR markers for identification of strawberry genotypes carrying red stele (*Phytophtora fragarie*i) resistance gene *Rpf1*. *Agron Res.*, **4**: 335-339.

Saez C, Esteras C, Martinez C, Ferriol M, Dhillon NPS, Lopez C and Pico B. 2017. Resistance to tomato leaf curl New Delhi virus in melon is controlled by a major QTL located in chromosome 11. *Plant Cell Rep.*, **36**: 1571-1584.

Sawangjit S, Chatchawankanphanich O, Chie so bat P, Attathom T, Dale J and Attathom S. 2004. Molecular characterization of tomato-infecting *Begomovirus*es in Thailand. *Virus Res.*, **109**:1-8.

Seal SE, vanden Bosch F and Jeger MJ. 2006. Factors influencing *Begomovirus* evolution and their increasing global significance: Implications for sustainable control. Crit Rev Plant Sci., **25**:23-46.

Sharma P, Rishi N and Malathi VG. 2005. Molecular cloning of coat protein gene an Indian cotton leaf curl virus (CLCuV-HS2) isolate and its phylogenetic with others members of *Geminiviridae*. *Virus Genes.*, 30:85-91.

Srivasthava MK, Li C and Li Y. 2012. Development of sequence characterized amplified region (SCAR) marker for identifying drought tolerant sugarcane genotypes. *Phytochemistry.*, **6**: 763–767.

Subiastuti AS, Hartono S and Daryono BS. 2019. Detection and identification of *Begomovirus* infecting *Cucurbitaceae* and *Solanaceae* in Yogyakarta, Indonesia. *Biodiversitas.*, **20**:738-744.

Swanson, MM, Varma A, Muniyappa V, and Harrison BD. 1992. Comparative epitope profiles of the particle proteins of whitefly-transmitted geminiviruses from nine crop legumes in India. *Ann. Appl. Biol*., **120**: 425–433.

Tsai W, Shih S, Rauf A, Safitri R, Hidayati N, Huyen BTT and Kenyon L. 2013. Genetic diversity of legume yellow mosaic *Begomovirus*es in Indonesia and Vietnam. *Ann Appl Biol*., **163**: 367-377

Venkataravanappa V, Reddy CNL, Saha S and Reddy MK. 2018. Recombinant Tomato leaf curl New Delhi virus is associated with yellow vein mosaic disease of okra in India. *Physiol Mol Plant Pathol.*, **104**:108-118.

Wasswa P, Otto B, Maruthi MN, Mukasa SB, Monger W and Gibson RW. 2011. First identification of a sweet potato *Begomovirus* (sweepovirus) in Uganda: characterization, detection, and distribution. *Plant Pathol.*, **60**: 1030-1039.

Yadav A, Ahmad J and Ahmad A. 2012. Development of Randomly Amplified Polymorphic DNA-Sequence Characterized Amplified Region Marker for Authentication of Swertia Chirayita, an Endangered Himalayan Plant. *J Plant Mol Biol Biotehnol*., **3**: 27–34.

Yousif MT, Kheyr-Pour A, Gronenborn B, Pitrat M and Dogimont C. 2007. Sources of resistant to watermelon chlorotic stunt virus in melon. *Plant Breed*., **126**: 422-427.

JJBS

Volume 13, Number 2, June 2020
ISSN 1995-6673
Pages 153 - 158

Jordan Journal of Biological Sciences

Phytotoxicity of Zinc-oxide Nanoparticles on Seedling Growth and Antioxidant Activity of Red gram (*Cajanus cajan L.*) Seed

K. V. Pavani*, G. Sai Poojitha and M. Beulah

Department of Biotechnology, Gokaraju Rangaraju Institute of Engineering and Technology, Bachupally, Hyderabad, India

Received March 28, 2019; Revised June 18, 2019; Accepted July 11, 2019

Abstract

The present study is aimed at investigating the effects of zinc oxide nanoparticles (ZnO NPs) on *Cajanus cajan* L. seeds. Seeds were exposed to five different concentrations of ZnO NPs (5, 10,15,20,25 mg/100ml). The results show that at higher concentrations (20, 25 mg/100ml ZnO NPs) there is reduction in the seed germination percentage, root length, shoot length, number of leaves, width of leaves and fresh and dry weight of plant. ZnO NPs had an increased effect on Glutathione Reductase **(**GR) and Guaiacol peroxidase (GPX), Hydrogen peroxide (H_2O_2) and ascorbic acid content, had a decreased effect on Catalase (CAT) activity. Transmission Electron Microscopy studies showed aggregated nanoparticles around the cell wall of the seed, which clearly indicates the absorption of nanoparticles by *Cajanus cajan* L. seed and shows negative effects on seedling growth. Reactive oxygen species (ROS) stress was caused by ZnONPs in seed and leaf. This study shows that direct exposure to ZnONPs causes significant phytotoxicity. This highlights the necessity for safe disposal of wastes containing nanoparticles.

Keywords: Zinc oxide nanoparticles, *Cajanus cajan* L., Seed germination, Antioxidant activity, Transmission Electron Microscopy

1. Introduction

Recent advances in nanotechnology facilitated finding practical applications in biomedical, electronics, agriculture, renewable energy and green technologies (Ma *et al.,* 2015). The unrestricted use of nanoparticles in many aspects of daily life has led researchers to consider the problems and consequences of their environmental impact (Gottschalk *et al.,* 2015). Nanoparticles enter into the environment through effluents, agricultural application, atmospheric deposition, surface runoff or other pathways and will ultimately accumulate in the soil. Exposure modelling indicated that the concentrations of nanoparticles in soil are higher than those in water or air. So soils may be the main source of nanoparticles released into the environment (Gottschalk *et al.,* 2009). Nanoparticles in the soil will interact with plants accumulate in plant biomass, pass through the food chain and accumulate in higher trophic levels of consumers (Zhu *et al.,* 2008). Zn is an important molecule of key enzymes like Cu-Zn SOD (Broadley 2007), metabolism of carbohydrates and protein (Singh *et al.,* 2013). Plants can absorb ZnO nanoparticles (Zhao *et al.,* 2012), and accumulate Zn. They have both positive and negative effects on organisms (Salah and Naif, 2016).

In recent years, research in this area has been focused on the interaction between plants and nanoparticles. The effect of nanoparticles on germination depends on concentrations of nanoparticles and varies from a plant to another. De la Rosa *et al.* (2013) applied different concentrations of ZnONPs on cucumber, alfalfa and tomato, and found that only cucumber seed germination was enhanced. Zhang *et al.* (2015) reported that corn exposed to ZnONPs showed no significant negative physiological effects. Most studies showed that nanoparticles could produce toxic effects above a certain concentration (Rico *et al.,* 2011). Therefore, a better understanding of behavior and impact of nanoparticles on the health of plants and hence on environment is highly demanding (Chow *et al.,* 2005). This study can be helpful in understanding the effects of environmentally released ZnO NPs on *Cajanus cajan L.*

2. Materials and Methods

Zinc oxide nanoparticles of mean size of 100 nm diameter (Sigma Aldrich) was used in the study. Different concentrations of ZnO NPs solutions were prepared by directly suspending the nano-particles in deionised water and magnetic bars were placed in the suspensions for stirring before use to avoid aggregation of the particles.

Cajanus cajan L. (Red gram) was collected from local market. Seeds were surface sterilized with 0.1% sodium hypochlorite for 5 min to prevent any fungal contamination. After that, the seeds were washed with deionised water and dried between two paper towels. The seeds were then soaked in 5, 10,15,20,25 mg/100ml of ZnO NPs solution, deionised water (control) for 8 hours. *Cajanus cajan L.* seeds that are soaked in ZnO NPs solution were sown in pots (20 cm × 40 cm) filled with red soil and a layer of coco peat.

The effect of ZnO NPs on *Cajanus cajan L.* was determined by studying growth (germination percentage,

* Corresponding author e-mail: pavani_20042003@yahoo.co.in.,poojthasai2013@gmail.com; mallula.beualh@gmail.com,.

root and shoot length, leaf length, leaf width, no. of leaves, fresh weight, dry weight) and biochemical (Total Sugars, Reducing Sugars, Protein, chlorophyll**)** parameters on 20th, 40th, 60th and 80th day of experiment. The number of seeds germinated was counted and the germination percentage was calculated by using the following formula:

Germination percentage = (number of seeds germinated / number of seeds sown) *100.

The physiological parameters of the seedlings were analysed in terms of root, shoot length, leaf length and leaf width with the help of standard scale, fresh weight and dry weight with the help of electrical balance. After the fresh weight was taken, the seedlings were kept in a hot air oven at 60 ° C for 48 hrs then the weight of dry matter was recorded.

Protein content was determined by the method of (Lowry et al., 1951) Total Sugars, Reducing Sugars and chlorophyll were estimated by the recommended methods of (AOAC, 2000). Experiments were carried out in triplicate.

2.1. Antioxidants Enzymes

Antioxidant potential was investigated through monitoring the activity of different antioxidative enzymes including, catalase (CAT), Guaiacol Peroxidase (GPX), Glutathione Reductase (GR) and Hydrogen Peroxide (H_2O_2), Ascorbic acid.

2.2. Enzyme extraction

0.2g of sample (seed and leaf) was homogenized in 2 ml of extraction buffer having 50mM sodium phosphate with pH 7.0, 0.1% phenyl methyl sulfonyl fluoride (PMSF) and 0.1% EDTA. The homogenate was centrifuged at 12000g for 25 minutes and the supernatant was used as enzyme source.

2.3. Giaiacol peroxidase (GPX)

Guaiacol peroxidase was assayed following (Chance and Maehly, 1955) method. A reaction mixture consisting of 50mM phosphate buffer (pH 7.0) 20mM guaiacol, 10mM H_2O_2 and 100 µl enzyme extract was used to measure POX activity. Guaiacol peroxidase activity was measured by the increase in absorbance at 470nm (A_{470}) due to guaiacol oxidation. One unit of POX is defined as the amount of enzyme need to convert 1 µmol. Of H_2O_2 min^{-1} at 25°C. It is expressed as µ mol. Guaiacol/min-1g-1 FW or activity U/g FW.

2.4. Catalase (CAT)

Catalase enzyme activity was measured by following (Aebi, 1984) method. A reaction mixture having 50mM Sodium Phosphate buffer (pH 7.0) and 50 µl of enzyme extract was utilized to this mixture. 10mM H_2O_2, was added gradually and its consumption was measured for 2 minutes to measure CAT activity. CAT activity was assayed by following the decline in absorbance of H_2O_2 at 240nm (A_{240}). One unit of activity is defined as the amount of enzyme that catalyses the oxidation of 1 µmol. Of H_2O_2 min^{-1} under the assay conditions. It is expressed as µ mol. H_2O_2 / mg protein min^{-1} or activity U/g FW.

2.5. Glutathione Reductase (GR)

Glutathione reductase was assayed using (Carlburg and Mannervik, 1985) method. 50mM Tris-HCl buffer (pH 7.5), 3mM MgCl2, 0.5mM GSSG, 0.2mM NADPH and 250µl of enzyme extract was taken and made up to 1.5ml reaction mixture. GR activity was determined by monitoring the oxidation of NADPH at 340nm (A_{340}).

2.6. Hydrogen Peroxide (H2O2)

Hydrogen peroxide activity was determined by the (Velinkovar *et al.*, 2000) method. 500mg leaf sample weighed and homogenized in an ice cold bath wih 5 ml of 0.1% (w/v) trichloroacetic acid. The homogenate was centrifuged at 10,000g for 15 minutes and 0.5ml of the supernatant was added to 0.5 ml of 10mM potassium phosphate buffer (pH 7.0) and 1 ml of 1M KI. The absorbance of the supernatant was measured at 390nm.

2.7. Ascorbic acid

Ascorbic acid activity was determined using (Oser, 1979) method. 0.1g leaf was homogenized in 6% TCA. From the homogenate, 4ml was taken and to this 2ml of 2%DNPH, 1 drop of 10% thiourea was added. The content was boiled for 15 minutes in water bath and cooled. After cooling, 5ml of 80% (v/v) H_2SO_4 was added. The absorbance was read at 530nm. 2% DNPH (2,4 dinitrophenyl hydrazine) was prepared by dissolving 2g of DNPH in 100ml of 0.5 N H_2SO_4. 10% thiourea was prepared by dissolving 10g in 100ml of 70% ethanol.

2.8. TEM analysis

In 25mg/100ml ZnO NPs solution, red gram seeds were soaked for 8 hrs and later fixed in 2.5% gluteraldehyde in 0.1M phosphate buffer(PH 7.2). The samples were fixed for 24 h at 4°C, and rinsed with PBS for 4 times each sample and then fixed in 1% aqueous Osmium Tetroxide, later rinsed for 6 times with distilled water. This was followed by dehydration in series of graded alcohols and later infiltrated with in araldite 6005 resin or spur resin(spur,1969) . For polymerization samples were incubated for 72h at 80°C. Ultra-thin (60 nm) sections were made with a glass knife on ultra-microtome (Leica Ultra cut UCT-GA-D/E-1/00), mounted on copper grids and stained with saturated aqueous Urenyl acetate (UA) and counter stained with Reynolds lead citrate (LC) **(**John J, 1998**)**. The samples were viewed and photographed under TEM(Hitachi, H-7500 from JAPAN) at required magnifications.

2.9. Statistical Analysis:

Data recorded from three replications were subjected to single way analysis of variance (ANOVA) and critical differences were calculated at p=0.05 level.

3. Results

The desired concentrations (5, 10 ,15,20 and 25mg/100ml ZnONPs) used to testify their effect on growth parameters of *Cajanus cajan* L. Seedlings were selected based on a preliminary test on seed germination. The seedling growth parameters have been considered as primary indicator for the phytotoxicity of ZnONPs, especially in 80 days with higher concentrations. Significant decrease in the germination percentage, root length, number of leaves, width of leaves and increase in fresh and dry weight of plant was observed upon exposure to higher concentrations of ZnONPs. On the other hand, the results showed that the exposure of red gram seeds upto 15mg/L of ZnONPs exhibited a significant increase in

the growth of root and shoot length and number, length and width of leaves as compared to higher concentrations (25 mg/Lof ZnONPs). The results indicated that nano-ZnO in an appropriate concentration promoted root and shoot length of red gram(Fig.1-4).

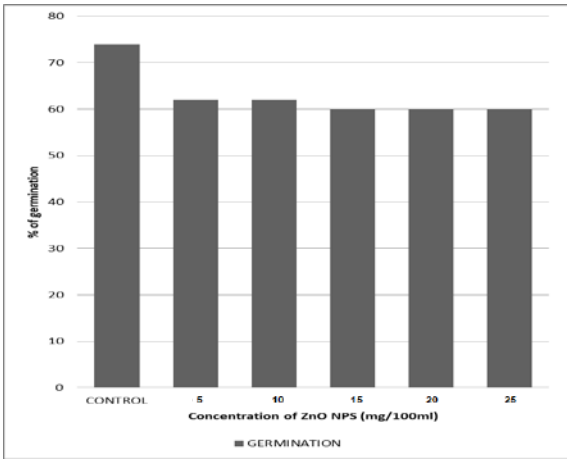

Figure 1. Germination % of *Cajanuscajan L.* grown in ZnO NPs

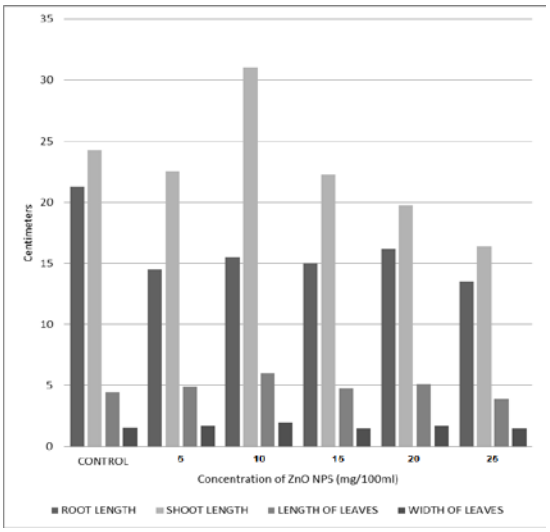

Figure 2. Lengths of Roots, Shoots and Leaves, and Widths of Leaves of *Cajanuscajan L.* grown in ZnO NPs

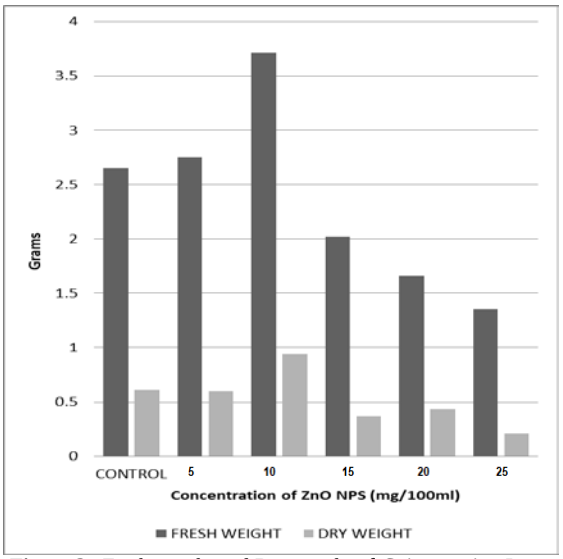

Figure 3. Fresh weight and Dry weight of *Cajanuscajan L.* grown in ZnO NPs

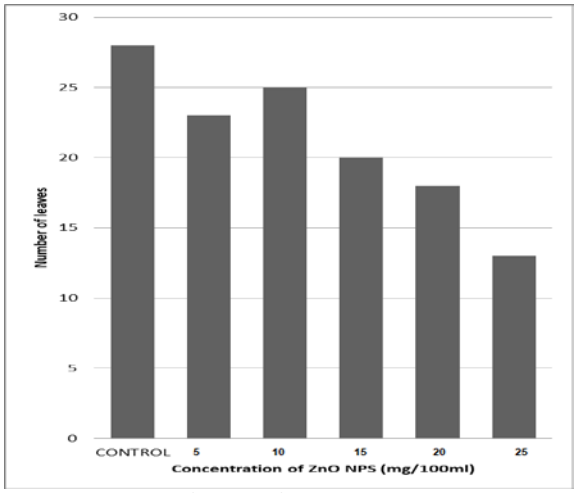

Figure 4. Number of Leaves of Cajanuscajan L. grown in ZnO NPs

In this study, a significant increase in carbohydrate, protein and chlorophyll of red gram seeds was found in response to the application of ZnONPs. The highest reducing sugars and protein content was recorded for seeds treated with 10 mg/100ml ZnONPs (Fig.5). Compared with the control, the chlorophyll content was found to be significantly increased in the plants grown with the 25 mg/100ml ZnO NPs treatment (Fig.6).

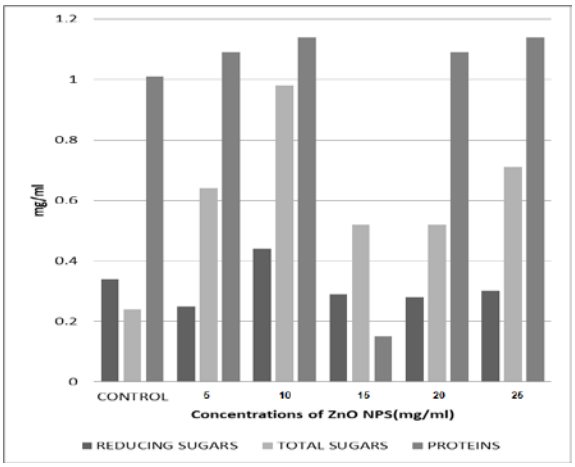

Figure 5. Reducing Sugar, Total sugar and Protein content of *Cajanuscajan L.* grown in ZnO NPs

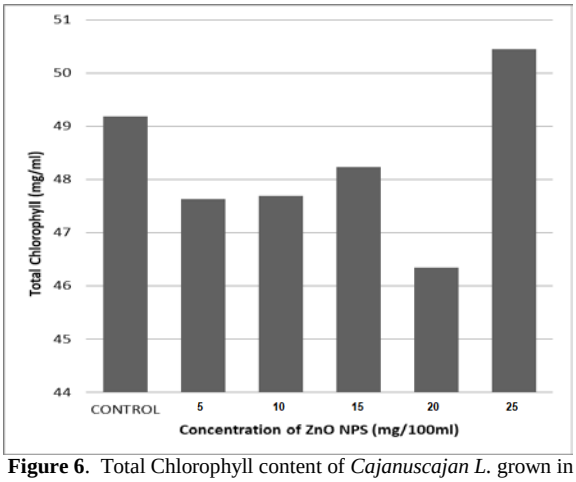

Figure 6. Total Chlorophyll content of *Cajanuscajan L.* grown in ZnO NPs

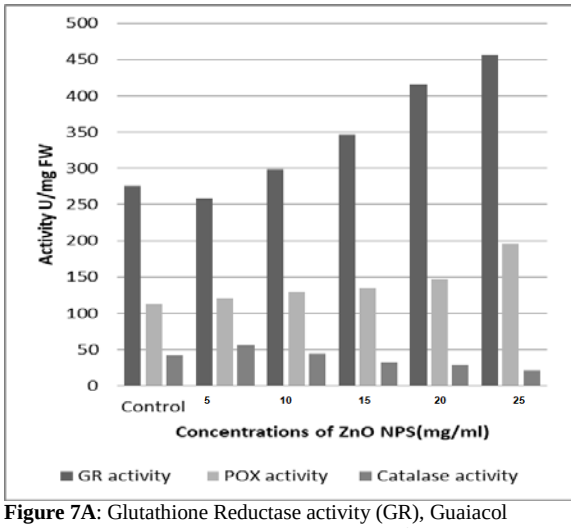

Figure 7A: Glutathione Reductase activity (GR), Guaiacol peroxidase (POX) activity, Catalase activity of *Cajanuscajan L.* Seed grown in ZnO NPs.

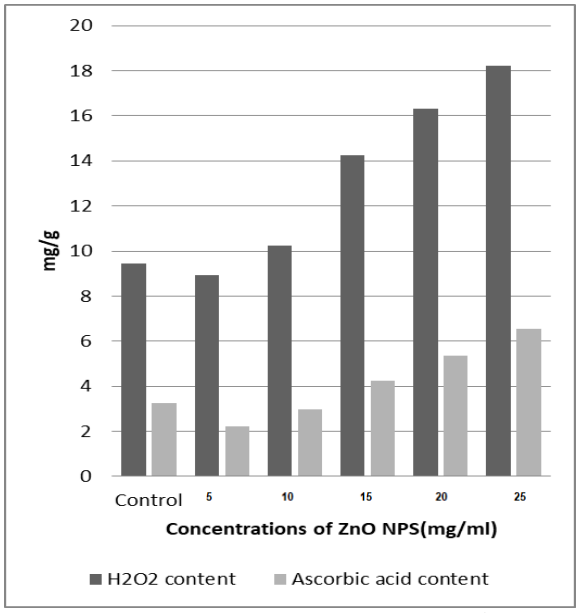

Figure 7B. H_2O_2 content and Ascorbic Acid content of *Cajanuscajan L.* Seed grown in ZnO NPs.

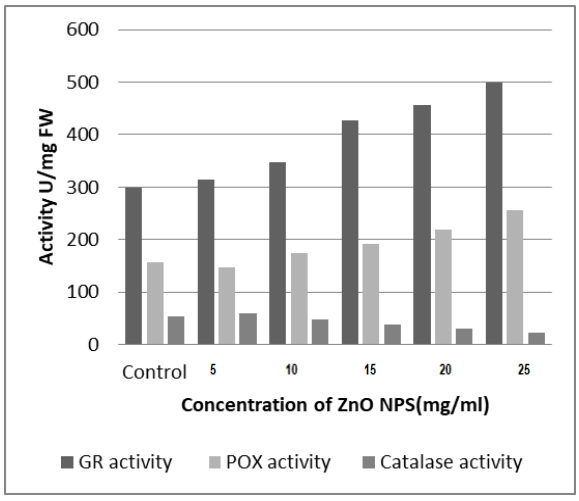

Figure 8A. Glutathione Reductase activity(GR), Guaiacol peroxidase (POX) activity, Catalase activity of *Cajanuscajan L.* Leaf grown in ZnO NPs

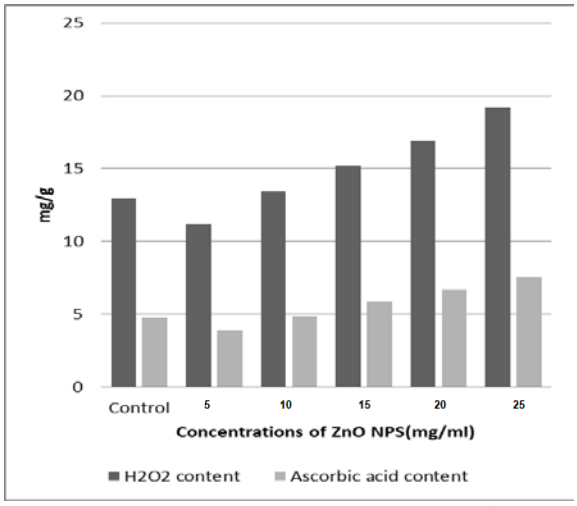

Figure 8B. H_2O_2 content and Ascorbic Acid content of *Cajanuscajan L.* Leaf grown in ZnO NPs.

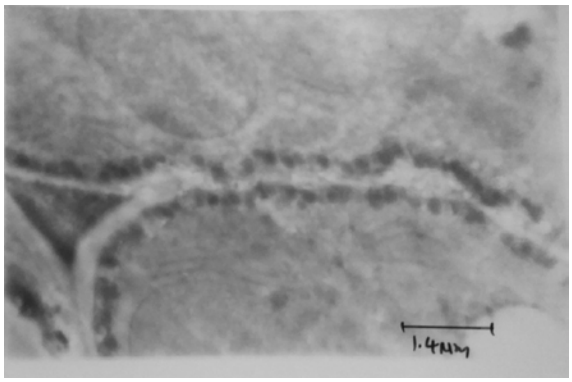

Figure 9. TEM image of red gram seed (Magnification: 13510X)

The activity of key antioxidant enzymes including, GR, GPX,CAT, Hydrogen Peroxide and Ascorbic acid in *Cajanus cajan L.* seeds that were grown in the presence of zinc oxide nanoparticles were analyzed. The activity of GR, POX and Hydrogen Peroxide was increased up to 25 mg/100 in seed compared to the control, whereas activities of CAT and Ascorbic acid were increased for concentrations up to 10 mg/100ml and were decreased with increasing NPs concentration. As shown in (Fig.7A-7B). GR, POX, Hydrogen Peroxide and Ascorbic acid activity in *Cajanus cajan L.* leaf in higher concentrations was significantly higher in comparison to the control. This is contrary to CAT activity. CAT activity is significantly decreased in the presence of NPs, except for 10 mg/100ml treatment. It should be noted that at the highest concentration, the activity for every antioxidant enzymes was significantly increased (Fig.8A-8B).

TEM analysis of the *Cajanus cajan L.*seeds treated with 25 mg/ml ZnONPs revealed clusters of nanoparticles along the cell wall of seed cells (Fig.9). Nanoparticles of different sizes were found inside the cell, however average size of 1.4 µm were predominantly recorded.

4. Discussion

Objectives of the present study were to investigate the effects of ZnONPs on the growth of red gram. On exposure to ZnONPs, our results had shown significant impact on the seed germination and seedling growth of red gram. (Lin and Xing, 2007) reported that ZnO NPs

inhibited seed germination in *Lolium multiflorum* and *Zea mays*. The damage to the structure of roots at higher concentration may be the reason for the germination of the seeds (Kwang *et al.*, 2018). Lee e*t al.* (2008) also found that the seedling growth parameters of mung bean and wheat plants were significantly decreased due to the presence of copper nanoparticles. Zhongzhou Yang *et al.* (2015) reported that there is no inhibition effect of ZnONPs on root and shoot length of rice. Mechanism of metal oxide NP phytotoxicity was related to the type of nanoparticles, test plants, concentration, chemical composition, surface modification and particle size (Brunner *etal.*, 2006). Sharma *et al.* (2012) also observed that AgNPs increased plants growth profile and biochemical attributes of common bean and corn.

ZnONPs treated red gram showed improvement in reducing sugars, total sugars, protein and chlorophyll content. Tarafdar (2013) reported that ZnONPs induced a significant improvement in *Cyamopsis tetragonoloba* chlorophyll and protein synthesis. But significant reduction of total chlorophyll and total protein contents were observed under the higher concentrations of AgNPs (Asma *et al.*, 2018). Mechanism of action of different kinds of nanoparticles is unclear in different plants (Mohamed *et al.*, 2014). The increase in biochemical parameters illustrate the importance of zinc in protein synthesis, chlorophyll production and activation of many enzymes on the biosynthetic pathway of secondary metabolites (Sasan and Sevedeh, 2017).

With increased concentration of ZnONPs, the activities of antioxidative enzymes increased in the seed and leaf except catalase and H_2O_2. Such increase in antioxidative enzyme activity may be due to the stress over the seedlings of *Cajanus cajan L.* Metal stress commonly generates toxic free radicles and superoxides and activates the production of anti-oxidative stress enzymes. These enzymes scavenge the ROS by reduction reaction and protect cells from any damage (Gao *et al.*, 2013; Garcia-Sanchez *et al.*, 2015). GPX, GR activity increased in Faba bean *(Vicia faba L)* seedling treated with ZnONPs (Salah M. H. Gowayed and Naif M. Kadasa, 2016). Repression of catalase might be caused by the accumulation of H_2O_2 (Yi *et al*., 2003). H_2O_2 can play an important role in the induced tolerance against oxidative stress by activation of the plant antioxidant system in a dose dependent manner. Reduced catalase activity can be compensated by alternative H_2O_2-scavenging mechanisms such as increased ascorbate peroxidase and glutathione peroxidase levels (Willekens *et al*., 1997).

The micrographs of the seed sections clearly show that the cell wall acts as primary accumulation sites for NPs. These results strongly point toward possible transformations and/or aggregation of ZnO NPs during or after their internalization. The TEM image clearly shows the transport of nanoparticles into the seeds, which is responsible for decrease in growth parameters and enhanced antioxidant activity.

5. Conclusion

ZnONPs caused significant inhibition on *Cajanus cajan.* L. seed germination, shoot and root growth, ZnONPs caused significant inhibition on *Cajanus cajan.L.* seed germination, shoot and root growth, number of leaves, fresh and dry weight of plants upon exposure to higher concentrations. But sugars, protein and chlorophyll content increased with higher concentrations. We also observed increase in Glutathione Reductase and Peroxidase activity, H_2O_2 and ascorbic acid content. But upon exposure to higher concentrations of ZnONPs, decrease in catalase activity of seeds and leaves of *Cajanus cajan.L.* was observed. TEM image of red gram clearly showed translocation of ZnONPs into the seed. According to our results, we can conclude that inhibition of seedling growth and antioxidant activity differ significantly with the nanoparticle concentration. It can be speculated that the toxic effects of ZnONPs on plants is due to formation of ROS, following the NPs uptake. Since red gram is the most staple food, NPs can find their way into the human body and interact with the cells with unexpected consequences. Therefore, more investigations are needed to determine the positive or negative effects of ZnONPs on red gram/ plants.

Acknowledgements

The authors acknowledge University Grants Commission (UGC) for the financial support under UGC minor project and Sri Venkateswara Veterinary University for the technical assistance during TEM analysis.

References

Aebi H. 1984. Catalase. Methods in Enzymology .**105**:121–126.

AOAC. Official methods of analysis. 200. AssoOffi Anal Chem, Arlington, VA.

Asma A Al-Huqaila, Maysa M Hatatab, d Arwa A AL-Huqail C and Mohamed M Ibrahimd. . 2018.Preparation, characterization of silver phyto nanoparticles and their impact on growth potential of Lupinus termis L. Seedlings. *Saudi J Biol Sci,* **25(2)** : 313–319.

Broadley M R. 2007. Zinc in plants. *New Phytologist,* **173**: 677–702.

Brunner TJ , Wick P, Manser P, Spohn P , Grass R N, Limbach LK, Bruinink A, Stark WJ.2006. In vitro cytotoxicity of oxide nanoparticles: Comparison to asbestos, silica, and the effect of particle solubility. *Environ. Sci. Technol,* **40**: 4374–4381.

Carlberg I and Mannervik B. 1985. Glutathione reductase. In: Meister, A. (ed.), Methods in Enzymology. Academic Press, New

York. **113:** 484–490.

Chance B and Maehly SK. 1955. Assay of catalase and peroxidase. Methods Enzymol. **2:** 764-775.

Chow JC, Watson JG, Savage N , Solomon CJ, Cheng YS, McMurry PH, Corey LM , Bruce GM, Pleus RC, Biswas P and Wu CY. 2005. Nanoparticles and the Environment. *Journal Air and Waste Management Association*,**55**:1411–1417.

De la Rosa G, Lopez-Moreno ML, De Haro D, Botez CE, Peralta-Videa JR, Gardea-TorresdeyJL 2013. Effects of ZnO nanoparticles in alfalfa, tomato, and cucumber at the germination stage: root development and X-ray absorption spectroscopy studies. *Pure Appl Chem,* **85(12):** 2161–2174.

Gao J , Xu G, Qian H, Liu P , Zhao P and Hu Y. 2013. Effects of nano-TiO2 on photosynthetic characteristics of Ulmuselongata seedlings. *Environ Pollut,* **176:** 63–70.

Garcia-Sanchez S, Bernales I, and Cristobal S. 2015. Early response to nanoparticles in the Arabidopsis transcriptome compromises plant defence and root-hair development through salicylic acid signalling. *BMC Genomic.,* **16 (341)** : 2-16.

Gottschalk F, Lassen C, Kjoelholt J, Christensen F, Nowack B. 2015. Modeling flows and concentrations of nine engineered nanomaterials in the Danish environment. *Int J Environ Res Public Health*, **12**:5581–5602.

Gottschalk F, Sonderer T, Scholz RW, Nowack B. 2009. Modeled environmental concentrations of engineered nanomaterials (TiO2, ZnO, Ag, CNT, fullerenes) for different regions. *Environ Sci Technol*, **43** : 9216–9222.

John J Bozzola and Lonnie DRussell. 1998. In: Electron Microscopy Principles and Techniques for Biologists 2nd Edn. Jones and Bartlett Publishers, Sudbury, Massachusetts. 19 - 45 and 72 - 144.

Kwang-Yeol Yang, Stephanie Doxey, Joan E McLean, David Britt, Andre Watson, Dema Al Qassy, Astrid Jacobson, Anne J Anderson. 2018.Remodeling of root morphology by CuO and ZnO nanoparticles: effects on drought tolerance for plants colonized by a beneficial pseudomonad. *Botany*, **96(3)** : 175-186.

Lee WM, An YJ, Yoon H, Kweon HS. 2008. Toxicity and bioavailability of copper nanoparticles to the terrestrial plants mung bean (Phaseolusradiatus) and wheat (Triticumaestivum): plant agar test for waterinsoluble nanoparticles. *Environ Toxicol Chem*, **27:**1915–1921.

Lowry OH, Rosebrough NJ, Farr NJ, Randall RJ. 1951. Protein measurement with the folin phenol reagent. *J BiolChem* , **193:** 265-275.

Lin D and Xing B. 2007. Phytotoxicity of nanoparticles inhibition of seed germination and root growth. *Environmental pollution*, **150** : 243-250.

Ma C, White JC, Dhankher OP, Xing B. 2015. Metal-based nanotoxicity and detoxification pathways in higher plants. *Environ Sci Technol*, **49:**7109–7122.

Mohamed MI, Amal AH, Afaf IS, Gehan AE, Abdul-Aziz A, Farid MA, Humaira HR, Nadine, M. 2014. Synthesis of eco-friendly silver nanoparticles using plant extracts and assessment of their antimicrobial activity. *Fresenius Environ. Bull*, **23 (1a):** 184–189.

Oser B L. 1979. Hawk's Physiological Chemistry. Mc Graw Hill, New York, pp.702-705.

Rico CM, Majumdar S, Duarte-Gardea M, Peralta-Videa JR, GardeaTorresdey JL. 2011. Interaction of nanoparticles with edible plants and their possible implications in the food chain. *J Agric Food Chem*, **59:**3485–3498.

Salah M H Gowayed and Naif M. Kadasa.2016. Effect of Zinc oxide aseedling exposed to Cadmium *Life Science Journal*, **13(3):** 18-27.

Sasan M Sevedeh Sara M . 2017. Zinc Sulphate and Nano-Zinc Oxide Effects on Some Physiological Parameters of *Rosmarinus officinalis. Astrophysical journal Supplement*, **8**,2635-2649.

Sharma P, Bhatt D, Zaidi MG, Saradhi P, Khanna P,Arora PK. 2012. Silver nanoparticlemediated enhancement in growth and antioxidant status of *Brassica juncea. Appl. Biochem. Biotechnol*, **167:**2225–2233.

Singh N B, Nimisha Amist, Kavita Yadav, Deepti Singh, Pandey JK, and Singh SC. 2013. Zinc Oxide Nanoparticles as Fertilizer for the Germination, Growth and Metabolism of Vegetable Crops. Journal of Nanoengineering and Nanomanufacturing. **3:** 353–364.

Spurr AR. 1969. *J. Ultrastructural Res.*, **26:** 311.

Torney F, Trewyn BG, Lin VS-Y, Wang K .2007. Mesoporous silica nanoparticles deliver DNA and chemicals into plants. *Nature Nanotechnolgy*, **2**:295–300.

Velikova V, Yordanov I and Edreva A. 2000. Oxidative Stress and Some Antioxidant Systems in Acid Rain-Treated Bean Plants: Protective Role of Exogenous Poly-amines. *Plant Science.*, **151:** 59-66.

Willekens H, Chamnongpol S, Davey M, Schraudner M, Langebartels C, Montagu MV, Inze D, Camp WV. 1997. Catalase is a sink for H_2O_2 and is indispensable for stress defense in C3 plants. *EMBO J.*, **16:** 4806-4816.

Yi SY, Yu SH, Choi D, 2003. Involvement of hydrogen peroxide in repression of catalase in TMV-infected resistant tobacco. *Molecules and Cells* , **15**: 364-369.

Zhao L, Peralta-Videa JR, Ren M, Varela- Ramirez A, Li C , Hernandez-Viezcas J A, Aguilera RJ, Gardea-Torresdey JL. 2012. Transport of Zn in a sandy loam soil treated with ZnO NPs and uptake by corn plants: Electron microprobe and confocal microscopy studies. *Chemical Engineering Journal*, **184** : 1– 8.

Zhongzhou Yang , Jing Chen , Runzhi Dou , Xiang Gao , Chuanbin Mao and Li Wang . 2015. Assessment of the phytotoxicity of metal oxide nanoparticles on two crop plants, maize (*Zea mays L.*) and rice (*Oryza sativa L.) International J ournal of Environmental Research Public Health* , **12** : 15100–15109. doi:10.3390/ijerph121214963.

JJBS

Volume 13, Number 2, June 2020
ISSN 1995-6673
Pages 159 - 164

Jordan Journal of Biological Sciences

Antibacterial Activity and Chemical Composition of *Arum hygrophilum* Boiss Crude Extracts

Hatim M. Jaber , Khawla D. Al-Hamaideh., Hala I. Al-Daghistani , Nabil H. Amer , Moayyad N. Nassar , Saleh MH. Abd Al–Latif and Abdulameer HD. Al-Nuaimi *

Department of Basic Medical Sciences, Faculty of Medicine, Al-Balqa Applied University, P.O.Box: Al-Salt 19117Jordan.

Received June 6, 2019; Revised July 8, 2019; Accepted July 11, 2019

Abstract

Plants are an important origin of novel pharmacological compounds. In Jordan, *Arum hygrophilum* Boiss plant is utilized as food and used as traditional medicine for the management of many diseases. This study was designed to evaluate the antibacterial activity and investigate the chemical components of *Arum hygrophilum* Boiss extracts. Water, methanol and ethanol extracts of the plant were prepared and dissolved in Dimethyl sulfoxide to a final stock concentration of 500mg/ml. The antibacterial effect of the extracts was performed using the well diffusion method against the following bacteria: *Staphylococcus aureus, E.coli, Pseudomonas aeruginosa, Enterococcus faecalis, Klebsiella pneumonia, Salmonella typhi.* In addition, antifungal activity was studied using *Candida albicans, Candida tropicalis, Candida krusei,* and *Candida rugose.* As compared with the standard inhibition zone of some antibiotics, the water extract exhibited a significant inhibition zone against *P. aeruginosa* (30 mm ± 3.0), whereas methanol extract showed significant inhibition zones against *P. aeruginosa* (21± 2.5 mm) and against *E. faecalis* (15 ± 0.37mm). No antifungal activity was detected in all plant extracts. Chemical compounds identification was carried out applying Gas Chromatography-Mass Spectroscopy (GC-MS) analysis. Test of the extracts revealed the presence of 21 chemical components in the methanol extract, 11 compounds were detected in the water extract and 23 compounds in the ethanol extract. Among these chemicals, alkaloids were detected; two in methanol extract, (3H)-Pyrimidinone and pyrrolidin-2-one and one alkaloid in the water extract, 1H-Imidazole, 2-ethyl-4,5dihydro. The water extract also contained Tert-butyl hydroxy anisole (phenolic compound). Other important components included: Tetrahydropyranis in methanol extract, Butanoic acid in methanol and water extracts, and 2-amino-1,3-propanediol in the water extract. Since the global scheme is now changing towards the use of traditional plant products to control infectious diseases, we believed that the findings in this study are promising, providing a therapeutic potential, and should be further investigated for their medicinal applications.

Keywords: Medicinal plants, Arum *hygrophilumb* Boiss, Antimicrobial activity, Chemical components of plant extracts, Gas Chromatography- Mass Spectrometry analysis (GC-MS).

1. Introduction

Plants are widely used for a variety of purposes in all human cultures; they are utilized as food, culinary spices, medicinal herbs, and cosmetic products. It was announced that about 80% of people in developing countries are using the plants and their extracts as a primary source of healthcare and traditional medical practice (Bodeker *et al.*, 2005). Worldwide, there are about four billion people depending on herbal drugs; some are used for the treatment of chronic diseases such as diabetes, some neurological disorders and cancer (Salim *et al.*, 2008; Lahlou, 2013).

Medicinal plants are an important source for drug discovery; moreover, many newly approved drugs were generated from certain habits of different cultures (Balunas and Kinghorn, 2005). In the field of infectious diseases, 75% of the used drugs are of natural origin; they are in the top 35 worldwide selling ethical drug sales of 2000-2002 (Rates, 2001; Newmann *et al.*, 2003; Balunas and Kinghorn, 2005). In cancer treatment area, 62% of the consumed drugs are of natural origin (Balunas and Kinghorn, 2005).

Despite the progressive increase in the literature on phytochemistry, only a small number of plant species has been screened biologically. There are still a huge number of plants waiting for future investigation, particularly with the development of highly sensitive analytical screening methods (Evans, 2002; Balunas and Kinghorn, 2005).

Jordan is located at the junction of four different biogeographical sectors: the Sudanian or tropical, the Saharo-Arabian, the Irano-Turanean and the Mediterranean (Alali *et al*., 2006; Alali *et al*., 2008; Feinbrun-Dothan,1986; Al Eisawi, 1998); it is known for its various typography and climate. Jordan is rich and biodiverse in its flora and fauna; where 2,500 plant species of about 900 genera and 140 families were documented, it is nearly 20% of the overall flora that are used in tradition medicine (Oran, 2015). In Jordan, a restricted number of plants has been chemically investigated for their biological

* Corresponding author e-mail: abdulameerh@bau.edu.jo & abdulameerh@yahoo.com.

activities (Hudaib and Aburjai, 2007; Abu-Dahab and Afifi, 2007; Quran, 2009).

Araceae plant family (arum family) has 107 genera and over 3700 species that are distributed worldwide (Afifi *et al*., 2017). In Jordan, four arum species were mentioned in the list of flowering plants of Jordan, they are *Arum hygrophilum*, *Arum dioscorides*, *Arum elongatum* and *Arum palaestinum* (Al-Eisawi, 2013). These four species are collectively called Louf. Jordan's Louf is utilized as spices and cooked like leafy crops; it is used in folk medicine to treat cases with cancer, circulatory system, obesity, internal bacterial infection, diabetic symptoms and poisoning problems.

Arum grows naturally in the mountains, rocky places, forests, red soils, alluvial soils, near water canals, and in the upper Jordan Valley. It is also available in many areas including: Ajlun, Jarash, Irbid, Al-Balqa', Wadi-Shua'ib, in addition to Amman (Al-Eisawi, 1998).

Only few reports are available on the chemical and biological characteristics of Arum species (Afifi *et al*., 2017). Extracts of *Arum palaestinum* were found effective against leukemia (k562) and colon cancer (Hatmal*et al*., 2017); fortified *Arum palaestinum* Boiss had blocked the growth of prostatic tumors in mice (Cole *et al*., 2015). Antimicrobial effect of *Arum palaestinum* was also detected by Afifi *et al*. (1997). Antibacterial effect of *Arum maculatum* leave extracts was also detected by Mansour *et al.* (2015). Extract obtained from *A. hygrophilum* revealed some biological activity *in vitro* and *in vivo*. It inhibits the gastrointestinal enzymes involved in the digestion and absorption of carbohydrate and lipid. In addition, it augmented β-cell proliferation in a dose dependent manner (Afifi *et al.*, 2017).

This project was designed to evaluate the antibacterial activity and investigate the chemical composition of *Arum hygrophilum* Boiss stem and leave extracts.

2. Materials and Methods

2.1. Preparation of Plant Extracts

Stems and leaves of *Arum hygrophilum* Boiss were collected from Al- Salt region in Jordan in the flowering period from March to April, 2018. The harvested plant parts (stems and leaves) were thoroughly washed, chopped into bits, dried and grinded using a blender. Aliquots of 10g dry powdered plant material were extracted with 100ml of solvent by refluxing method. The following solvents were used; hot water, methanol and ethanol for 72h at room temperature (except for hot water at 50C°) with continuous shaking at 170rpm. All extracts were filtered through white canvas and filter units of 0.22-0.45μm pore size. Thereafter, solvents were evaporated using rotary evaporator; the crude extracts weighed and dissolved in Dimethyl sulfoxide (DMSO) to a final stock concentration of 500 mg/ml, and kept at 4°C until use.

2.2. Antibacterial and Antifungal Activity of the Extracts

2.2.1. Agar well diffusion method

Antibiotic assay was performed on Petri dishes containing 20 ml of Mueller Hinton (MH) agar. Following the guidelines given by the Clinical and Laboratory Standards Institute (CLSI, 2018), test cultures of *Staphylococcus aureus* (ATCC 29213), *E.coli* (ATCC 25922), *Pseudomonas aeruginosa* (ATCC 27853), *Enterococcus faecalis* (ATCC 51299), *Klebsiella pneumonia*, *Salmonella typhi*, *Candida albicans*, *Candida tropicalis*, *Candida krusei*, and *Candida rugosa* from overnight growth cultures on nutrient agar were taken and suspended in 3 ml of sterile normal saline; that was to achieve the correct inoculums turbidity that matched 0.5 MacFarland standard turbidity in test tubes. Sterile swab sticks were dipped into the inoculum suspension, and the excess fluid was removed by squeezing the swab against the inner sidewall of the test tube. The swabs were used to streak the entire agar surface of each MH plate; the plates were rotated at 90^o angle each time to ensure an uniform distribution of the inoculums over the whole agar plate. The plates were then allowed to dry for two minutes. Four holes with a diameter of 8 mm were punched aseptically in the agar with a sterile tip; then a volume of 150 µL of each arum extract, water, methanol and ethanol and the control Dimethyl sulfoxide (DMSO) solvent were introduced into a well. Petri-dishes were incubated overnight at an optimum temperature of 37^{o}C for 24 hours. Zones of inhibition were scored depending on the activity of antimicrobial compounds in each extract. Experiments were repeated three times and the inhibition zones were recorded as a mean and compared with the positive control.

2.3. Identification of chemical compounds

Chemical screening of the active compounds present in water, ethanol, and methanol extracts was analyzed using GC-MS analysis. Each sample was reconstituted using 1 ml Dichloromethane (DCM) (Aldrich Chemical Co. ltd., USA.) and passed through a glass wool to expel the solid materials. GC-MS system consisted of an HP 5890 series II plus GC and 5972 quadruple mass selective detector (MSD), and Vectra XM24/100i computer workstation was used. Forty microliter of the collection in triplicate was transferred into auto-sampler glass vials having Teflon covers, and the composition was analyzed. The injector temperature was 250°C, the injection mode was Splitless, and the running time was 39min. The dilution rate was 1- 5 for methanol and water extracts, whereas ethanol extract was analyzed without dilution. Identification of components was created using a computer program that utilized a similarity index, match factor or purity between the unknown spectrum and standard library spectra.

2.4. Statistical analysis

Results were summarized as mean ± standard deviation. Independent t-test was used for statistical analysis. Results were considered significant when $P < 0.05$

3. Results

3.1. Antibacterial activity of Arum hygrophilum Boiss extracts

Water and methanol plant extracts displayed some antibacterial activity. Using *Pseudomonas aeruginosa* ATCC 27853, water extract revealed inhibition zone (30.0 ± 3.0 mm), followed by methanol extract (21 ±2.5 mm) (Figure 1 and Table 1). No inhibition zone appeared with ethanol and DMSO (the negative control) (Figure 1). The inhibition zone of water extract against *P. aeruginosa* was

significant as compared with the standard inhibition zone of some antibiotics including Tetracycline (12.0 ±1.0 mm) (p = 0.001), Polymyxins B (13.0 ±1.5 mm) (p = 0.001) and Gentamycin (11.0 ±1.5 mm) (p = 0.001). The inhibition zone of water extract was as much as that of Ciprofloxacin (32 ± 3.0 mm), the difference between them is not significant (P = 0.460) (table 2).

Methanol extract reveled a significant inhibition zone against *P. aeruginosa* in comparison to Tetracycline (p = 0.001), Polymyxins B (p = 0.003) and Gentamycin (p = 0.001). Methanol extract also revealed inhibition zone (15.0 ± 0.37 mm) against *E. Faecalis.*

Ethanol extract showed no inhibitory effects against all the tested microorganisms (Table 1).

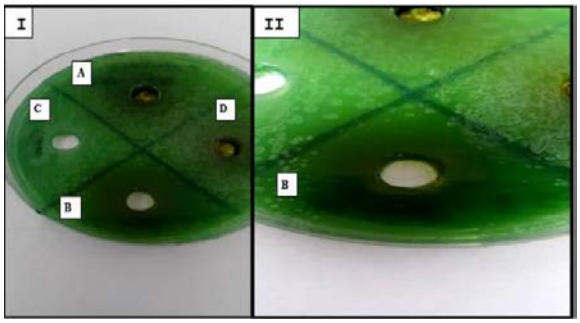

Figure 1.(I) Inhibition zone of *Arum hygrophilum* Boiss on *Pseudomonas aeruginosa* ATCC 27853 using methanol extract (A), water extract (B), ethanol extract (C), and DMSO (D). (II) Inhibition zone of *Arum hygrophilum* Boiss (B) on *Pseudomonas aeruginosa* ATCC 27853 using water extract.

Table 1. Antibacterial activity (zone of inhibition) of different *Arum hygrophilum* Boiss extracts.

Pathogens	Diameter of inhibition zone (mm) mean ± SD		
	Ethanol extract	Methanol extract	Hot water extract
P. aeruginosa	0.0 ± 0.0	21.0 ± 2.5	30.0 ± 3.0
E. coli	0.0 ± 0.0	0.0 ± 0.0	0.0 ± 0.0
E. faecalis	0.0 ± 0.0	15.0 ± 0.37	0.0 ± 0.0
S. aureus	0.0 ± 0.0	0.0 ± 0.0	0.0 ± 0.0
K. pneumoniae	0.0 ± 0.0	0.0 ± 0.0	0.0 ± 0.0
S. typhi	0.0 ± 0.0	0.0 ± 0.0	0.0 ± 0.0
C. albicans	0.0 ± 0.0	0.0 ± 0.0	0.0 ± 0.0
C. tropicalis	0.0 ± 0.0	0.0 ± 0.0	0.0 ± 0.0
C. krusei	0.0 ± 0.0	0.0 ± 0.0	0.0 ± 0.0
C. rugosa	0.0 ± 0.0	0.0 ± 0.0	0.0 ± 0.0

Table 2. The inhibition zone of water extract of *Arum hygrophilum* Boiss (30 ± 3.0 mm) against *P. aeruginosa* as compared with the standard inhibition zone of some antibiotics

Pseudomonas aeruginosa		
Antibiotics	Inhibition zone (mm) Mean ± SD	P – value
Chloramphenicol (30 µg)	R	
Tetracycline (30 µg)	12 ± 1.0	0.001
Trimethoprim (25 µg)	R	
Erythromycin (15 µg)	R	
Clarithromycin (15 µg)	R	
Penicillin G (10 U)	R	
Polymyxins B (15µg)	13 ± 1.5	0.001
Gentamycin (10 µg)	11 ± 1.5	0.001
Kanamycin (10 µg)	R	
Ciprofloxacin (25 µg)	32 ± 3.0	0.460

3.2. Antifungal activity:

All different Arum extracts were tested against pathogenic *Candida spp*. including; *C. albicans, C. tropicalis*, *C. krusei*, and *C. rugose* (isolated from patients at the Jordan University Hospital). No antifungal activity was detected with different extract.

3.3. Identification of Chemical Components of Arum hygrophilum Boiss extracts

GC-MS chromatography was based on the peak area percentages, retention time, molecular formula and molecular weight. It revealed the presence of 21 chemical compounds in the methanol extract (Table 3), 11 compounds in the water extract (Table 4), and 23 compounds in the ethanol extract (Table 5).

Among the detected chemical components of the extracts, two alkaloids (4(3H)-Pyrimidinone, and Pyrrolidin-2-one) were identified in the methanol extract, and one alkaloid, 1H-Imidazole, 2-ethyl-4,5dihydro in the water extract (Tables 3, 4). The water extract further revealed the presence of phenolic compound, Tert-butyl hydroxy anisole (Table 4).

Table 3: Chemical components of methanol extract of *Arum hygrophilum* Boiss detected by GC-MS

NO.	Name of compounds	Molecular formula	Molecular weight
1	1,2- Butanediol	C4H10O2	90
2	1,2-Dideoxy-1-erythro-pentitol	C5H12O3	120
3	3-Methyl-oxirane-2-carboxylic acid	C5H8O3	116
4	3-(Methoxyethoxymethoxy)-2-methylpentan-1	C10H22O4	154
5	Propane,1,2,3- trimethoxy	C6H14O3	134
6	Butanoic acid, 4-(2-methoxy-1-methyl-2-oxoethoxy)-, methyl ester	C9H16O5	204
7	Decene,3,3,4-timethyl	C13H26	182
8	Borane	C7H18BN	127
9	Tridecane, 3-methylene	C14H28	196
10	Cyclobutane, 2-hexyl- 1,1,4-trimethyl	C13H26	182
11	2-Undecene, 3-methyl	C12H24	168
12	4-Cyclopentene-1,3-dione	C5H4O2	96
13	4(3H)-Pyrimidinone	C4H4N2O	96
14	But-1-ene-3-yne,1-ethoxy	C6H8O	96
15	Pentanoic acid,2-methylphenyl ester	C12H16O2	192
16	Pyrrolidin-2-one	C11H15NO2	193
17	Butibufen	C14H20O2	220
18	Tetrahydropyran	C5H10O	86
19	6- Methyl-cyclohex-2-en-1-ol	C7H12O	112
20	Cyclopentane, 1,2,3-trimethyl	C8H16	112
21	Octane, 4,5-dimethyl	C10H22	142

Table 4. Chemical components of water extract of *Arum hygrophilum* Boiss detected by GC-MS

NO.	Name of compound	Molecular formula	Molecular weight
1	2-Amino-1,3-propanediol	C3H9NO3	91
2	Butanoic acid, 4-chloro	C4H7ClO2	122
3	Cyclohexene, bromo	C6H11Br	162
4	1,2-Ethanediol, monoformate	C3H6O3	90
5	1-Cyclopenten-3-one	C8H10O4	170
6	1-Penten-3-one,2-methyl	C6H10O	98
7	4-Hexen-3-one,2,2-dimethyl	C8H14O	126
8	1H-Imidazole, 2-ethyl-4,5dihydro	C5H10N2	98
9	Glycine, N-cyclopropylcarbonyl-, methyl ester	C7H11NO3	157
10	Tert-butyl-hydroxy anisole	C11H16O2	180
11	Cyclohexane	C6H11N3	125

Table 5. Chemical components of ethanol extract of *Arum hygrophilum* Boiss detected by GC-MS

NO.	Name of compounds	Molecular formula	Molecular weight
1	2,2-Bioxirane	C4H6O2	86
2	1,3-Dioxane,2,4-dimethyle	C6H12O2	116
3	1,3-Dioxane,4-methyl	C5H10O2	102
4	1,3-Dioxepane,2-heptyl	C12H24O2	200
5	Ethanol,2-trimethylsilyl	C5H14O2Si	134
6	Silanol, trimethyl- propanoate	C6H14O2Si	146
7	Silanol, allyldimethyl	C5H12OSi	116
8	3-Hexanol,3-methyl	C7H16O	116
9	2,5-Dimethyl-4-hydroxy-3-hexanone	C8H16O2	144
10	Silane, diethylmethyl	C5H14Si	102
11	2,4-Hexadienal	C6H8O	96
12	2-Hexyne, 4-methyl	C7H12	96
13	2,2-Dimethylcyclopropancarboxylic acid	C8H11NO2	153
14	Methyl-3,3-dimethyl cyclopropane	C9H14O4	186
15	3,3-Dimethylcyclopropane	C7H10O4	158
16	Cyclohexylmethylethylphosphonofluoridate	C9H18FO2P	208
17	Dispiro	C14H22O4	254
18	2-Butenamide	C7H12N2O2	156
19	Phosphonofluoridic acid	C8H16FO2P	194
20	2,2-Dimethyl-3-trans-beta-cyclo-propanecarboxylic acid	C10H16O2	168
21	Eucalyptol	C10H18O	154
22	Benzeneacetaldehyde	C8H8O	120
23	Benzene, propyl	C9H12	120

4. Discussion

Arum hygrophilum Boiss is a well-known plant in Jordan; it is widely consumed as food and used as traditional folk medicine for the management of a variety of diseases. Only few studies are available on the biochemical components and potential medical effect of this plant. This study investigated the antimicrobial activity and chemical components of the plant.

The final stock concentration of the plant extracts (500mg/ml) used in this study was determined on the recommendation of the *Environmental Protection Agency* (*EPA*), being the maximum acceptable total dissolved solids level in drinking water **(**Investopedia, 2019**).**

Antibacterial activity assessment of *Arum hygrophilum* Boiss demonstrated that the water and methanol extracts had a significant antibacterial activity against *P. aeruginosa.* Methanol extract further revealed an inhibitory effect on *E. Faecalis*, whereas ethanol extract displayed no antibacterial influence against all the tested microorganisms. All type of extracts didn't show antifungal activity. However, previous study revealed that ethanol extract of *Arum hygrophilum* displayed an antifungal activity (Khalil and Dababneh, 2007), while petroleum ether, chloroform, ethyl acetate and 70% methanol extracts of *Arum maculatum* manifested greater antimicrobial activities against *E. coli and Staphylococcus aureus* (Mansour *et al*., 2015). It seems that the type of solvent used in preparing the plant extract displays an important role in drawing out the effective ingredients.

The Significant antibacterial effect of *Arum hygrophilum* Boiss against the most resistant bacteria (*P. aeruginosa* and *E. Faecalis*) reveals a promising hope in their eradication.

Fruits and vegetables have antioxidant and scavenging free radical properties; it is due to its polyphenolics, flavonoids and vitamin contents. The GC-MS analysis used in this study revealed the presence of Tert-butyl hydroxy anisole (phenolic compound) in the water extract of *Arum hygrophilum* Boiss; that finding approves its scavenging and antioxidant properties and goes with the reported results of Afifi et al. (2017) on the same plant.

Furthermore, the GC-MS analysis showed the presence of three alkaloids in the *arum hygrophilum* extracts, two in the methanol, (4(3H)-Pyrimidinone and pyrrolidin-2-one) and one in the water extracts (1H-Imidazole, 2-ethyl-4,5dihydro). Alkaloids have a wide variety of physiological effect; they have direct antibacterial, antibiotic enhancing activities, and antivirulence effects (Cushnie *et al*., 2014). The (3H)-Pyrimidinone compound present in the arum extract is commonly used as antibacterial, antifungal, anti-HIV, anticancer, anti-inflammatory, and antiulcer agent (Boukharsa *et al*., 2014), whereas the pyrrolidin-2-one possesses a promising antibacterial, anticancer, and larvicidal potentialities (Suresh *et al*., 2016). The 1H-Imidazole, 2-ethyl-4,5dihydro is one of the Imidazole derivatives; it is used as a base for building up promising antibacterial compounds (Rani *et al*., 2013).

Among the important chemical components of *Arum hygrophilum* methanol extract, Tetrahydropyranis is used as a core in developing non fluoroquinolones compounds; these products exhibited strong antibacterial activity against gram positive bacteria (Surviet *et al*., 2013). Further modification on Tetrahydropyranis, the Dibasic tetrahydropyran-based compounds demonstrated wider antibacterial effects; they are influential against Gram-positive and Gram-negative bacteria including *Staphylococcus aureus*, Enterobacteriaceae, *Pseudomonas aeruginosa*, and *Acinetobacter baumannii* (Surviet *et al*., 2017).

Another important chemical compound detected in the methanol and water extracts is Butanoic acid. This chemical structure has various beneficial effects, such as antimicrobial activities, anti-inflammatory and positive effects on animal production, including enhancement of gut development (Bedford and Gong, 2018). Serinol (2-amino-1,3-propanediol) compound present in the water extract is a serine amino acid structural analogue. This compound is usually used in the synthesis of chloramphenicol antibiotic, and has several applications through its derivatives (Andreeßen and Steinbüchel, 2011).

Afifi *et al*. (2017) had identified flavonoids and several plant acids in *Arum hygrophilum* Boiss ethanol extracts. They carried out their investigation through column chromatography and the HPLC-MS. These components are scavenging and antioxidant agents (Amarlal *et al*., 2009; Scalbert *et al*., 2005); and having antimicrobial activities (Cushnie and Lamb, 2005; Daglia, 2012), whereas analysis of ethanol extract of *Arum hygrophilum* Boiss in this study denied the presence of flavonoids and plant acids among the 23 detected chemical components. It seems that the column chromatography and HPLC-MS analysis is more informative than the GC-MS analysis specially if the plant extract involved other component difficult to be detected by GC-MS including some inorganic ions, polymers, nucleotides, and proteins.

More studies are required to monitor the medicinal applications and exploring the toxic effect of *Arum hygrophilum* Boiss and its extracts on vital body organs.

5. Conclusion

In addition to the previously mentioned potentialities of *Arum hygrophilum* Boiss extract, this study demonstrated the importance of the plant components as antibacterial and antioxidants agents used for treatment of various types of infection.

Acknowledgements

The authors are very grateful to the Dean of the Faculty of Medicine and to Al-Balqa Applied University for their help and encouragement.

References

Abu-Dahab R and Afifi F. 2007. Antiproliferative activity of selected medicinal plants of Jordan against a breast adenocarcinoma cell line (MCF7). Scientia Pharmaceutica, **75(3):**121–136.

Afifi F, Kasabri V, Litescu S and Tawaha K. 2017. Phytochemical and Biological Evaluations of Arum hygrophilum Boiss. (Araceae). Pharmacogn Mag, **13(50):** 275–280.

Afifi, F, Shervington, A and Darwish, R. 1997. Phytochemical and biological evaluation of Arum palaestinum. Part 1: Flavone C-glycosides. Acta Technologiae Et Legis Medicamenti, **8(2):**105-110.

Al Eisawi DMH. 1998. Field guide to wild flowers of Jordan and neighbouring countries. Commercial Press, Jordan.

Alali FQ, Tahboub YR, Ibrahim ES, Qandil AM, Tawaha K, Burgess J P, Sy A, Nakanishi Y, Kroll DJ and Oberlies NH. 2008. Pyrrolizidine alkaloids fromEchiumglomeratum (Boraginaceae). Phytochemistry**, 69(12):** 2341-2346.

Alali FQ, Tawaha K, El-Elimat T, Qasaymeh R, Li C, Burgess J, Nakanishi Y, Kroll DJ, Wani MC and Oberlies NH. 2006. Phytochemical studies and cytotoxicity evaluations of Colchicum tunicatumFeinbr and Colchicum hierosolymitanumFeinbr (Colchicaceae): two native Jordanian meadowsaffrons. Nat. Prod. Res, **20(6):** 558-566.

Al-Eisawi DMH. 2013. Flora of Jordan Checklist, Revised 1st ed. The University of Jordan Press, Jordan.

Amarlal S, Mira L, Nogueira JM, Da Silva AP and Helena Florêncio M. 2009. Plant extracts with anti-inflammatory properties-a new approach for characterization of their bioactive. Bioorg Med Chem., **17(5):** 1876-83.

Andreeßen B and Steinbüchel A. 2011. Serinol: small molecule - big impact. AMB Express, **1:**12.

Balunas MJ and Kinghorn AD. 2005. Drug discovery from medicinal plants. Life Sciences, **78(5):** 431-441.

Bedford A and Gong J. 2018.Implications of butyrate and its derivatives for gut health and animal production. Anim Nutr., **4(2):** 151–159.

Bodeker C, Bodeker G, Ong CK, Grundy CK, Burford G and Shein K. 2005. WHO Global Atlas of Traditional, Complementary and Alternative Medicine. World Health Organization, Geneva, Switzerland.

Boukharsa Y, Zaoui Y, Taoufik J and Ansar M. 2014. Pyridazin-3(2H)-ones: Synthesis, reactivity, applications in pharmacology and agriculture. Journal of Chemical and Pharmaceutical Research, **6(12):** 297-310.

Clinical and Laboratory Standards Institute CLSI. 2018. M100 Performance Standards for Antimicrobial Susceptibility Testing, 28th ed. USA.

Cole C, Burgoyne T, Lee A, Stehno-Bittel L and Zaid G. 2015. Arum Palaestinum with isovanillin, linolenicacid and β-sitosterol inhibits prostate cancer spheroids and reduces the growth rate of prostate tumors in mice. BMC Complement Altern Med., **15:**264.

Cushnie TPT and Lamb AJ. 2005. Antimicrobial activity of flavonoids. International Journal of Antimicrobial Agents, **26(5):** 343-356.

Cushnie TPT, Lamb AJ and Cushnie B. 2014.Alkaloids: An overview of their antibacterial, antibiotic-enhancing and antivirulence activities. International Journal of Antimicrobial Agents, **44(5):** 1-45.

Daglia M. 2012. Polyphenols as antimicrobial agents. Current Opinion in Biotechnology, **23(2):**174–181.

Evans WC. 2002. Trease and Evans Pharmacognosy, 5th edition. Elsevier (A Divisionof Reed Elsevier India Pvt. Limited).

Feinbrun-Dothan N. 1986. Flora Palaestina part 4: Text. Alismataceae to Orchidaceae. Israel Academy of Sciences and Humanities, Jerusalem: **2:** p 462.

Hatmal MM, Abderrahman S MandAlsholi D. 2017. Determining the anti – tumor effects of different extracting methods of Arum palaestinum on different cancer cell lines by In vitro assay. PharmacologyOnLine, **1:** 28-45.

Hudaib M and Aburjai T. 2007. Volatile components of *Thymus vulgaris* L. from wild-growing and cultivated plants in Jordan. Flavour and Fragrance Journal, **22(4):** 322-327.

Investopedia, 2019. Environmental Protection Agency (online) Available at: https://www.investopedia.com/terms/e/environmental-protection-agency.asp (Accessed 9 May 2019).

Khalil A and Dababneh B F. 2007.Inhibition of Phytopathogenic Fungi by Extracts from Medicinal Plants in Jordan. J. Bio. Sci., **7(3):** 579-581.

Lhlou M. 2013. The Success of Natural Products in Drug Discovery. Pharmacology and Pharmacy, **4:** 17-31.

Mansour O, Salamma R and Abbas L. 2015.Screening of Antibacterial Activity In vitro of Arum maculatum L. Leaves Extracts. Int. J. Pharm. Sci. Rev. Res., **31(2):** 231-234.

Newman DJ, Cragg GM and Snader KM. 2003. Natural products as sources of new drugs over the period 1981-2002. Journal of Natural Products, **66(7):** 1022-1037.

Oran SAS. 2015. Selected wild plant species with exotic flowers from Jordan.Inter. J. Biod. Cons.,**7(5):** 308-320.

Quran S. 2009. Ethnopharmacological survey of wild medicinal plants in Showbak, Jordan. Journal of Ethnopharmacology, **123(1):** 45-50.

Rani N, Sharma A and Singh R. 2013.Imidazoles as Promising Scaffolds for Antibacterial Activity: A Review. Mini-Reviews in Medicinal Chemistry, **13(12):** 1812-1835.

Rates S. 2001. Plants as sources of drugs. Toxicon, **39(5):** 603-613.

Salim AA, Chin YW and Kinghorn AD. 2008. Drug discovery from plants.In: Ramawat KG and Merillon JM, Bioactive Molecules and Medicinal Plants.Springer Berlin Heidelberg, pp. 1-24.

Scalbert A, Johnson IT and Saltmarsh M. 2005.Polyphenols: antioxidants and beyond. The American Journal of Clinical Nutrition, **81(1):** 215S–217S.

Suresh M, Padusha S and Raja A. 2016. Antimicrobial and larvicidal activities of 2-hydroxypyrrolidine/piperidine derivatives. SOJ Pharm PharmSci, **3(1):** 1-6.

Surivet JP, Zumbrunn C, Rueedi G, Hubschwerlen C, Bur D, Bruyere T, Locher H, Ritz D, Keck W, Seiler P, Kohl C, Gauvin JC, Mirre A, Kaegi V, Dos Santos M, Gaertner M, Delers J, Enderlin-Paput M and Boehme M. 2013. Design, synthesis, and characterization of novel tetrahydropyran-based bacterial topoisomerase inhibitors with potent anti-Gram-positive activity. J Med Chem, **56(18):** 7396−7415.

Surivet JP, Zumbrunn C, Bruyere T, Bur D, Kohl C, Locher HH, Seiler P, Ertel EA, Hess P, Enderlin-Paput M, Enderlin-Paput S, Gauvin JC, Mirre A, Hubschwerlen C, Ritz D and Rueedi G. 2017. Synthesis and Characterization of Tetrahydropyran-Based Bacterial Topoisomerase Inhibitors with Antibacterial Activity against Gram Negative Bacteria. J Med Chem, **60(9):** 3776 -3794.

JJBS

Volume 13, Number 2, June 2020
ISSN 1995-6673
Pages 165 - 176

Jordan Journal of Biological Sciences

Leaf Morphology and Venation Patterns of *Euphorbia* L. (Euphorbiaceae) in Egypt with Special Notes on Their Taxonomic Implications

Abdel Aziz A. Fayed[1], Mohamed S. Ahamed[2], Ahamed M. Faried[1] and Mona H. Mohamed[1*]

[1]*Botany and Microbiology Department, Faculty of Science, Assiut University, Assiut,* [2]*Botany and Microbiology Department, Faculty of Science, Helwan University, Helwan, Egypt.*

Received April 30, 2019; Revised June 16, 2019; Accepted July 12, 2019

Abstract

Euphorbia L. (Euphorbiaceae) is the largest genus of flowering plants in the flora of Egypt. The present paper deals with the study of leaf architecture including venation patterns, marginal configuration and leaf shape characters in the *Euphorbia* species in Egypt. A classical clustering analysis (UPGMA) and principle component analysis (PCA) by PAST 2.17c softwere are conducted based on 37 architectural leaf characters to discriminate the investigated taxa. Plates of light microscope for cleared leaf, marginal ultimate veins details as well as tooth shape for studied taxa were provided. Results from multivariate analysis are kept in line with the traditional taxonomic sections of the genus in Egypt. The obtained phenogram is slightly matched with the tradition and modern classification of genus *Euphorbia*. The arrangement and attachment of leaves, laminar size, apex and base leaf features, symmetry of base and medial of blade, primary vein framework, major secondary veins course, minor secondary veins, tertiary veins course and areolation development have been considered to be the most important distinguishable characters in *Euphorbia*. Leaf morphology and venation characters can be considered as good taxonomic indicators in segregating *Euphorbia heterophylla* in a distinct section (*Poinsettia*) within subgenus *Chamaesyce*, in addition they can discriminate the closely related species of *Euphorbia* as shown in the constructed key.

Keywords: Areolation, *Euphorbia*, Idioblasts, PCA, Venation, Architecture, UPGMA.

1. Introduction

Euphorbiaceae *sensu lato* is one of the six largest plant families after Orchidaceae, Asteraceae, Fabaceae, Rubiaceae and Poaceae (Christenhusz, and Byng, 2016). It includes around 8000–9000 species in 340 genera, and strongly represented in the tropical regions of the world (Radcliffe-Smith, 1980; Govaerts *et al.*, 2002; Secco *et al.*, 2012). According to Webster (1994), Euphorbiaceae *s.l.* comprises 52 tribes and 5 subfamilies: Phyllanthoideae, Oldfieldioideae, Acalyphoideae, Crotonoideae and Euphorbioideae. Recently, the Angiosperm Phylogeny Group (APG, 2016) recognized five lineages of Euphorbiaceae *s.l.* at family level: Phyllanthaceae, Putranjivaceae, Pandaceae, Picrodendraceae and Euphorbiaceae *sensu stricto*.

Euphorbia L. is one of the largest genera of angiosperms and the largest genus of Euphorbiaceae; it has a cosmopolitan distribution with about 2150 species (Govaerts *et al*., 2000; Bruyns, 2006). Despite its great vegetative diversity, the genus is morphologically characterized by having a cyathiate inflorescence and a highly reduced inflorescence that resembles a single flower (Steinmann and Porter, 2002). Based on geographical distribution, habit, leaves and stipules characters, branching of inflorescence, number and morphology of involucral glands and seed characters, the genus has been divided into four subgenera: *Esula* Pers., *Athymalus* Neck., *Chamaesyce* Raf., and *Euphorbia*.

Regionally, *Euphorbia* is considered as the largest genus in the flora of Egypt, represented by 41 species, distributed in all phyto-geographical regions of the country with different habits and habitats (Boulos, 2000).

El-Hadidi (1973), critically revised sect. *Anisophyllum* (Haw.) Roeper, while Fayed (1973) made a taxonomic revision of 20 species represented in different sections namely: *Anisophyllum*, *Lyciopsis* Boiss., *Poinsettia* (Graham) Boiss., *Pseudoacalypha* Boiss., *Tirucalli* Boiss., and *Tithymalus* Boiss. Accordingly, Fayed(1973) indicated the importance of some morphological characters, such as habit, leaves, cyathia, capsules, and seed features in distinguishing the Egyptian taxa of *Euphorbia*.

According to Laraño and Buot (2010), the leaf architecture and other vegetative characters are often ignored by some taxonomist in identification and classification of plant taxa due to their belief that these characters have high grade of phenotypic plasticity; however, it can be pointed out that leaf characters, particularly venation patterns are, in general, genetically

* Corresponding author e-mail: monaalam92@yahoo.com.

fixed and can be used as a taxonomic tool. Moreover, foliar micromorphology and architecture can be used as a valuable aid to taxonomy in various groups (e.g, Abd El-Ghani *et al.*, 2007 Laraño and Buot Jr, 2010; Salvaña and Buot Jr, 2013; Thepsithar and Thongpukdee, 2013)

The plant leaves are commonly used in taxonomic analyses, particularly in fitting with morphometric analysis (Viscosi and Cardini, 2011). Leaf characters may stand as appropriate taxonomic characters mainly in plant fossils in which the flowering organs are degenerated or absent (Hickey, 1973; Dilcher, 1974; Hickey and Taylor, 1991). Many authors discriminated and identified different taxa based only on morphological characters of leaves (Levin, 1986 a, b; Todzia and Keating, 1991; Hershkovitz, 1992; Christophel *et al.*, 1996; Roth-Nebelsick *et al*., 2001; Wang *et al.* 2001; Luo and Zhou, 2002; Fuller and Hickey, 2005; Loutfy *et al.*, 2005; Martínez-Millán and Cevallos-Ferriz, 2005; Cervantes *et al.*, 2009; Pacheco-Trejo *et al.*, 2009).

Recently, Sarala and Vijay (2014) studied the foliar micromorphology and architecture of 44 species belonging to 20 genera in Euphorbiaceae, and showed that these characters can be used for differentiating taxa. Kakkar and Paliwal (1972) made detailed studies on the leaf anatomy of the genus *Euphorbia* with regard to tracheoid idioblasts and vein endings. Sehgal and Paliwal (1974) studied the leaf venation patterns of 150 species of *Euphorbia* and they divided the genus into three major groups (uni-, bi- and tri-veined).

The present investigation was conducted to evaluate the importance of leaf morphological characters as well as patterns of venation in studying the diversity and patterns of variation of 21 taxa of *Euphorbia* in Egypt.

2. Materials and Methods

2.1. Sampling

The present study was based mainly on specimens preserved in ASTU Herbarium (Table 1) as well as fresh materials of the most species that collected from their appropriate localities.

Table 1: Tribal and sectional classification as well as source of taxa under investigation. Herbarium acronym is following Thiers (2017).

Subgenus	Section	Taxa	Collection
Euphorbia subgenus Chamaesyce Raf.	*Anisophyllum* (Haw.) Roeper	*E. hirta* L.	Nile valley, Assiut university ground, 5-5-2018, Mona Hassan (ASTU)
		E. indica Lam.	Nile valley, Assiut university ground, 5-5-2018, Mona Hassan (ASTU)
		E. peplis L.	Mediterranean region, Alexandria: Baltim, 31-7-1990, Fayed & El- Garf (ASTU)
		E. lasiocarpa Klotzsch	Nile valley, Cairo: Maadi garden, 27-9-2011, Fayed (ASTU)
		E. hyssopifolia L.	Nile valley, Giza, no date, Abdel Salam Galaly (ASTU)
		E. forsskaolii J. Gay	Nile valley, Assiut El Jadida, 9-4-2018, Mona Hassan (ASTU)
		E. scordifolia Jacq.	Gebel Elba, Haliab Triangle Area: Wadi Umm Shleem, 13-1-2005, Kadry Abdel Khalik (ASTU)
		E. granulata Forssk. var. *granulata*	Gebel Elba, Haliab Triangle Area: Wadi Umm Sheeb, 13-5-2013, Kadry Abdel Khalik (ASTU)
		E. serpens Kunth	Nile valley, Assiut university ground, 5-5-2018, Mona Hassan (ASTU)
		E. prostrata Ait.	Nile valley, Assiut university ground, 5-5-2018, Mona Hassan (ASTU)
	Poinsettia (Graham) Boiss.	*E. heterophylla* L.	Nile valley, Assiut university ground, 5-5-2018, Mona Hassan (ASTU)
Euphorbia subgenus *Athymalus* Neck.	*Lyciopsis* Boiss.	*E. cuneata* Vahl	Gebel Elba, Haliab Triangle Area: Sambeek Embeek, no date, Usama Abdel Rady (ASTU)
Euphorbia subgenus *Esula* Pers.	*Pachycladae* (Boiss.) Tutin	*E. dendroides* L.	Gebel Elba, Sollum plateau, 15-4-2016, Faried and Banhawy (ASTU)
		E. terracina L.	Mediterranean region, Alexandria-Burg-El-Arab, 6-4-2015, Faried *et al.* (ASTU)
	Chylogala (Fourr.) Prokh.	*E. retusa* Forssk.	Mediterranean region, wadi Hagol, 13-4-2010, Zareh and Aboul-Ela (ASTU)
	Helioscopia Dumort.	*E. arguta* Banks & Sol.	Assiut University ground, 1-1961, Badari (ASTU)
		E. helioscopia L.	Nile valley, Assiut university ground, 12-1-2018, Mona Hassan (ASTU)
	Exiguae (Geltman) Riina & Molero	*E. dracunculoides* Lam.	Gebel Elba, Haliab Triangle Area: Wadi Maarafawy, 4-2-2005, Kadry Abdel Khalik (ASTU)
	Tithymalus Boiss.	*E. peplus* L.	Nile valley, Assiut university ground, 17-4-2018, Mona Hassan (ASTU)
		E. chamaepeplus Boiss.	Gebel Elba, Gebel Serbal region, wadi Rem, 23-4-2004, Fayed *et al.* (ASTU)
	Pithyusa (Raf.) Lázaro	*E. obovata* Decne	Southern Sinai: Wadi Gebal region, wadi Gebal, 13-5-2004, Fayed *et al*. (ASTU)

2.2. Leaf clearing

For leaf venation study, method of Yu and Chen (1986) was followed with some modifications. Leaves were boiled in water for 10-20 minutes, then placed in 1-5% NaOH, the strength depending on the thickness of the material. NaOH solution was changed every 1-2 days during the clearing process, which generally took 2-10 days. Cleared leaves were then rinsed in running water thoroughly, dried, stained in 1% safranin, and mounted on

slides with Glycerin. Leaves were examined and photographed by Olympus SZ61 stereomicroscope provided with a digital Olympus camera SC100. Characters and characters states of leaf morphology were described based on terminologies of Melville (1976), Hickey (1973), Pole (1991), Ash *et al.* (1999) and Ellis *et al.* (2009).

2.3. Numerical analysis

For the numerical analysis, PAST version 2.17 c program of Hammer *et al.* (2001) was used. Hamming/P-distance clustering algorithms test was used to assess the degree of similarity inside data matrix by un-weighted pair-group method with arithmetic means (UPGMA) to generate the current phenograms (Figure 1).

3. Results

Samples of 21 species of *Euphorbia* were undergone for analysis. The morphological characters and character states were evaluated and recorded (Table 2). Data were analyzed by the software PAST version 2.17c (Hammer *et al.*, 2001) using the data matrix organized for 21 OUTS x 57 binary and multistate traits (Table 3). Within the current study, the phenogram (Figure 1) was performed by UPGMA; it achieved the highest co-phenetic correlation coefficient (0. 8745) which showed a good fit between the phenogram and the distance matrix. PCA was performed to check the uniformity of the grouping achieved with cluster analysis by using combined data in which the cumulative variance for PC1 and PC2 increased 52% of the variation for the two first principal components and accounted 100% for the first 20 principal components (Table 4). The arrangement and attachment of leaves, laminar size, symmetry of leaves base, medial symmetry of blade and primary vein framework, major secondary veins course have been considered to be important distinguishable characters in *Euphorbia* at cluster level. The numerical analysis separated the 21 taxa into three major clusters (Figure 1).

The constructed phenogram showed that *E. heterophylla* in section *Poinsettia* was separated from the rest of the examined taxa and form the most basal cluster (C1) at the similarity level of 0.7; the second cluster (C2) includes ten taxa which was separated into three main groups (A, B and C) at similarity level 0.39: the basal group (A) comprises *E. hirta*, *E. lasiocarpa*, *E. hyssopifolia* and *E. indica*, the second group (B) included *E. peplis* and *E. scordifolia*, *E. forsskaolii*, *E. prostrata*, the last group (C) included two species, *E. serpens* and *E. granulata* var. *granulata.* Group A was further divided into two subgroups at the similarity level 0.29, *E. hirta* in the first subgroup, *E. indica*, *E. lasiocarpa* and *E. hyssopifolia* were included in second subgroup. Group B was classified into two subgroups at the same last similarity level includes *E. prostrata* in third subgroup and *E. forsskaolii*, *E. peplis* and *E. scordifolia* in fourth subgroup. *Euphorbia peplis* was separated in a single clade in the same last subgroup (Figure 1). The third cluster (C3) includes ten species: *E. helioscopia*, *E. arguta*, *E. terracina*, *E. retusa*, *E. cuneata*, *E. dracunculoides*, *E. dendroides*, *E. peplus*, *E. chamaepeplus* and *E.* obovata. These species were separated in two major groups (D and E). Group D included four species segregated into two sub-groups at similarity level of 0.3; the basal sub-groups (subgroup 5) included three species: *E. terracina*, *E. helioscopia* and *E. arguta*, *E. terracina* was separated. The second subgroup (subgroup 6) was represented by *E. retusa*. Group E included six species which can be separated in four sub-groups at similarity level of 0.22. The most basal subgroups (subgroup 7) consists of only of *E. dendroides*, the second one (subgroup 8) consists of *E. dracunculoides*, the third subgroup (subgroup 9) consists of *E. peplus*, *E. chamaepeplus*, and the last one (subgroup 10) consists of *E. obovata* and *E. cuneata*.

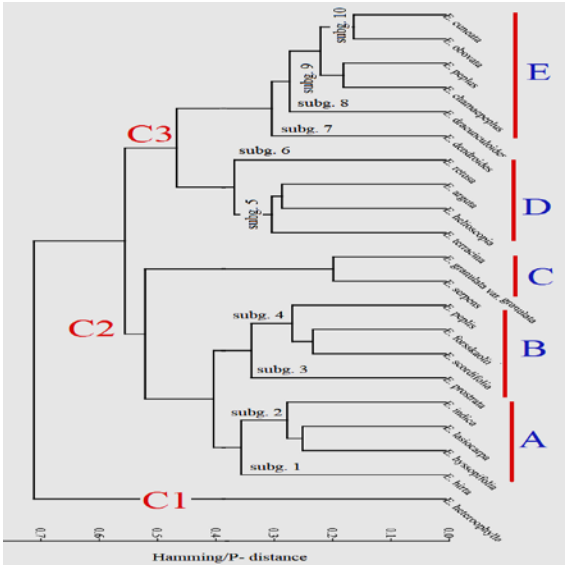

Figure 1. UPGMA dendrogram of the 21 taxa of *Euphorbia* using Hamming/ P- distance measure (0.8684) based on 57 architectural characters, the letters refer to divided groups, (C1, C2, C3) main clusters; (A-E) different groups.

Table 2. Characters and character states and their codes; NA= Non Applicaple.

Code	Morphological characters	Characters state	Code	Morphological characters	Characters state
1	Leaf attachment	Petiolate (1); Sessile (2); Subsessile (3)	6	Laminar ratio	Less than 1.5 cm (1); 2–3 cm (2); 4–7 cm (3); > 8 cm (4)
2	Leaf arrangement	Alternate (1); Opposite (2); Sub-opposite (3)	7	Laminar size	Leptophyll(1); Nanophyll (2); Microphyll (3); Notophyll (4)
3	Leaf organization	Simple (1); Compound (2)	8	Laminar shape	Elliptic (1); Obovate (2); Ovate (3); Oblong (1); Linear (5); Oblong-lanceolate (6); Oblong-ovate (7); Linear-lanceolate (8); Spathulate (9); Oblong-obovate (10); Oblong-elliptic (11)
4	Petiole features	Terete (1); NA (2)	9	Medial symmetry	Symmetry (1); Asymmetry (2)
5	Position of lamina attachment	Marginal (1); NA (2)	10	Base symmetry	Symmetry (1); Asymmetry with basal width (2); Asymmetry with basal extension (3); Asymmetry with basal insertion (4)

Code	Morphological characters	Characters state	Code	Morphological characters	Characters state
11	Lobation	Unlobed (1); Lobed (2)	34	Intersecondary frequency	Less than one per intercostal area (1); usually one per intercostal area (2); more than one per intercostal area (3); NA (4)
12	Margin type	Untoothed (1); Toothed (2)	35	Intercostal tertiary vein	Percurrent (1); Reticulate (2)
13	Type of teeth	Dentate (1); Serrate (2); Serrate-crenate (3); NA (4)	36	Course of percurrent tertiary	Mixed (opposite-alternate) (1); NA (2)
14	Special margin features	Involute (1); Papillate (2); Erose (3); NA (4)	39	Epimedial tertiary	Alternate percurrent (1); Reticulate (2); Ramified (3); Mixed (4)
15	Apex angle	Acute (1); Obtuse (2); Reflex (3)	40	Proximal course of epimedial tertiary	Parallel to percurrent (1); NA (2)
16	Apex shape	Straight (1); Convex-rounded (2); Acuminate (3); Emarginate (4); Convex-truncate (5); Convex rounded or convex truncate (6)	41	Distal course of epimedial tertiaries course	Parallel to percurrent (1); NA (2)
17	Base angle	Acute (1); Obtuse (2); Reflex (3); Oblique-reflex (4)	42	Exterior tertiaries course	Absent (1); Looped (2); Terminating at margin (3)
18	Base shape	Cuneate (1); Convex rounded (2); Convex truncate (3); Convex with basal extension (4); Decurrent (5); Cordate (6); Concave-convex (7)	43	Quaternary vein fabric	Percurrent (1); Irregular reticulate (2); Absent (3)
19	Terminal apex features	Mucronate (1); Retuse (2); NA (3)	44	Quinternary vein fabric	Irregular reticulate (1); NA (2)
20	Surface texture	Glabrous (1); Pubescent on both surface (2); sparse pubescent on one side (3)	45	Areolation	Poor development (1); Moderate development (2); Good development (3)
21	Surficial glands	Marginal (1); NA (2)	46	Freely Ending Veinlets (FEVs)	Absent (1); Mostly unbranched (2); mostly one branch (3); Dichotomous branching (4); Dendritic (5)
22	Primary vein framework	Pinnate (1); Palmate basal actiondromous (2); Palmate basal acrodromous (3)	47	FEVs terminal	Simple (1); Tracheoid idioblasts (2)
23	Number of basal veins	One (1); 3-4 (2); 5-6 (3)	48	Marginal ultimate venation	Absent (1); Incomplete loops (2)
24	Major secondary vein framework	Semicraspedodromous (1); Festooned semicraspedodromous (2); Cladodromous (3); brochidodromous (4); Festooned brochidodromous (5)	49	Tooth spacing	Regular (1); Irregular (2); NA (3)
25	Minor secondary	Craspedodromous (1); Semicraspedodromous (2); Brochidodromous (3); NA (4)	50	Order of teeth	One (1); Two (2); NA (3)
26	Perimarginal veins	Intramarginal secondary (1); Fimbrial vein (2); Absent (3)	51	Number of teeth per 0.5 cm	4-7 (1); 8-12 (2); NA (3)
27	Major secondary spacing	Regular (1); Irregular (2); Gradually increasing proximally (3); Abruptly increasing proximally (4)	52	Sinus shapes	Angular (1); Rounded (2); NA (3)
28	Variation of major secondary angle to midvein	Uniform (1); Inconsistent (2); Smoothly decreasing proximally (3)	53	Tooth shapes	CC/ ST – CC/ CC (1); ST/ RT (2); ST/ St (3); RT/ RT- RT/ CC (4); CC/ CC- CC/ FL (5); RT /ST (6); CC/ RT (7); CV/ CC (8); ST/ CC (9); CC/ CC (10); NA (11)
29	Major secondary attachment to midvein	Decurrent (1); Basally Decurrent (2); Deflected (3); Excurrent (4)	54	Principle vein	Present (1); Absent (2)
30	Intersecondary veins	Present (1); Absent (2)	55	Principle vein terminating	Submarginal (1); At apex of tooth (2); On proximal flank (3); On distal flank (4); At nadir of superjacent sinus (5); NA (6)
31	Intersecondary proximal course	Parallel to major secondary (1); Perpendicular (2); NA (3)	56	Course of accessory veins	Looped (1); Straight to concave (2); NA (3)
32	Intersecondary length	Less than 50% (1); More than 50% (2); NA (3)	57	Special features of tooth apex	Simple (1); Glandular (2); Cassidate (3); NA (4)
33	Intersecondary distal course	Reticulate or ramifying (1); Parallel (2); Perpendicular (3); Basiflexed (4); NA (5)			

Table 3: Matrix obtained from scoring (21 OTUs x 57 characters)

Characters / OUTS	1	2	3	4	5	6	7	8	9	10	11	12	13	14	15	16	17	18	19	20	21	22	23	24	25	26	27	28	29	30	31	32	33	34	35	36	37	38	39	40	41	42	43	44	45	46	47	48	49	50	51	52	53	54	55	56	57
F. hirta	1	?	1	1	1	?	?	6	?	?	1	?	?	4	1	1	4	4	?	?	1	?	?	?	1	?	?	?	?	?	4	1	?	1	?	1	?	?	?	?	?	?	?	?	?	?	?	1	1	1	1	1	9	?	4	1	?
E. indica	1	2	1	1	1	2	3	4	2	3	1	2	2	4	2	2	3	4	3	2	2	2	3	1	2	2	3	1	1	1	2	1	4	2	2	2	2	2	2	2	2	3	2	2	3	4	2	1	2	2	1	2	1	2	3	3	3
E. lasiocarpa	1	2	1	1	1	2	2	6	2	2	1	2	2	4	2	2	3	6	3	3	2	2	3	1	2	2	2	2	1	1	1	1	2	1	2	2	2	2	4	2	2	3	3	2	3	3	2	1	1	1	2	1	1	2	5	3	1
E. hyssopifolia	1	2	1	1	1	2	2	6	2	2	1	2	2	4	1	2	3	6	3	1	2	2	3	1	2	2	2	2	1	1	1	1	1	2	1	2	2	2	2	4	2	2	3	3	2	3	3	2	1	2	2	1	2	2	1	1	3	3
F. peplis	?	?	1	1	1	1	?	4	?	4	1	?	?	1	4	?	4	4	4	?	1	?	?	?	?	1	?	?	?	?	1	1	?	1	?	1	1	1	?	?	?	?	4	?	?	?	?	?	?	1	?	?	1	?	?	1	?	1
E. granulans var. granulans	1	2	1	1	1	1	1	7	2	4	1	1	4	4	2	3	4	6	2	2	2	2	2	2	3	4	1	2	2	2	2	3	3	3	4	2	2	2	2	4	2	2	1	3	2	2	2	2	1	3	3	3	3	11	2	6	3	4
E. serpens	1	2	1	1	1	1	1	4	2	2	1	1	4	4	3	4	3	4	2	1	2	2	2	3	4	1	2	1	1	2	3	3	5	4	2	2	2	2	3	2	2	1	3	2	1	2	2	1	3	3	3	3	11	2	6	3	4
E. forsskaolii	1	2	1	1	1	1	2	11	2	4	1	2	3	4	2	5	4	4	3	3	2	2	2	3	1	1	2	1	2	1	1	1	1	1	2	2	2	2	4	2	2	3	3	2	1	2	2	1	2	2	2	2	4	2	1	3	1
E. scordifolia	1	2	1	1	1	1	2	7	2	4	1	2	2	4	2	2	4	4	3	2	2	2	2	2	3	4	3	2	2	3	1	1	2	1	1	2	2	2	2	4	2	2	3	3	2	3	2	2	2	1	1	1	2	5	2	1	3	1
E. prostrata	1	2	1	1	1	1	1	1	2	2	1	2	2	4	2	2	4	4	3	2	2	2	2	1	2	2	2	2	2	1	1	2	4	2	2	2	2	2	3	2	2	2	3	2	1	2	2	1	1	1	1	2	6	2	1	3	1
E. heterophylla	1	3	1	1	1	4	4	3	1	1	1	2	2	4	1	1	1	5	3	2	1	1	1	5	3	3	1	1	1	1	1	2	1	2	1	1	1	1	1	1	1	2	1	1	3	3	1	2	1	1	2	1	10	1	2	2	2
E. cuneata	2	1	1	2	1	2	2	9	1	1	1	1	4	4	2	6	1	1	1	1	2	1	2	1	4	3	1	3	1	1	1	2	1	1	2	2	2	2	2	2	2	2	2	2	2	3	2	2	3	3	3	3	11	2	6	3	4
E. dendroides	2	1	1	2	1	3	3	8	1	1	1	1	4	4	2	3	2	3	1	1	2	1	2	4	4	3	2	3	2	1	1	1	1	1	2	2	2	2	3	2	2	1	2	1	3	5	1	2	3	3	3	3	11	2	6	3	4
E. retusa	2	1	1	2	1	2	3	5	1	1	1	2	2	1	1	1	2	2	3	1	2	1	3	1	4	3	4	2	1	2	3	3	5	4	2	2	2	2	2	2	2	2	2	2	3	5	2	2	2	2	2	1	1	7	1	2	2	1
E. arguta	2	1	1	2	1	3	3	6	1	1	1	2	2	2	1	1	2	3	3	2	2	1	2	2	4	3	2	1	1	1	1	2	1	1	2	2	2	2	4	2	2	2	2	2	3	2	2	1	2	2	1	2	10	1	1	2	1
E. helicocopta	2	1	1	2	1	3	3	2	1	1	1	2	2	4	2	2	1	3	3	1	2	1	2	2	4	3	4	1	1	1	1	1	1	2	2	2	2	2	2	2	2	2	2	2	3	2	2	1	1	1	1	1	8	2	1	3	1
E. drawneuloides	2	1	1	2	1	2	2	8	1	1	1	1	4	3	1	2	2	2	1	1	2	1	2	1	4	3	3	2	1	1	1	1	1	1	2	2	2	2	2	2	2	2	3	2	3	5	2	1	3	3	3	3	11	2	6	3	4
E. peplus	1	1	1	1	1	2	2	2	1	1	1	1	4	4	2	2	1	2	3	1	2	1	1	2	4	3	2	1	1	1	1	1	1	1	2	2	2	2	2	2	2	2	2	2	1	2	1	2	3	3	3	3	11	2	6	3	4
E. chamaepeplus	1	1	1	1	1	1	2	3	1	1	1	1	4	4	2	2	2	7	1	1	2	1	2	1	4	3	2	1	3	1	1	1	3	1	2	2	2	2	2	2	2	3	3	2	1	2	2	2	3	3	3	3	11	2	6	3	4
E. oblonata	2	1	1	2	1	1	2	2	1	1	1	1	4	4	2	2	1	5	1	1	2	3	2	1	4	3	2	2	3	1	1	1	1	1	2	2	2	2	2	2	2	2	3	2	2	3	2	2	3	3	3	3	11	2	6	3	4
E. terracina	2	1	1	2	1	3	3	6	1	1	1	2	2	4	1	2	2	2	2	1	2	1	2	4	4	3	3	3	3	1	1	1	1	3	2	2	2	2	2	2	2	2	2	3	3	5	2	2	2	2	1	2	9	2	6	3	1

Table 4. Eigenvalue, percentage of variance and cumulative percentage of variance of the first 20 principal components

PC	Eigenvalue	% variance	% Cumulative variance
1	22.2015	37.557	37.557
2	8.24882	13.954	51.511
3	7.43225	12.573	64.084
4	4.74229	8.0222	72.1062
5	4.21551	7.1311	79.2373
6	2.71919	4.5999	83.8372
7	2.54534	4.3058	88.143
8	1.45054	2.4538	90.5968
9	0.971608	1.6436	92.2404
10	0.791265	1.3385	93.5789
11	0.724165	1.225	94.8039
12	0.687639	1.1632	95.9671
13	0.51345	0.86857	96.83567
14	0.471354	0.79736	97.63303
15	0.353922	0.59871	98.23174
16	0.309592	0.52372	98.75546
17	0.23223	0.39285	99.1483
18	0.216522	0.36628	99.51459
19	0.163111	0.27592	99.7905
20	0.123952	0.20968	100.000

4. Key to the taxa

Leaves notophyll, intercostal tertiary veins fabric mixed percurrent.....**E.heterophylla**

Leaves microphyll, nanophyll or leptophyll, intercostal tertiary veins fabric reticulate or absent ……..…...**2**

2- Leaf base asymmetrical; primary vein palmately basal actinodromous ……...…**3**

Leaf base symmetrical; primary vein pinnate or palmately basal acrodromous…….....**12**

3- Leaves margin toothed……..**4**

- Leaves margin entire……..……..**11**

4- Leaves leptophyll …….. **E. prostrata**

Leaves nanophyll or microphyll ……..……..**5**

Major secondary veins and minor secondary veins semicraspedodromous ……..…….…….…….…**6**

Major secondary veins cladodromous; minor secondary veins craspedodromous or absent ……...**9**

6- Leaves microphyll, pubescent; major secondary veins attachment excurrent to the midvein, tooth apex glandular ……..…… **E. hirta**

- Leaves nanophyll, sparsely hairy or entirely glabrous, major secondary veins attachment decurrent to the midvein, tooth apex eglandular ……...…….. **7**

7- Leaves oblong, base convex with oblique reflex extension; major secondary veins abruptly increasing proximally, uniformly angled ……**E. indica**

Leaves oblong-lanceolate, base cordate with reflex width; major secondary veins irregular, inconsistently angled……...……**8**

8- Leaves sparsely hairy; tooth spacing regular, tooth number up to 7 per 5 mm, sinus shapes angular, principle vein terminating at nadir of superjacent sinus, tooth apex simple ……..…….... **E. lasiocarpa**

Leaves entirely glabrous; tooth spacing irregular, tooth number less than 5 per 5 mm, sinus shapes rounded, principle vein terminating at submarginal, tooth apex cassidate ……...…….……. **E. hyssopifolia**

9- Leaves entirely glabrous, apex reflex-emarginated, asymmetrical base insertion, margin dentate ……..…. **E. peplis**

- Leaves pubescent, apex convex; asymmetrical base extension; margin serrate ……...…….. **10**

10- Leaves sparsely pubescent on one surface, apex rounded-truncate; craspedodromous minor secondary veins; perimarginal secondary veins present; secondary veins angle uniform, attachment to midvein basely decurrent; tooth spacing irregular ……..... **E. forsskaolii**

- Leaves pubescent on both surfaces, apex convex rounded; minor secondary veins absent; perimarginal

secondary veins absent; secondary veins angle inconsistent, attachment to midvein deflected; tooth spacing regular, ……..... **E. scordifolia**

Table 5: Correlation between the morphological characters and the first two principal components PC1, PC2; (1) indicates traits with high scores in PC1, while (2) indicates traits with high scores in PC2

Code	Morphological characters	PC 1	PC 2
1	Leaf attachment	0.022	-0.038
2	Leaf arrangement	-0.068	0.037
3	Leaf organization	0.000	0.000
4	Petiole features	0.051	-0.049
5	Position of lamina attachment	0.000	0.000
6	Laminar ratio	0.028	-0.179
7	Laminar size	-0.006	-0.176
8	Laminar shape [2]	0.150	0.558
9	Medial symmetry [2]	-0.071	0.107
10	Base symmetry [2]	-0.071	0.107
11	lobation	0.000	0.000
12	Margin type	-0.088	-0.05
13	Type of tooth	0.102	0.046
14	Special margin features	-0.007	0.052
15	Apex angle	-0.008	0.071
16	Apex shape [2]	-0.002	0.268
17	Base angle [2]	-0.139	0.295
18	Base shape [1]	-0.141	0.079
19	Terminal apex features	-0.136	-0.072
20	surface texture	-0.074	0.012
21	Surficial glands	-0.000	0.036
22	Primary vein framework	-0.052	0.086
23	Number of basal veins	-0.058	0.076
24	Major secondary framework	0.085	-0.088
25	Minor secondary course [1]	0.176	-0.047
26	Perimarginal veins [2]	0.055	-0.169
27	Major secondary spacing	-0.027	-0.080
28	Variation of major secondary angle	0.033	0.084
29	Major secondary attachment to midvein	0.018	0.027
30	Inter secondary	0.017	0.055
31	Intersecondary proximal course	0.004	0.121
32	Intersecondary length	0.029	0.066
33	Intersecondary distal course [2]	0.006	0.216
34	Intersecondary frequency	0.026	0.112
35	Intercostal tertiary vein fabric	-0.001	0.035
36	Course of Percurrent tertiary	-0.001	0.035
37	Angle of percurrent tertiary	-0.001	0.035
38	Intercostal tertiary vein angle variability	-0.001	0.035
39	Epimedial tertiaries [2]	-0.068	0.182
40	Proximal course of epimedial tertiaries	-0.001	0.035
41	Distal course of epimedial tertiaries	-0.001	0.035
42	Exterior tertiary course [1]	-0.103	-0.022
43	Quaternary vein fabric	-0.026	0.127
44	Quinternary vein fabric	-0.031	0.059
45	Areolation	-0.044	-0.038
46	Freely Ending Veinlets branching	0.056	0.003
47	FEVs terminal	-0.025	0.047
48	Marginal ultimate venation	0.053	-0.058
49	Tooth spacing	0.126	0.104
50	Order of teeth	0.126	0.104
51	Number of teeth per 0.5 cm [1]	0.153	0.091
52	Sinus shape	0.108	0.112
53	Tooth shapes [1,2]	0.735	-0.233
54	Principle vein	0.014	0.049
55	Principle vein terminating [1,2]	0.384	0.265
56	Course of accessory veins	0.002	0.063
57	Specific tissue on teeth apex [1,2]	0.208	0.157

11- Leaves glabrous; apex reflex-emarginated, base cordate, reflexed angle; major secondary veins angle variation uniform; decurrent attachment to midvein; epimedial third veins ramified; areolation poor ……. **E. serpens**

- Leaves pubescent; apex obtuse; base convex with basal extension, oblique reflexed angle; major secondary veins angle variation inconsistent, basally decurrent attachment to midvein; epimedial third veins mixed; areolation moderate…**E. granulata var. granulata**

12- Leaves margin toothed ……..……...…….…….……**13**

- Leaves margin entire…….. **16**

13- Leaves linear, margin involute; major secondary veins semicraspedodromous; inter secondary veins absent..... **E. retusa**

- Leaves oblong-lanceolate or obovate, margin features papillate or absent; major secondary veins festooned semicraspedodromous or simple brochidodromous; inter secondary veins present ……..……...**14**

14- Leaves apex mucronate; major secondary veins simple brochidodromous, angle variation smoothly decreasing proximally; marginal ultimate venation incomplete loops…….……. **E. terracina**

Leaves apex obtuse or acute; major secondary veins festooned craspedodromous, angle variation uniform; marginal ultimate venation looped ……..……..…… **15**

15- Leaves obovate, glabrous, apex convex rounded, margin features not papillate; major secondary veins spacing abruptly increasing proximally; tooth spacing regular, sinus shape angular …… … **E. helioscopia**

Leaves oblong-lanceolate, pubescent, apex acute, margin features papillate; major secondary veins spacing irregular; tooth spacing irregular, sinus shape rounded ……..……**E. arguta**

16-Leaves linear-lanceolate……**17**

- Leaves ovate or obovate ……**18**

17- Leaves microphyll, margin entire; major secondary veins simple brochidodromous, spacing irregular; freely ending veins termination simple; marginal ultimate veins incomplete looped…….....**E. dendroides**

Leaves nanophyll, margin erose; major secondary veins semicraspedodromous, spacing smoothly increasing proximally; freely ending veins termination freely tracheoid idioblasts; marginal ultimate veins absent ……...…..**E. dracunculoides**

18- Leaves petiolate; major secondary veins angle variation uniform ……**19**

Leaves sessile; major secondary veins angle variation inconsistent or smoothly decreasing proximally ……..**20**

19- Leaves obovate, apex not mucronate, base decurrent; major secondary veins festooned brochidodromous with decurrent attachment to the midvein; quaternary veins present; freely ending veins termination simple ……...……...…….**E. peplus**

Leaves ovate, apex mucronate, base obtuse; major secondary veins semicraspedodromous with deflected attachment to the midvein; quaternary vein absent, freely

ending veins termination tracheoid idioblasts ……. **E. chamaepeplus**

20- Leaves obovate; primary vein palmately basal acrodromous; major secondary angle variation inconsistent, spacing irregular, deflected attachment to the midvein……..……**E. obovata**

- Leaves spathulate; primary vein pinnate; major secondary angle variation smoothly decreasing proximally, spacing regular, decurrent attachment to the midvein ……..……**E. cuneata**

5. Discussion

This study emphasizes the significance of leaf characters for recognizing most of the taxa under investigation. Leaf shapes and venation patterns are considered as essential traits that generally play a significant role in discriminate *Euphorbia* members at either subgeneric or sectional levels. The PCA is providing the numerical values correlative to the morphological traits used in this taxonomic analysis. PCA is considered as a standard multivariate statistical method that aims to make analysis to obtained numerical data (Mardia *et al.*, 1979). In this study, PCA results are slightly consistent with the latest taxonomic studies using the leaf morphology as the most important factor for classification of angiosperms.

Our primary phenetic data cannot yet reflect the true evolutionary history and the phylogeny among *Euphorbia* species in Egypt; however our findings are somewhat consistent with the previous traditional sectional classification of Pax and Hoffmann (1931) and recently with the molecular circumscriptions of the some studies such as Yang *et al.* (2012), Peirson *et al*. (2013), Riina *et al*. (2013). Leaf shapes, venation patterns and tooth characters were considered as essential traits that generally play a significant role in delimiting *Euphorbia* members both subgeneric and sectional

levels and can be considered as good taxonomic indicators in segregating closely related species in *Euphorbia.* In this study, only three subgenera covering all members of *Euphorbia* are selecting (Table 1). The first one is *E.* subgen. *Chamaesyce* which includes 11 taxa, the second is *E.* subgen. *Esula* with nine taxa, while the last one is *E.* subgen. *Athymalus* which is representing here by only one taxon (Table 1).

Euphorbia subgen. *Chamaesyce* is represented in our study by two sections, namely: *Anisophyllum* and *Poinsettia*. Section *Poinsettia* is represented by only one species, *E. heterophylla.* Morphologically, this species is unique in having some synapomorphic characters such as opposite-alternate leaves, glandular stipules, peltate glands which are often reduced to one gland, and seed caruncle reduced or minute (Boulos, 2000). Our results showed that *E. heterophylla* differs from all investigated taxa mainly by having notophyll leaves, mixed percurrent intercostal tertiary veins, alternate percurrent epidermal tertiaries and percurrent quaternary veins (Figures 3A and 5A).Based on these characters, it was solitarily placed in cluster C1 (Figure 1). All taxa of section *Anisophyllum* are characterized by a number of unique characters, such as opposite leaves, asymmetrical base, stipulate, clustered cyathium, axillary or terminal cythial, glands often with membranous appendages and ecarunculate seeds (Radcliff-Smith, 1980). Hooker (1885) stated that "*sect. Anisophyllum is forever multiplied*"; in addition, El-Ghazaly & Chaudhary (1993) showed that this section is heterogamous in respondence to the shape of aperture and sexine pattern of its pollen grains. Based on the current results, the architectural characters of species belonging to sect. *Anisophyllum* are rather variable. Furthermore, the phylogenetic results obtained by Yang *et al.* (2012) using the ITS and chloroplast *ndhF* sequence proved that *Anisophyllum* is monophyletic group. In our study, the represented taxa of this section share numerous characters (e.g. opposite leaves, asymmetrical base, asymmetrical medial and palmately basal actiondromous veins), (Figure 2). In this study, ten species of sect. *Anisophyllum* are grouped together in cluster C2 (Table 1 and Figure 1), which is divided into three groups: A, B, and C. Within the species of sect. *Anisophyllum*, leaf characters and venation patterns provide a significant value to distinguish the studied taxa. *Euphorbia hirta*, *E. lasiocarpa*, *E. hyssopifolia*, and *E. indica* were placed together in group A (Figure 1), and share some macro-morphologically characters, such as: erect to ascending habit and cyathia clustered into capitates inflorescences (Boulos, 2000; Zohary, 1972).

Boulos (2000) and Zohary (1972) recognized *E. hirta* (sect. *Anisophyllum*) by its densely pubescent leaves and leaves length reaching to 4–4.5 cm in length. Nevertheless, leaf architectural characters of *E. hirta* (e.g. microphyll leaves with densely serrate margin, glandular tooth) were considered as good diagnostic characters and can be used to circumscribe the distinct Subgroup 1 (Figures 1, 2A and 4A).

On the other hand, *E. lasiocarpa*, *E. hyssopifolia* and *E. indica* (sect. *Anisophyllum*) share some morphological characters such as oblong to oblong-lanceolate leaves, loose clustered cyathia terminated at lateral or axiallary shoots (Boulos, 2000). The current results show that these taxa are clustered together in the distinct Subgroup 2 (Figure 1) by having a similar architectural characters such as nanophyll leaves; major and minor secondary veins are semicraspedodromous, fimbrial perimarginal veins terminating at margin, major secondary veins decurrently attached to midvein and exterior tertiary terminating at leaf margin (Figures 2B, 2C, 2D, 4B, 4C and 4D). Radcliffe-Smith (1980) remarked that there is morphological ambiguity among *E. hyssopifolia* and *E. indica*; however, based on its narrow leaves as well as black seeds, El-Hadidi (1973) considered that *E. hyssopifolia* is a distinct species and differs from *E. indica*. El-Hadidi's (1973) aspect has been approved by the current results that *E. hyssopifolia* exhibits glabrous lanceolate leaves, with asymmetrical basal width, acute apex, cordate base with reflex angle, angles of secondary veins are inconsistent, proximal course of intersecondary veins is parallel, reticulate intersecondary veins course, quaternary veins fabric absent and freely ending veins (FEVs) with one branch (Figures 2D and 4D). Moreover, *E. indica* have hairy oblong leaves, with asymmetrical basal extension, obtuse apex, cordate base with oblique reflex angle, secondary veins angles uniform, intersecondary veins proximal course perpendicular, intersecondary veins course basiflexed, quaternary veins fabric presented and freely ending veins with dichotomous branching (Figures 2B and 4B). According to Boulos (2000), *E. lasiocarpa* seems to be more closely related to *E. indica* than other

taxa; they share some morphological characters such as sparsely hairy leaves with obtuse apex; however, the present results offer distinct architectural characters between the both species with a low similarity index (25%); *Euphorbia lasiocarpa* can be recognized by presence of sparse hairs towards the margin of leaf base (while being spread out on whole leaf in *E. indica*); in addition, *E. lasiocarpa* is characterized by cordate leaf base with reflex angle, inconsistent secondary veins angles are, regular tooth spacing, angular sinus shape and the principle vein is terminating at the nadir of superjacent sinus (Figures 2C and 4C).

Morphologically, *E. forsskaolii*, *E. scordifolia*, *E. prostrata* and *E. peplis* have small leaves (c. 1.5 x 0.5 cm) and a solitary cyathium (El-Hadidi, 1973; Fayed, 1973; Boulos, 2000). The dendrogram (Figure 1) reveals the location of the four species together in Cluster C2, group B by sharing architectural leaf features such as: oblique reflex base with convex basal extension, irregular spacing of secondary veins, mostly unbranched FEVs, round sinus, simple submarginal principle veins in the tooth apex.

The dendrogram (Figure 1) shows that group B is subdivided into two subgroups: subgroup 3 and subgroup 4. Based on floral and seeds characters documented by Fayed (1973), Boulos (2000) and Fayed and Hassan (2007), *E. prostrata* is easily distinguished from the related taxa by having minute appendage glands and transversely wrinkled seeds. Our results revealed that *E. prostrata* can be separated from all involved taxa by having elliptic leptophyll leaves with inequal basal width, minor semicraspedodromous secondary veins and the fimbrial perimarginal veins (Figures 2J and 4J). These differentiated characters confirm the placement of *E. prostrata* in a separate subgroup (Subgroup 3) away from *E. forsskaolii*, *E. peplis* and *E. scordifolia* (Figure 1).

Within subgroup 4, *E. forsskaolii*, *E. peplis* and *E. scordifolia* share architectural characters, such as nanophyll leaves and cladodromous secondary veins course. *E. peplis* is morphologically different from other taxa within this subgroup by having glabrous leaves, and seed length over 1.5 mm with 4-angles in transverse section (El-Hadidi, 1973; Fayed, 1973; Fayed and Hassan, 2007); these characters are in agreement with architectural results showing in figures 2E and 4E, in which *E. peplis* have entirely glabrous leaves, reflex-emarginated apex, asymmetrical insertion base, dentate margin, and fimbrial perimarginal veins.

Euphorbia scordifolia and *E. forsskaolii* are distinguishable on macro-morphological characters (Fayed, 1973) and seed characters (Fayed and Hassan, 2007); in addition, our results show a similarity value reaching to 21% due to the discriminating characters between those two taxa, in which the major secondaries veins are deflected in attachment to midvein, exterior tertiary veins terminating at margin, areolation is well developed and tooth spacing is regular in *E. scordifolia* (Figures 2I and 4I), while *E. forsskaolii* is characterized by decurrent major secondaries veins, absence of exterior tertiary veins, tooth spacing being irregular and areolation is poorly developed (Figures 2H and 4H).

The group C in cluster C2 is represented by two taxa, *E. serpens* and *E. granulata* var. *granulata*, they share the leptophyll leaves with untoothed margin, absence of inter secondary veins (Figures 2F, 4F, 2G and 4G), but can easily be discriminated in morphology.

The second subgenus involved in this study is *Athymalus* which is representing by one section, *Lyciopsis*, with only one species *Euphorbia cuneata*. The dendrogram (Figure 1) shows that, *E. cuneata* placed together with *E.* obovata (subgenus *Esula*, section *Pithyusa*) with a similarity value reaching to 18%. According to Fayed and Hassan (2007), *E. cuneata* shares smooth seeds as character with some members of subgenus *Esula*. Our results cannot be used to place *E. cuneata* in a separate cluster; it will be useful to discriminate this species from all other involved specie.

The third subgenus involved in present study is *Euphorbia* subgen. *Esula*. It is represented in this study by nine species within six sections (Table 1). Most members of *E*. subgen. *Esula* are characterized by exstipulate leaves, absence of petaloid appendages, dichasial cyathia, and carunclate seeds (Zohary, 1972; Fayed, 1973; Boulos, 2000). They distribute mainly in temperate region particularly in the Mediterranean regions. Figure 1 shows the placement of all taxa belonging to *E*. subgen. *Esula* in a separate cluster (C3). Only one species, *Euphorbia retusa*, of the first section, *Chylogala*, was sampled in this study. According to Riina *et al.* (2013) and Boulos (2000), *E. retusa* can be easily separated from related taxa by having caruncle (about half as long as the seeds). Based on our results, *E. retusa* is placed solitarily as subgroup 6 (Figure 1), with involute margin and without intersecondary veins (Figures 3D and 5D).

Two species: *Euphorbia helioscopia* and *E. arguta*, of (the second section, *Helioscopia*) were sampled in this study. They were grouped together with *E. terracina* (section *Pachycladae*) in the same subgroup 5 (Figure 1) with a similarity index 31%. However, *E. helioscopia* and *E. arguta* are closer with each other than to *E. terracina* because they share absence of terminal mucronate apex and festooned semicraspedodromous secondary veins (Figures 3E, 5E, 3F and 5F).

According to Riina *et al.* (2013), *E. terracina* is placed in *Pachycladae* (the third sampled section) with *E. dendroides* by sharing some seed characters and their geographical distribution. Our result is not agreement with this view, whereas *E. terracina* and *E. dendroides* were placed in subgroups 5 and 7 respectively (Figure 1). In this study, the analysis of leaf architectural characters confirms the placements of *E. terracina* and *E. dendroides* in different sections as reported by Pax and Hoffmann (1931). *Euphorbia terracina* differs from *E. dendroides* mainly in having oblong-lanceolate leaves, toothed margin, major secondary spacing abruptly increasing proximally (linear lanceolate, untoothed margin, irregular spacing in *E. dendroides*), Figures (3C, 5C, 3K and 5K).

The fourth sampled section within subgenus *Esula* is *Exiguae*, which is represented here by *E. dracunculoides*. Morphological characters of leaves can be helpful to distinguish *E. dracunculoides* from all other involved taxa, it is unique in having linear-lanceolate leaves with mucronate apex, semicraspedodromous major secondary veins, well developed areolation as well as dendritic freely ending veins (Figures 3G, 5G). The placement of *E. dracunculoides* in subgroup 8 (Figure 1) is in agreement with the morphological and molecular results of Riina *et*

al. (2013) in which, *E. dracunculoides* was located in a separate clade within section *Exiguae*.

According to Boulos (2000) and Riina *et al.* (2013), *E. peplus* and *E. chamaepeplus* are included in section *Tithymalus* (the fifth sampled section). They are closely related by having some morphological characters. Figure 1 shows the clustering of both species together within subgroup 9 based on leaf morphology and venation patterns. Although, *E. peplus* and *E. chamaepeplus* shared characters such as petiolate leaves, uniform secondary veins variation, irregular spacing, poorly developed areolation, unbranched freely ending veins, *E. peplus* can be easily distinguished from *E. chamaepeplus* by some leaf characters, *E. peplus* is characterized by obovate leaves, apex features absence festooned brochidodromous major secondary veins with decurrent attachment to midvein, irregular reticulate quaternary veins and simple freely ending veins (Figures 3H and 5H), while *E. chamaepeplus* can easily be distinguished by ovate leaves, mucronate apex, semicraspedodromous major secondary veins with deflected attachment to midvein, quaternary veins absent, tracheoid idioblasts freely ending veins (Figures 3I and 5I).

Finally, *E. obovata* is included in *Pithyusa* (the sixth sampled section) based on characters of capsule and seeds (Riina *et al.*, 2013). However, our results placed *E. obovata* together with *E. cuneata* (subgenus *Athymalus*, section *Lyciopsis*) in subgroup 10 (Figure 1). *E. obovata* is the only species with palmate and basal acrodromous primary veins (Figure 3 J).

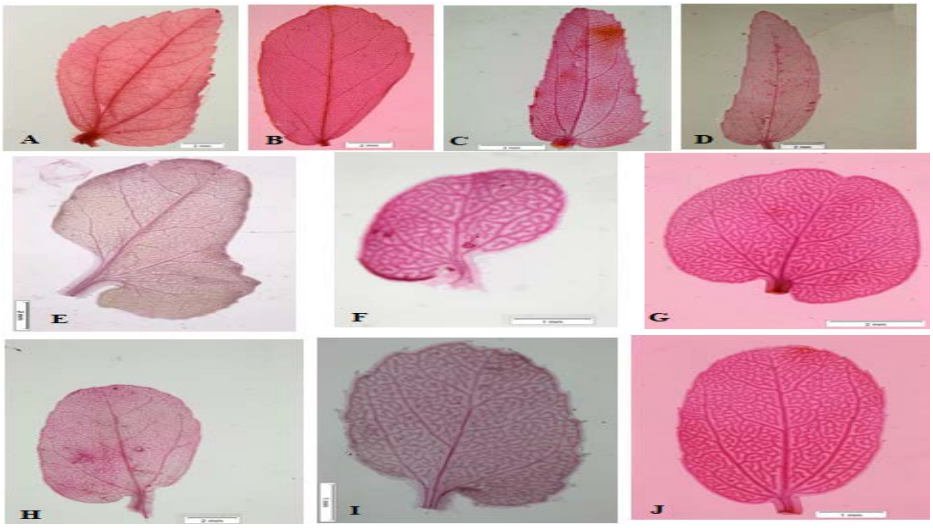

Figure 2: Light microscope micrographs of leaf blade of Euphorbia species, **A**. E. hirta, **B**. E. indica, **C**. E. lasiocarpa, **D**. E. hyssopifolia, **E**. E. peplis, **F.** E. granulata var. granulata, **G.** E. serpens, **H.** E. forsskaolii, **I** E. scordifolia, **J.** E. prostrata.

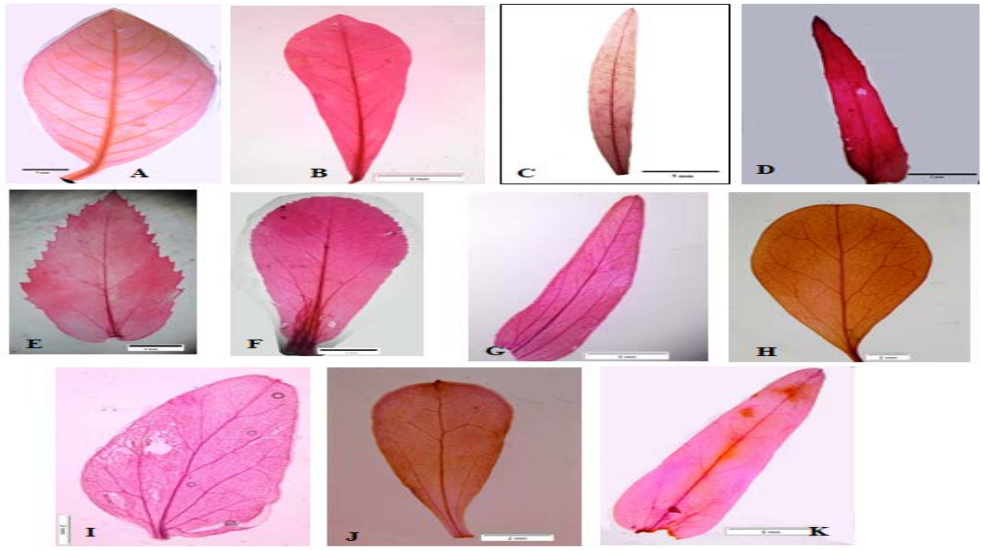

Figure 3: Light microscope micrographs of leaf blade of Euphorbia species, **A**. E. heterophylla, **B**. E. cuneata, **C**. E. dendroides, **D**. E. retusa, **E**. E. arguta, **F.** E. helioscopia, **G.** E. dracunculoides, **H.** E.peplus, **I.** E. chamaepeplus, **J.** E. obovata, **K.** E. terracina**.**

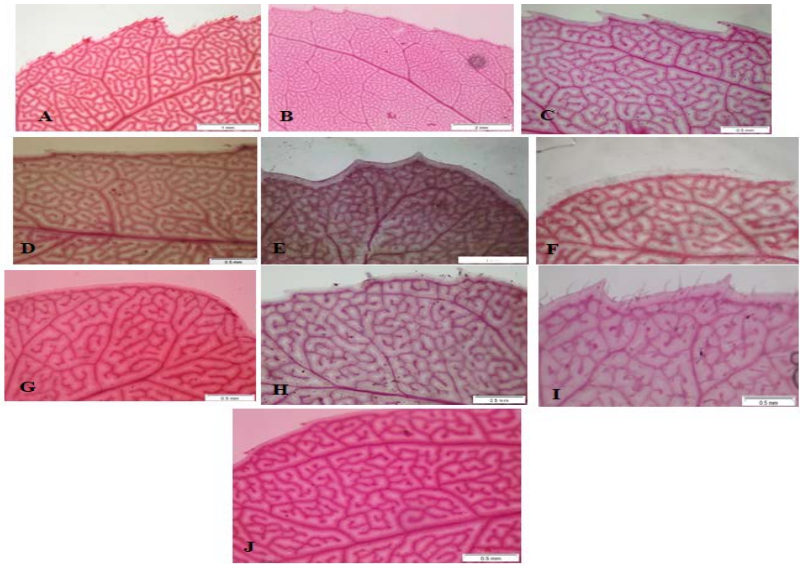

Figure 4. Light microscope micrographs of middle and marginal regions of leaves of Euphorbia species, A. E. hirta, B. E. indica, C. E. lasiocarpa, D. E. hyssopifolia, E. E. peplis, F. E. granulata var. granulata, G. E. serpens, H. E. forsskaolii, I. E. scordifolia, J. E. prostrata.

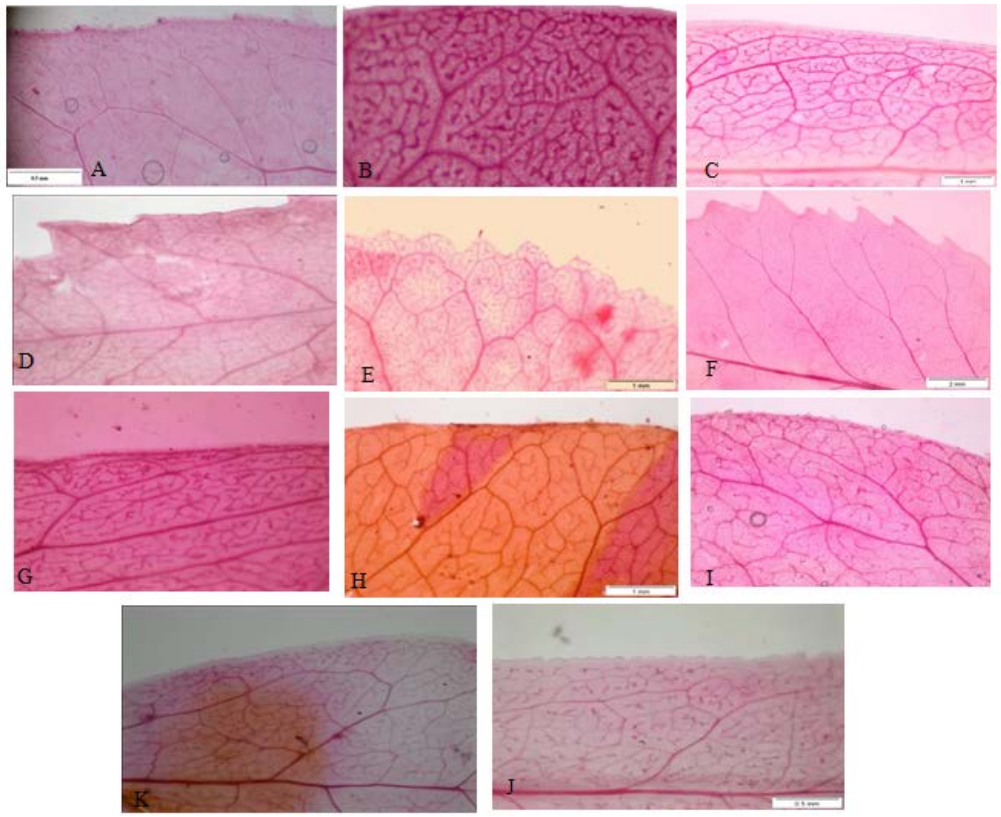

Figure 5: Light microscope micrographs of middle and marginal regions of leaves of *Euphorbia* species, **A**. *E. heterophylla*, **B**. *E. cuneata*, **C**. *E. dendroides*, **D.** *E. retusa*, **E.** *E. helioscopia*, **F.***E. arguta*, **G.** *E. dracunculoides*, **H.** *E. peplus*, **I.** *E. chamaepeplus*, **J.** *E. obovata*, **K.** *E. terracina*.

6. Conclusion

Since the time of Linnaeus, the identification and reconstruction of relationships between different plants have been based greatly on features of the reproductive organs. Although characters of seed, fruit and flower have proved very useful in plant taxonomy, there are situations in which these organs are not available for study. So, the current study was conducted to assess the importance of leaf morphological characters as well as venation patterns in identification and studying the diversity of 21 taxa of *Euphorbia* in Egypt. Our results are, to some degree, in line with the traditional classification sections of Pax and Hoffmann (1931), especially in placement of *Euphorbia terracina* and *Euphorbia dendroides* in different sections; in addition, our results agree with recently phylogenetic classification in placement of *Euphorbia heterophylla* in distinct section (*Poinsettia*). The arrangement and attachment of leaves, symmetry of base and median part blade, the primary vein and intersecondary veins are considered the most important characters to distinguished taxa at subgeneric and sectional levels, while laminar size, apex and base features of leaf, secondary veins characters, minor secondaries veins, tertiary veins, areolation, tracheoid idioblasts and tooth characters were considered as distinguished characters at species level. Results indicated that leaf architecture features, particularly venation patterns, are genetically fixed and can be used as a good taxonomic tool either in identification or classification of *Euphorbia* species in Egypt.

References

Abd El-Ghani MM, Kamel W and El Bous M. 2007. The leaf architecture and its taxonomic significance in Capparaceae from Egypt. *Acta Biologica Szegediensis*, **51(2):** 125-136.

APG IV. 2016**.** An update of the Angiosperm Phylogeny Group classification for the orders and families of flowering plants: APG IV. *Bot J Linn Soc*, **181(1)**: 1-20.

Ash A, Hickey LJ, Ellis B, Wilf P, Johnson K and Wing S. 1999. **Manual of Leaf Architecture–morphological description and categorization of dicotyledonous and net-veined monocotyledonous angiosperms by Leaf Architecture**. Smithsonian Institution, Washington.

Boulos L. 2000. **Flora of Egypt (Geraniaceae-Boraginaceae)**. Vol. 2. Al-Hadara Publishing, Cairo-Egypt.

Bruyns PV, Mapaya RJ and Hedderson TJ. 2006. A new subgeneric classification for *Euphorbia* (Euphorbiaceae) in southern Africa based on ITS and psbA-trnH sequence data. *Taxon*, **55 (2):** 397-420.

Cervantes A, Terrazas T and Hernández HM. 2009. Foliar architecture and anatomy of *Bernardia* and other genera of Acalyphoideae (Euphorbiaceae). *Brittonia*, **61(4)**: 375-391.

Christenhusz MJ and Byng JW. 2016. The number of known plants species in the world and its annual increase. *Phytotaxa*, **261 (3):**201-217.

Christophel D, Kerrigan R and Rowett A. 1996. The use of cuticular features in the taxonomy of the Lauraceae. *Anna Missouri Bot Gard*, **83 (3):** 419-432.

Dilcher DL. 1974. Approaches to the identification of angiosperm leaf remains. *Bot Rev*, **40(1):** 1-157.

El-Hadidi MN. 1973. The genus *Euphorbia* L. in Egypt I.: Section *Anisophyllum* Roep. B*ulletin du Jardin botanique National de*

Belgique / Bulletin van de Nationale Plantentuin van België, **43(1/2):** 83-100.

El-Ghazaly GA, Chaudhary R. 1993. Pollen morphology of some species of the genus *Euphorbia* L. *Review palaeobot Palynolo*, **78(3-4):** 293-319.

Ellis B, Daly DC, Hickey LJ, Johnson KR, Mitchell JD, Wilf P and Wing SL. 2009. **Manual of leaf architecture**. Vol. 190. Cornell University Press, Ithaca.

Fayed AA. 1973. Studies on the genus *Euphorbia* L. in Egypt. M. Sc. Thesis, Faculty of Science, Cairo University.

Fayed AA, and Hassan NM. 2007. Systematic significance of the seed morphology and seed coat sculpture of the genus *Euphorbia* L. (Euphorbiaceae) in Egypt. *Flora Mediterrinea* **17:** 47-64.

Fuller DQ and Hickey LJ. 2005. Systematics and leaf architecture of the Gunneraceae. *Bot Rev*, **71(3):** 295-353.

Govaerts R, Frodin D, Radcliffe-Smith A, Carter S. 2000. **World checklist and bibliographyof Euphorbiaceae.** Vol. 2. Royal Botanic Gardens, Kew.

Hammer Ø, Harper DA and Ryan PD. 2001. PAST-Palaeontological statistics software package for education and data analysis. *Palaeontologia electronica*, **4:** 9.

Hershkovitz MA. 1992. Leaf morphology and taxonomic analysis of *Cistanthe tweedyi* (nee *Lewisia tweedyi*; Portulacaceae). *Systematic Botany*, **17(2):** 220-238.

Hickey LJ and Taylor DW. 1991. The leaf architecture of *Ticodendron* and the application of foliar characters in discerning its relationships. *Ann Missouri Bot Gard*, **78(1):** 105-130.

Hickey LJ. 1973. Classification of the architecture of dicotyledonous leaves. *Am J Bot*, **60(1):** 17-33.

Hooker JD. 1885. **The Flora of British India,** Vol. 5. L. Reeve & Co, Ltd, England.

Kakkar L and Paliwal GS. 1972. Studies on the leaf anatomy of *Euphorbia* IV. Terminal idioblasts. *J Indian Bot Soc*, **51:** 118-126.

Larano AAP and Buot Jr IE. 2010. Leaf architecture of selected species of Malvaceae sensu APG and its taxonomic significance. *Philipp J Syst Biol*, **4:** 21-54.

Levin GA. 1986. Systematic foliar morphology of Phyllanthoideae (Euphorbiaceae).I. Conspectus. *Ann Missouri Bot Gard*, **73 (1):** 29-85.

Levin GA. 1986. Systematic foliar morphology of Phyllanthoideae (Euphorbiaceae). III. Cladistic analysis. *Sys Bot*, **11(4):** 515-530.

Loutfy M HA, Karakish E AK, Khalifa ASF and Mera ERA, 2005. Numerical taxonomic evaluation of leaf architecture of some species of genus *Ficus* L. *Int J Agric Biol*, **7:** 352-357.

Luo Y and Zhou ZK, 2002. Leaf architecture in *Quercus* subgenus *Cyclobalanopsis* (Fagaceae) from China. *Bot J Linn Soc*, **140(3):**283-295.

Mardia K, Kent J and Bibby J. 1979. **Multivariate Analysis**. Academic press, London.

Martínez-Millán M and Cevallos-FerrizSR. 2005. Arquitectura foliar de Anacardiaceae. *Rev Mex Biodivers*, **76(2):** 137-190.

Melville R. 1976. The terminology of leaf architecture. *Taxon*, **25(5/6):** 549-561.

Pacheco-Trejo J, Terrazas T and Ochoterena H. 2009. Leaf architecture of the genus *Didymaea* Hook. f. (Rubiaceae). *Plant Syst Evol*, **281(1-4):** 137-149.

Pax F and Hoffmann K. 1931. Euphorbiaceae. In: Engler-Prantl (Ed.), **Nat. Pflanzenfam** Wilhelm Engelmann, Leipzig, Germany, PP. 128-134.

Peirson JA, Bruyns PV, Riina R, Morawetz JJ and Berry PE. 2013. A molecular phylogeny and classification of the largely succulent and mainly African *Euphorbia* subg. *Athymalus* (Euphorbiaceae). *Taxon*, **62(6):** 1178-1199.

Pole M. 1991. A modified terminology for angiosperm leaf architecture. *J. R. Soc. N. Z.*, **21(4):** 297-312.

Radcliffe-Smith A. 1980. *Euphorbia* L. In: Townsend CC and Guest E (Eds.), **Flora of Iraq**, Vol. 4. Ministry of Agriculture; Bentham-Moxon Trust, Baghdad, pp. 327-362.

Riina R, Peirson JA, Geltman DV, Molero J, Frajman B, Pahlevani A, Barres L, Morawetz, JJ, Salmaki Y and Zarre S. 2013. A worldwide molecular phylogeny and classification of the leafy spurges, *Euphorbia* subgenus *Esula* (Euphorbiaceae). *Taxon*, **62 (2):** 316-342.

Roth-Nebelsick A, Uhl D, Mosbrugger V and Kerp H. 2001. Evolution and function of leaf venation architecture: a review. *Ann Bot*, **87(5):** 553-566.

Salvaña FRP and Buot Jr I E. 2013. Leaf architectural study of *Hoya coriacea*, *Hoya halconensis* and *Hoya buotii* (Apocynaceae). *International Research Journal of Biological Sciences*, **3(3):** 37-44.

Sarala C and Bhadane Vijay V. 2014. Leaf architecture in some Euphorbiaceae. *Indian J. Applied & Pure Bio.*, **29(2):** 343-360.

Secco RdS, Cordeiro I, Senna-Vale Ld, Sales MFd, Lima LRd, Medeiros D, Sá Haiad Bd, Oliveira ASd, Caruzoand MBR and Carneiro-Torres D. 2012. An overview of recent taxonomic studies on Euphorbiaceae s.l. in Brazil. *Rodriguésia* **63 (1):** 227-242.

Sehgal L and Paliwal G. 1974. Studies on the leaf anatomy of *Euphorbia*: II. Venation patterns. *Bot J Linn Soc*, **68 (3):**173-208.

Steinmann VW and Porter JM. 2002. Phylogenetic relationships in Euphorbieae (Euphorbiaceae) based on ITS and ndhF sequence data. *Ann Missouri Bot Gard*, **89(4):** 453-490.

Thepsithar C and Thongpukdee A. 2013. Comparative MicroMorphology, Anatomy and Architecture of Leaf of *Physalis*. I*nternational Journal of Biological, Biomolecular, Agricultural, Food and Biotechnological Engineering*, **7(8):** 806-810.

Thiers B. 2017. Index herbariorum. A global directory of public herbaria and associated staff. New York Botanical Garden‘s Virtual Herbarium, New York. Available from: http:// sweetgum.nybg.org/science/ih.

Todzia CA and Keating RC.1991. Leaf architecture of the Chloranthaceae. *Ann Missouri Bot Gard*, ٧٨**(1):** 476-496.

Viscosi V and Cardini A. 2011. Leaf morphology, taxonomy and geometric morphometrics: a simplified protocol for beginners. *PloS one*, **6:** e25630.

Wang YF, Ferguson DK, Zetter R, Denk T, Garfi G. 2001. Leaf architecture and epidermal characters in *Zelkova*, Ulmaceae. *Bot J Linn Soc*, **136 (3):** 255-265.

Webster GL. 1994. Synopsis of the genera and suprageneric taxa of Euphorbiaceae. *Ann Missouri Bot Gard*, **81(1):** 33-144

Yang Y, Riina R, Morawetz JJ, Haevermans T, Aubriot X and Berry PE. 2012. Molecular phylogenetics and classification of *Euphorbia* subgenus *Chamaesyce* (Euphorbiaceae). *Taxon*, **61(4):** 764-789.

Yu C and Chen Z. 1986. Leaf architecture of the woody dicotyledons from South China:1. Terminology and methods. *Acta Bot Austro Sinica*, **2:** 83-97.

Zohary M. 1972. Euphorbiaceae. In: Zohary M (Ed.), **Flora Palaestina**, Part 2**.** Israel Academy of Sciences and Humanities, Jerusalem, pp. 264-423.

JJBS
Jordan Journal of Biological Sciences

Volume 13, Number 2, June 2020
ISSN 1995-6673
Pages 177 - 181

Establishment of a Cutoff Value of Phenylalanine for Phenylketonuria among West Bank-Palestinian Neonates

Ibrahim A. Ghannam*, Akram T. Kharroubi, Renad M. Mustafa, Sumaia M. Jamous, Shahd M. Almufreh and Nelly M. Othman

Medical Laboratory Sciences Department, Al-Quds University, P.O. Box:66, Abu Dies, East Jerusalem, Palestine

Received June 24, 2019; Revised July 10, 2019; Accepted July 12, 2019

Abstract

Phenylketonuria (PKU) is an autosomal recessive disease due to a deficiency in phenylalanine hydroxylase that converts phenylalanine to tyrosine; this deficiency will lead to serious consequences like mental retardation. The purpose of this study was to establish a cutoff value of phenylalanine for the Palestinian neonates and to determine the incidence of PKU. A retrospective cohort study was carried out using data obtained from the Palestinian Central Public Health Laboratory (CPHL). During 2017, a total of 75,744 dried blood specimens had been tested for PKU using IBL international Kit with an enzymatic colorimetric principle. The data was analyzed using Receiver Operating Characteristics (ROC) curve to obtain the cutoff value of phenylalanine for PKU. Descriptive statistics and independent sample T-test were also used in the statistical analysis. ROC curve analysis revealed blood phenylalanine cutoff value of 3.3 mg/dL with 100% sensitivity and 99.۸% specificity. Among the 75,744 tested, 27 were positive (incidence rate of 35.6 per 10^5 newborns per year), 16 (59.3%) males, and 11 (40.7%) females. The cut off value (3.3 mg/dL) established in this study can be used with strong confidence, so we recommend that this value be adopted and used in Palestine.

Keywords: PKU, ROC Curve, Phenylalanine, Cutoff Value

1. Introduction

Phenylketonuria (PKU) is an autosomal recessive disease due to a mutation in the gene responsible for the production of phenylalanine hydroxylase (PAH) found on chromosome number 12. This enzyme converts phenylalanine (which is an essential amino acid important in the protein synthesis in the body) into Tyrosine (which is also an amino acid produced by the body used to support energy and motivation, promotes focus and mental clarity and improves mood and stress response) (Schuck *et al.*, 2015). Tyrosine is also the precursor of catecholamine, melanin and thyroid hormones (Figure 1). So, deficiency in PAH enzyme or its absence will cause phenylalanine build up in the infant's body leading to mental retardation, organ damage, abnormal posture and pale skin (Schlegel *et al.*, 2016). The damage is unfortunately irreversible, and these dangerous symptoms will become apparent in the first weeks of the infant's life (van Wegberg *et al.*, 2017).

This disease is considered an inborn error of metabolism where blockage of phenylalanine metabolism leads to the alternative pathway where phenylalanine is converted into phenylpyruvate and phenylacetate which are excreted by the kidney and seen in the urine, which is why it is called Phenylketonuria (PKU) (Williams *et al.*, 2008) and was first discovered by Asbjorn Folling (Folling, 1994).

There are 3 types of PKU disorders based on phenylalanine concentration in the infant's body: classic-type 1 with a concentration of >20 mg/dL, type 2 with a concentration of 10-20 mg/dL, and benign-type 3 with a concentration of <10 mg/dL (Hanley, 2004; Williams *et al.*, 2008).

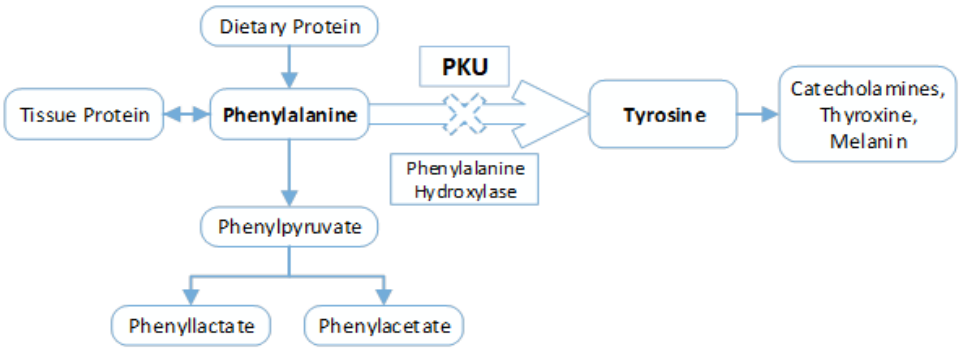

Figure 1. Phenylalanine metabolism pathway in Phenylketonuria.

Sample collection time for PKU screening differs depending on the method used, but most methods agree that it should not be less than 24-hours in order to differentiate between phenylalanine levels in those who are healthy and those who potentially have the disorder when quantitative methods are used, and 72-hour is believed to be the best time for testing because the baby will have got the appropriate amount of phenylalanine from the breastfeeding (van Wegberg *et al.*, 2017). Several methods can be used in PKU screening, such as Bacterial Inhibition Assay (Guthrie method) (Guthrie & Susi, 1963), Enzymatic Colorimetric method, Tandem Mass Spectrometry, enzymatic Fluorometric method, and newly emerging Molecular Methods (Blau *et al.*, 2014; Borrajo, 2016; Williams *et al.*, 2008).

This disease can be controlled by following a low phenylalanine diet; a restricted diet composed of less than usual breastfeeding along with formula milk free of Phenylalanine should be used to make sure the infant gets sufficient amount of Phenylalanine required for normal growth and development without causing harm (Kose *et al.*, 2018), or a milk formula with a little amount of Phenylalanine could be used alone but never breastfeeding alone (NIH, 2019).

According to a meta-analysis study done in European countries, patients with Phenylalanine concentration below 5.95 mg/dL should remain untreated as this concentration will not cause any symptoms to appear and has no effect on neurons. However, patients with Phenylalanine concentration below 5.95 mg/dL should be followed up and monitored during the first year of life because of the possibility of blood phenylalanine concentration increasing with age. So, according to this study, 5.95 mg/dL is considered as the upper target phenylalanine concentration (van Wegberg *et al.*, 2017). Some studies recommended a restricted diet for life (Guest *et al.*, 2013; Merrick *et al.*, 2003), while another study recommended a restricted diet until adulthood (Williams *et al.*, 2008). Mothers having PKU should follow a restricted diet during pregnancy in order to prevent building up and accumulation of Phenylalanine in infant's body causing fetal damage (Manta-Vogli & Schulpis, 2017).

Since there is no specific PKU cutoff value of Phenylalanine for the Palestinian population, the CPHL that performs this test for all Palestinian neonates from West Bank uses a cutoff value specified by the PKU neonatal Screening Assay Kit by IBL International, Germany (3 mg/dL). However, due to variations in the PKU cutoff values of Phenylalanine in different countries, the cutoff value used should be examined. Therefore, the purpose of this study was to establish a cutoff value of Phenylalanine for PKU in the West Bank - Palestine and to determine its incidence.

2. Methodology

A retrospective cohort study was conducted using a data for 75,744 specimens obtained from the CPHL (which is the only laboratory in the West Bank that screens for PKU). These specimens were tested for PKU in 2017, the method used for testing was an enzymatic-colorimetric method using (PKU) neonatal Screening Assay kit (RE80015 / RE80019, IBL International, Germany), with no cross-reactivity with the typical substance tested (analytical specificity), 1.55 mg/dL for functional sensitivity (limit of detection). Blood samples were collected between 24 to 72 hours after birth. Regarding linearity, samples showing concentration above the highest standard should be calculated from the linear curve by multiplying the standard used by two. Sample dilution is not recommended because blood presents an endogenous phenylalanine concentration and matrix effects of other substance cannot be excluded according to the kit used.

Blood for testing was obtained from the heel prick of the infant into a cellulose filter paper. A 5-mm spot puncher was used to punch filter paper and get a blood spot, then phenylalanine on the spot paper was eluted with trichloroacetic acid (TCA 3%). Phenylalanine dehydrogenase was added to transform phenylalanine into phenylpyruvate and to reduce NAD+ to NADH, then a substrate -Tetrazolium Salt- (yellow) was added and transformed into violet substrate Formazan by the reduced NADH. The color intensity of Formazan was measured using a spectrophotometer at 570 nm.

The CPHL applies the procedure specified in the IBL kit, a concentration of 2.5-2.9 mg/dL is considered a gray zone and it should be repeated to make sure of the result. If the concentration is above 3 mg/dL after repetition, a new sample should be collected and analyzed again, if it's also above 3 mg/dl it's considered positive. If any sample either a new one or the first one after repetition is below 3 mg/dL, it is considered negative.

3. Ethical approval

The study was a records-based, and there was no direct intervention involvement with patients. However, Data collection forms issued by Palestinian Ministry of Health that include ethical considerations were filled and signed.

4. Statistical Analysis

Data was processed using IBM Statistical Package for Social Sciences (SPSS) version 23 and MedCalc program version 15.8. Receiver Operating Characteristics (ROC) curve analysis was used to calculate the cutoff value. Descriptive statistics were used to assess the percentages while independent sample t – test, paired sample t – test, and Fisher's Exact test were used for inferential statistics. *P*-value <0.05 was considered statistically significant.

5. Results

A total of 75,744 specimens were included in this study from all Palestinian newborns in West Bank region during 2017, from which the results of 1915 specimen were repeated for at least once based on the current methodology adopted by CPHL in Palestine. Among the whole cases, 27 were PKU positive with an incidence rate of (35.6 per 10^5 newborns per year); comprising 59.3% of males and 40.7% of females. This gender difference was statistically insignificant (p=0.108).

The cutoff value obtained by the ROC curve analysis was 3.3 mg/dL with an optimal sensitivity (100%) and specificity (99.^%). Figure 2 shows The Area Under the ROC Curve (AUC) which was found to be 1 (Confidence interval: 1 - 1).

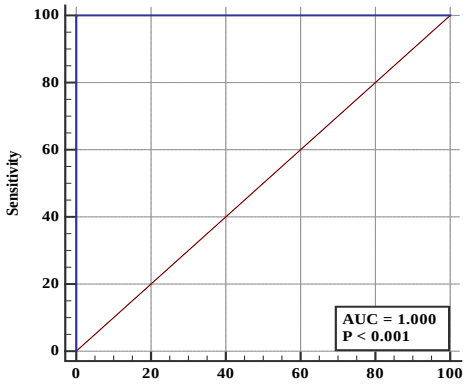

Figure 2. ROC curve analysis to establish the Phenylalanine cutoff value for PKU in the West Bank – Palestine.; AUC: Area under the Curve

Among specimens obtained, 75,576 (99.8%) were found to be true negative (TN), with 1.6 ± 0.467 mg/dL (mean ±SD). A value of 2.6 mg/dL was the most common (mode) among negative results, with a frequency of 397. Figure 3 shows Phenylalanine test results distribution among PKU true negative cases.

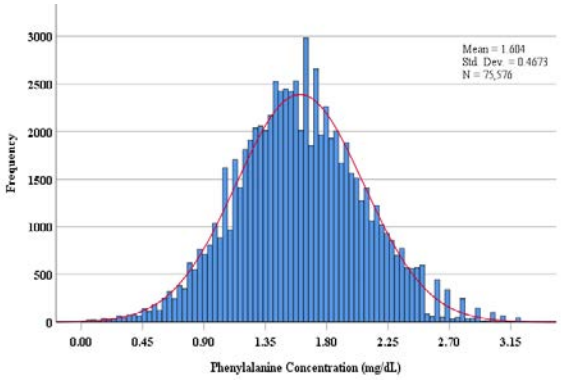

Figure 3. PKU test results distribution of Phenylalanine test results for PKU true negative cases among tested neonates.

However, 141 (0.2%) were found to be false positive (FP) as shown in Table 1. These numbers of TN and FP were obtained according to the calculated cutoff value of 3.3 mg/dL. Regarding true positive results, the highest value obtained was 29 mg/dL while the lowest value was 3.4 mg/dL.

Table 1. Frequency of PKU test result for False Positive and True Positive cases among tested neonates

Phenylalanine Concentration (mg/dL)	No. of FP cases	No. of TP cases
3.3 - 4.9	125	6
5.0 - 6.9	9	5
7.0 - 8.9	4	3
9.0 - 10.9	0	0
11.0 - 12.9	2	0
13.0 - 14.9	0	2
≥ 15.0	1	11
Total	141	27

PKU: phenylketonuria; FP: false positive; TP: True positive

The mean of Phenylalanine values for PKU true positive cases from the first sample without any repetition was 12.25 while the mean after retesting the first sample was 12.30 (p=0.89), while the mean of Phenylalanine value on a second sample that is collected after 10 days from the first one was 15.85 mg/dL. On the other hand, there was a sharp decline of mean Phenylalanine values from 4.05 to 2.52 for False positive results between the results of the first sample and the retesting of it (P <0.001).

Based on the 3.3 mg/dL cutoff value estimated by this study, the cutoff value usually used by CPHL in the West Bank (≥2.5 mg/dL) to distinguish positive from negative cases could be changed to a new one with much less false positive cases (141 case) than the usually estimated number (1888 case) (Figure 4).

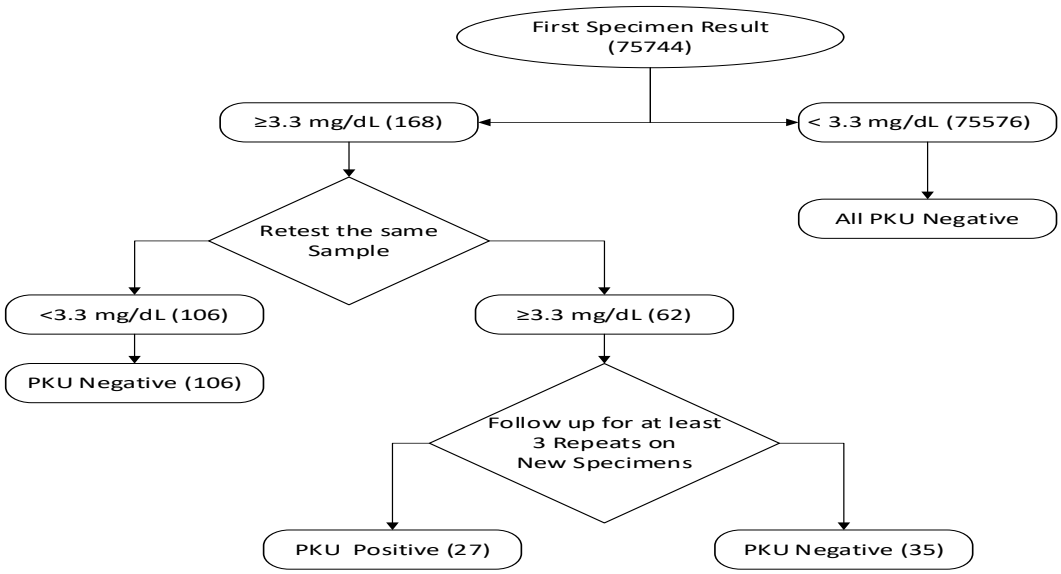

Figure 4. PKU Positive Cases identification based on a cutoff value of ≥ 3.3mg/dL for Phenylalanine

6. Discussion

The incidence rate of PKU in the West Bank of Palestine in 2017 was 35.6 per 10^5 newborns (1 : 2800) less than that in Turkey (1:2600) but Larger than average Arabian countries (1:6000) (Williams *et al.*, 2008). No significant incidence difference was found between males and females; this could be due to PKU being an autosomal recessive inherited disorder and not sex-linked (van Wegberg *et al.*, 2017). The optimum cutoff value of Phenylalanine for PKU for the Palestinian population living in West Bank based on ROC curve analysis was 3.3 mg/dL. Phenylalanine cutoff values for PKU vary from one population to another, for example, according to a study held in Bangkok the established cutoff value was 3.6 mg/dl using ELIZA method, 4 mg/dL using Guthrie method (Wasant *et al.*, 1999), another study in California gave a cutoff value of 4.3 mg/dL (Arnopp *et al.*, 1995). In Brazil, the cut off value was 5 mg/dL (Ramalho *et al.*, 2014). Regarding China, different cities had different cutoff values; 2 mg/dL in both Ankang and Fujian (Zhang & Jiang, 2011; Zhu *et al.*, 2004), 2.3 mg/dL in Shenzhen (Chun *et al.*, 2010), and 2.6 mg/dL in Daqing (Pan *et al.*, 2007).

In the ROC curve analysis, sensitivity refers to rate of true positive cases identified by the test divided by all true positive cases while the specificity refers to the rate of true negative cases identified by the test divided by all true negative cases. The analysis of this data revealed that sensitivity was 100% while specificity was 99.^%; this means that there are no false negative cases and all negative cases are true negative, so the established cutoff value estimated in this study can be used with strong confidence. The 141 (0.2%) false positive cases could be due to prematurity, improper sample collection time, procedural or personal error.

The AUC is a reflection of how good the test is at distinguishing patients with disease and those without the disease. In this study, it was found to be 1.0 for the ROC curve for the first sample, indicating that the test was excellent, and the 3.3 mg/dL value obtained is a definitive cutoff value

Phenylalanine concentrations of PKU cases ranged from >20 mg/dL for classic PKU (4 cases) and between 10 mg/dL to 20 mg/dL for mild PKU (9 cases), and <10 mg/dL for benign PKU (14 case). These different types of PKU according to phenylalanine concentrations could explain the variations in phenylalanine concentrations among the PKU positive cases (Williams *et al.*, 2008).

Repeated measures analysis for PKU for positive cases showed no significant difference between the mean of the first result and the retesting of the first sample, while the same analysis showed a sharp decrease in the mean concentration of phenylalanine in the false negative cases. So, the result of retesting the first sample is an excellent indicator for true positive cases. On the other hand, the mean phenylalanine concentration in the true positive cases increased dramatically between the first sample (12.25 mg/dL) and the second sample (15.85 mg/dL) that is tested after about 10 days, $p = 0.018$. This increase in phenylalanine concentration ascertains the presence of PKU in these neonates. Most false positive cases (115 case) became negative from the retesting of the first sample, while the rest (26 case) became negative on the second sample.

7. Recommendations

Some serious steps should be taken in preventing infants from leaving hospitals without making this important test. Also, parents should collaborate with centers and hospitals and follow the instructions when the test is performed. There is an urgent need to educate parents of PKU patients to follow the restricted diet. Moreover, the right protocol should be followed taking into account the appropriate sample collection time.

To reduce the cost of testing and repeating tests without actual need, we recommend the CPHL to adopt 3.3 mg/dl as a definitive cutoff value of Phenylalanine for PKU from the first test result. If the first test result is more than 3.3 mg/dL, then the sample must be retested, and new samples are necessary to rule out false positive cases.

Acknowledgments

The authors would like to acknowledge and thank the Palestinian Ministry of Health (PMOH) (Central Public Health Laboratory / Public Health Directorate) whose data was used in the creation of this publication. Also, we would like to extend our sincere gratitude to the Director General of Allied Medical Services, PMOH, Mr. Osama Najjar, for his assistance with data collection.

References

Arnopp JJ, Lorey FW, Currier RJ, Eastman JW, Velazquez KB, Morales DR, & Cunningham GC. 1995. Results of screening for phenylketonuria using a lower cutoff value in early collected specimens. *Screening*, **3(4)**, 193-199.

Blau N, Shen N, & Carducci C. 2014. Molecular genetics and diagnosis of phenylketonuria: state of the art. *Expert Rev Mol Diagn*, **14(6)**, 655-671. doi:10.1586/14737159.2014.923760

Borrajo GJ. 2016. Newborn Screening for Phenylketonuria: Latin American Consensus Guidelines. *Journal of Inborn Errors of Metabolism and Screening*, **4**, 1 - 5. doi: 10.1177/2326409816682764

Chun HX, Xin HX, & Qi Z. 2010. Exploration on cut off value of PKU screening in neonates by ROC analysis. *Maternal and Child Health Care of China*, **21**, 025.

Folling I. 1994. The discovery of phenylketonuria. *Acta Paediatr Suppl*, **407**, 4-10.

Guest JF, Bai JJ, Taylor RR, Sladkevicius E, Lee PJ, & Lachmann RH. 2013. Costs and outcomes over 36 years of patients with phenylketonuria who do and do not remain on a phenylalanine-restricted diet. *J Intellect Disabil Res*, **57(6)**, 567-579. doi:10.1111/j.1365-2788.2012.01568.x

Guthrie R, & Susi A. 1963. A Simple Phenylalanine Method for Detecting Phenylketonuria in Large Populations of Newborn Infants. *Pediatrics*, **32(3)**, 338-343.

Hanley WB. 2004. Adult phenylketonuria. *Am J Med*, **117(8)**, 590-595. doi:10.1016/j.amjmed.2004.03.042

Kose E, Aksoy B, Kuyum P, Tuncer N, Arslan N, & Ozturk Y. 2018. The Effects of Breastfeeding in Infants With Phenylketonuria. *J Pediatr Nurs*, **38**, 27-32. doi:10.1016/j.pedn.2017.10.009

Manta-Vogli PD, & Schulpis KH. 2017. Phenylketonuria Dietary Management and an Emerging Development. *J Acad Nutr Diet*. doi:10.1016/j.jand.2017.05.020

Merrick J, Aspler S, & Schwarz G. 2003. Phenylalanine-restricted diet should be life long. A case report on long-term follow-up of an adolescent with untreated phenylketonuria. *Int J Adolesc Med Health*, **15(2)**, 165-168.

NIH. (2019). What are common treatments for phenylketonuria (PKU)? https://www.nichd.nih.gov/health/topics/pku/conditioninfo/treatments (15.5.2019)

Pan JL, Zhao YQ, Chen YM, & Zhang FX. 2007. Study on Phe cut-off point of neonatal phenylketonuria screening in Daqing. *Chinese Journal of Birth Health & Heredity*, **2**, 65 - 71.

Ramalho AR, Ramalho RJ, Oliveira CR, Magalhaes MM, Santos EG, Sarmento PM, Matos DO, Oliveira MC, Oliveira AL, & Aguiar-Oliveira MH. 2014. Evaluation of effectiveness and outcome of PKU screening and management in the State of Sergipe, Brazil. *Arq Bras Endocrinol Metabol*, **58(1)**, 62-67.

Schlegel G, Scholz R, Ullrich K, Santer R, & Rune GM. 2016. Phenylketonuria: Direct and indirect effects of phenylalanine. *Exp Neurol*, **281**, 28-36. doi:10.1016/j.expneurol.2016.04.013

Schuck PF, Malgarin F, Cararo JH, Cardoso F, Streck EL, & Ferreira GC. 2015. Phenylketonuria Pathophysiology: on the Role of Metabolic Alterations. *Aging Dis*, **6(5)**, 390-399. doi:10.14336/AD.2015.0827

van Wegberg AMJ, MacDonald A, Ahring K, Belanger-Quintana A, Blau N, Bosch AM, Burlina A, Campistol J, Feillet F, Gizewska M, Huijbregts SC, Kearney S, Leuzzi V, Maillot F, Muntau AC, van Rijn M, Trefz F, Walter JH, & van Spronsen FJ. 2017. The complete European guidelines on phenylketonuria: diagnosis and treatment. *Orphanet J Rare Dis*, **12(1)**, 162. doi:10.1186/s13023-017-0685-2

Wasant P, Liammongkolkul S, & Srisawat C. 1999. Neonatal screening for congenital hypothyroidism and phenylketonuria at Siriraj Hospital, Mahidol University, Bangkok, Thailand--a pilot study. *The Southeast Asian journal of tropical medicine and public health*, **30**, 33-37.

Williams RA, Mamotte CD, & Burnett JR. 2008. Phenylketonuria: an inborn error of phenylalanine metabolism. *Clin Biochem Rev*, **29(1)**, 31-41.

Zhang L, & Jiang JY. 2011. Study on the cut-off value of screening test for phenylketonuria of neonate in Ankang area of Shanxi province. *Laboratory Medicine and Clinic*, **16**, 027.

Zhu WB, Chen HQ, & Wang J. 2004. Study on Phe cut-off point of neonatal phenylketonuria screening in Fujian province. *Chinese Journal of Birth Health & Heredity*, **4**, 94 -96.

JJBS

Volume 13, Number 2, June 2020
ISSN 1995-6673
Pages 183 - 189

Jordan Journal of Biological Sciences

Immunomodulatory and Anti-Arthritic Activities of *Stachys circinata*.

Wassila Slimani[1,2*], Sakina Zerizer[1,2*] and Zahia Kabouche[1]

[1]*Université des frères Mentouri-Constantine, Département de Chimie, Laboratoire d'Obtention de Substances Thérapeutiques (L.O.S.T), Constantine,* [2] *Département de Biologie Animale, Laboratory of Ethnobotany Palynology and Ethnopharmacology and Toxicology (E.P.E.T), Constantine, Algeria*

Received May 19 , 2019; Revised July 6, 2019; Accepted July 20, 2019

Abstract

The present study reports on the immunomodulatory and anti-arthritic activity of the dichloromethane extract of *Stachys circinata* L'her dried aerial parts (DMESC). Male *Mus Musculus* Albinos were used in all *in vivo* experiment. The toxicity was determined by the acute oral toxicity test administering DMESC orally, while the effect on phagocytosis was monitored by the blood carbon clearance assay. The formalin-induced arthritis (FIA) approach was used to measure the edema size during a 10 d period and quantify the C-reactive protein (CRP) and anti-cyclic citrullinated peptide (ACCP) at the end of the experiment. DMESC, did not produce visible signs of toxicity nor mortality and the LD resulted > than 2000 mg/kg. Phagocytic activity increased at all tested DMESC concentrations (50, 150 and 200 mg/kg) as evidenced by the half-life of colloidal carbon in the blood, the clearance rate was faster at 150 mg DMESC/kg. Also in the FIA test, DMESC supply at 150 mg/kg, revealed a significant decrease of the edema size, anti-CCP values ($P=0.000$) and CRP ($P<0.05$). As conclusion, the results clearly evidence that DMESC owns immune-stimulatory and anti-arthritic activity.

Keywords: *Stachys circinata*, Phagocytic activity, anti-inflammatory, CRP, Anti- CCP

1. Introduction

A large number of plants and their isolated constituents have been shown to potentiate health by exerting anti-inflammatory, anti-stress and anti-cancer effects by modulating the immune function (Bin-Hafeez *et al*., 2003). Macrophage is the first cell to recognize infectious agents and is central to cell-mediated and humoral immunities. It is a specialized phagocytic cell that attacks, destroys, and ingests cancer cells, foreign substances, and infectious microbes, by secreting pro-inflammatory cytokines, such as tumor necrosis factor-α (TNF-α) and interleukine-1 (IL-1) (Kim *et al*., 2013).

Rheumatoid arthritis (RA) is a frequent chronic inflammatory disease (Boissier *et al.*, 2012). RA is an unremitting multisystem disease accompanied by immune hyperactivity, persistent synovitis, and synovial hyperplasia along with deposition of autoantibodies to immunoglobulins leading to articular cartilage damage and resorption of osseous matter (Hasan and Alamgeer, 2018).

C-reactive protein (CRP) is an acute phase protein synthesized by hepatocytes in response to proinflammatory cytokines, in particular interleukin (IL)-6. It has been shown to be of great value as an inflammatory marker in RA and has been suggested to mediate part of the complement activation in RA (Singh *et al.*, 2013).

The presence of anti-citrullinated protein/peptide antibodies (ACPAs usually measured as anti-CCP) is highly specific for RA. ACPAs recognize citrullinated peptides found in many matrix proteins such as filaggrin, keratin, fibrinogen, and vimentin and found also in alpha-enolase (Svard *et al*., 2013). Citrulline derives from arginine by post-translational modification by peptidyl arginine deiminases (PADs) (Sakkas *et al.*, 2014). Citrullination of synovial antigens, especially fibrin, is an active process during synovial inflammation that probably allows the induction of anti-CCP antibody in RA patients (Del Val Del Amo *et al*., 2006).

The genus Stachys (Lamiaceae) is widely known in folk medicine and is worldwide distributed accounting for 300 species. In Algeria, this genus is represented by 14 species. Nassar *et al.* (2015) has revealed that three plant extracts belonging to Lamiaceae family exert antioxidant and immunostimulant effects. The study of Laggoune *et al*. (2016) has shown that the n-butanolic extract of the aerial parts of *Stachys mialhesi* exhibited significant antioxidant, antinociceptive and anti-inflammatory effects in laboratory animals. *In vivo* studies have revealed that *Stachys pilifera* possess significant anti-inflammatory effect (Sadeghi *et al.*, 2014), and considerable cytotoxic and anti-proliferative properties on HT-29 colorectal cell line (Panahi Kokhdan *et al*., 2018).

The current study was designed to evaluate the immunomodulatory and the anti-arthritic effects of the endemic species *S .circinata.*

* Corresponding author e-mail: zerizer.sakina@umc.edu.dz; wasbio@hotmail.fr; wassilaslimani25@gmail.com.

2. Materials And Methods

2.1. Plant Collection and authentication

Aerial parts of *S. circinata* L'Her were collected from Djebel El-Ouahch-Constantine (North Eastern Algeria) in April 2013 during the flowering stage. A voucher specimen (LOST SC04/13) has been deposited in the Laboratory of therapeutic substances, University frères Mentouri-Constantine and authenticated by Prof. G. De Belair (University of Annaba, Algeria).

2.2. Preparation of the dichloromethane extract

Air-dried and powdered aerial parts (1kg) of *S. circinata* were macerated three times at room temperature with MeOH-H2O (7:3, v/v) for 24h. After filtration, the filtrate was concentrated and dissolved in water (600 mL). The resulting solution was extracted successively with petroleum ether, CH_2CL_2, EtOAc and *n*-butanol. Concentration in vacuo at room temperature led to the following extracts: petroleum ether (2.3 g), dichlomethane (9 g) EtOAc (5 g) and *n*-butanol (25 g). The resulting dichlomethane extract of *S. circinata* (DMESC) was then used in all experiments.

2.3. Animals

Adult male *Mus Musculus* Albinos mice (2-2.5 mths old) were obtained from central pharmacy Institute, Constantine, Algeria. The animals used in all experiments had a weight range between 26 and 35 g. All the mice were kept under standard laboratory conditions at 24 ± 1°C relative humidity 55% with a 12 h light/dark cycle. They were fed with a stock rodent diet and tap water. The animal studies were conducted after obtaining clearance from Institutional Animal Ethics Committee and the experiments were conducted in strict compliance according to ethical principles and guidelines provided by the Committee for the Purpose of Control and Supervision of Experiments on Animals (CPCSEA).

2.4. Acute oral toxicity

The present study was conducted according to the guideline proposed by the Organization for Economic Cooperation and Development (OECD) revised up-and-down procedure for acute toxicity testing. This guideline is based on the procedure of Bruce *et al*. 1985.

A 2000 mg/kg dose was used in five adult male mice, the dose was given to a sole mouse, with the aim to monitor mortality and clinical signs (behaviors recorded: unusual aggressiveness, unusual vocalization, restlessness, sedation and somnolence movements, paralysis, convulsion, fasciculation, prostration and unusual locomotion). Observations lasted 48 h and were performed during the first hour and then each 3 h until the end. Upon survival of this mouse, four additional mice were given the same dose sequentially at 48 h intervals and again, clinical signs were monitored. All of the experimental animals were maintained under close observation for 14 d following DMESC administration, and the number of mice that died within the experimental period was noted. The lethal dose 50 (LD50) was established to be above 2000 mg/kg if no health disorders nor death was registered in three or more mice.

2.5. Phagocytosis (carbon clearance method)

Phagocytic activity of reticuloendothelial system (RES) was assayed by carbon clearance test. Phagocytic index was calculated as a rate of carbon elimination of RES by carbon clearance test determined by a reported method (Halpern *et al*., 1953).

Mice were divided into four groups each of 7 animals: group I (Control) received 0.5 mL of a 0.9% NaCl saline solution via intraperitoneal (i.p.) injection; groups II, III and IV were administred by i.p injection with 50, 150 and 200 mg/Kg of DMESC, respectively.

Forty eight hours after the i.p. injection of the treatment, a colloidal carbon ink suspension was injected via tail vein to all groups at a dose of 0.1 mL/10g. The ink suspension consisted of black carbon ink 3 ml, saline 4ml and 3% gelatin solution 4ml. Then, blood samples (≈14 drops or 25µL) were withdrawn from the retro-orbital plexus via heparin glass capillaries at interval of 5 and 15 min after carbon ink injection. Collected blood samples were lysed in a 0.1% sodium carbonate solution (4 mL) and optical density measured spectrophotometrically at 675nm. At the end of the experiment, liver and spleen were removed from each mice, weighted and values used to calculate the phagocytic index K.

Clearance kinetic was expressed by: 1) the phagocytic index K, which follows an exponential function of concentration to time and measures all the RES activity in contact with the circulating blood, and 2) the corrected phagocytic index α, which expresses this activity by, unit of active weight organs (liver and spleen). Finally, the clearance rate was expressed as the half-life period (t½, min) of the carbon ink in the blood. Parameters have been calculated using the following formulas according to Biozzi *et al*., 1970.

$$K = \frac{\text{LogOD1} - \text{LogOD2}}{t2 - t1} \qquad t\tfrac{1}{2} = \frac{0{,}693}{K}$$

$$\alpha = \sqrt[3]{K}\frac{\text{Body weight of animal}}{\text{Lever} + \text{spleen wt}}$$

OD1 and OD2 are the optical densities (at 675nm) recorded at time t1 (5 min) and t2 (15 min), respectively.

2.6. Formalin-induced arthritis

To perform this test, mice (20-30 g) were divided into four groups (F, FF, SC, D) of five animals each. Group 'F' remained untreated (negative control); group 'FF' (positive control) was subjected to the sole formalin treatment; group 'SC' to formalin + DMESC at 150 mg/kg and group 'D' to formalin + the anti-inflammatory standard drug (diclofenac of sodium) at 10 mg/kg. The administration was done orally by mixing the plant extract or diclofenac of the treated groups into a flour balls. The delivery of DMESC or diclofenac of sodium was carried out while maintaining the standard diet. In this experiment, the concentration with the highest efficacy of DMESC (150 mg/kg) was employed according to the results attained in the phagocytosis experiment.

According to the protocol of Mazumder *et al.* (2012), Formalin treatments were performed by injecting into the sub-plantar of the right hind paw 100 µL of formalin (2%) on the 1st and 3rd day of the experiment. Then, diclofenac and the DMESC were daily administered until the end of the experiment. During the 10 d experiment, a daily

measurement of the edema size was realized with a digital caliper.

2.7. Blood investigation

At the end of the experiments, animals from the entire groups were water-fasted overnight before collecting the blood samples. Blood samples were withdrawn as reported in the phagocytosis paragraph. The separated plasma was assayed for hs-C-reactive protein by an immunoturbidimetric method on a Cobas integra 400 plus analyser (Roche) and anti-CCP was measured by Stratec Biomedical Systems Gemini 6280 Automated Compact Microplate Processor.

2.8. Statistical analysis

The data are reported as mean ± SEM (standard error of the mean). Statistical analyses of the results were performed using one–way ANOVA test and Tukey's multiple comparison tests (SPSS version 20). The values of, $^{***}P<0.001$, $^{**}P< 0.01$and $^{*}P< 0.05$ were considered to indicate the significant levels.

3. Results

3.1. Acute toxicity study

According to the preliminary toxicity test, the DMESC was found to be safe up to 2000 mg/kg. Indeed, during the 14 day-assessment time, mice were not affected by the amendment of floor balls with 2000 mg/kg of DMESC and they remained healthy and with no visible signs of toxicity nor mortality. This result stand up for an LD50 higher than 2000 mg/kg.

3.2. Phagocytic activity

The results show a significant increase of K index mean values in mice belonging to DMESC supplied groups if compared to the control (NaCl group) with *P*= 0.001 (Fig. 1A). Index values for the DMESC administered groups were: 0.031 ± 0.004; 0.038 ± 0.005 and 0.035 ± 0.007 with 50, 150 and 200 mg/kg, respectively. The NaCl group attained a mean index value of 0.017 ± 0.005. The highest activity was monitored in the group of mice fed with 150 mg DMESC /kg (65.3% increase), but difference among DMESC doses was not significant. This indicates that DMESC enhanced the phagocytic activity by stimulating the RES. and according to the results, it seems that the tested concentrations lower or higher than 150 mg/kg do not improve the phagocytic index value.

DMESC supply to mice influenced significantly the calculated half time (t½) of colloidal carbon clearance which decreased by nearly 50% compared to the control (NaCl). Among DMESC supplied groups the probability was *P*= 0.01 with a t½ of 23.01 ± 3.14 min; 18.65 ± 2.52 min and 20.56 ± 2.83 min with 50, 150 and 200 mg/kg, respectively (Fig. 1B). The NaCl group owned a t½ of 40.62 ± 20.35 min. Compared to control, the clearance rate with150 mg DMESC/kg was lowered more than twice.

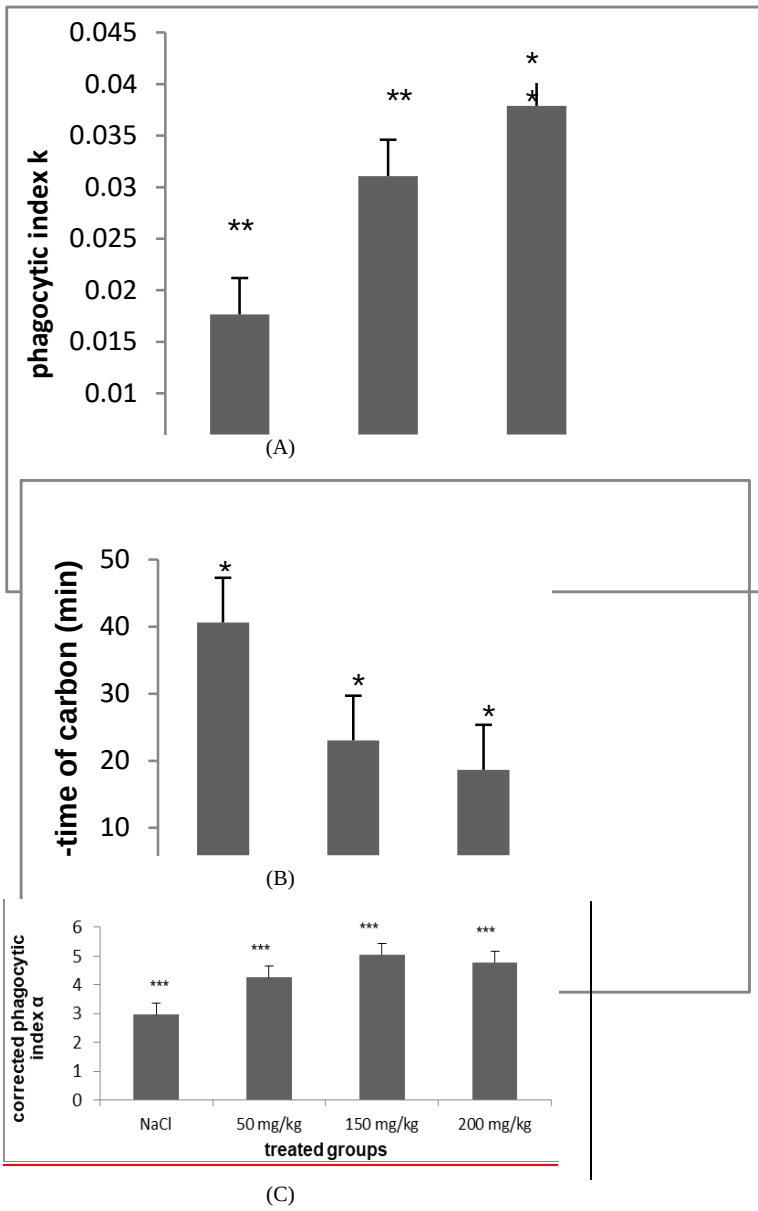

Fig. 1. Effect of dichloromethane extract *S. circinata* of aerial parts on phagocytic activity expressed as: (A) index phagcytic K; (B) half-time t1/2 of carbon in the blood; (C) corrected phagocytic index α. Values are mean ± SEM (n=7) and significant difference from the control group is shown as *p<0.05, **p<0.01, ***p<0.001

GI: Control group received NaCl; **GII:** group received dichloromethane extract of *S. circinata* at dose 50mg/kg; **GIII:** group received dichloromethane extract of *S. circinata* at dose 150mg/kg; **GIV:** group received dichloromethane extract of *S. circinata* at dose 200mg/kg.

In addition to the results reported in Fig.1A, B a significant increase in the corrected phagocytic index α occurred between DMESC groups *P*=0.000 (α= 4.26 ± 0.74; 5.05 ± 0.57; 4.78 ± 0.60 with 50, 150 and 200 mg/kg, respectively) and the control group (α= 2.97 ± 0.50) (Fig. 1C).

3.3. Formalin induced arthritis

The results evidenced a significant inhibition in the edema size in group 'SC' and 'D' (*P*=0.000) while, on the other hand a significant increase of the size occurred in

group 'FF' (*P*=0.000) in comparison to the negative control, group 'F' (*P*=0.000) (Fig. 2).

One day following the first injection of formalin, the edema size enlarged significantly in groups 'FF', 'SC' and 'D' (3.24 ± 0.37; 3.26 ± 0.08 and 3.10 ± 0.24 mm, respectively) in comparison to the negative control group 'F' (1.71 ± 0.016 mm), while, after the second injection of formalin, size increase on the 3rd day was negligible.

On the 4th d, size decreased significantly in group 'SC' and 'D' (2.98 ± 0.13 and 3.04 ± 0.11 mm, respectively) compared to the group 'FF', positive control, where the edema size increased until 5 days after the 2nd formalin injection (3.83 ± 0.28 mm).

From the 5th d until the end of the experiment, the sizes in group 'SC' and 'D' decreased slightly and mean values were almost identical, whereas a significant decrease occurred in the positive control group 'FF' (Fig. 2).By comparing the edema size of each group during the experimental period, the size of the negative control group 'F' remained nearly stable throughout the experiment with an average of 1.7 mm, while compared to the edema size in group 'FF' a decrease of about 77,6 and 79,2% was attained in treated groups 'SC' and 'D', respectively.

It is noteworthy to evidence that the edema development in group 'FF' progressed differently from group 'SC' and 'D' following the 2nd injection of formalin at the 3rd day. Indeed, in group 'FF' size continue to enlarge until day 8 and then decreased till 10th d (3.27 ± 0,44 mm). On the other hand, starting from day 4, edema in group 'SC' and 'D' slowly underwent a similar decease evidencing clearly a comparable anti-inflammatory effect of DMESC and diclofenac of sodium.

The C-reactive protein (CRP) concentration in mice blood following formalin injection decreased by supplying mice with 150 mg/kg DMESC (group 'SC') or with 10 mg/kg diclofenac of sodium (group 'D') and values were about 1.03 ± 0.74 and 0.68 ± 0.26 mg/L, respectively. However, the mean value of CRP (1.62 ± 0.82 mg/L) in group FF was increased but not significantly when it's compared to group 'SC' and 'D' (Fig. 3A).

The ACCP values were also influenced by treatments and had a similar trend to those of CRP but differences resulted a significantly lower (*P* = 0.000) in blood of mice supplied with DMESC or diclofenac of sodium. The concentration of ACCP is decreased in the groups 'SC' and 'D' (2.14 ± 0.38 and 1.57 ± 0.56 UI/mL, respectively) when it's compared to the group 'FF' (positive control) which had the highest ACCP values (3.13 ± 0.96 UI/mL) (*P* = 0.000), while the group 'F' (negative control) had the lowest (0.62 ± 0.32 UI/mL) values as shown in Fig. 3B.

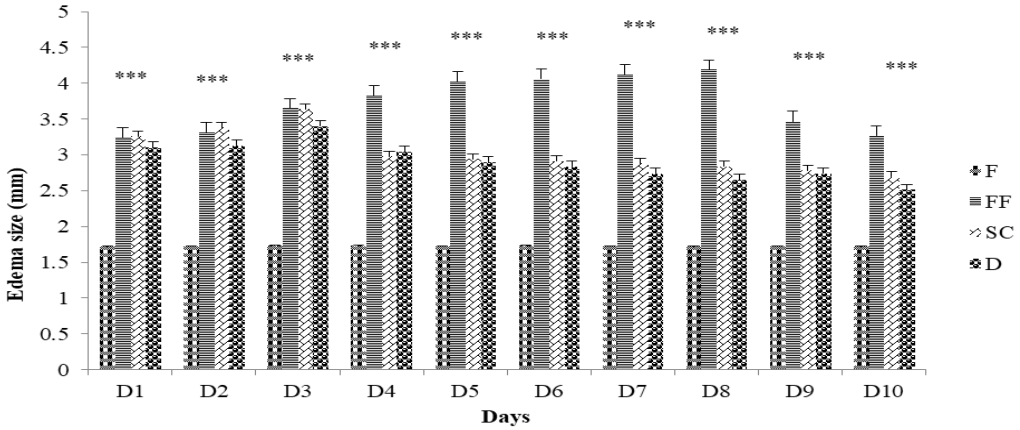

Figure 2: Anti-inflammatory effect dichloromethane extract of *S. circinata* aerial parts on the formalin induced mice hind paw edema during a 10 day experimental period. Values are mean ± SEM (n=8) and significant difference from the control group is shown as *p<0.05, **p<0.01, ***p<0.001. Treatments: F= untreated (negative control); FF= (positive control) sole formalin treatment; SC= formalin + DMESC (150 mg/kg); D= formalin + diclofenac of sodium (10 mg/kg).

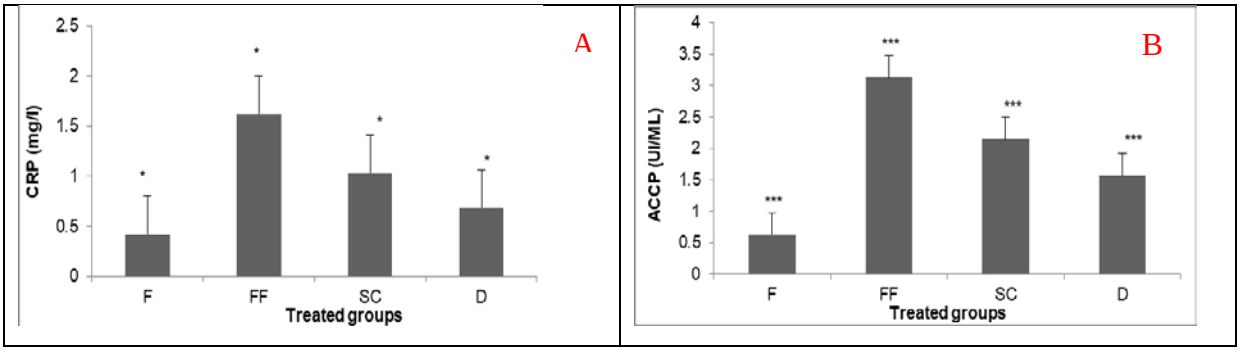

Figure 3: Effect of dichloromethane extract of *Stachys circinata* on serum parameters in Formalin-induced arthritis in mice. (A) Blood levels of C-Reactive Protein (CRP) in mice following formalin-induced arthritis as influenced by the dichloromethane extract of *S. circinata* aerial parts (DMESC) and diclofenac of sodium; (B) Anti-cyclic citrullinate peptide (ACCP) levels in mice blood following formalin-induced arthritis as influenced by the dichloromethane extract of *S. circinata* aerial parts (DMESC) and diclofenac of sodium. Values are mean ± SEM (n=7) and significant difference from the control group is shown as *p<0.05, **p<0.01, ***p<0.001. Group F: untreated (negative control); Group FF: (positive control) formalin inflammation; Group SC: formalin inflammation+ DMESC (150 mg/kg); Group D: formalin inflammation+ diclofenac of sodium (10 mg/kg).

4. Discussion

The use of herbal medicines as alternative or adjuvant treatment has been increasing worldwide and gaining popularity in developing countries where ethnobotanical practices are still very popular. Although medicinal plants may have biological activities that are beneficial to humans, the potential toxicity of these bioactive substances has not been well established. Thus, the safety and efficacy of these plants must be studied thoroughly to maximize their benefits for mankind (Elsnoussi *et al*., 2011).

In our study, we have demonstrated that the dichloromethane extract of *S. circinata* is not toxic by oral administration in mice up to 2000 mg/kg, similar toxicological concentrations were achieved for plant extracts of *Argania spinosa, Citrullus colocynthis* and *Boswellia serrata* by Aribi, 2015.

The evaluation of the immunomodulatory effect of DMESC took into account that the immune cells and mediators are directly involved in the processing of antigens, removal of microorganisms by, phagocytosis, lysis of bacteria, viruses or tumor cells. Many malignant diseases are caused by, a decreased number or function of immune competent cells. Hence, modification of immune response either through suppression or stimulation may be helpful in avoiding diseases related to the immune system (Sharma *et al*., 2012).

Currently several of the available therapeutic drugs have potential side effects. Thus, medicinal plants and their active components as a source of immunomodulatory agents are gaining importance (Sharma *et al*., 2012).

The results of the present study showed that DMESC may stimulate cell mediated immunity as shown by an increase in macrophage induced phagocytosis in carbon clearance test. When ink containing colloidal carbon is injected into the systemic circulation, the macrophages engulf the carbon particles of the ink and the rate of clearance of ink from blood is known as phagocytic index (George *et al*., 2014). DMESC stimulated the RES by, a high significant increase in the phagocytic index. Our results are in agreement with those of Benmebarek *et al*. (2014) who indicated that *Stachys ocymastrum* extract appears immune stimulatory at low concentrations and immunosuppressive at high concentrations as it exhibited a biphasic effect on the phagocytic activity of the RES and with those of Nassar *et al.* (2015) who reported that the *n* butnolic extract of *Stachys circinata* increased the phagocytic index at 150 mg/kg.

The improvement in phagocytic function by DMESC may be due to a number of actions of different effector components of the phagocytes. However, the most important mechanism is the up-regulation of receptors that are required to interact with the pathogens which include mannose and toll like receptors. It may also be due to the increased opsonization of carbon particles by complement proteins and immunoglobulins. So, the immunostimulate activity of the DMESC which acted by activating the function of the RES is due to the fact that it contains natural physiologically active substances such as terpenoids, phenolic compounds and flavonoids (Laggoune et al., 2016), which increase the humoral response, by stimulating the macrophages and B-lymphocytes subsets involved in antibody synthesis (Dash *et al*., 2006).

In our work we are searching for a new therapeutic drugs for arthritis because synthetic drugs, in recent years, are accompanied by numerous unwanted side effects, such as the Non Steroidal Anti-Inflammatory Drugs (NSAIDs) that produce gastric ulcer, and as major side effects glucocorticoids are associated with adrenal suppression (Boddawar *et al*., 2016). In addition, their use cannot halt the development of rheumatoid arthritis and Disease Modifying Antireheumatic Drugs (DMARDs) have been impeded by their potential of long-term side effects, toxicity and immunosuppression (Tag *et al.,* 2014). So, it is very important to search for new therapeutic drugs from a natural source with greater efficiency and lower toxicity.

Findings of the present study have revealed that DMESC treatment exerts anti-arthritic effect. It decreased the inflammation compared to the control group as observed by the decrease in the edema size, the concentration of ACCP and CRP values. These results agree with those of Mazumder *et al.* (2012) who reported that in the formaldehyde induced arthritis inflammation test (FIA), the methanol extract of *Barleria lupulina* owned a significant inhibition of the edema formation during the experimental period of 10 days. Our results are in agreement with those of Kehili *et al.* (2016) who reported that ACCP and CRP are decreased in mice injected with formalin and treated with Algerian *Phoenix dactylifera* fruit. Benmebarek *et al*. (2013) reported a decrease of hs-CRP when mice was treated with extracts of *S. mialhesi* following an inflammation induction by hyperhomocysteinemia.

FAI is one of most commonly used acute models for assessing anti-arthritic potential of plant extract (Kore *et al*., 2011). Injection of formalin into hind paw produces localized pain and inflammation, which is biphasic response, an early neurogenic component followed by a later tissue-mediated response (Shastry *et al*., 2011).

The initial phase of the edema is due to the release of histamine and serotonin and the edema is maintained during the plateau phase by kinin like substance and the second accelerating phase of swelling due to the release of prostaglandin like substances (Manguesh *et al*., 2010); this phase seems to be an inflammatory response with inflammatory pain that can be inhibited by anti-inflammatory drugs (Vasudevan *et al.*, 2006).

The anti-inflammatory activities of many plants have been attributed to their saponin, terpenoids, flavonoids and steroids contents (Shastry *et al*., 2011). Flavonoids were considered to be the active components responsible for the biological actions of the genus *Stachys.* In addition, this genus has been shown to possess various biological properties related to antioxidant, anti-nociceptive and anti-inflammatory mechanisms by targeting reactive oxygen species and prostaglandins which are involved in the late phase of acute inflammation and pain perception (Kehili *et al*., 2016; Laggoune *et al*., 2016). These results are compatible with those of Peng *et al.* (2016) who reported that the flavonoids and alkaloids in the ethanol extract of the roots of *Caragana pruinosa* might be responsible for its anti-arthritic activity. In our research, we evidence that DMESC had accelerated the anti-inflammatory activity in a similar pathway as diclofenac and this is remarkable by lower volume of edema, CRP and Anti-CCP values.

The initiation of RA involves the activation of auto-reactive T cells and the recruitment of these T cells along

with other leukocytes into the joints. These leukocytes produce a variety of mediators of inflammation. Prominent among these mediators are arachidonic acid metabolites, pro-inflammatory cytokines, free radicals and matrix-degrading enzymes. These mediators modulate the processes relating to cell migration into the joints as well as angiogenesis and degradation of the extracellular matrix within the joints, leading to the arthritic inflammation (Venkatesha *et al*., 2011).

Naderi *et al*.(2016) reported that phenolic compounds in the Ginger decrease the pro-inflammatory factors of TNF-α and IL-1β. Both mediators induce NF-kB, which is a ubiquitous eukaryotic transcription factor with a pivotal role in inflammatory pathways. In addition, these crucial compounds suppress the synthesis of prostaglandin and leukotriene by inhibiting the COX-2 and lipoxygenase pathways and also inflammation-involved pathways diminishing the inflammation. Therefore the active compounds obtained by Lggoune *et al*.(2016), could play same role for inhibition of TNF-α and IL-1β.

Serum CRP, a surrogate marker of disease severity that correlates with final outcome of arthritis is also a potent endogenous ligand for TLR-2 present on the surfaces of synovial fibroblasts, PMNs and macrophages and its transcription is regulated by pro-inflammatory cytokines including IL-6 (Adhikary *et al*., 2016).Serum concentration of CRP, the most common type of acute phase proteins was tested in our experiments and was found to be significantly attenuated in case of FAI in mice treated with DMESC. This explains a protective role of DMESC against liver damage and inflammatory reactions in hepatic tissues during pathogenesis of FIA.

Immune complexes (IC) deposited into the synovial joints elevate pro-inflammatory cytokines in serum, through induction of mononuclear cells, these immune complexes can stimulate PMNs and macrophages to secrete pro-inflammatory cytokines, like TNF-α. In both ways, there is activation of synovial macrophages which ultimately results in increased production of TNF-α, IL-1β and other pro- inflammatory cytokines like IL-6, IL-12 and IL-15 which are involved in RA pathogenesis (Adhikary *et al*., 2016). However, IC containing citrullinated fibrinogen have been detected in the peripheral blood of anti-citrullinated protein/peptide antibody (ACPA) -positive RA patients and also in synovial pannus (Fisher, 2014). These IC stimulate macrophage TNFα production and the accumulation of multiple ACPA specificities is correlated with preclinical inflammation (elevation of TNF-α, IL-6, and IFN-γ) preceding clinical arthritis (Sakkas *et al*., 2014).

A considerable improvement in the management of RA has been obtained since the advent of biological agents such as (TNF)-α inhibitors (adalimumab, certolizumab, etanercept, golimumab or infliximab) anti-B cell agent (rituximab), anti-IL-6 receptor inhibitor (tocilizumab), T cell modulator (abatacept) (Atzeni *et al*., 2013). A problem facing the practicing physician is to prescribe the most appropriate biological agent to individual patient, in other words, to match a biological agent with a patient profile, given the high cost of biological (Boissier *et al*., 2012). The presence of ACPAs was associated with reduced response to anti-TNFα agents (Potter *et al*., 2009).

From the DMESC, a variety of secondary metabolites were isolated and fifteen known compounds have been identified, among them flavonoids such as luteolin, apigenin, isorhamnetin, triterpenoids such as betulinic acid, ursolic acid and olealonic acid, sterols such as stigmasterol and β-sitosterol (Lggoune *et al*., 2016). However the effect shown by DMESC that ameliorates FIA induced inflammation and progressive bone damage is an outcome of a cumulative effect of all these bioactive compounds; therefore, further studies are warranted on these chemical constituents from DMESC after purifying them and administering them separately in animal models with respect to formalin-induced arthritis.

5. Conclusion

These findings provide a basis for the therapeutic potential of *S. circinata* for the control and management of diseases in which the immune system needs to be stimulated and for inflammatory conditions like rheumatoid arthritis.

Acknowledgements

The authors are grateful to the MESRS (Ministry of Scientific Research, Algeria)

Conflicts Of Interest

All authors report no conflicts of interest regarding this manuscript.

References

Adhikary R, Majhi A, Mahanti S, Bishayi B. 2016. Protective effects of methanolic extract of *Adhatoda vasica* Nees leaf in collagen-induced arthritis by modulation of synovial toll-like receptor-2 expression and release of pro-inflammatory mediators. *J Nutr Inter med Metab*, **3**: 1-11.

Aribi B. 2015. Biological activities of some medicinal plants on rheumatoid arthritis induced by hyperhomocysteinemia and formalin and on tumoral process. Thesis submitted for the degree of doctorat 3ème CYCLE Option: Immuno-Oncology. Departement of Animal Biology. Faculty of Life and Natural Sciences. University frères Mentouri, Constantine. Algeria

Atzeni F, Benucci M, Sallì S, Bongiovanni S, Boccassini L, Sarzi-Puttini P. 2013. Different effects of biological drugs in rheumatoid arthritis. *Autoimmun Rev*, **12**:575-579.

Benmebarek A, Zerizer S, Laggoune S and Kabouche Z. 2013. Effect of *Stachys mialhesi* de Noé on the inflammation induced by hyperhomocysteinemia in cardiovascular diseases. *Pharm Lett*, **5 (2):**212-223.

Benmebarek A, Zerizer S, Laggoune S, Lakhal H,and Kabouche Z. 2014. Biphasic dose response effect of *Stachys ocymastrum. Inter J Pharm Pharma Sci*, **6(2):**534-537.

Bin-Hafeez B, Haque R, Parvez S, Pandey S, Sayeed I, Raisuddin S. 2003. Immunomodulatory effects of fenugreek (*Trigonella foenum graecum* L.) extract in mice. *Inter Immunopharmacol*, **3 :** 257-265.

Biozzi G, Stiffel C, Mouton D, Decreusefond C, Corradetti A, Verolini F, *et al*. 1970. Effect of irradiated *Plasmodium berghei* vaccination on the phagocytic activity of the reticuloendothelialsystem during rat infection with this *plasmodium*. *Bull World Health Organ*, **42:** 163-168.

Boddawar GD, Dhawale SC, Shaikh SS. 2015. Assessment of anti-inflammatory potential of *Sesbaniabi spinosa* Linn. leaf

extracts and fractions by acute and chronic models. *Alex J Med*, **52:** 289-293.

Boissier MC, Semerano L, Challal S, Saidenberg-Kermanac'h N, Falgarone G. 2012. Rheumatoid arthritis: From autoimmunity to synovitis and joint destruction. *J Autoimmun*, **39:** 222-228.

Bruce RD. 1985. An Up-and-Down Procedure for Acute Toxicity Testing. *Fundam Appl Toxicol*, **5:** 151-157.

Dash S, Nath LK, Bhise S, Kar P, Bhattacharya S. 2006. Stimulation of immune function activity by the alcoholic root extract of *Heracleum nepalense* D. Don. *Indian J Pharmacol*, **38:** 336-340.

Del Val Del Amo N, Ibanez Bosch R, Fito Manteca C, Gutierrez Polo R, Loza Cortina E. 2006. Anti-cyclic citrullinated peptide antibody in rheumatoid arthritis: Relation with disease aggressiveness, *Clin Exp Rheumatol*, **24:** 281-286.

Elsnoussi AHM, Chung PL, Ebrika OS, Asmawi MZ, Sadikun A, Yam MF. 2011. Toxicity evaluation of a standardised 50% ethanol extract of *Orthosiphon Stamineus*. *J Ethnopharmacol*, **133**: 358-363.

Fisher BA. 2014. Chapter 90 - Antibodies to specific citrullinated proteins in rheumatoid arthritis. **Autoantibodies**. 3rd edition. Birmingham, UK, University Hospitals Birmingham NHS Foundation Trust, pp 761-769.

George A, Chinnappan S, Choudhary Y, Bommu P, Sridhar M. 2014. Immunomodulatory activity of an aqueous extract of *Polygonum minus* Huds on swiss albinos mice using carbon clearance assay. *Asian Pac J Trop Dis*, **4:** 398-400.

Halpern BN, Benacerraf B, Biozzi G. 1953. Quantitative Study of the Granulopectic Activity of the Reticulo-Endothelial System. I: The effect of the ingredients present in India ink and of substances affecting blood clotting *in vivo* on the fate of carbon particles administered intravenously in rats, mice and rabbits. *Br J Exp Pathol*, **34:** 426-440.

Hasan UH and Alamgeer. 2018. Antiarthritic efficacy of *Clematis orientalis*. *Bangladesh J Pharmacol*, **13:** 142-148.

Kehili HE, Zerizer S, Beladjila KA, Kabouche Z. 2016. Anti-inflammatory effect of Algerian date fruit (*Phoenix Dactylifera*)**.** *Food Agric Immunol*, **27:** 820-829.

Kim TH, Lee SJ, Rim HK, Shin JS, Jung JY, Heo JS, *et al.* 2013. *In vitro* and *in vivo* immunostimulatory effects of hot water extracts from the leaves of *Artemisia princeps* Pampanini cv. Sajabal. *J Ethnopharmacol*, **149:** 254-562.

Kore K J, Shete R V, Desai N V. 2011. Anti-Arthritic activity of Hydroalcoholic extract of Lawsonia *Innermis Int. J. Drug Dev. & Res*, **3 (4):** 217-224

Laggoune S, Zeghib A, Kabouche A, Kabouche Z, Maklad YA., Leon F, *et al.* 2016. Components and anti-oxidant, anti-inflammatory, anti-ulcer and anti-nociceptive activities of the endemic species *Stachys mialhesi* de Noé. *Arabian J Chem*, **9:** S191-197.

Laggoune S, Zeghib A, Kabouche A, Kabouche Z. 2016.Secondary metabolites, evaluation of the DPPH free-radical scavenging effect by electron spin resonance and antibacterial activity of the endemic species *Stachys circinata* l'Her. *Chem Nat Compd*, **52:** 552-553.

Mangesh SB, Virendra GK, Ashwin DS. 2010. Evaluation of Analgesics and Anti-inflammatory Activity of a Poly-Herbal Formulation. *Int J Pharm Tech Res.* 2010, **2:** 1520-1527.

Mazumder PM, Mondal A, Sasmal D, Arulmozhi S, Rathina velusamy P. 2012. Evaluation of anti-arthritic and immunomodulatory activity of *Barleria lupulina*. *Asian Pac J Trop Biomed*, **2:** S1400-1406.

Naderi Z, Mozaffari-Khosravi H, Dehghan A, Nadjarzadeh A, Huseini HF. 2016. Effect of *ginger* powder supplementation on nitric oxide and C - reactive protein in elderly knee osteoarthritis patients: A 12-week double-blind randomized placebo-controlled clinical trial. *J Tradit Complement Med*, **6:** 199-203.

Nassar M, Zerizer S, Kabouche Z, Kabouche A, Bechkri S . 2015. Antioxidant and the immunomodulatory activities exhibited by three plants from Lamiaceae family. *Inter J Pharm Pharm Sci*. **(7) 9:** 331-334.

Panahi Kokhdan E, Sadeghi H, Ghafoori H, Sadeghi H, Danaei N, Javadian H, Reza Aghamaali M.. 2018. Cytotoxic effect of methanolic extract, alkaloid and terpenoid fractions of Stachys pilifera against HT-29 cell line. *Res Pharm Sci*, **13(5):** 404-412.

Peng W, Wang L, Qiu X, Jiang Y, Han T, Pan L, *et al*. 2016. Therapeutic effects of *Caragana pruinosa* Kom. roots extract on type II collagen-induced arthritis in rats. *J Ethnopharmacol*, **191:** 1-8.

Potter C, Hyrich KL, Tracey A, Lunt M, Plant D, Symmons DP, *et al*. 2009. Association of rheumatoid factor and anti-cyclic citrullinated peptide positivity, but not carriage of shared epitope or PTPN22 susceptibility variants, with anti-tumour necrosis factor response in rheumatoid arthritis. *Ann Rheum Dis*, **68:** 69-74.

Sadeghi H, Zarezade V, Sadeghi H, Akbartabar Toori M, Barmak M J, Azizi A, Ghavamizadeh M, Mostafazadeh M. 20014. Anti-inflammatory Activity of Stachys Pilifera Benth. Iran Red Crescent Med J, **16(9):** e19259.

Sakkas LI, Bogdanos DP, Katsiari C, Platsoucas CD. 2014. Anti-citrullinated peptides as autoantigens in rheumatoid arthritis-relevance to treatment. *Autoimmun Rev*, **13:** 1114-1120.

Sharma U, Bala M, Kumar N, Singh B, Munshi RK, Bhalerao S. 2012. Immunomodulatory active compounds from *Tinospora cordifolia*. *J Ethnopharmacol*, **141:** 918- 926.

Shastry VM, Patil VR, Chaudhari RY. 2011. Acute and chronic anti-inflammatory activity of *Pergularia Daemia* whole plant in various experimental animal models. *Int J Pharm Pharm Sci*, **3:** 241-244.

Singh HV, Shrivastava AK, Raizada A, Singh SK, Panday A, Singh N, *et al*. 2013. Atherogenic lipid profile and high sensitive C-reactive protein in patients with rheumatoid *arthritis. Clin Biochem*, **46:** 1007-1012.

Svärd A, Kastbom A, Sommarin Y, Skogh T. 2013. Salivary IgA antibodies to cyclic citrullinated peptides (CCP) in rheumatoid arthritis. *Immunobiology*, **218:** 232-237.

Tag HM, Kelany OE, Tantawy HM, Fahmy AA. 2014. Potential anti-inflammatory effect of lemon and hot pepper extracts on adjuvant-induced arthritis in mice. *J Basic Appl Zool*, **67:** 149-157.

Vasudevan M, Gunnam K K, Parle M. 2006. Antinociceptive and Anti-Inflammatory Properties of *Daucus carota* Seeds Extract. *J Health Sci*, **52(5):** 598-606.

Venkatesha SH, Berman BM, Moudgil KD. 2011. Herbal medicinal products target defined biochemical and molecular mediators of inflammatory autoimmune arthritis. *Bioorg Med Chem*, **19:** 21-29.

JJBS

Volume 13, Number 2, June 2020
ISSN 1995-6673
Pages 191 - 196

Jordan Journal of Biological Sciences

Plasma MicroRNA-133a as a Potential Biomarker for Acute Coronary Syndrome

Heba F. El Sayed Turky[1*], Wafaa Abdel Latif E. Mohammed[1], Sally M. Shalaby[1], Rasha L. Etewa[1,2], Nader T. Kandil[3] and Islam Galal[3]

[1] *Medical Biochemistry & Molecular Biology Department , Faculty of Medicine, Zagazig University, Zagazig, Egypt;* [2]*College of Medicine , Jouf University , Sakaka , Al- Jouf , Saudi Arabia ;* [3] *Cardiology Department, Faculty of Medicine, Zagazig University, Zagazig, Egypt*

Received June 7, 2019; Revised July 14, 2019; Accepted July 28, 2019

Abstract

Background: In clinical practice, there is still a need for novel biomarkers, which can reliably rule in or rule out acute coronary syndrome (ACS) immediately on admission.

Aim of the study: To evaluate the role of plasma miRNA-133a (miR-133a) as a novel biomarker for early diagnosis of ACS.

Patients and Methods: A total of 72 subjects with chest pain suggestive of ACS were admitted as early as possible from the onset of chest pain to the ICU of Cardiology Department, Faculty of Medicine, Zagazig University and were enrolled in this cross sectional study. They included 18 controls (group 1) and 54 ACS patients (group 2). Group 2 was subdivided into 3 subgroups: unstable angina (UA), non ST-segment elevation myocardial infarction (NSTEMI) and ST-segment elevation myocardial infarction (STEMI). Immediately at enrollment, blood samples were taken for estimation of plasma miR-133a expression levels by real time PCR.

Results: The present study showed a significant up-regulation of miR-133a expression in ACS patients when compared to the controls ($p<0.001$). The same results have been found for ACS subgroups when compared to the healthy control group ($p<0.001$ for each). Also, there were higher miR-133a expression levels in NSTEMI than UA patients ($p<0.001$) and a significant up-regulation of this miRNA expression in STEMI group compared to the NSTEMI group ($p<0.001$). Furthermore, there was a significant positive correlation between miR-133a expression and cardiac troponin (Hs-cTnT) levels.

ROC analysis revealed that the AUC of miR-133a level in plasma of ACS patients was 0.92, with specificity of 93 % and sensitivity of 88.2 %, indicating that miR-133a may be considered as a good predictor marker of ACS.

Conclusions: Plasma miR-133a expression level may represent a sensitive predictor for diagnosing ACS. This is of particular interest in patients with UA and NSTEMI in whom diagnostic uncertainty is high.

Keywords: ACS, STEMI, NSTEMI, Real time PCR, miR-133a

1. Introduction

Acute coronary syndrome (ACS) describes the spectrum of clinical manifestations which follow disruption of a coronary arterial plaque, complicated by thrombosis, embolization and varying degrees of obstruction to myocardial perfusion. It includes three diseases involving the coronary arteries: ST-segment elevation myocardial infarction (STEMI), non-ST-segment elevation myocardial infarction (NSTEMI) and unstable angina (UA) (Condorelli *et al.,* 2014).

In clinical practice, there is still a need for novel biomarkers, which can reliably rule in or rule out ACS immediately on admission. This is of particular interest in patients with UA and NSTEMI in whom diagnostic uncertainty is high (Falk *et al.,* 2013).

The golden standard for diagnosing acute myocardial infarction is still cardiac troponins (cTn) but blood cTn concentrations may be falsely elevated in certain cardiac as well as non-cardiac diseases such as severe heart failure, atrial fibrillation, chronic kidney disease, severe sepsis and septic shock (Giannitsis and Katus, 2013). Therefore, it is necessary to investigate novel biomarkers with high sensitivity and specificity for early identification of ACS.

MicroRNAs (miRNAs) are endogenous small non-coding RNAs with 21-25 nucleotides in length. By pairing with the 3' UTR of target mRNAs, miRNAs can regulate protein-coding genes at the posttranscriptional level via degradation of mRNAs or repression of protein translation (Ha and Kim, 2014). MicroRNAs are easily detected and quantified in body fluids by microarray assays, northern blot, and real-time polymerase chain reaction (qRT-PCR) (Ha and Kim, 2014).

MiR-133a is one of the most abundant miRNAs in the heart. The combination of experimental models of human pathologies with tools that modulate miR-133a activity has provided important insights on the role played by this miRNA and their targets in very prevalent

* Corresponding author e-mail: dr.hebaturky@gmail.com.

cardiovascular pathologies (Van Rooij and Kauppinen, 2014).

Previous studies demonstrated that miR-133a had a low level presence in the plasma of healthy people, and it was expressed differentially in different cardiovascular diseases (D'Alessandra *et al.*, 2010). Furthermore, it has been reported that the elevated miR-133a is released into peripheral circulation from the injured myocardium after Ca2+ stimulation (Ahlin *et al.*,2016).

The aim of our work was to identify the role of plasma miR-133a as a novel biomarker for acute coronary syndrome.

2. Subjects and Methods

The study was conducted in Medical Biochemistry & Molecular Biology Department and Cardiology Department - Faculty of Medicine, Zagazig University & Medical Scientific Research Center, Zagazig University in the period from July 2017 to September 2018. A total of 72 subjects presenting with chest pain suggestive of ACS were admitted as early as possible from the onset of chest pain to the ICU of Cardiology Department and enrolled in this cross sectional study. Subjects were classified into 2 groups: Group (1): included (18) healthy subjects served as controls who were admitted to hospital for their complaints of pericardial discomfort. It was further confirmed by cardiac catheterization that those people turned out to have no coronary artery lesions. Therefore, they were selected as control. Group (2): included 54 ACS patients. Patient (ACS) Group (2) was subdivided into 3 subgroups: Group (I): included 18 UA patients, group (II): included 18 NSTEMI patients and group (III): included 18 STEMI patients. We excluded patients with chronic kidney disease as the elevated levels of cTn due to impaired clearance may result in false positive data. Also, patients with heart faliure , severe aortic stenosis , stress cardiomyopathy, hypertrophic obstructive cardiomyopathy (HOCM) were excluded, as in these patients false positive results regarding plasma miR-133a level may interfere with the study. All participants were subjected to the following: - Full history: including history of diabetes, hypertension, smoking & family history. - Complete physical & clinical examination. - Electrocardiography: to find out ischemic changes. - Laboratory investigations: Fasting blood glucose, lipid profile and high sensitive troponin T (Hs-cTnT) were taken from patient sheet. - Immediately at enrollment, blood samples were taken for analysis of plasma miR-133a expression levels by real time PCR. - Coronary angiography: for diagnosis of ischemia.

Written consent was obtained from every participant after explanation of the procedure. Medical research and ethics committee approved the study. The work has been carried out in accordance with The Code of Ethics of the World Medical Association (Declaration of Helsinki) for studies involving humans.

3. Real time PCR analysis for miR-133a expression

miRNA extraction from plasma was done using miRNeasy kits from Qiagen, Germany, catalogue No RY43 .Then miRNA was reverse transcribed using miScript IIRT kit from Qiagen, Germany, catalogue no: 218161. The amplification was performed in a 20 µL mixture containing 5µL of the cDNA, 100 pmol/mL of each primer miRNA-133 a Cat. no MS00045857) or RNU6 as internal control (Cat. no. MS00033740), 10 µL 2x QuantiTect SYBR Green PCR Master Mix (Qiagen) and 4 µL Dd H2O. The amplification was carried out using real time PCR (Stratagene Mx3005P) qPCR System according to the following protocol; 95ºC for 15 min initial activation step then 40 cycles of (95ºC for 15 sec, 55ºC for 30 sec then 70ºC for 30 sec). A melting curve was analyzed to validate the results after the PCR amplification. The amplitude of change of the miRNA expression observed in patients in relation to control group was analyzed by the $2^{-\Delta\Delta Ct}$ method.

4. Statistical analysis

All data were statistically analyzed using SPSS 20.0 for windows (SPSS Inc., Chicago, IL). Receiver Operating Characteristic (ROC) curve analysis was used to identify optimal cut-off values of miR-133a with sensitivity and specificity for diagnosis of ACS.

5. Results

Regarding demographic data, the present study showed that there were no significant differences between the ACS patients and healthy controls regarding age, body mass index, gender, smoking, diabetes mellitus, dyslipidemia and family history ($p>0.05$) while there was statistically significant difference as regard the hypertension status ($p<0.05$) (Table 1).

The present study showed a significant up-regulation of miR-133a expression in ACS patients when compared to the controls ($p<0.001$) (fig 1). The same results have been found for ACS subgroups (UA, NSTEMI and STEMI patients) when compared to the healthy control group ($p<0.001$ for each) (Table 2). In the present study, there were higher miR-133a expression levels in NSTEMI than UA patients ($p<0.001$). Also, there was a significant up-regulation of this microRNA expression in STEMI group compared to the NSTEMI group ($p<0.001$) (Table 2).

Regarding miR-133a expression levels, there was statistically highly significant difference between control group & case group ($p<0.001$) (Table 3). As for cardiac troponin (Hs-cTnT), there was statistically highly significant difference between control group & case group ($p<0.001$) (Table 3).

Furthermore, there was a significant positive correlation between miR-133a expression and cardiac troponin (Hs-cTnT) levels (fig 2).

ROC analysis showed that cardiac troponin level (Hs-cTnT) has specificity of 61.1 % and sensitivity of 76.9 % with cut off value = 3.65 when discriminating between ACS patients and controls (fig 3). ROC analysis revealed that the AUC of miR-133a level in plasma of ACS patients was 0.92, with specificity of 93 % and sensitivity of 88.2 % with cut off value = 1.24 when discriminating between ACS patients and controls indicating that miR-133a may be considered as a good predictor marker of ACS (fig 4). Additionally, ROC curve revealed that the AUC of miR-133a expression was 0.93 with specificity of 91.6 % and sensitivity of 87.5 % with cut off value = 4.3 when discriminating between myocardial infarction (MI) patients and controls in myocardial infarction (MI) patients

indicating that miR-133a level may be considered as a predictor marker of myocardial infarction (fig 5).

Table (1): Descriptive statistics of the demographic parameters in the studied groups: group 1(control group) and group 2 (ACS group). The data presented in table (1) showed that there were no significant differences between the ACS patients and healthy controls when comparing age, body mass index, onset of chest pain , gender, smoking, diabetes mellitus, dyslipidemia and family history (p>0.05) while there was statistically significant difference when comparing hypertensive status (p<0.05).

Variable	**Control group 1 (n=18)**	ACS group2 (n=54)	T test	P-Value
	X ±SD	**X ±SD**		
Age	45.11 ± 6.5	48.54 ± 7.63	-1.71	0.091
Body mass index (Kg/m^2)	29.6 ± 2.81	30.98 ± 4.09	-1.32	0.188
Onset of chest pain	5.32±4.21	6.11±4.32	-0.68	0.501

Continued Table (1):

Variable	**Control group 1 (n=18)**		ACS group2 (n=54)		χ^2	**P value**
	N	**%**	**N**	**%**		
Gender					0.46	0.49
Male	8	44.4	31	57.4		
Female	10	55.6	23	42.6		
Smoker					0.19	0.661
Yes	5	33.3	18	33.3		
No	13	66.7	36	66.7		
Hypertension					6.01	**<0.05**
Yes	5	33.3	33	61.1		**(S)**
No	13	66.7	21	38.9		
Dyslipidemia					0.46	0.49
Yes	8	44.4	29	53.7		
No	10	55.6	25	46.3		
Diabetes mellitus					3.45	0.063
Yes	3	16.7	22	40.7		
No	15	83.3	32	59.3		
Family History					3.46	0.062
Yes	4	22.2	25	46.3		
No	14	77.8	29	53.7		

Table (2): Comparison of miR-133a expression level between UA group I , NSTEMI group II , STEMI group III & the control group. The data presented in (table 2) showed that miR-133a expression level, was (3.6 ± 1.3) in UA group, (4.63 ± 0.8) in NSTEMI patients, (5.89 ± 1.12) in STEMI patients and (1.06 ± 0.06) in control group. The data indicated that there was high statistically significant difference when comparing miR-133a expression level between control group and different ACS subgroups (UA , NESTMI & STEMI) with (P < 0.001).

Variable	UA group I (n=18)	NSTEMI group II (n=18)	STEMI group III (n=18)	Control group (n=18)		P-Value	
	X ±SD	X ±SD	X ±SD	X ±SD	F		LSD
miR -133a expression level	3.6 ± 1.3	4.63 ± 0.8	5.89± 1.12	1.06 ± 0.06	84.2	< 0.001 (HS)	< 0.001[1] < 0.001[2] < 0.001[3] < 0.001[4] <0.001[5] < 0.001[6]

F is for ANOVA test

LSD is for least significant difference

P1: Group IV compared to group I. `P2: Group IV compared to group II. P3: Group IV compared to group III. P4: Group II compared to group I. `P5: Group III compared to group I. P6: Group III compared to group II.

Table (3): Comparison of cardiac tropnonin (Hs-cTnT) values & miR-133a expression level between control group and case group. The data presented in table (3) showed that there was statistically highly significant difference between control group & case group (p<0.001).

Variable	**Control group 1 (n=18)**	**ACS group2 (n=54)**	Mann whitney test/ t-test	P-Value
Cardiac Troponin (pg/ml)			164.5	**< 0.001 (HS)**
X ±SD	3.51 ± 0.82	86.52 ± 111.16		
Median	3.6	46.64		
Range	(1.94-4.85)	(2.15-394.6)		
miR -133a expression level			-10.67	**< 0.001 (HS)**
X ±SD	1.06 ± 0.06	4.71± 1.43		
Median	1.055	4.74		
Range	(0.97-1.2)	(1.14-7.34)		

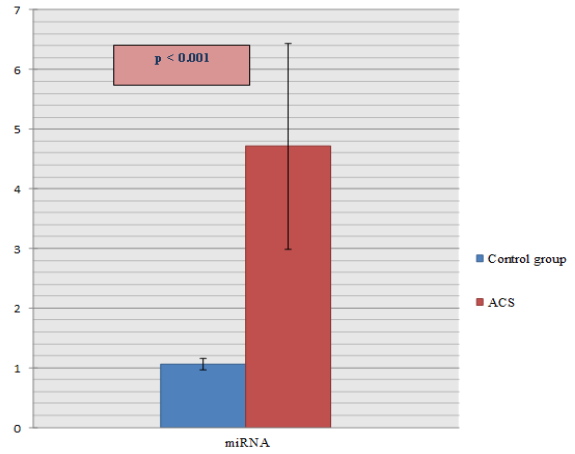

Figure 1. Showing comparison of miR-133a expression level between control group { (n=18) with mean ± SD : 1.06 ± 0.06 } and case group { (n= 54) with mean ± SD : 4.71 ± 1.43 } . The data in fig (1) showed a significant up-regulation of miR-133a expression in ACS patients when compared to the controls ($p<0.001$) .

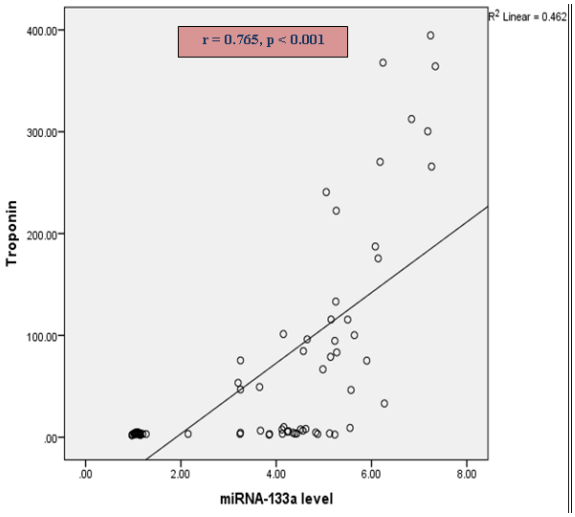

Figure 2. Correlation between cardiac troponin (Hs-cTnT) value and miR-133a expression level. The data in fig (2) showed a significant positive correlation between miR-133a expression level and cardiac troponin (Hs-cTnT) levels , r = 0.765 with $p < 0.001$.

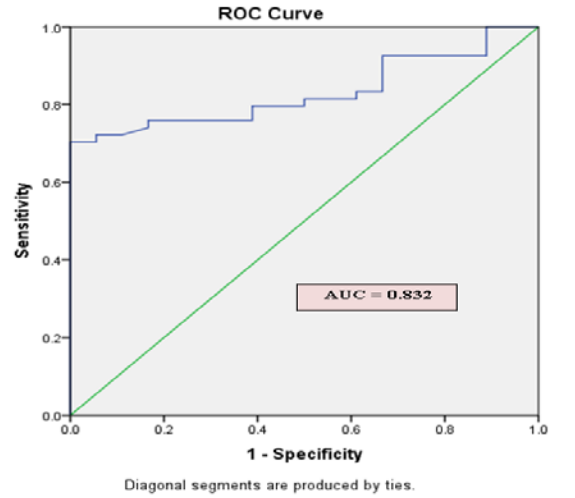

Figure 3. ROC analysis showed that cardiac troponin level (Hs-cTnT) has specificity of 61.1 % and sensitivity of 76.9 % with cut off value = 3.65 when discriminating between ACS patients and controls.

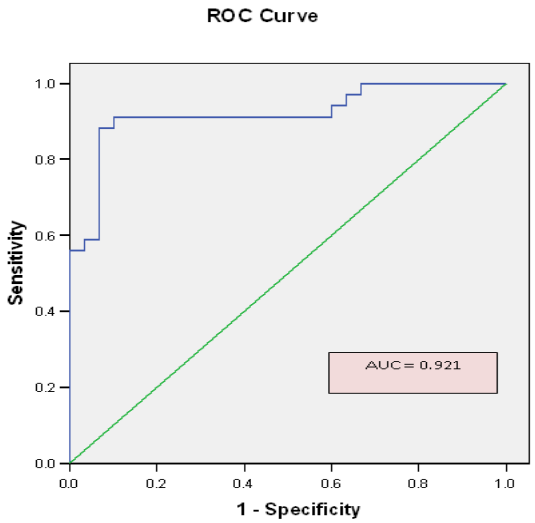

Figure 4. ROC curve detecting sensitivity and specificity of miR-133a level in ACS patients .The data in fig (4) revealed that the miR-133a level with specificity of 93 % and sensitivity of 88.2 % with cut off value = 1.24 when discriminating between ACS patients and controls.

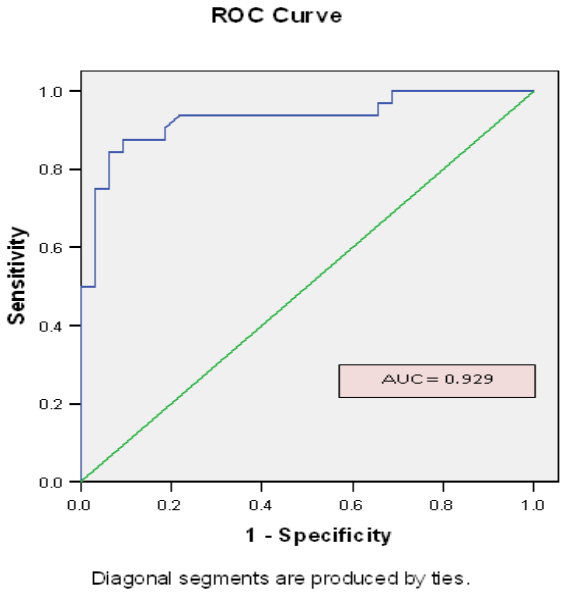

Figure 5. ROC curve detecting sensitivity and specificity of miR-133a level in myocardial infarction (MI) patients .The data in fig (5) revealed that the miR-133a level with specificity of 91.6 % and sensitivity of 87.5% with cut off value = 4.3 when discriminating between myocardial infarction (MI) patients and controls.

6. Discussion

It is very critical to diagnose myocardial infarction in chest pain patients as soon as possible. Up to date, the most commonly used biomarkers for MI are cardiac troponins; cardiac troponin I and T (cTnI and cTnT). Unfortunately, these biomarkers are not consistently elevated within the first hours after the onset of symptoms, demanding subsequent measurements and delaying early diagnosis (Anderson *et al.*, 2011). Therefore, it is still a clinical need for novel biomarkers, which can reliably rule in or rule out ACS immediately on admission.

It has been reported that the human genome includes thousands of miRs, 300 of which are roughly expressed in

the heart (Hu G1 *et al.,* 2012). Cardiomyocyte-enriched miRNAs, including miR-1, miR 208a, miR-208b, miR-133a, miR-133b, and miR-499 have been suggested as potential diagnostic markers in patients with AMI (Shalaby *et al.,* 2016; Parizadeh *et al.,* 2018).

We selected miR-133a because of its known high expression in cardiac muscle (Wang GK *et al.,* 2010). MiR-133a shows low expression levels in the plasma of healthy individuals, while it is released into peripheral circulation from the injured myocardium after calcium stimulation (Liu *et al.,* 2008).

The present study found a significant up-regulation of miR-133a expression in ACS patients when compared to the controls indicating that it can be used as a diagnostic biomarker for ACS. Also, our study showed a statistically significant difference between control group and ACS patients regarding cardiac tropnonin (Hs-cTnT) values.

Although both cTnT and miR-133a showed significant elevation with ACS, the priority factors for using miR-133a as a biomarker for ACS might include: (i) microRNAs are detected in circulating blood in a remarkably stable form, which can withstand enzymatic degradation, repetitive freezing, and thawing cycles (Dimmeler and Zeiher 2010); and (ii) miR-133a may be superior to cardiac troponin for detecting myocardial injury in individuals with renal dysfunction, since troponin would increase in end-stage renal disease, even in the absence of an ACS (Abbas *et al,.* 2005).

In the present study, we found that there was no significant difference between UA group and control group concerning Hs-cTnT values while there was a significant up-regulation of miR-133a expression levels in UA patients when compared to controls.

Detectable quantities of cTnT are released only in the setting of irreversible myocardial injury, for example myocardial necrosis, thereby leaving the patients with UA, which by definition indicates myocardial ischemia without necrosis, undiagnosed with cTnT (Wu *et al.,* 2006). In the present work, we observed the elevation of miR-133a in UA patients indicating that this miRNA might be helpful for accelerating the diagnosis of UA, so better management could be allowed. The release mechanism of miRNAs is unclear, but they may be freed to the bloodstream as a consequence of passive release of the cell contents as apoptotic bodies, exosomes and microparticles (Martinez *et al .,* 2011). Microparticles containing miRs may be formed during myocardial ischemia as well as during necrosis (Martinez *et al.,* 2011). Additionally, miRNA microarray analysis and in situ hybridization indicated that miR-133a was released from infarcted and peri-infarcted myocardium (Kuwabara *et al.,* 2011). Therefore, we hypothesized that the elevated levels of miR-133a in the state of UA could result from its passive release from ischemic myocardial tissue.

Kuwabara *et al.,* 2011 studied the miR-133a expression levels in UA patients (Kuwabara *et al.,* 2011). Although the sample sizes were small, the serum level of miR-133a increased significantly in patients with UA (n=8, $P<0.05$) compared with other patients without ACS (Kuwabara *et al.,* 2011).

In the present study, there were higher miR-133a expression levels in NSTEMI than UA patients. Also, there was a significant up-regulation of this microRNA expression in STEMI group compared to the NSTEMI group. These results indicated that miR-133a expression levels could be discriminate between UA, NSTEMI and STEMI patients. Our results are consistent with a large cohort comprised of 444 patients with ACS (Widera *et al.,* 2011).

In our study, there was a significant up-regulation of miR-133a in both NSTEMI and STEMI patients compared to control group. Our results are consistent with many studies. It has been reported that miR-1, miR-133, miR-499 as well as miR-208a levels in plasma from AMI patients were significantly higher than those in healthy subjects, CHD patients without AMI, or patients with other cardiovascular diseases (Wang *et al.,* 2010). However, the amplitudes of the increase were different among the 4 types of miRNAs; the highest increase was the miR-133 (Wang *et al.,* 2010). Recently, based on the meta-analysis of ten case-controlled studies including 1074 patients, it was found that the level of miR-133a in blood serum or plasma may be used as a diagnostic biomarker of AMI (Zhu *et al*., 2018).

However, other studies disagreed with our findings and showed that miR-133 is not a good biomarker for AMI diagnosis (D'Alessandra *et al.,* 2010 *;* Roberta De Rosa *et al.,* 2017) Among these is a study done by Wang et al which showed that miR-133a was detected with higher levels in plasma from the AMI group, but there were no statistically significant differences in its level among the healthy, non-CHD ,and CHD groups or miR-133 levels not significantly increased in patients with AMI (n=32) compared with healthy individuals (n=36) (Wang *et al.,* 2010). We suggest that these differences may be due to the variation in the time from the onset of symptoms to sampling the circulating blood or the relative small sample size of the studies.

In the present study, ROC analysis revealed that the AUC of miR-133a level in plasma of ACS patients was 0.92, with specificity of 93 % and sensitivity of 88.2 %, indicating that miR-133a may be considered as a good predictor marker of ACS.

ROC analysis revealed also that the AUC of miR-133a in plasma of AMI patients was 0.93 with specificity of 91.6 % and sensitivity of 87.5%.; indicating that miR-133a may be a clinically practicable biomarker for AMI diagnosis. ROC curve of Hs-cTnT was plotted and showed specificity of 61.1 % and sensitivity of 76.9 % in ACS patients and specificity of 88.9 % and sensitivity of 61.1% in AMI patients. These results revealed that circulating miR-133a is more informative than cTnT for ACS and AMI diagnosis.

Consistently, miR-133 showed an AUC of 0.912, with a sensitivity of 81.1% and a specificity of 91.2% in AMI compared with non-AMI (Liu P *et al*., 2014). Wang et al. found that the ROC curves of CHD subcategories revealed that circulating miR-133a is more sensitive for AMI diagnosis than cTnI in CHD patients (Wang *et al.,* 2013). Recently, the meta-analysis of ten case-controlled studies including approximately 1 thousand AMI patients suggested that miR-133a could be used as a biomarker for AMI diagnosis, particularly considering that the pooled AUC of the ROC curve is 0.88 (95% CI 0.85–0.90) with the sensitivity of 0.83 % and the specificity of 0.78% (Zhu *et al*., 2018).

In contrary to our results, Devaux *et al.* (2015) prospectively investigated the use of six different miRs in n=1155 acute chest pain patients. Finally, n=179 patients

were diagnosed as NSTEMI and n=45 patients as suffering from STEMI. MiR-133a, miR-208b and miR-499 were identified as univariate predictors of myocardial infarction as these three miRs control cardiomyocyte identity (Xin *et al*., 2013). However, their predictive value did not remain significant after correction for troponin levels. Furthermore, the AUC were low (AUC: 0.53–0.76) compared to high sensitive troponin (AUC: 0.94) (Devaux *et al.*, 2015).

The main concern of our study was that we analyzed miR-133a in suspected ACS patients at the time of their enrollment at the emergency department. Other studies investigated the miR-133a levels at later time points or in established diagnosed cases. Early diagnosis of ACS can definitely help decrease the morbidity and the mortality outcomes.

7. Conclusion

Plasma miR-133a expression levels were up-regulated in all ACS groups when compared to controls indicating that circulating miR-133a may be a novel and potent biomarker for ACS, especially for UA. Our results suggested that circulating miR-133a may be a potentially promising predictor for accelerating the diagnosis of ACS patients in the clinical practice.

Conflict of interest

None.

References:

Abbas NA, John RI, Webb MC, Kempson ME, Potter AN, Price CP , Vickery S and Lamb EJ .2005. Cardiac troponins and renal function in nondialysis patients with chronic kidney disease. *Clin Chem* , **51**: 2059-2066.

Ahlin F, Arfvidsson J, Vargas K G, Stojkovic S, Huber K and Wojta J.2016 . MicroRNAs as circulating biomarkers in acute coronary syndromes: *Areview. Vascul. Pharmacol. pii* , **81**:15-21.

Anderson, JL., Adams CD, Antman EM, Bridges CR, Califf RM, Casey DE Jr, Wright RS, Ettinger SM, Fesmire FM, Ganiats TG, Jneid H, Lincoff AM, Peterson ED, Philippides GJ, Chavey WE 2nd, Fesmire FM, Hochman JS, Levin TN, Theroux P, Wenger NK and Zidar JP. 2011.ACCF/AHA Focused Update Incorporated Into the ACC/AHA 2007 Guidelines for the Management of Patients With Unstable Angina/Non- ST-Elevation Myocardial Infarction: a report of the American College of Cardiology Foundation/American Heart Association Task Force on Practice Guidelines. *Circulation* , **123** : 426–579.

Condorelli G, Latronico MV and Cavarretta E .2014. microRNAs in cardiovascular diseases: current knowledge and the road ahead. *J Am Coll Cardiol* , **63**: 2177–2187.

D'Alessandra Y, Devanna P, Limana F, Straino S, Di Carlo A, Brambilla PG, Rubino M, Carena MC, Spazzafumo L, De Simone M, Micheli B, Biglioli P, Achilli F, Martelli F, Maggiolini S, Marenzi G, Pompilio G and Capogrossi MC. 2010. Circulating microRNAs are new and sensitive biomarkers of myocardial infarction. *Eur Heart J* , **31**: 2765–73.

Devaux Y, Mueller M, Haaf P , Goretti E, Twerenbold R, Zangrando J , Vausort M, Reichlin T, Wildi K, Moehring B, Wagner DR and Mueller C.2015. Diagnostic and prognostic value of circulating microRNAs in patients with acute chest pain. *J Intern Med* , **277 (2)** : 260-271.

Dimmeler S and Zeiher AM. 2010. Circulating microRNAs: novel biomarkers for cardiovascular diseases? *Eur Heart J* , **31**: 2705-2707.

Falk E, Nakano M, Bentzon J F, Finn AV and Virmani R. 2013 . Update on acute coronary syndromes: the pathologists' view. *Eur. Heart J* , **34** : 719–728.

Giannitsis E and Katus HA. 2013. Cardiac troponin level elevations not related to acute coronary syndromes. *Nat Rev Cardiol* , **10 (11)** : 623-34.

Ha M and Kim VN .2014. Regulation of microRNA biogenesis. *Nat Rev Mol Cell Biol* , **15** : 509–24.

Hu G, Drescher KM and Chen XM. 2012. Exosomal miRNAs: Biological Properties and Therapeutic Potential. *Front Gene* , **20** : 3:56.

Kuwabara Y, Ono K, Horie T, Nishi H, Nagao K, Kinoshita M , Watanabe S, Baba O, Kojima Y, Shizuta S, Imai M, Tamura T, Kita T and Kimura T. 2011. Increased microRNA-1 and microRNA-133a levels in serum of patients with cardiovascular disease indicate myocardial damage. *Circ Cardiovasc Genet* , **4** :446–54.

Liu N, Bezprozvannaya S, Williams AH, Qi X, Richardson JA, Bassel-Duby R and Olson EN.2008. microRNA-133a regulates cardiomyocyte proliferation and suppresses smooth muscle gene expression in the heart. *Genes Dev* , **22** : 3242–54.

Liu Peng, Qiu Chun-guang , Li Bei-fang , Ding Xue-zhi, Wang Zi-hao, Li Yun-fu,Dang Yan-ping, Liu Yang-gui, Li Wei-guo, Hu Tian-yong and Huang Zhen-wen.2014. Clinical impact of circulating miR-133, miR-1291 and miR-663b in plasma of patients with acute myocardial infarction. *Diagn Pathol* , **9 (1) :** 89.

Martinez, M. C., Tual-Chalot and Andriantsitohaina R . 2011. Microparticles: targets and tools in cardiovascular disease. *Trends Pharmacol. Sci.* , **32** : 659–665.

Parizadeh SM , Ghandehari M , Parizadeh MR, Ferns GA, Ghayour-Mobarhan M , Avan A and Hassanian SM.2018. The diagnostic and prognostic value of circulating microRNAs in coronary artery disease: A novel approach to disease diagnosis of stable CAD and acute coronary syndrome. *J Cell Physiol* , **233 (9)** : 6418-6424.

Roberta De Rosa , Salvatore De Rosa , David Leistner, Jes-Niels Boeckel, Till Keller,Stephan Fichtlscherer, Stefanie Dimmeler and Andreas M. Zeiher.2017. Transcoronary Concentration Gradient of microRNA-133a and Outcome in Patients With Coronary Artery Disease. *Am J Cardiol* , **120 (1)** :15–24.

Shalaby Sally M , El-Shal Amal S, Shoukry Amira ,Mohamad H. Khedr and Nader Abdelraheim. 2016. Serum miRNA-499 and miRNA-210: A Potential Role in Early Diagnosis of Acute Coronary Syndrome. *International Union of Biochemistry and Molecular Biology* , **68 (8)** : 673–682.

Van Rooij E and Kauppinen S. 2014. Development of microRNA therapeutics is coming of age. *EMBO Mol Med* , **6** : 851–64.

Wang F, Long G, Zhao C, Huaping Li, Sandip Chaugai, Yan Wang , Chen Chen, and Dao Wen Wang. 2013.Plasma microRNA-133a is a new marker for both acute myocardial infarction and underlying coronary artery stenosis. *J Transl Med* , **11**: 222.

Wang GK, Zhu JQ, Zhang JT, Li Q, Li Y, He J and Qin YW, Jing Q. 2010.Circulating microRNA: a novel potential biomarker for early diagnosis of acute myocardial infarction in humans. *Eur Heart J* , **31**: 659–66.

Widera, C., Gupta, S. K ., Bang C, Bauersachs J, Bethmann K, Kempf T, Wollert KC and Thum T.2011. Diagnostic and prognostic impact of six circulating microRNAs in acute coronary syndrome. *Journal of Molecular and Cellular Cardiology* , **51** : 872–875.

Wu AH, Fukushima N, Puskas R, Todd J and Goix P. 2006. Development and preliminary clinical validation of a high sensitivity assay for cardiac troponin using a capillary flow (single molecule) fluorescence detector. *Clin Chem* , **52**: 2157–2159.

Xin M, Olson EN and Bassel-Duby R. 2013. Mending broken hearts: cardiac development as a basis for adult heart regeneration and repair. *Nat Rev Mol Cell Biol* , **14** : 529–541.

Zhu L, Liu F, Xie H and Jin Feng. 2018. Diagnostic performance of microRNA-133a in acute myocardial infarction: *A meta-analysis.Cardiol J* , **25 (2)** : 260-267.

JJBS

Jordan Journal of Biological Sciences

Volume 13, Number 2, June 2020
ISSN 1995-6673
Pages 197 - 205

Diversity and Antimicrobial Activity of Endophytic Fungi from the Medicinal Plant *Pelargonium graveolens* (geranium) in Middle Egypt

Manal M. Yasser, Marym A. Marzouk, Nadia M. El-Shafey and Salwa A. Shaban*

Botany and Microbiology Department, Faculty of Science, Beni-Suef University, Egypt

Received June 13, 2019; Revised July 25, 2019; Accepted July 28, 2019

Abstract

This study assesses the diversity and antimicrobial activity of the *Pelargonium graveolens*-associated endophytic fungi in Beni-Suef, Egypt. *P. graveolens* is a medicinal plant very common in Beni-Suef area and is used basically as a source of the expensive geranium oil. A total of 280 isolates belonging to 20 morphologically different fungal species have been isolated from root, leaf, and stem of *P. graveolens*. Identification of the isolates has been carried out by combining the morphological and molecular methods. Also, antifungal activity against plant and human pathogens has been tested using a dual culture method.

Results show that *P. graveolens* is extensively colonized by fungi that live inside it systematically at least during the test. The root exhibits the highest colonization frequency CF% and isolation rate IR% (96% and 99% respectively). All the isolates belong to the phylum ascomycetes, and phylogenetic analysis shows that they are relatively related genetically. The most occurring genera are *Aspergillus* and its teleomorph *Emericella* (CF=28%). Most of the isolates exhibit antifungal activity against one or more of the tested pathogens. The maximum inhibition rate is for *Emericella nidulans* (E6658) against *Microsporum audouinii* (80%). *Aspergillus niger* (E6657) and *Penicillium* sp. (E6651) show very strong activity against all the tested pathogenic fungi.

Keywords; Endophytic Fungi, Medicinal Plant, Molecular Identification, Phylogenetic Tree, *Pelargonium Graveolens*. Antifungal Activity.

1. Introduction

Endophytic microorganisms live inside plant tissues imperceptibly for at least part of their life cycle without any negative effect on their host (Kusari et al., 2012). Fungi are considered the most occurring endophytes (Staniek et al., 2008). They are highly diverse and polyphyletic and exist in all parts of the plants in any environment investigated till now (Yan et al., 2015). All plants form an endophytism relation with one or more fungi (Haddadderafshi, 2015).

Despite the new techniques, identification of fungi still depends on morphological features using light microscope examination. However, this may not be very accurate as it depends on the examiner taxonomic expertise. Besides, many endophytes grow in culture media as sterile mycelia (Ginting et al., 2013). Molecular identification is an effective way to identify the most related species. For fungi, this technique basically depends on the analysis of specific fragments of the ribosomal rDNA like 18S rDNA sequence or internal transcribed spacer (ITS), 28S subunit, and 5.8S rDNA sequence. ITS sequence analysis is widely used for the identification of endophytic fungi (Diaz et al., 2012). It was reported that molecular analysis of morphologically different isolates proved belonging them to the same species (Ginting et al., 2013). Endophytic fungi, therefore, are usually identified using a combination of morphological and molecular techniques (Zhang et al., 2006).

Plant-endophyte association is dependent on both partners (fungi and host plant) phylogeny and environmental factors. It was reported that endophytes from related host species are relatively phylogenetically related than those from unrelated plants. Moreover, endophytes from related hosts from different environments are found to be unrelated and unrelated plants from the same environment incorporate related species of endophytes (Arnold, 2007).

Endophytes have been reported to help plant in many ways. They may help to adapt environmental stress (adaptation benefits) like drought and salts stress or may help their host to resist invading by pathogens, insects, weeds or even herbivore (Rodriguez et al., 2009).

Endophytic fungi can produce wide varieties of bioactive secondary metabolites such as phenols, alkaloids, steroids, peptides, flavonoids, quinones, and terpenoids which may stimulate plant growth or used as therapeutic agents against plant and human diseases (Zhao et al., 2019). They also have been reported to produce one or

* Corresponding author e-mail: micro_sa2010@yahoo.com.

more of their host's metabolites. For example, endophytes isolated from the medicinal plant *Salacia oblonga*, which is known for its production of taxol (anticancer agents), was found to produce taxol by using genomic mining approach to detect two genes incorporated in the production of taxol (Roopa et al., 2015) and other several examples have been reported. Such studies led to discover new compounds and commercial production of these therapeutic compounds in large scale by the cheap and easy fermentation process.

The endophytic *Curvularia pallescens* (URM 6048) isolated from *Calotropis procera* has shown antagonistic effect against the plant pathogenic fungus *Colletotrichum dematium*, and against human pathogens *Staphylococcus aureus* and *Streptococcus pyogenes* (Nascimento et al., 2015). In a study on the diversity of endophytes isolated from *Opuntia humifusa* in the United states, six of the isolates was found to inhibit the plant pathogenic fungus *Phomopsis obscurans*

Studies on endophytic fungi and their antimicrobial activity help understanding their diversity, interaction with their host, and metabolites production. The diversity and antimicrobial activity of endophytic fungi associated with *P. graveolens* from Egypt environment have never been studied before.

Pelargonium graveolens (geranium) is a medicinal, aromatic plant dominant in Egypt, especially in Beni-Suef governorate. Its genera belong to the family Geraniaceae. *Pelargonium graveolens* has an abundance of positive benefits. These benefits include antibacterial, antifungal and antioxidant activity and others. Traditionally, the plant has been used to treat a variety of symptoms including: nephritis, wounds, fever, colds and sore throats, inflammation, heavy menstrual flow, hemorrhoids, dysentery, cancer gastrointestinal diseases, hyperglycemia, insomnia, heart disease, asthma, nausea and vomiting, fever and tuberculosis (Ćavar and Maksimović, 2012; Hsouna and Hamdi, 2012). It is mainly used to produce geranium oil. As only about 1 kg of geranium oil can be produced from 500 kgs of fresh weight (Centre, 2015), its production is very expensive. Studying its mutualistic communities may help in improving its production.

The aims of this study are to 1) assess the diversity of fungi isolated from the medicinal plant *P. graveolens* collected from Beni-Suef, middle Egypt, 2) investigate the genetic relation between the isolates and 3) evaluate the antifungal activity of the isolated endophytes against plant and human pathogenic fungi.

2. Materials and methods

2.1. Collection of the samples

Pelargonium graveolens samples were collected from 7 different fields in Beni-Suef governorate, Egypt. Sampled plants that were mature enough, healthy, and have no disease symptoms, based on the visual investigation of plant organs (leaves, stem, flowers and root), were chosen. Every sampled plant placed in a sterile bag and sealed well then labeled. Samples were preserved in the refrigerator until the next step for at most four days to avoid contamination.

2.2. Preparation of segments for isolation

Plants were washed carefully with tap water to remove mud and debris and let to dry on towels at room temperature. In the laminar air hood, the plant parts were cut into small pieces (about 1 cm) using sterile scalpels and numbered.

2.3. Sterilization of the samples' surfaces

The samples were surface sterilized using 75% ethanol for 1-3 minutes to remove wax and kill epiphytes followed by immersion in 4% sodium hypochlorite for 30-60 seconds for further sterilization depending on the structure of the tissues of the samples. Then the segments were rinsed with distilled sterile water three times and allowed to dry on sterile petri dishes containing sterile towels or filter papers.

2.4. Culturing

1-4 segments of a single part of the geranium plant (leaf, root, stem) were placed in a plate containing PDA media supplemented with 0.5 ml/l chloramphenicol and incubated at 25°C for 10 -20 days in the dark.

The effectiveness of the surface sterilization protocol was tested by imprint method of Schulz *et al.*, (Schulz, 1993) where a surface sterilized leaf segment was pressed and placed on the surface of a sterile PDA plate for 5 minutes then removed and the plate incubated with the other plates. Any appearing of growth indicate that the surface sterilization was not enough to eliminate epiphytes, and more sterilization period would be required.

Fungi that appeared to grow slowly from the inside plant tissues only were considered endophytes. While plates containing fast growing fungi and surface contaminates were discarded.

The isolated fungi were purified on antibiotic-free PDA media. A single spore of each fungal isolate was isolated and stored for further investigations.

2.5. Single spore isolation

Two drops of tween 80 were added to a tube containing 10 ml sterile distilled water and inoculated with the aerial mycelium of fungi from pure culture and shaken well. The suspension was then streaked by a sterile cotton swap on a thin film of PDA media in a petri dish and incubated at 25°C. After 24 h, the plates were examined for tiny hyphal growth arises from a single spore. The chosen germinating spore was cut off and transferred into another sterile PDA plate and incubated at 25°C for 5-10 days and used for preservation and subculturing for identification and further investigations. The isolates were stored in slants containing Czapecks media at 4°C.

2.6. Diversity of the isolated fungi

A number of segments colonized by endophytic fungi from each distinct tissue was recoded. Colonization frequency (CF%) and isolation rate (IR%) for each tissue also were calculated using the following equations (Wang et al., 2015) :

$$CF\% = \frac{\text{Number of segments colonized with isolated fungi}}{\text{Totall number of segments investigated}} \times 100 \quad (1)$$

$$IR\% = \frac{\text{Number of isolated fungi recovered from a tissue}}{\text{Totall number of the tissue segments investigated}} \times 100 \quad (2)$$

2.7. Microscopic identification of fungal endophytes

Isolates were identified based on the morphology of the fungi in the plates and direct microscopic examination of mycelium, conidia, fruiting bodies and spores using standard manual Moubasher, 1993 (Moubasher, 1993).

2.8. Molecular identification of fungal endophytes

The molecular identification was conducted in Microbiology and Applied Genomics Group, Institute of Chemical, Environmental & Bioscience Engineering Vienna, University of Technology, Austria. Genomic DNA was extracted from mycelia grown on 3% MEA (Malt Extract Agar) and incubated at 28°C then harvested after 2 days with the Plant DNeasy Minikit (QIAgen GmbH, Hilden, Germany) according to the manufacturer's instructions. A region of nuclear DNA containing the ITS1 and two regions of the rRNA gene cluster was amplified by PCR using the primer combinations SR6R and LR1 (White et al., 2014) as described by Kullnig-Gradinger et al.,(Kullnig-Gradinger et al., 2002). PCR products were sequenced. ITS sequences of the isolates were subjected to sequence similarity comparison of the sequences from the NCBI GenBank database (www.ncbi.nlm.nih.gov) using blast search. Sequences were aligned using the Clustal W program. The phylogenetic tree was built using MEGA X software (Kumar et al., 2018).

2.9. Calculation of the colonization frequency (CF%) of the isolates

$CF\%$ indicates the abundance of the isolates in their host plant and has been calculated for the isolates on the level of genera as described in equation (1).

2.10. Antifungal activity of the isolates

A total of 20 isolated endophytic fungi were screened for their antimicrobial activity against three plant pathogenic fungi (*Rhizoctonia solani*., *sclerotium rolfsii*, *Fusarium solani*) and against a human pathogen (*Microsporum audouinii*). Dual culture method presented by Morton and Stroube (1955) was used where seven-day-old pure cultures of endophytes and pathogens grown on PDA media were used in the experiment. A 5 mm disc from endophyte plate was cut by a sterile cork poorer and moved to one side of a sterile plate containing SDA (Sabouraud dextrose agar) media. Another disc of the pathogen was placed on the opposite side of the test plate. The control plate was done by replacing the endophyte disc by a sterile PDA disc (without mycelia). Plates were incubated in the dark at 27°C for seven days, then the radius of the growth of the pathogen has been measured at three dimensions, and their average was recorded as the radius of the growth. The activity of endophytes to inhibit the pathogenic fungal growth was expressed as the inhibition rate which was calculated as;

RP; is the radius of pathogen growth in the test plate.

RC; is the radius of pathogen growth in the control plate.

2.11. Statistical analysis of data

The results of inhibition rate were compared using one-way ANOVA and a Post Hoc-Tukey HSD test ($P<0.05$). The analyses were conducted using SPSS v.19.

3. Results

3.1. Isolation of endophytes

A total of 50 plants of Pelargonium graveolens were collected for the isolation of endophytic fungi from Beni-Seuf governorate in Egypt. The collection and isolation have done on 10 separated experiments. A total of 435 segments (150 leaf segments,150 stem segments, and 135 root segments) were inoculated on PDA media. Twenty morphologically different fungi have been successfully isolated and purified, as shown in Figure 1.

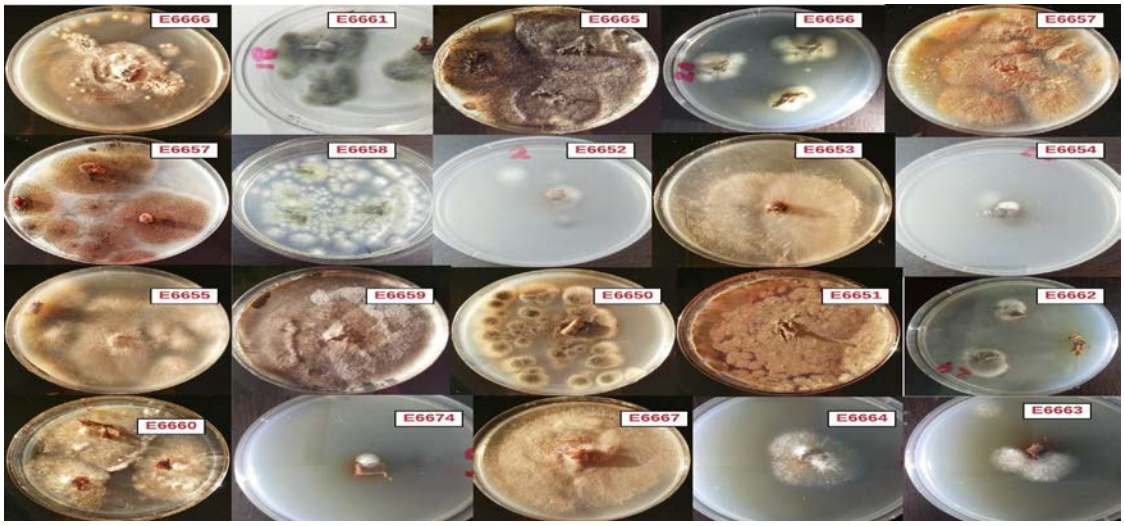

Figure 1. Different morphologically fungi isolated on PDA media

3.2. Morphological identification of the isolates

Twenty different taxa were identified depending on macro and micromorphology, including characteristics of colonies on plates, reverse colony color, pigment diffusion, sporophore and spore chain characteristics as presented in Table 1.

Table.1 List of the morphologically identified fungal species with their morphological features and the tissue source of isolation.

Code	Name	Morphological structure	Tissue
E6666	*Acremonium* sp.	White to cream- conidia one- celled	Stem
E6661	*Alternaria* sp.	Dark olive to black-conidia globose	Leaf
E6665	*Alternaria* sp.	Dark gray to black-conidia straight, elliptical- septate	Leaf
E6656	*Asperigillus* sp.	Golden yellow-coninial heat columner- smooth – conidia globose	Leaf-stem
E6675	*Asperigillus terrus*	Golden yellow to brown-conidial heads large-conidia globose rough	Root
E6657	*Aspergillus niger*	Dark black- conidia globose- conidiophores smooth	Root-stem-leaf
E6658	*Emericella nidulans*	Faint green- reverse grayed-orange-ascospores with no equatorial ridges	Leaf
E6652	*Fusarium* sp.	Pale pink-microconidia-globose	Root
E6653	*Fusarium* sp.	White to cream-microconidia-fusiform	Root
E6654	*Fusarium* sp.	Pale purple-macroconidia-	Root
E6655	*Fusarium* sp.	White buff -micro and macroconidia	Root
E6659	*Stemphylium* sp.	Dark grayed olive- smooth rounded conidia-conidiophore nodose-transverse and longitudinal septa	Root-stem
E6650	*Peicillium duclauxii*	Green- white margin-conidia elliptical-symmetrical	Root
E6651	*Penicillium corylophilum*	diffuse Dark green-conidia globose - asymmetrical- red pigment in the media	Stem
E6662	Black sterile mycelium	Dark black gray hyphal tip	Leaf
E6660	Sterile mycelium	Pale yellow white margin-sterile white mycelium	Leaf
E6664	Sterile mycelium	Cream color- sterile hypha	Root
E6674	Sterile mycelium	Light gray- white margin	Leaf
E6667	Sterile mycelium	Buff to cream	Leaf
E6663	*Ulocladium botrytis*	Dark gray, light gray margin- conidia verruculose-transverse septa	Root

* (the code of the isolates "E and numbers": E refers to endophyte, the numbers refer to the TUCIM No. [Collection of Industrially Important Microorganisms, Vienna University of Technology]).

Most of the isolates have recovered from a single organ except for *Stemphylium* sp. (E6659) which has been isolated from both leaf and stem of the plant and *Aspergillus* sp. (E6656) Which has been isolated from root and stem. *Aspergillus niger* (E6657) was found to recover from all plant tissues (leaf, stem, and root). All Fusaria species have been isolated only from the root of *P. graveolens*. 15% of the isolates have failed to produce spores in culture media.

Table.2 The colonization frequency (CR%) and isolation rate (IR%) of different tissues of Pelargonium graveolens.

Parameter	Leaves	Stem	Root	Total
No. of segments	150	150	135	435
No. of segments with isolates	70	58	129	257
No. of isolated fungi	87	72	133	292
colonization frequency (CF%)	47%	39%	96%	59%
Isolation rate (IR%)	58%	48%	99%	67%

Total of 257 isolates have been recovered from the investigated plants. Data in table. 2 show that root harbors most of the isolates with colonization frequency (CF)=96% and isolation rate (IR)=99%. Leaf tissues exhibit CF=47% and IR=58%. The stem shows the lowest CF% and IR% (39% and 48% respectively). Total plant tissues exhibit relatively high frequency (CF=59%) and richness of isolates (IR=67%). These results indicate that, *P. graveolens* is extensively colonized by endophytic fungi, specially the root of the plant.

3.3. Molecular identification of strains

Molecular analysis of the isolates has been carried out using ITS rDNA sequences to confirm the microscopic identification and study the phylogenetic relation between related species and the relation between all the isolates that colonize *p. graveolens* as endophytes. The most related taxa from GenBank and their accession number are listed in table 3. The score, E value, and query coverage and identity percentage are also displayed. Sequences that exhibited the highest identity and query coverage percentage have been chosen. From table 3, all chosen sequences exhibit at least 99% identity and 95% query coverage with one or more species or genera in the GenBank.

3.4. Phylogenetic analysis of the molecular data

Alignment of the sequences and construction of the phylogenetic tree have been carried out for choosing the most genetically related taxa to the isolates and understanding the genetic relation between the isolates. The sequences of the isolates and sequences chosen from the GenBank have been aligned using the Clustal W program. MEGA X software has been used to build the tree, using Neighbor- joining method (Saitou and Nei, 1987) with p-distance model and pairwise deletion of gaps.

A number of taxa that exposed to the analysis are 48 (20 query sequences of the isolates and 28 taxa with the closet sequences from GenBank) with a bootstrap of 500 replicates. The produced tree has 1822 sites and sum of branch length 1.1397. Branches with bootstrap value $\leq$ 50% is considered supported. The phylogenetic tree placed the isolated fungi in to 4 clades as shown in fig. 2.

All belong to the phylum Ascomycota. Clade (A) contains 6 query sequences and 9 from GenBank. All belong to the order Hypocreales with high branch support (100%) and divided into two subclades. One includes 5 fungi from the family Nectriaceae (E6652, E6654, E6653, E6655 and E6664) and all identified as *Fusarium* sp. with 100% support.

Table.3 Molecular identification of the isolates and the closest similar taxa from GenBank.

Isolates	Most closely related taxa from GenBank	Max score	Total score	Query cover (%)	E value	Identities (%)	Accession	Length
E6650	*Talaromyces* sp.	1016	1016	98	0	99.64	MG745311.1	579
	Talaromyces flavus var. *flavus* strain	1013	1013	100	0	99.12	MH860587.1	1124
	Penicillium pinophilum	1002	1002	98	0	99.11	HQ392503.1	588
E6651	*Talaromyces flavus var. flavus* strain	1020	1020	99	0	99.12	MH860587.1	1124
	Penicillium sp.	1007	1007	95	0	100.0	KX008642.1	560
E6652	*Fusarium oxysporum*	976	976	99	0	99.81	LT970803.1	1419
	Fusarium oxysporum	963	1073	97	0	100.0	KY587331.1	616
E6653	*Fusarium oxysporum*	970	970	99	0	99.44	LT746252.1	1407
E6654	*Fusarium oxysporum*	961	961	99	0	100.0	KX421425.1	1419
E6655	*Fusarium verticillioides*	983	983	97	0	100.0	MF682356.1	572
	Fusarium oxysporum	998	998	99	0	99.82	KU872849.1	1052
	Fusarium nygamai	998	998	99	0	99.82	HF546381.1	963
	Fusarium nygamai	983	983	97	0	100.00	KY039301.1	534
E6656	*Aspergillus terreus*	1086	1086	99	0	99.50	JX188057.1	1341
E6675	*Aspergillus terreus*	1079	1079	97	0	100.0	KY200574.1	608
E6657	*Aspergillus niger*	1062	1062	97	0	100.0	FJ668837.1	625
E6658	*Aspergillus sublatus*	1011	1011	99	0	99.64	KU866668.1	748
	Aspergillus quadrilineatus	1011	1011	99	0	99.64	NR_131289.1	587
	Emericella rugulosa	1011	1011	99	0	99.64	AB244780.1	590
	Aspergillus nidulans	1000	1000	96	0	100.0	MG459155.1	553
	Emericella nidulans	1000	1000	96	0	100.0	KC466534.1	567
	Aspergillus floriformis	998	998	96	0	100.0	KU866568.1	556
E6659	*Stemphylium vesicarium*	1026	1026	100	0	99.64	MG065799.1	1005
	Pleospora herbarum	1016	1016	98	0	100.0	KP334719.1	582
E6660	*Chaetomium madrasense*	985	985	95	0	100.0	MH864195.1	597
	Chaetomium ascotrichoides	985	985	95	0	100.0	MH861550.1	586
E6661	*Alternaria alternate*	1007	1007	100	0	100.0	MH221088.1	596
	Dothideomycetes sp.	1007	1007	100	0	100.0	KX908431.1	1074
	Alternaria tenuissima	1007	1007	100	0	100.0	KX664335.1	1110
E6662	*Alternaria alternate*	1003	1003	100	0	99.82	KY676196.1	865
	Dothideomycetes sp.	1003	1003	100	0	99.82	KX908365.1	1074
	Alternaria tenuissima	1003	1003	100	0	99.82	KX664322.1	1117
E6663	*Gilmaniella humicola*	904	904	94	0	100.0	MH855915.1	534
	Zopfiella longicaudata	878	878	92	0	100.0	KF811038.1	475
E6664	*Fusarium verticillioides*	983	983	97	0	100.0	MF682356.1	572
	Fusarium nygamai	983	983	97	0	100.0	KY039301.1	534
	Hypocreales sp.	981	981	97	0	100.0	GQ923973.1	558
	Fusarium oxysporum	998	998	99	0	99.82	KU872849.1	1052
E6665	*Alternaria alternate*	1009	1009	100	0	99.82	KX115416.1	678
	Dothideomycetes sp.	1009	1009	100	0	99.82	KX909052.1	1070
	Alternaria tenuissima	1009	1009	100	0	99.82	KX664335.1	1110
E6666	*Acremonium sclerotigenum*	990	990	97	0	100.0	MG980070.1	576
	Scopulariopsis sp.	989	989	97	0	100.0	KU523862.1	574
	Acremonium alternatum	989	989	97	0	100.0	KT192193.1	575
	Peniophora sp.	989	989	97	0	100.0	HQ607928.1	598
E6667	*Chaetomium subaffine*	1007	1007	97	0	100.0	MG770272.1	559
E6674	*Botryotrichum murorum*	1000	1000	97	0	100.0	MG770259.1	548

In the other subclade E666 fungus is placed near 2 different species of *Acremonium* (*A. alternatum* and *A. sclerotigenum*) with very strong bootstrap value (100%), E666 is defined as *Acremonium* sp. by combining the microscopic examination with the genetic analysis. Clade (B) includes 4 fungi belong to the family Caetomiaceae. E6663 is located near a sister clade containing two different genera (*Gilmaniella humicola* and *Zopfiella longicaudata*) with a very strong bootstrap value (98%) which has been denoted as unidentified genus as the

microscopic examination does not match with any of them. E6674 is defined as *Botryotrichum murorum* with 100% support. E6667 is *C. subaffine* with 89% support. E6660 locates in the same subclade with 2 different *Chaetomium* sp. so it is defined on the level of genera as *Chaetomium* sp. Cluster (c) involves 6 isolated fungi. All belong to Aspergillaceae family with 100% bootstrap value. In Clade (D), 4 fungal species belonging to the family Pleosporaceae, and are divided in to 2 subclades with 100% support. E6659 fungus is in the same subclade with 2 different genera (*Stemphylium vesicarium* and *Pleospora herbarum*), but it clustered in a sister clade with *Stemphylium vesicarium* with 60% bootstrap value which supports the morphological examination. E6665, E6662 and E6661 are in the same subclade with more than one Alternaria species. E6665 and E6662 are identified as *Alternaria alternate* with 63% and 75% support respectively, while E6661 fungus is identified as *Alternaria tenuissima* with 73% bootstrap value.

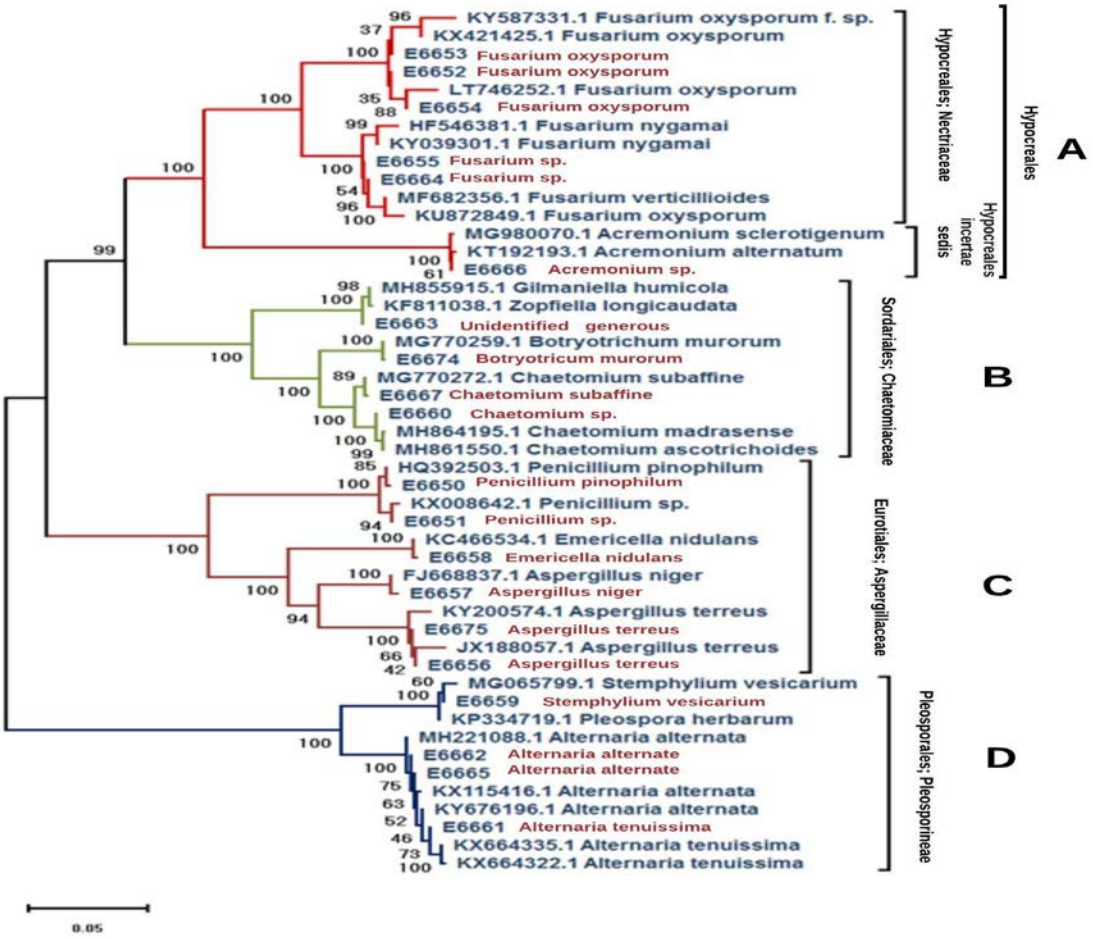

Figure 2. neighbor joining phylogenetic tree of the isolates with 500 replicates bootstrap

3.5. Colonization frequency of the isolated fungi

The colonization frequency indicates the abundance of the endophytes in their host plant. As shown in fig.3, Aspergillus and its teleomorph (Emericella) are the most occurring isolated genera with 28% colonization frequency followed by Fusarium 21%, then Penicillium 16%. Stemphlium and Alternaria have the same frequency 12%, whereas Chaetomium, Acremonium and botyotrichum sp. show low colonization abundance with frequency 4%, 3%, and 2% respectively. An isolate (E6663) could not be able to determine its genera and is represented as unidentified genus with low CF% (2%).

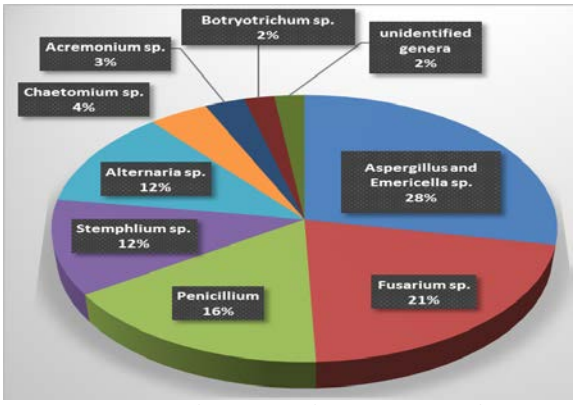

Figure 3. The CF% of the isolated fungi on the level of genera.

3.6. Antimicrobial activity of the isolates

Most of the fungi exhibit antagonistic activity against *Fusarium solani* with inhibition rate ranging from 60% for *Emericella nidulans* (E6658) to 4% for *Alternaria*

sp.(E6662). *Penicillium* sp.(E6651), *Aspergillus terreus* (E6675) and *Aspergillus niger* (E6657) are, also, very active against *F.solani* with inhibition rate 45%, 47 and 28% respectively. Five fungal isolates (*Alternaria alternate* (E6665), *Alternaria tenuissima* (E6661), *Fusarium* sp. (E6664), *Acremonium* sp. (E6666) and *Chaetomium subaffine* (E6674)) have negative inhibition rate indicating that they stimulate the growth of the tested pathogen fig.4(a)

Out of the 20 isolated fungi, only 4 fungal isolates exhibit antifungal activity against *sclerotium rolfsii*. *Aspergillus niger* (E6657) has a maximum inhibition rate (72%). Both *Penicillium* sp. (E6651) and *Chaetomium subaffine* (E6667) inhibit *S. rolfsii* by 50%, and *Emericella nidulans* (E6658) exhibits 31% inhibition rate against *S. rolfsii* fig.4(b).

Six fungal species exhibit antifungal activity against *Rhizoctonia solani*. The highest inhibition rate is recorded for *Aspergillus niger* (E6657), and the lowest rate is for *Aspergillus terreus* (E6656) (27%), and the rest of the tested fungi show no antimicrobial activity Fig.4(c).

As shown in Fig.4(d), most of the isolates exhibit antagonistic activity against *Microsporum audouinii*. *Emericella nidulans* (E6658) exhibits the highest rate of inhibition (80%). *Acremonium* sp. (E6666) shows no effect on the tested pathogen and *Chaetomium subaffine* (E6667) has negative inhibition rate, which reveals that it stimulated the growth of the pathogen.

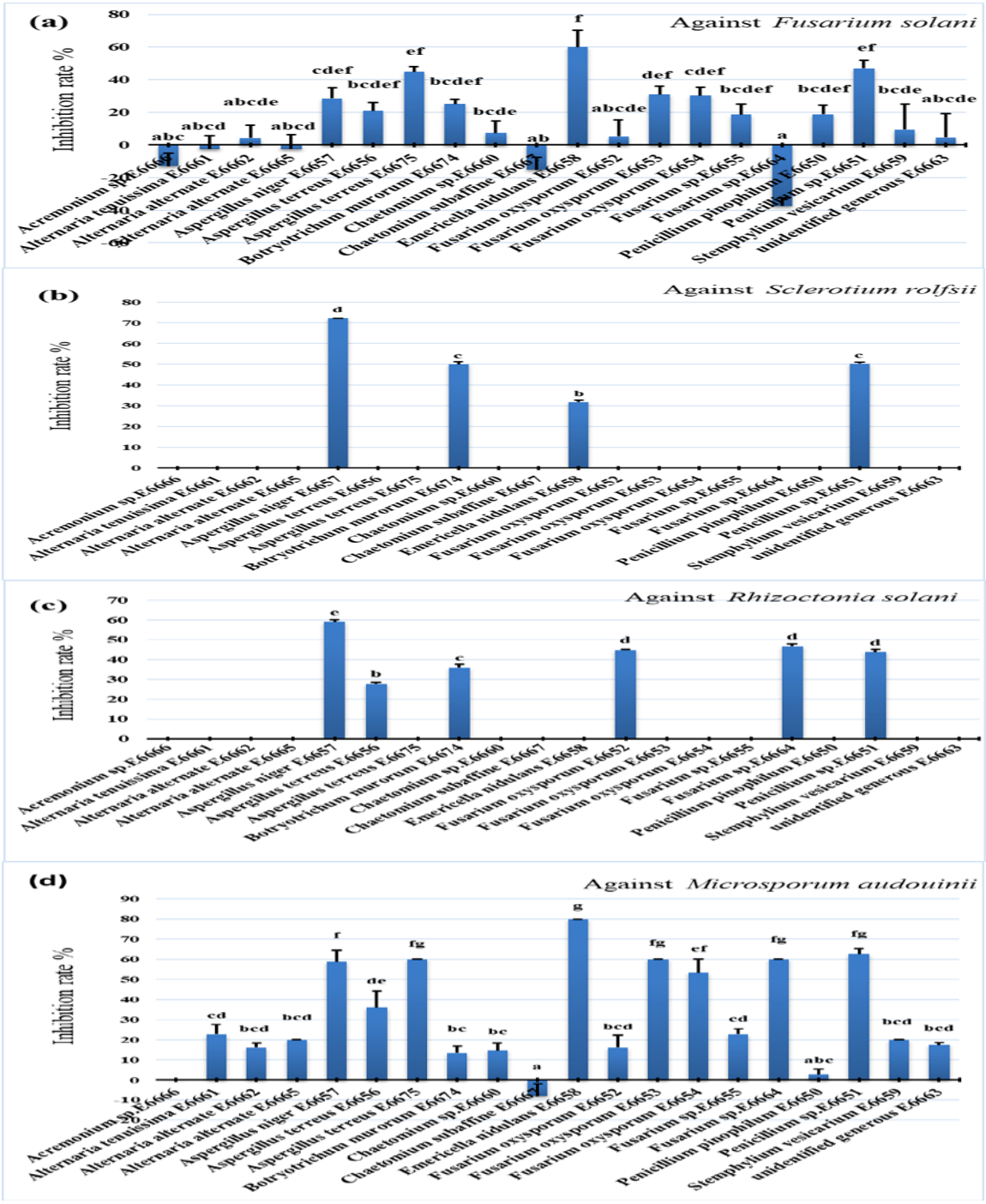

Figure 4. Inhibition rate IR% values of the isolated fungi against pathogenic fungi. Error bars represent the standard error SE± of three replicates. Significant differences between the mean values are represented as different letters on the bars (P ≤0.05) by Tukey HSD test.

4. Discussion

In the current study, a total of 274 fungi have been isolated from leaf, root, and stem of *P. graveolens* plant. Plant root exhibits the highest CF% (96%) and IR% (99%) than leaf and stem. These results match with the study of M. Manganyi, et al., who reported higher colonization rate of endophytic fungi in the root (28%) of Pelargonium sidoides than the leaf (25%) (Manganyi et al., 2018). This may be due to the exposure of the root to rich microbial community from the surrounding soil. Stem harbors the lowest number of isolates (CF=39% and IR=48%). The variation in the isolates diversity among plant organs may also be due to differences in the chemical composition of these organs (Huang et al., 2008). Composition of endophytic fungi community from different organs display a tissue-specific manner as most of the isolates were recovered from a specific organ while *Stemphylium* sp. (E6659) has been isolated from the leaf and stem of the plant. *Aspergillus* sp. (E6656) has been isolated from the root and stem. *Aspergillus niger* (E6657), also, was found to recover from all plant tissues (leaf, stem and root). All *Fusarium* species have been isolated only from the root of *P. graveolens*. This indicates that the isolated fungi may develop a specific relationship with their host plant organ. This finding is supported by many studies on endophytes. From a previous study on *Angelica sinensis*-associated endophytes, many fungi exhibited specificity to certain organ such as *Alternaria* sp. that recovered only from the leaf (JIANG et al., 2013).

The isolated fungi were grouped into 20 morphologically different fungi. Morphological identification has been able to determine most of the isolates genera and detect the sexual phase (teleomorph) if exist. Microscopic examination, also, were able to identify the species of some genera. As many isolated fungi were reported to fail to sporulate in culture media, Non-sporulated isolates have hampered their identification and classified as Mycelia sterilia. The identities of the isolated fungi have been confirmed by combining morphological with molecular identification. ITS region is one of the most frequently utilized tool to identify fungi at the species level. However, it has complications and cannot serve as the universal barcode of fungi (Diaz et al., 2012). In this study, ITS sequences of the isolates have been analyzed and subjected to sequence similarity comparison using blast search. In our study, molecular identification effectively identifies 9 fungi on the level of species with at least 99% identity and 95% query coverage, including fungi that are identified as Mycelia sterilia in microscopic examination.

In many cases, fungi exhibit similarity with more than one species or even genera or with the sexual and asexual phase of a fungus strain. A study on endophytic fungi isolated from *Glycine max* has faced the same complication (Fernandes et al., 2015). These cases were confirmed by microscopic examination. Some fungi that exhibit different morphological feature were identified as the same species in molecular analysis. Similar results were reported (Ginting et al., 2013). Therefore these isolates may differ at the sub- species level. Only one fungus could not be identified on the level of genera as it exhibits similarity with two different genera from GenBank and microscopic examination did not match one of them.

Calculation of the phylogenetic tree illustrates the close phylogenetic relation between the fungi exposed to the analysis. They are clustered into 4 clades. All belong to the phylum Ascomycetes and 4 orders Hypocreales (30%), Sordariales (20%), Eurotiales (30%) and Pleasporales (20%) and five families. All the isolate represents 10 genera: Fusarium, Aspergillus, Emericella, Acremonium, Chaetomium, Penicillium, Stemphylium, Alternaria, Botryoticum, and an unidentified genus. In many studies, most of these fungi isolated in high frequency as endophytes, especially from medicinal plants (Nair and Padmavathy, 2014).

Aspergillus and its telemorph Emericella are the most abundant isolated genera (CF=28%) followed by Fusarium (CF=21%) and Penicillium (CF=16%). Stemphylium and Alternaria exhibit the same CF value (12%). Other isolated genera show frequency values equal to or less than 4%. These results, however, cannot be compared with other studies as it depends on many factors including host and endophyte progeny, their chemical composition, other microbial communities associated with the plant and the environmental factors (Schulz and Boyle, 2006).

In the current study, all the isolated fungi exhibit antifungal activity against at least one of the tested pathogens except for *Acremonium* sp. (E6666) and *Chaetomium subaffine* (E6667). The maximum inhibition rate is for *Emericella nidulans* (E6658) (IR=80%) against *M. audouinii*. Many of the isolates exhibit strong activity against more than one of the tested pathogenic fungi. For example, *A. niger* (E6657) and *Penicillium* sp. (E6651) show very strong activity against the four pathogenic fungi. These results reveal that endophytic fungi isolated from *P. gravoelons* can be a source of bioactive metabolites, involving those able to control plant and human diseases(Chi et al., 2019).

5. Conclusion

The current study suggests that *P. gravoelons* plant is symbiotically associated with rich endophytic fungi community. Identification of these fungi is best done by combining morphological and molecular analysis. The diversity of these fungi varied among different organs. Some of the isolates exhibit a manner of specificity than the others. The isolated fungi are closely related, and all belong to Ascomycetes. Most of the isolates exhibit antifungal activity against some tested pathogens, which reveal that they may be a source of bioactive compounds against plant and human diseases.

Although using the ITS marker was valuable for species identification in this study other markers are recommended to offer more resolution to ITS and avoid the limitations of a single-marker barcoding system. These markers such as the largest (RPB1) and second largest (RPB2) subunits of RNA polymerase, translation elongation factor 1-alpha (tef1), beta-tubulin (tub2) and partial calmodulin (CaM).

Acknowledgments

Authors thank Marica Grujic and Dr. I. S. Druzhinina (the leader of the Microbiology and Applied Genomics Group), Microbiology and Applied Genomics Group, Institute of Chemical, Environmental & Bioscience Engineering Vienna University of Technology, Austria for their help during the molecular identification of isolates.

References

Arnold, A.E. 2007. Understanding the diversity of foliar endophytic fungi: progress, challenges, and frontiers. *Fungal Biology Reviews* **21 (2–3)**: 51–66.

Ćavar, S., and Maksimović, M. 2012. Antioxidant activity of essential oil and aqueous extract of Pelargonium graveolens L'Her. *Food Control* **23 (1)**: 263–267.

Centre, I. trade. 2015. The IFEAT socio-economic study of geranium oil. *IFEAT World http://www.intracen.org/uploadedFiles/intracenorg/Content/Exporters/Market_Data_and_Information/Market_information/Market_Insider/Essential_Oils/Geranium%20oil.pdf* (July): .

Chi, W.C., Pang, K.L., Chen, W.L., Wang, G.J., and Lee, T.H. 2019. Antimicrobial and iNOS inhibitory activities of the endophytic fungi isolated from the mangrove plant Acanthus ilicifolius var. xiamenensis. *Botanical Studies* **60 (1)**: .

Diaz, P.L., Hennell, J.R., and Sucher, N.J. 2012. Genomic DNA Extraction and Barcoding of Endophytic Fungi. *Springer Science+Business Media* **862 (862)**: 171–179.

Fernandes, E.G., Pereira, O.L., Silva, C.C. da, Bento, C.B.P., and Queiroz, M.V. de. 2015. Diversity of endophytic fungi in Glycine max. *Microbiological Research* **181**: 84–92.

Ginting, rohani cinta badia, Sukarno, N., Widyastuti, U., Darusman, latifah kosim, and Kanaya, S. 2013. Diversity of Endophytic Fungi from Red Ginger (Zingiber officinale Rosc.) Plant and Their Inhibitory Effect to Fusarium oxysporum Plant Pathogenic Fungi. *HAYATI Journal of Biosciences* **20 (3)**: 127–137.

Haddadderafshi, N. 2015. Diversity and antagonistic activity of endophytic fungi from sweet cherry and pepper. .

Hsouna, A. Ben, and Hamdi, N. 2012. Phytochemical composition and antimicrobial activities of the essential oils and organic extracts from pelargonium graveolens growing in Tunisia. *Lipids in Health and Disease* **11 (1)**: 1.

Huang, H., Rong, H., Li, X., Tong, S., Zhu, Z., Niu, L., and Teng, M. 2008. The crystal structure and identification of NQM1/YGR043C, a transaldolase from Saccharomyces cerevisiae. *Proteins* **73 (4)**: 1076–1081.

JIANG, S., QIAN, D., YANG, N., TAO, J., and DUAN, J. 2013. Biodiversity and Antimicrobial Activity of Endophytic Fungi in Angelica sinensis. *Chinese Herbal Medicines* **5 (4)**: 264–271.

Kullnig-Gradinger, C.M., Szakacs, G., and Kubicek, C.P. 2002. Phylogeny and evolution of the genus Trichoderma: A multigene approach. *Mycological Research* **106 (7)**: 757–767.

Kumar, S., Stecher, G., Li, M., Knyaz, C., and Tamura, K. 2018. MEGA X : Molecular Evolutionary Genetics Analysis across Computing Platforms. **35 (6)**: 1547–1549.

Kusari, S., Hertweck, C., and Spiteller, M. 2012. Chemical ecology of endophytic fungi: Origins of secondary metabolites. *Chemistry and Biology* **19 (7)**: 792–798.

Manganyi, M.C., Regnier, T., Kumar, A., Bezuidenhout, C.C., and Ateba, C.N. 2018. Biodiversity and antibacterial screening of endophytic fungi isolated from Pelargonium sidoides. *South African Journal of Botany* **116**: 192–199.

Moubasher, A.H.. e. al. (1993). *Soil fungi in Qatar and other Arab countries*. The Centre for Scientific and Applied Research, University of Qatar.

Nair, D.N., and Padmavathy, S. 2014. Impact of endophytic microorganisms on plants, environment and humans. *The Scientific World Journal*.

Nascimento, T.L., Oki, Y., Lima, D.M.M., Almeida-Cortez, J.S., Fernandes, G.W., and Souza-Motta, C.M. 2015. Biodiversity of endophytic fungi in different leaf ages of Calotropis procera and their antimicrobial activity. *Fungal Ecology* **14**: 79–86.

Rodriguez, R.J., White Jr, J.F., Arnold, A.E., and Redman, R.S. 2009. Fungal endophytes: diversity and functional roles. .

Roopa, G., Madhusudhan, M.C., Sunil, K.C.R., Lisa, N., Calvin, R., Poornima, R., Zeinab, N., Kini, K.R., Prakash, H.S., and Geetha, N. 2015. Identification of Taxol-producing endophytic fungi isolated from Salacia oblonga through genomic mining approach. *Journal of Genetic Engineering and Biotechnology* **13 (2)**: 119–127.

Saitou, N., and Nei, M. 1987. The Neighbor-joining Method : A New Method for Reconstructing Phylogenetic Trees '. **4 (4)**: 406–425.

Schulz, B., and Boyle, C. 2006. What are Endophytes? 9: 1–14.

Schulz, H.J. 1993. HJ Schulz, Phys. Rev. Lett. 71, 1864 (1993). *Phys. Rev. Lett.* **71**: 1864.

Staniek, A., Woerdenbag, H.J., Kayser, O., Staniek, A., Woerdenbag, H.J., and Kayser, O. 2008. Endophytes : exploiting biodiversity for the improvement of natural product-based drug discovery Endophytes : exploiting biodiversity for the improvement of natural product-based drug discovery. 9145 (May): .

Wang, Y., Gao, B.L., Li, X.X., Zhang, Z. Bin, Yan, R.M., Yang, H.L., and Zhu, D. 2015. Phylogenetic diversity of culturable endophytic fungi in Dongxiang wild rice (Oryza rufipogon Griff), detection of polyketide synthase gene and their antagonistic activity analysis. *Fungal Biology* **119 (11)**: 1032–1045.

White, T.J., Bruns, T., Lee, S., and Taylor, J. 2014. Amplification and Direct Sequencing of Fungal Ribosomal Rna Genes for Phylogenetics. *PCR Protocols* (**January**): 315–322.

Yan, J.F., Broughton, S.J., Yang, S.L., and Gange, A.C. 2015. Do endophytic fungi grow through their hosts systemically? *Fungal Ecology* **13**: 53–59.

Zhang, H.W., Song, Y.C., and Tan, R.X. 2006. Biology and chemistry of endophytes. *Natural Product Reports* **23 (5)**: 753–771.

Zhao, X., Zhang, Y., Shi, J., Liu, Y., Lu, Y., and Lian, Z. 2019. Biosynthesis of antibacterial compound against multidrug resistant foodborne pathogens by Phomopsis sp. XP-8. *Food Control* 95 (April 2018): 223–231.

JJBS

Volume 13, Number 2, June 2020
ISSN 1995-6673
Pages 207 - 211

Jordan Journal of Biological Sciences

Angiotensin Converting Enzyme (ACE) Gene Polymorphism in Jordanian Type-1 and Type-2 Diabetic Patients

Ahmad Barghash[1], Samer I. Al-Gharabli[2*], Malak Jweihan[2], Maisam Tanbouz[2], Esra'a AlBarahmieh[2], Eyad Hamad[3], Nafisah Al-Rifai[2], Hussam AlHawari[4] and Lubna H. Tahtamouni[5*]

[1]*Department of Computer Science, School of Electrical Engineering,* [2]*Department of Pharmaceutical and Chemical Engineering, School of Applied Medical Sciences,* [3]*Department of Biomedical Engineering, School of Applied Medical Sciences, German Jordanian University,* [4]*Department of Internal Medicine, Faculty of Medicine, The University of Jordan, Amman,* [5]*Department of Biology and Biotechnology, Faculty of Science, The Hashemite University, Zarqa, Jordan*

Received June 28, 2019; Revised July 31, 2019; Accepted August 5, 2019

Abstract

Epithelial cells of the endothelial surfaces incorporate a gene for angiotensin-converting enzyme (ACE) that encodes metallopeptidase proteins. In this work, molecular characterization of the ACE gene by investigating the presence of two specific variants of 287 bp fragment (Alu element), have been studied. Therefore, the insertion (I allele) and the deletion (D allele) of this gene fragment were controlled. A group of Jordanian patients with Type-I and Type-II Diabetes Mellitus (DM) was selected for this study. The investigated sample contains 26 subjects with Type-I DM, 45 subjects with Type-II DM in addition to a control group of 44 healthy subjects. ACE genotypes of the patients and control groups were achieved using PCR of the DNA amplification. Results reveal no significant statistical differences in ACE genotype distribution among the focus group and the control one. Therefore, there is no significant association between DM and ACE genotype distribution variants of the proposed insertion. The ACE gene polymorphism is not directly correlated to diabetes.

Keywords: Angiotensin; ACE gene; Diabetes mellitus, Differential expression, Alu element.

1. Introduction

The epithelial cells of endothelial surfaces combine genes for angiotensin-converting enzymes (ACE) that encrypt a metallopeptidase. In this research, the molecular characterization of ACE has been studied by the means of the hypothesis of presence and absence of two specific variants of 287 bp fragment based on the previous researches (Castellon and Hamdi, 2007; Hamdi and Castellon, 2003; Hamdi, *et al*., 2002). It has been based on the hypothesis of the insertion of (I allele) and the deletion of (D allele) of this gene fragment.

In order to test this hypothesis, a focus group of Jordanian patients with Type-I and Type-II Diabetes Mellitus (DM) have been used. In addition, a control group of 44 healthy subjects, and a focus group contain 26 subjects with type 1 diabetes mellitus (T1DM) and 45 with type 2 diabetes mellitus (T2DM).

Diabetes mellitus (DM) is a metabolic chronic health illness identified by a raised blood sugar levels (Zhong, *et al*., 2015). DM has been categorized into two main groups; group one is called type 1 diabetes mellitus and it has been known and denoted by (T1DM) and the second group is called type 2 diabetes mellitus and it has been known and denoted by (T2DM) (Piero, *et al*., 2015; Saucă, *et al*., 2012). Diabetes mellitus patients suffer from various health difficulties such as diabetic nephropathy, diabetic retinopathy and cardiovascular disease (CVD) (Golmohamadi, *et al*., 2006)

The angiotensin-converting enzyme (ACE) (EC 3.4.15.1) plays a vital role in inducing the conversion of angiotensin I to angiotensin II, which is the primary effector molecule of the Renin-Angiotensin-Aldosterone System (RAAS) (Golmohamadi, *et al*., 2006; Song and Lee, 2015). Angiotensin II allows for the constriction of blood vessels leading to an increment of blood pressure.

ACE gene polymorphism is classified based on either the presence/insertion, denoted (I), or absence/deletion, denoted (D) of 287 bp *Alu* elements at intron 16 of chromosome 17 which results in three different genotypes; DD and II homozygotes and ID heterozygote. Plasma ACE levels are 30% and 60% higher in the ID heterozygotes and DD homozygotes, respectively, when compared to the II homozygotes. Therefore, individuals who carry the DD and ID genotypes have a more active Renin-Angiotensin-Aldosterone System (RAAS) (Al-Serri, *et al*., 2015).

Various research groups have investigated the correlation of the *ACE* gene I/D polymorphism and T1DM and T2DM. However, the results are inconsistent. Some studies did not find a relative correlation between *ACE* gene polymorphism and developing DM or one or more of its complications (Jayapalan, *et al*., 2010; Kumar, *et al*., 2013; Pasha, *et al*., 2002; Schmidt, *et al*., 1995; Zhou, *et*

* Corresponding author e-mail: Samer.gharabli@gju.edu.jo; lubnatahtamuni@hu.edu.jo.

al., 2012). On the other hand, other studies suggested that the DD genotype marks for higher risk of certain diseases like diabetic nephropathy and hypertension (Tseng, *et al*., 2011). Huang and colleagues (2001) showed that an increment in ACE gene levels is adequate to develop nephropathy in diabetic mice (Huang, *et al*., 2001). In addition, the DD genotype was abided to increase risk of severe hypoglycemia in T1D patients (Freathy, *et al*., 2007).

Various researches explored the diversity of the ACE gene haplotypes. It has been shown that the frequency distributions of the haplotypes vary among people in different countries (Farheen, *et al*., 2011). The D allele was found to be present more frequently in Africans and Caucasians, while the I allele is present more frequently among Asians (Farheen, *et al*., 2011). The frequency distributions of ACE gene haplotypes were studied in few Arab populations (Al-Hinai, *et al*., 2002; Frossard, *et al*., 1997; Motawi, *et al*., 2016) but not in Jordanians. In addition, the relation between the ACE gene polymorphism insertion/deletion and T2DM have been studied and discussed in some Arab populations but not among Jordanian DM patients (Al-Harbi, *et al*., 2012; Al-Rubeaan, *et al*., 2013; Al-Serri, *et al*., 2015; Alsafar, *et al*., 2015; Chmaisse, *et al*., 2009). Therefore, we aimed at investigating the relationship between *ACE* I/D polymorphism and T1DM and T2DM Jordanian patients. Additionally, we aimed at investigating possible roles of *ACE* expression in DM through a broad gene expression analysis of a set of available large-scale National Center for Biotechnology Information Gene Expression Omnibus (NCBI GEO) datasets.

2. Materials and methods

2.1. Study subjects

Seventy-one type 1 (n=26) and 2 diabetes mellitus (n=45) patients were recruited from three hospitals; Jordan Hospital, Dr Jameel Tutanji Hospital, and the University of Jordan Hospital, Amman, Jordan. The inclusion criteria for the current study were: T1DM and T2DM patients (who already diagnosed by consultant diabetologist), being treated for DM without any other complication(s) beside DM. All patients completed informed consent. Information regarding age, treatment and complications was collected from patients using a written questionnaire or interview. 44 subjects were recruited as Age-matched healthy control subjects (n=44). This study was approved by the Institutional Review Board (IRB), Faculty of Medicine at the University of Jordan, that conforms to the World Medical Association Declaration of Helsinki.

2.2. ACE genotyping

Each participant provided a sample of 3 mL of peripheral blood which has been withdrawn on EDTA tube using a venous puncture, followed by the DNA extraction from 300 µL blood; this has been performed using a commercially kit (AccuVis Bio, UAE).

Genomic DNA from each of the control and DM patients groups analyzed by amplification of polymerase chain reaction (PCR) in 30 µL cuvette that includes various components: 1 µL of forward primers (GGACTCTGTAAGCCACTGCTGGAGACC), 1 µL of reverse primers (GGATGTGGCCATCACATTCGTCAGAT) , 8 µL of nuclease-free water, 15 µL of the master mix (New England Biolabs, USA) and finally 5 µL of DNA sample.

The PCR reaction recipe was 35 cycles of denaturation at 96 ^{o}C for 30 seconds, followed by annealing for another 30 seconds and finally elongation at 68 ^{o}C for 30 seconds (Hamdi, *et al*., 2002). This reaction has been conducted using a thermal cycler (MyCycler) (Bio-Rad, USA). The phase of amplification of the DNA was stopped by adding 0.25 M EDTA on ice. Electrophoresis has been performed on the amplified products on 2% (w/v) agarose gel.

2.3. Analysis of NCBI Gene Omnibus (GEO) datasets

In this work, we analyzed three preprocessed and normalized DNA microarrays from the NCBI GEO project. Two T1D datasets; GSE43488 (Lietzen, *et al*., 2018) with 357 samples from 18 autoantibody-positive children (Case) and their matched controls (Control) and GSE30210 (Kallionpää, *et al*., 2014) with 247 samples from 18 prediabetes children and their matched controls. The last dataset GSE9006 (Kaizer, *et al*., 2007) is a super series with 234 samples belonging to three classes; T1DM (162 samples), T1DM (24 samples), and healthy samples (48 samples).

2.4. Statistical analysis

Based on the verification of the Hardy-Weinberg equilibrium, the obtained genotypes and alleles frequencies were compared with predicted frequencies. The Statistical software, StatSoft Inc, Tulsa, OK, USA (version 7.0) has been used to perform both of Chi-square test and Fisher's exact test to obtain the polymorphism frequency. The analysis of NCBI GEO datasets was performed using the R-cran statistical environment similar to the method described in (Barghash, *et al*., 2016). Differential gene expression analysis was checked using the Kolmogorov–Smirnov (KS) test. Bear in mind, that all tests were two-sided, with the assumption of any obtained value of $p<0.05$ would be considered statistically significant.

3. Results

DNA was successfully extracted from 44 control subjects, 26 T1DM patients and 45 T2DM patients (Figure 1).

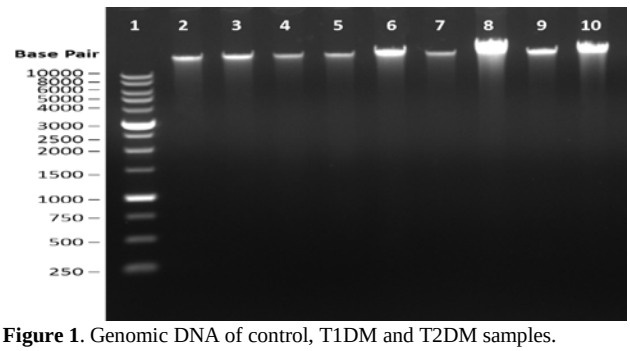

Figure 1. Genomic DNA of control, T1DM and T2DM samples. Lane 1: 1 kb DNA molecular weight marker; Control: Lanes 2-4; T1DM: Lanes 5-7; T2DM: Lanes 8-10.

The PCR amplification products of the 287-bp Alu region of the ACE gene are shown in Figure 2.

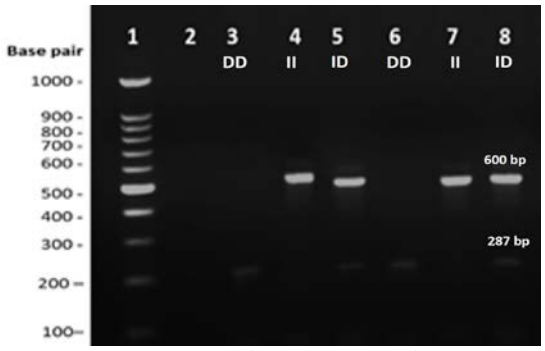

Figure 2. illustrates an amplified Alu segment of the ACE gene that exploits insertion (II) and/or deletion (DD) segment. Lane 1:100 bp Ladder, Lane 2: negative control, Lanes 3 and 6: Alu deletion (DD) at 287 bp, Lanes 4 and 7: Alu insertion (II) at 600 bp, Lanes 5 and 8: Alu insertion and deletion (ID) at 287 bp and 600 bp.

The PCR amplification revealed results that indicate all three genotypes, II (600bp), ID (600/287bp), DD (287bp) were observed in each of the control and DM patients. The highest genotype frequency in control and T1DM patients was the DD genotype (77.3% and 56.5%, respectively) (Table 1). The opposite way, the ID genotype was the most frequent genotype (62%) among T2DM patients (Table 1). Alternatively, the obtained results showed no significant difference in the I and D allelic frequency between the non-diabetic and diabetic groups (Table 1).

Table1. Genotypic and allelic distributions of the ACE gene in control and diabetic populations.

	Genotype			**Allele**	
	II	**ID**	**DD**	**I**	**D**
Control	11.4%	11.4%	77.2%	0.17%	0.83%
T1DM	8.7%	34.8%	56.5%	0.26%	0.74%
T2DM	2.0%	62.0%	36.0%	0.20%	0.80%
P value	0.2501	0.0164	0.0435	0.3628	0.3628

Similarly, we observed that ACE did not show differential expression between the case and control samples in any of the analyzed GEO datasets where KS test consistently resulted in very high p-values. Figure 3 A and B presents a similar expression behavior in T1DM and healthy samples.

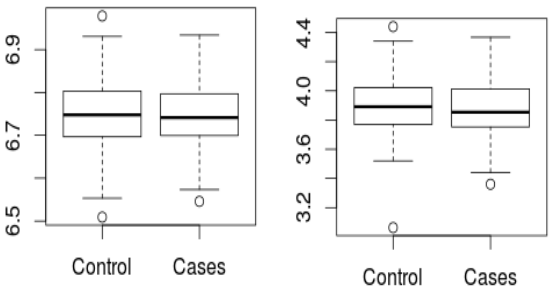

Figure 3. Analysis of ACE gene expression in GEO datasets GSE30210 (left) and GSE43488 (right). No differential expression is detected in ACE expression in GEO datasets GSE30210 or GSE43488.

Additionally, we analyzed GSE9006 which contains a mixture of healthy, T1DM, and T1DM samples to get an overall idea about the possible occurring change in ACE expression. However, no differential expression was detected between the analyzed sample types as presented in figure 4.

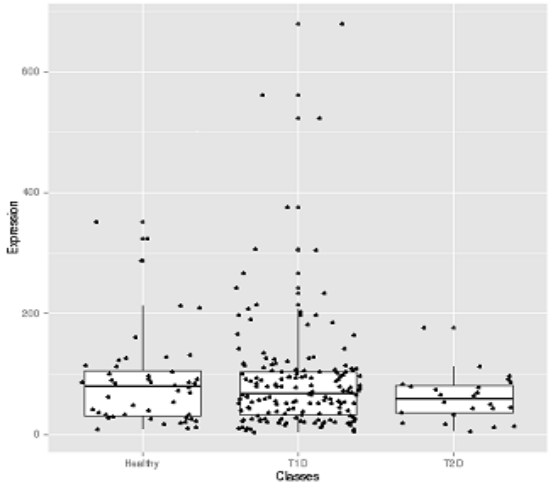

Figure 4. Analysis of ACE gene expression in GEO dataset GSE9006. No differential gene expression is found between the Healthy, T1D, and T2D classes

4. Discussion

Angiotensin-converting enzyme (ACE) cleaves angiotensin I protein converting it into the active angiotensin II hormone. Angiotensin II allows for the constriction of blood vessels; this leads an increment in blood pressure. The ACE gene is considered to be part of either the Renin-Angiotensin-Aldosterone System (RAAS) or Renin-Angiotensin System (RAS). RAAS is normally involved in regulating blood pressure and maintaining balanced body fluids and salts. As a part of RAAS, angiotensin II induces the delivery of hormone aldosterone. Aldosterone, in turn, induces the kidneys to absorb salt and water (Remuzzi, *et al*., 2005). An increment in ACE levels has been noted and correlated to induce nephropathy in diabetic mice (Huang, *et al*., 2001).

Genetic polymorphism is the presence of genetic variations that give different forms of individuals in a population of a certain species. Genetic polymorphism is one cause of diversity. In addition, polymorphism plays a leading role in diseases, such as cardiovascular and age-related diseases. The risk of developing various diseases can be increased many times by inheritance of risk alleles of the various genes at susceptibility loci (Ma, *et al*.).

An insertion/deletion polymorphism is one type of genetic polymorphism where a specific nucleotide sequence in a gene is either insertion or is deletion, i.e. presence or absence. The gene variant with the insertion of the sequence is called the insertion (I) allele, while the other variant that does not have the sequence is called the deletion (D) allele. The first report mentioning ACE I/D polymorphism has been released in 1990 by Rigat and colleagues (Rigat, *et al*., 1990). ACE I/D polymorphism involves either the insertion or deletion of 287 base pairs (*Alu* element) at intron 16 of chromosome 17. ACE I/D polymorphism is the most common type of genetic variations encountered in the RAAS system (Ma, *et al*.). Each person has two copies of the ACE gene, one from each parent. Therefore, each individual could have two D-alleles (DD), or two I-alleles (II), or one I-allele and one D-allele (ID).

Individuals that carry the DD genotype produce more ACE protein and therefore have a more active RAAS system (van Zuydam, *et al*., 2018). Many studies show that the II genotype provides a protective advantage to diabetes type 1 and 2 patients against developing nephropathy (Ha, 2014). In addition, the D allele was found to be present more frequently in Africans and Caucasians, while the I allele is present more frequently among Asians (Ma, *et al*.). It has been proposed that the DD genotype marks for higher risk of certain diseases like diabetic nephropathy and hypertension (Marre, *et al*., 1995; Tseng, *et al*., 2011), as well as increased risk of severe hypoglycemia in T1D patients (Freathy, *et al*., 2007; Pena, *et al*., 2012), but not for T2D patients (Freathy, *et al*., 2007). However, another study found that Taiwanese T2D patients who carry the DD genotype and have other risk factors like hypertension and smoking are at significate risk of peripheral arterial Disease (Tseng *et al*., 2012). The D allele of the ACE gene I/D polymorphism was found to be linked to Diabetes Type 2 in Caucasian male patients (Stephens, *et al*., 2006)

However, other researchers reported a null association between ACE I/D polymorphisms and the susceptibility of T1DM patients to nephropathy (Elhawary, *et al*., 2011; Hibberd, *et al*., 1997) or T2DM patients (Jayapalan, *et al*., 2010). It should be stated that differences in results by the different researchers regarding ACE I/D polymorphism and development of DM owe to ethnic differences, duration of sickness, and the interaction with the environment (van Zuydam, *et al*., 2018).

The results achieved in our study were found to be contradictory to most studies -up to our knowledge- that revealed an association between *ACE* DD genotype and DM (Table 1). Our result revealed a decrement in the frequency of the *ACE* DD genotype in the diabetic groups when correlated to the control group ($p<0.05$) (Table 1). This was in accordance with many studies (Doshi, *et al*., 2015; Jayapalan, *et al*., 2010; Schmidt, *et al*., 1995; Sikdar, *et al*., 2013), but against the findings of others (Baroudi, *et al*., 2009; Ergen, *et al*., 2004; Feng, *et al*., 2002) who found that *ACE* DD genotype in the T2DM is greater than the control group in Turkish, Tunisian and Chinese population, respectively. Nevertheless, the results did not provide any significant association between the I or D alleles of the *ACE* gene and DM (Table 1).

In conclusion and due to the limited number of blood samples collected, a firm understanding on the association of ACE I/D polymorphism and diabetes mellitus could not be reached. Nevertheless, there are around 450 genes associated with diabetes mellitus type 1 based on the susceptibility genes of this disease. These genes were identified using a genome-wide based association analysis, differential expression analysis, replication studies, and functional annotation clustering analysis (Qiu, *et al*., 2014). Those novel-risk genes associated with T1DM imply how important the current analysis is in either predicting or detecting disease susceptibility across the human genome.

References

Al-Harbi EM, Farid EM, Gumaa KA and Singh J. 2012.Genotypes and allele frequencies of angiotensin-converting enzyme (ACE) insertion/deletion polymorphism among Bahraini population with type 2 diabetes mellitus and related diseases. *Mol Cell Biochem*. **362**:219–23.

Al-Hinai AT, Hassan MO, Simsek M, Al-Barwani H and Bayoumi R. 2002. Genotypes and allele frequencies of angiotensin converting enzyme (ACE) insertion/deletion polymorphism among Omanis. *SQUMJ*. **4**:25–27.

Al-Rubeaan K, Siddiqui K, Saeb AT, Nazir N, Al-Naqeb D and Al-Qasim S. 2013. ACE I/D and MTHFR C677T polymorphisms are significantly associated with type 2 diabetes in Arab ethnicity: a meta-analysis. *Gene*. **520**:166–177.

Al-Serri A, Ismael FG, Al-Bustan SA and Al-Rashdan I. 2015. Association of the insertion allele of the common ACE gene polymorphism with type 2 diabetes mellitus among Kuwaiti cardiovascular disease patients. *J Renin-Angio-Aldo S*. **16**:910–916.

Alsafar H, Hassoun A, Almazrouei S, Kamal W, Almaini M, Odama U and Rais N. 2015. Association of angiotensin converting enzyme insertion-deletion polymorphism with hypertension in emiratis with type 2 diabetes mellitus and its interaction with obesity status. *Dis Markers*. **2015**:1–7.

Barghash A, Golob-Schwarzl N, Helms V, Haybaeck J and Kessler SM. 2016. Elevated expression of the IGF2 mRNA binding protein 2 (IGF2BP2/IMP2) is linked to short survival and metastasis in esophageal adenocarcinoma. *ONCOTARGET*. **7**:49743–49750.

Baroudi T, Bouhaha R, Moran-Moguel C, Sanchez-Corona J, Ben Maiz H, Kammoun Abid H and Benammar-Elgaaied A. 2009. Association of the insertion/deletion polymorphism of the angiotensin-converting enzyme gene with type 2 diabetes in two ethnic groups of Jerba Island in Tunisia. *J Renin-Angio-Aldo S*. **10**:35–40.

Castellon R and Hamdi H. 2007. Demystifying the ACE Polymorphism: From Genetics to Biology. *Curr Pharm Design* .**13**:1191–1198.

Chmaisse HN, Jammal M, Fakhoury H and Fakhoury R. 2009. A study on the association between Angiotensin-I converting enzyme I/D dimorphism and type-2 diabetes mellitus. *SJKDT*. **20**:1038–1046.

Doshi DD, Shah DB, Singh KM and Patel RK. 2015. Comparative Study of I/D Polymorphism of ACE Gene in Diabetes TYPE-2 Patients and Control Group in Unrelated Gujarati Population. *Genetika*. **47**:1013–1019.

Elhawary NA, Bogari N, Rashad M and Tayeb MT. 2011. Null genetic risk of ACE gene polymorphisms with nephropathy in type 1 diabetes among Egyptian population. *EJMHG*. **12**:187–192.

Ergen HA, Hatemi H, Agachan B, Camlica H and Isbir T. 2004. Angiotensin-I converting enzyme gene polymorphism in Turkish type 2 diabetic patients. *EMM*. **36**:345–350.

Farheen S, Basu A and Majumder PP. 2011. Haplotype variation in the ACE gene in global populations, with special reference to India, and an alternative model of evolution of haplotypes. *The HUGO journal*. **5**:35–45.

Feng Y, Niu T, Xu X, Chen C, Li Q, Qian R, Wang G and Xu X. 2002. Insertion/deletion polymorphism of the ACE gene is associated with type 2 diabetes. *Diabetes*. **51**:1986–1988.

Freathy RM, Weedon MN, Bennett A, Hyppönen E, Relton CL, Knight B, Shields B, Parnell KS, Groves CJ, Ring SM and Pembrey ME. 2007. Type 2 Diabetes TCF7L2 Risk Genotypes Alter Birth Weight: A Study of 24,053 Individuals. *AJHG*. **80**:1150–1161.

Frossard PM, Obineche EN, Elshahat YI and Lestringant GG. 1997. Deletion polymorphism in the angiotensin-converting enzyme gene is not associated with hypertension in a Gulf Arab population. *Clin Genet*. **51**:211–213.

Golmohamadi T, Nikzamir A, Nakhjavani M, Zahrai M, Amirzargar A and Saffari R. 2006. Association of angiotensin converting enzyme (ACE) gene polymorphism and diabetic nephropathy. *Iran J Public Health*. **35**:14–21.

Ha SK. 2014. ACE insertion/deletion polymorphism and diabetic nephropathy: clinical implications of genetic information. *J Diabetes Res*. **2014**:1–8.

Hamdi H and Castellon R. 2003. ACE inhibition actively promotes cell survival by altering gene expression. *Biochem Bioph Res Co*. **310**:1227–1235.

Hamdi HK, Reznik J, Castellon R, Atilano SR, Ong JM, Udar N, Tavis JH, Aoki AM, Nesburn AB, Boyer DS and Small KW. 2002. Alu DNA polymorphism in ACE gene is protective for age-related macular degeneration. *Biochem Bioph Res Co*. **295**:668–672.

Hibberd M, Millward B and Demaine A. 1997. The angiotensin I-converting enzyme (ACE) locus is strongly associated with age and duration of diabetes in patients with type I diabetes. *J Diabetes Complicat*. **11**:2–8.

Huang W, Gallois Y, Bouby N, Bruneval P, Heudes D, Belair MF, Krege JH, Meneton P, Marre M, Smithies O and Alhenc-Gelas F. 2001. Genetically increased angiotensin I-converting enzyme level and renal complications in the diabetic mouse. *P Natl A Sci India B*. **98**:13330–13334.

Jayapalan JJ, Muniandy S, and Chan SP. 2010. Null association between ACE gene I/D polymorphism and diabetic nephropathy among multiethnic Malaysian subjects. *J Hum Genet*. **16**:78–86.

Kaizer EC, Glaser CL, Chaussabel D, Banchereau J, Pascual V and White PC. 2007. Gene expression in peripheral blood mononuclear cells from children with diabetes. *JCEM*. **92**:3705–3711.

Kallionpää H, Elo LL, Laajala E, Mykkänen J, Ricaño-Ponce I, Vaarma M, Laajala TD, Hyöty H, Ilonen J, Veijola R and Simell T. 2014. Innate immune activity is detected prior to seroconversion in children with HLA-conferred type 1 diabetes susceptibility. *Diabetes*. **63**:2402–2414.

Kumar R., Sharma RK and Agarwal S. 2013. Genetic predisposition for development of nephropathy in type 2 diabetes mellitus. *Biochem Genet*. **51**:865–875.

Lietzen N, An LT, Jaakkola MK, Kallionpää H, Oikarinen S, Mykkänen J, Knip M, Veijola R, Ilonen J, Toppari J and Hyöty H. 2018. Enterovirus-associated changes in blood transcriptomic profiles of children with genetic susceptibility to type 1 diabetes. *Diabetologia*. **61**:381–388.

Carter M, Mendel R, Jun Cui MS and Li S. 2018. Genetic risk determination of hypercholesterolemia and coronary artery disease at the individual patient level. *Risk*. **130**:500–503.

Marre M, Lievre M, Chatellier G, Plouin PF, Wills C and Keir S. 1995. ACE inhibitors and diabetics with albuminuria. *The Lancet*. **346**:1638.

Motawi TK, Shaker OG, Shahin NN and Ahmed NM. 2016. Angiotensin-converting enzyme insertion/deletion polymorphism association with obesity and some related disorders in Egyptian females: a case-control observational study. *Nutr Metab*. **13**:1–11.

Pasha MQ, Khan AP, Kumar R, Ram RB, Grover SK, Srivastava KK, Selvamurthy W and Brahmachari SK. 2002. Variations in angiotensin-converting enzyme gene insertion/deletion polymorphism in Indian populations of different ethnic origins. *J Biosciences*. **27**:67–70.

Pena AS, Couper JJ, Harrington J, Gent R, Fairchild J, Tham E and Baghurst P. 2012. Hypoglycemia, but not glucose variability, relates to vascular function in children with type 1 diabetes. *Diabetes Technol The*. **14**:457–462.

Piero MN, Nzaro GM and Njagi JM. 2015. Diabetes mellitus-a devastating metabolic disorder. *AJBPS*. **4**:1–7.

Qiu YH, Deng FY, Li MJ and Lei SF. 2014. Identification of novel risk genes associated with type 1 diabetes mellitus using a genome-wide gene-based association analysis. *J Diabetes Invest*. **5**:649–656.

Remuzzi G, Perico N, Macia M and Ruggenenti P. 2005. The role of renin-angiotensin-aldosterone system in the progression of chronic kidney disease. *Kidney Int*. **68**:S57–S65.

Rigat B, Hubert C, Alhenc-Gelas F, Cambien F, Corvol P and Soubrier F. 1990. An insertion/deletion polymorphism in the angiotensin I-converting enzyme gene accounting for half the variance of serum enzyme levels. *JCI*. **86**:1343–1346.

Saucă OE, Carpini SD, Zagato L, Zerbini G, Manunta P and Cojocaru D. 2012. Role of angiotensin-converting enzyme insertion/deletion polymorphism in type i diabetes nephropathy. *Rom J Diabetes Nutr Metab Dis*. **19**:143–149.

Schmidt S, Schöne N and Ritz E. 1995. Association of ACE gene polymorphism and diabetic nephropathy?. *Kidney Int*. **47**:1176–1181.

Sikdar M, Purkait P, Raychoudhury P, Bhattacharya SK, Naidu JM and Sarkar BN. 2013. ACE gene insertion/deletion polymorphism and type-2 diabetic nephropathy in Eastern Indian population. *Hum Biol*. **2**:66–76.

Song GG and Lee YH. 2015. The insertion/deletion polymorphism in the angiotensin-converting enzyme and susceptibility to schizophrenia or Parkinson's disease: A meta-analysis. *J Renin-Angio-Aldo S*. **16**:434–442.

Stephens JW, Dhamrait SS, Acharya J, Humphries SE and Hurel SJ. 2006. A common variant in the ACE gene is associated with peripheral neuropathy in women with type 2 diabetes mellitus. *J Diabetes Complicat*. **20**:317–321.

Tseng CH, Tseng FH, Chong CK, Tseng CP and Cheng JC. 2011. Angiotensin-converting enzyme genotype and peripheral arterial disease in diabetic patients. *Exp Diabetes Res*. **2012**:1–7.

Van Zuydam NR, Ahlqvist E, Sandholm N, Deshmukh H, Rayner NW, Abdalla M, Ladenvall C, Ziemek D, Fauman E, Robertson NR and McKeigue PM. 2018. A genome-wide association study of diabetic kidney disease in subjects with type 2 diabetes. *Diabetes*. **67**:1414–1427.

Zhong W, Jiang Z and Zhou TB. 2015. RETRACTED: Association between the ACE I/D gene polymorphism and T2DN susceptibility: The risk of T2DM developing into T2DN in the Asian population. *J Renin-Angio-Aldo S*. **16**:NP35–NP35.

Zhou D, Ruiter R, Zhang J, Zhou MA, Liu H, Liu W and Wang S. 2012. Angiotensin-converting enzyme I/D polymorphism is not associated with type 2 diabetes in a Chinese population. *J Renin-Angio-Aldo S*. **13**:372–378.

Stephens JW, Dhamrait SS, Acharya J, Humphries SE and Hurel SJ. 2006. A common variant in the ACE gene is associated with peripheral neuropathy in women with type 2 diabetes mellitus. *J Diabetes Complicat*. **20**:317–321.

Tseng CH, Tseng FH, Chong CK, Tseng CP and Cheng JC. 2011. Angiotensin-converting enzyme genotype and peripheral arterial disease in diabetic patients. *Exp Diabetes Res*. **2012**:1–7.

Van Zuydam NR, Ahlqvist E, Sandholm N, Deshmukh H, Rayner NW, Abdalla M, Ladenvall C, Ziemek D, Fauman E, Robertson NR and McKeigue PM. 2018. A genome-wide association study of diabetic kidney disease in subjects with type 2 diabetes. *Diabetes*. **67**:1414–1427.

Zhong W, Jiang Z and Zhou TB. 2015. RETRACTED: Association between the ACE I/D gene polymorphism and T2DN susceptibility: The risk of T2DM developing into T2DN in the Asian population. *J Renin-Angio-Aldo S* **16**:NP35–NP35.

Zhou D, Ruiter R, Zhang J, Zhou MA, Liu H, Liu W and Wang S. 2012. Angiotensin-converting enzyme I/D polymorphism is not associated with type 2 diabetes in a Chinese population. *J Renin-Angio-Aldo S*. **13**:372–378.

JJBS

Volume 13, Number 2, June 2020
ISSN 1995-6673
Pages 213 - 218

Jordan Journal of Biological Sciences

Effect of Edible Bird's Nest Supplement on Hepato-renal Histomorphology of Rats Exposed to Lead Acetate Toxicity

Abdulla A. Albishtue [1, 4], Hazem Kareem Almhanna[4], Nurhusien Yimer[1*], Md Zuki A. Zakaria[2], Abd Wahid Haron [1] and Bahaa H. Almhanawi[3]

[1]Department of Veterinary Clinical Studies, [2]Department of Veterinary Preclinical Sciences, Faculty of Veterinary Medicine, [3]Department of Pathology, Faculty of Medicine and Health Sciences, University Putra Malaysia, 43400 Serdang, Selangor, Malaysia. [4]Department of Anatomy and Histology, Faculty of Veterinary Medicine, University of Kufa, Najaf, Iraq.

Received May 20, 2019; Revised July 29, 2019; Accepted August 8, 2019

Abstract

Lead acetate (LA) has been shown to cause hepato-renal damages through induction of oxidative stress. Edible bird's nest (EBN) has reportedly been shown to alleviate these damages, but no studies have been conducted on this area. The present study was aimed to evaluate the protective effects of EBN supplement on the liver and kidney of rats exposed to LA toxicity. Five groups of rats were used and grouped as follows: group 1 (positive control, C), was given distilled water; group 2 (positive control, T0), was administered with LA (10 mg/kg BW); and groups 3 (T1), 4 (T2), and 5 (T3), were given LA (10 mg/kg BW) plus graded concentrations of 30, 60, and 120 mg/kg BW of EBN, respectively. At day 35, blood was collected via cardiac puncture, serum was used for biochemical analysis, and rats were euthanized to collect liver and kidney for histo-morphological study. Laboratory analysis revealed significantly elevated liver enzymes, urea and creatinine levels in the T0 and T1 compared to C and T3 ($p<0.05$). The level of aspartate aminotransferase (AST) and alkaline phosphatase (ALP) was significantly lower in the T3 and C compared to T0 and T1 ($p<0.05$). Histo-morphological studies showed that exposed rats to LA without EBN supplement with portal and central vein dilatation and congestion evidenced by hepatocyte necrosis and degeneration as well as increased number of kupffer cells, while degree of damage was decreased in EBN treated groups. The animals in T3 showed ameliorating effects against LA toxicity, as well as decreased number of kupffer cells. In T0 and T1 rats, histopathological lesions of the kidneys were characterized by the degenerations of the tubular system, while T2 and T3 groups showed no such lesions. In conclusion, the findings showed that EBN can protect the hepatic and renal tissues from the damaging effects of LA toxicity and modulate biochemical alterations.

Keywords: EBN, lead acetate, liver, kidney, Kupffer cell

1. Introduction

Adverse effects of industrialization and urbanization increase the risk of daily exposure to a variety of chemical contaminants. Lead (Pb) is considered one of most important hazardous and cumulative environmental pollutants. Environmental levels of lead have increased more than 1000-fold over the past three centuries as a result of human activity and due to increasing worldwide use of leaded gasoline (ASDR, 2007). Lead has a negative impact on animal and human physiological, behavioral and biochemical functions, including liver, kidneys, reproductive system, hematopoietic system, central and peripheral nervous system, cardiovascular system, and endocrine glands (ASDR, 2007). Lead acetate can accumulate in human and animal tissues and can be induced by various factors such as age or hormone production to re-release Pb into the general circulation. Consequently, it also has long half-life (Horiguchi et al., 2013; Rzymski et al., 2014). Several studies have shown that Pb toxicity has a negative effect on vital organs associated with hepatic and renal damage (Farrag, 2007; Assi et al., 2017 a). One of the important mechanisms underlying Pb toxicity is the induction of oxidative stress because of reactive oxygen species and the depletion of the antioxidant defense system (Gupta, 2011). Edible bird's nest (EBN) is a natural product from swiftlet saliva and is traditionally considered a powerful medicine used by the Chinese community for centuries to alleviate several ailments (Koon, 2002). Research on various aspects of EBN has recently gained momentum, including its nutritional and health benefits. The traditional beliefs are largely supported by scientific explanations. Results from emerging researches have shown that EBN has a number of biological properties. These biological properties of EBN may have an impact on hepatic and renal diseases (Yida et al., 2015). Studies carried out in areas other than toxicity on the influence of EBN have reported important biological properties of EBN, which may reflect its ameliorating effect on the influence of heavy metal toxicity. EBN has been shown to be a potent antioxidant, but its role in mitigating the effect of Pb toxicity on liver and kidney is unknown. Therefore, the general objective of the present study was to evaluate the ameliorating effects

* Corresponding author e-mail: nurdeg2006@gmail.com.

of EBN supplement on hepato- renal histomorphology of rats exposed to lead acetate (LA) toxicity.

2. Materials and Methods

2.1. EBN preparation

EBN was purchased from Nest Excel Resources Sdn Bhd, maintained at 25 ℃ to 30 ℃. EBN extract was prepared in accordance with Chinese tradition as indicated by the local suppliers. The samples were cleaned, dried at room temperature, and ground into powder using a mixer (BUCHI-400, Switzerland). The ground EBN extract was maintained at 4 ℃. EBN solution was prepared by dissolving 1 g of EBN powder in 100 mL of distilled water, followed by heating in a water bath at 60 ℃ for 45 min. Lastly, the EBN solution was cooled down to room temperature and administered to the rats at doses based on their body weights (BW).

2.2. Preparation of lead acetate solution

Lead acetate with molecular formula Pb (C2H3O2)2, was purchased commercially from Oxford Lab. Co., India (CAS: 6080-56-4). A 1% (w/v) solution of lead acetate in distilled water was initially prepared and individual rats of the treated groups were given orally at a dose of 10 mg/kg of body weight using a gavage tube (straight 18 gauge, China).

2.3. Animals and experimental design

The study used 30 female Sprague–Dawley rats (12 weeks of age) from the Animal Resource Center, Faculty of Veterinary Medicine, Universiti Putra Malaysia (UPM). The rats were housed in groups for acclimatization period of 7 days with free access to water and standard rat diet (Gold Coin Brand Animal Feed). Approval to the use of rats for the experiment was obtained from the Institute for Animal Care and Use Committee, UPM (UPM/IACUC/AUP-R009/2016) and animals were handled in accordance with the guidelines. After 7 days of acclimatization, the rats were randomly grouped into 5 with 6 animals per group and administered LA at 10 mg/kg BW with oral supplement of EBN according to Albishtue et al. (2018a). Rats were divided into five groups, namely: Control (C), given distilled water orally; Positive control (T0), given LA (10 mg/kg); Treatment 1 (T1), given EBN (30 mg/kg) and LA (10 mg/kg), orally, daily; Treatment 2 (T2), given EBN (60 mg/kg) and LA (10 mg/kg); and Treatment 3 (T3), was given EBN (120 mg/kg) and LA (10 mg/kg). Both LA and EBN were administered orally once daily for a period of 35 days. The rats were euthanized after 35 days by CO_2 asphyxiation method following a general anaesthesia procedure, which included injection of ketamine (30 mg/kg BW) and xylazine (10 mg/kg BW) and blood collected by cardiac puncture according to the method of Albishtue et al. (2018 b).

2.4. Evaluation of biochemical parameters

An automated chemistry analyzer (Siemens, USA) was used to assess biochemical parameters from the sera obtained from the whole blood of the rats according to the methods of Assi *et al*. (2017 a).

2.5. Macroscopic and microscopic examinations of the liver and kidney

After sacrificing the rats, the livers and kidneys were excised and physically examined for any evidence of gross tissue abnormality. The tissue samples were fixed in 10% formalin for 24 h, processed, sectioned, and stained using hematoxylin and eosin (H&E) for histomorphological examinations. Stained tissues were examined under light microscopy and viewed with image analyser microscope. Three microscopic areas of similar region for each tissue sections were studied at various magnifications (40x and 100x magnifications). Sections were randomly selected for analysis using the Medical Image Analyser (Motic Image plus 2.0, China). The samples were observed under the microscope for histomorphological changes. Numbers of hepatocyte vacuolations and pyknotic hepatocytes in an area were counted at a magnification of 40x. Lesion severity was scored from 0 to +3 (0, no lesion; 1, mild lesion (<30%); 2, moderate (<60%); 3, severe (>60%) (Assi *et al*., 2017a). Number of Kupffer cells of the liver in an area was counted at a magnification of 40x.

Similarly, degeneration score of the tubular systems of the kidney in an area was also counted at a magnification of 40x using the same image analyser. Three microscopic areas of similar region for each tissue sections were studied. Lesion severity was scored according to Assi *et al*. (2017a) from 0 to +3 (0; no lesion; 1, mild lesion (<30%); 2, moderate (<60%); 3, severe (>60%)).

2.6. Statistical analysis

All data were expressed as means (M) ± standard error of mean (SE) and analysed with Graph Pad Prism 6.0 (Graph Pad Software, San Diego, California). Data obtained were checked for normal distribution using Shapiro-Wilk test. One-way analysis of variance (ANOVA) with Tukey multiple comparison post-hoc test was used to compare number of Kupffer cells and the concentrations of AST, ALP, Urea and Creatinine in the sera. Comparison between histopathological lesions in the liver and kidney were made using a Kruskal-Wallis (non-parametric) test. A value of $p<0.05$ was considered significant.

3. Results

3.1. Biochemical findings

The results of AST, ALP, Urea and creatinine activities in the serum from all the groups are summarized in Figures 1.A and B. The level of AST activity was elevated in the T0 group ($p<0.05$), while T1 was unchanged when compared to the control. On the other hand, AST activity was reduced in the T2 and T3 groups. Similarly, ALP activity was significantly higher in T0 group compared to group T3. There were no significant changes in T1 and T2 groups. The concentration of urea was significantly higher in T0 and T1 groups compared to the Control ($p<0.05$). However, T3 had low level of urea when compared to other treatment groups and control group ($p<0.05$) (Figure 1.C). On day 35, there was no significant difference between the treatment groups in creatinine concentration (Figure 1.D).

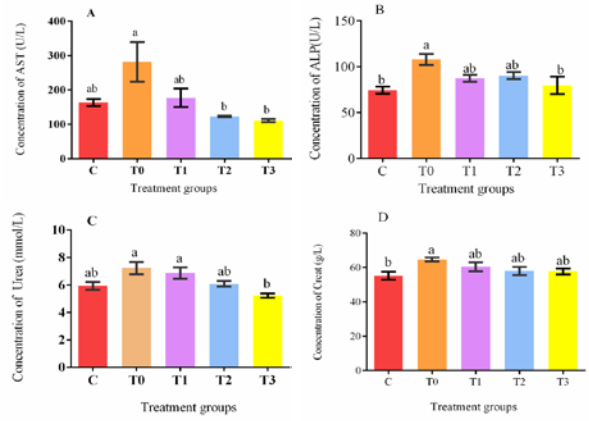

Figure 1. Effect of EBN on the serum biochemistry of LA exposed rats. AST = Aspartate aminotransferase; ALP = alkaline phosphatase; Creat = creatinine. Data are expressed as means ± S.E.M. Different letters a and b denotes significant difference at $p < 0.05$. Note: C = control; T0 = positive control, LA (10mg/Kg BW); T1= EBN (30mg/Kg BW) + LA (10mg/Kg BW); T2 = EBN (60mg/Kg BW) + LA (10mg/Kg BW); T3= EBN (120mg/Kg BW) + LA (10mg/Kg BW).

3.2. . Histomorphological findings in the livers and kidneys of rats exposed to lead acetate and supplemented with EBN

There were no apparent gross pathological lesions found in the liver and kidney of the rats. Nevertheless, histomorphological inspection of liver and kidney of the different groups except C and T3, showed lead-induced histopathological alterations, which involves portal and central veins dilatation and congestion evidenced by hepatocyte necrosis and degeneration, increased infiltration of inflammatory cells, and damaged tubular system of kidney. However, T3 supplemented with the highest EBN dose showed normal hepatic and renal structures as in the control group (Figures 2 and 3).

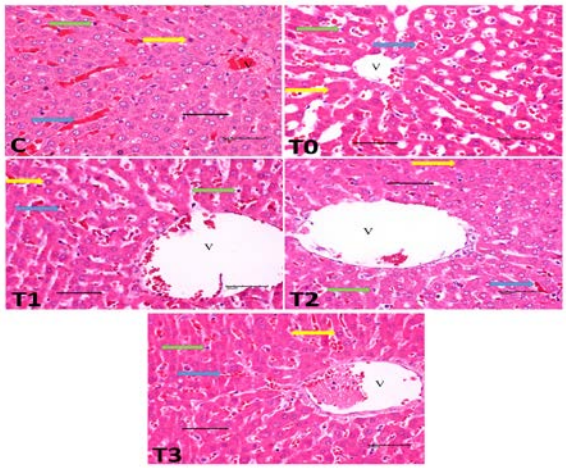

Figure 2. Histomorphological sections of the liver showing the effects of EBN in LA exposed female rats. T0 and T1 showing moderate vacuolation of the hepatocytes (black arrows) and pyknotic hepatocytes cells (yellow arrows) with a congested central vein (V). Notice Kupffer cells (green arrows); vascularization (blue arrows); C=control; T0= positive control, LA .(10mg/Kg BW); T1= EBN (30mg/Kg BW) + LA (10mg/Kg BW); T2= EBN (60mg/Kg BW) + LA (10mg/Kg BW); T3= EBN (120mg/Kg BW) + LA (10mg/Kg BW) (measure of scale bar = 50 µm, H & E 40 x magnification).

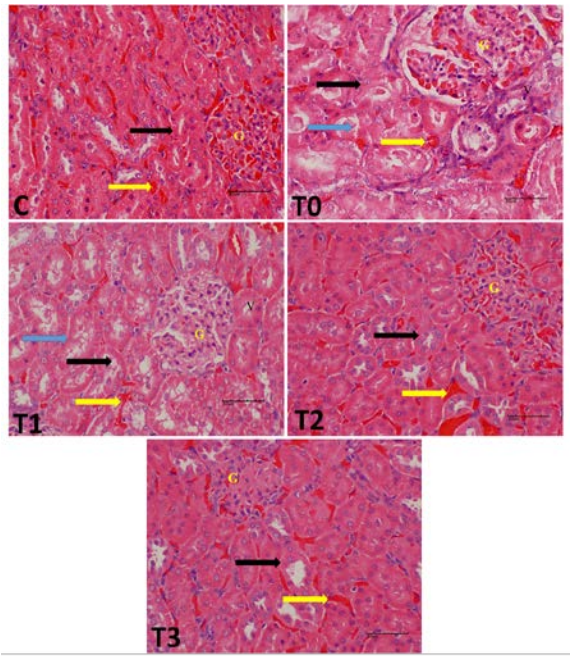

Figure 3. Histomorphological sections of the kidney showing the effects of EBN in LA exposed female rats. Notice degenerative changes of tubular systems (blue arrows) at T0 and T1. Renal structure of tubular systems (black arrows) and glomeruli (G) of nephrons and vascularization (yellow arrows). Note: C = control; T0 = positive control, LA (10mg/Kg BW); T1= EBN (30mg/Kg BW) + LA (10mg/Kg BW); T2= EBN (60mg/Kg BW) + LA (10mg/Kg BW); T3= EBN (120mg/Kg BW) + LA (10mg/Kg BW) (measure of scale bar = 50 µm, H & E 40 x magnification).

The results of histopathological lesion scores of the liver are presented in Figure 4. The results showed a statistically significant difference in the hepatocyte lesions with vacuolations and pyknotic hepatocytes among the experimental groups ($p<0.05$). The hepatocyte vacuolations and pyknotic hepatocytes were higher in T0 and lowest in T3 group (Figure 4). Kupffer cell proliferation had the lowest value at 120 mg/kg body weight of EBN (T3) compared to T0. The number of Kupffer cells found to decrease in a dose dependent manner with EBN. T2 had comparable with T1 and T3 (Figure 5).

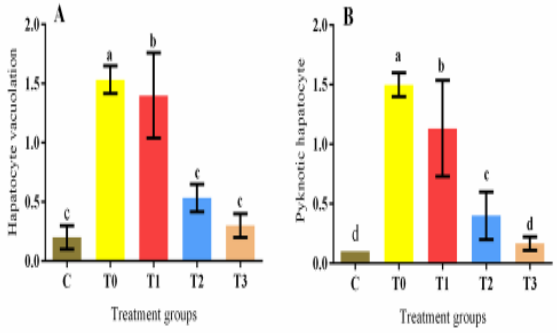

Figure 4. Effects of EBN on histopathological lesion scores in LA exposed livers of rats. C = control; T0 = positive control LA (10mg/Kg BW); T1= EBN (30mg/Kg BW) + LA (10mg/Kg BW); T2= EBN (60mg/Kg BW) + LA (10mg/Kg BW); T3= EBN (120mg/Kg BW) + LA (10mg/Kg BW) (positive control magnification).

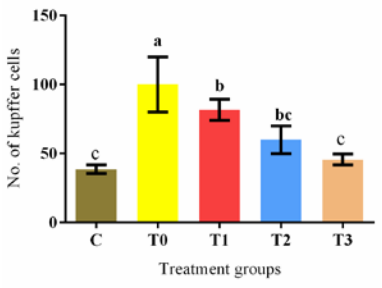

Figure 5. Effects of EBN on histomorphometric parameters in LA exposed liver of rats. Notice the greater quantity of Kupffer cells in T0 and T1, than the other groups. Data are expressed as means ± standard error (SE). Error bars with different alphabets (a, b, and c) denotes significant difference at $p < 0.05$.

Representative photomicrographs showing tubular degenerations and the histological sections of the kidneys of all experimental groups as well as their differences in scores are shown in Figure 6. Tubular degeneration score in the kidney was significantly higher in T0 group than in the T1 group ($p<0.05$).

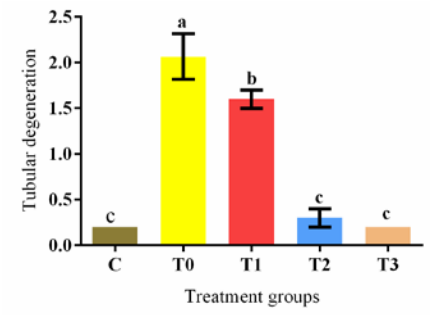

Figure 6. Effects of EBN on histopathological lesion scores in LA exposed kidneys of rats. C = control; T0 = positive control, LA (10mg/Kg BW); T1= EBN (30mg/Kg BW) + LA (10mg/Kg BW); T2= EBN (60mg/Kg BW) + LA (10mg/Kg BW); T3= EBN (120mg/Kg BW) + LA (10mg/Kg BW).

4. Discussion

The liver is a vital organ for storage, biotransformation and detoxification of toxic substances, particularly absorbed heavy metal materials (Ohkawa et al., 1979). In the present study, although laboratory findings have shown different alterations in the physiological functions of the animals, LA showed no gross pathological lesions in the liver and kidney. Examination of the tissue sections of the liver exposed to LA revealed that the portal and central veins underwent dilatation and congestion as evidenced by hepatocyte necrosis and degeneration. Kupffer cells represent 15% of the total liver cells and cover inside endothelial walls where they protrude and are found predominantly in the periportal region, which may represent the best location for the cell to exhibit their endocytic role for blood-born materials entering the liver (Arii and Imamura, 2000). The phagocytic capacity of Kupffer cells is characterized by very high, and numerous phagocytic structures and a large number of different types of very well developed lysosomes (Arii and Imamura, 2000). The liver can be damaged by different injuries such as chemical substances, toxins and pharmacological agents (Winwood and Arthur, 1993; Su, 2002). The immediate resulting effects of liver injuries are increased hepatocellular necrosis, which is one of the principal sources of Kupffer cells activation (Kolios et al., 2006). This is in agreement with the present study, which confirmed LA effect on the number of Kupffer cells. Another pertinent finding observed in the present study was the elevated levels of ALS and ALP in T0 group. The ALT and AST are two important enzymes that signify liver function in animals. An increased level of these enzymes indicates possible hepatocellular damage or injury (Assi et al., 2017a).

Prior studies have revealed that lead toxicity resulted in elevated serum ALT, AST, liver homogenate tumor necrosis factor-a (TNF-a), caspase-3, malondialdehyde (MDA), nitric oxide (NO) levels and a significant decline of total serum proteins, liver homogenate reduced glutathione (GSH) levels and superoxide dismutase (SOD) activity (El-Tantawy, 2016). On the other hand, the administration of LA could have generated a high level of oxidative stress which can cause defects in mitochondrial membrane permeability, resulting in outflow of free radicals and cytochrome-c from the mitochondria to bind with another protein called apoptotic protease activating factor-1 (Apaf-1), which stimulates the activation of caspase 3, leading to cell death (Liu *et al.*, 2005: Liu *et al*., 2012). Omobowale *et al.* (2014) undertook investigation of Pb-induced oxidative stress in the rat liver. Animals were administered with different doses for six weeks and then were not treated for another six weeks. The result revealed disturbances in homaginized liver ALT, AST, ALP, MDA and H_2O_2 concentrations, and a decrease in antioxidant enzymes SOD, catalase (CAT), glutathione peroxidase (GPx), glutathione S-transferase (GST) activities and lower concentration of GSH. According to the observations of Omobowale *et al.* (2014), in the liver, Pb caused the stimulation of MDA levels and lipid peroxidation that is considered as source of the modification of membrane integrity and fatty acid composition (Liu *et al*., 2012). In a similar finding, Pb-induced oxidative stress increase in liver (measured by MDA levels) in dose and time-dependent manner, and a consequence of the oxidative stress and apoptosis leading to influence mitogen-activated protein kinases in hepatocytes were reported (Mujaibel and Kilarkaje, 2015). Interestingly, histological examination of the livers of EBN treated groups in the present study showed significant protection. EBN supplemented groups especially T3 showed normal hepatic structure as in the control despite exposure to LA toxicity. Furthermore, it was observed that powdered EBN acted as a regulator for the levels of AST and ALP in treated rats. In previous studies, there was evidence of decreased GSH and SOD enzyme levels in rats exposed to LA (Assi *et al*., 2017 b); however, it is a limitation of the present study that these parameters were not assessed.

The EBN has been used as a hormonal replacement prophylactic agent in various conditions such as in the form of anti-aging, anti-cancer, and immunity enhancement. The protective role of the EBN supplement observed might be attributed to its biological properties such as cellular proliferation. The composition of EBN reported to consists of reproductive hormones including testosterone, estradiol (E2), progesterone (P4), LH, FSH and prolactin (Ma and Liu, 2012; Albishtue *et al.*, 2019a). EBN contains sialic acid which has some molecular mechanisms of causing cell proliferation being regulated

by the hormone E2. EBN is also known to contain VEGF and IL-6 which prevent apoptosis of embryonic neurons by interfering with the activation of caspase three leading to suppression of apoptosis in cells (Jin *et al*., 2001). A previous study had suggested that there is a synergistic relationship between VEGF, FSH and estradiol in preventing apoptosis, inhibiting caspase 3 activation and stimulating proliferation (Vitale *et al*., 2002; Bussmann *et al*., 2006; Irusta *et al*.,2010). EBN has Epidermal Growth Factor (EGF) – like activity (Kong *et al*., 1987), resulting in its stimulatory effect on cell growth and regeneration (Ng *et al*., 1986; Kong *et al*., 1989; Zhiping *et al*., 2015). Oxidative stress created by LA exposure is a major disorder contributor, which causes the development of toxicity that indicates significant pathological lesions on the vital organs (Oyagbemi *et al*., 2015). EBN has been shown to regulate antioxidant and inflammatory genes (Yida *et al*., 2015) and have many therapeutic benefits.

Presence of LA in the hepatocytes has been reported to induce necrosis, degeneration, and fatty change in a dose-dependent manner (Mudipalli, 2007). Although the present study has a limitation to provide evidence as to what happen to the oxidative stress and anti-oxidant biomarkers, we have demonstrated a similar positive effect of EBN on oxidative stress in our previous study (Albishtue et al., 2019b). Hence, based on the information on histo-morphological findings, it can be deduced that EBN prevents damage to the hepatocytes possibly through modulation of oxidative stress, and this may imply a strong ameliorative effect of EBN against LA toxicity on the hepatic tissues through an integrated mechanism.

The present study has shown that LA exposure for extended time stimulates gradual loss of membrane integrity and changes in tubular cells. Moreover, the toxicity results in the present study showed that urea and creatinine levels in LA alone administered groups were significantly higher than those in other groups supplemented with EBN. Laboratory findings revealed that concentration levels of urea and creatinine were higher in rats exposed to LA compared to the control. According to most authors, renal toxicity of LA can be characterised with evidence of degenerations of the tubular epithelium associated with nuclear bodies, which contain lead-protein complexes, and impaired tubular transport (Assi *et al*., 2017a). Most of the authors agreed that LA induces production of lipid peroxidation. Sharma and Singh (2014) have administered 10 and 150 mg/kg BW LA for 24 h and stimulated increased in renal TBARS levels and reduce SOD and CAT activities in the kidney of Balb-c mice. Interestingly, histological examination of the kidney of EBN treated groups in our study showed significant protection. Moreover, despite exposure to LA toxicity, EBN supplemented groups (especially T3) showed normal renal structure similar to the control. Furthermore, it was also observed that powdered EBN acted as a regulator for the levels of urea and creatinine in treated rats. Assessment of additional parameters such as fatty degeneration and intranuclear inclusion rates in kidneys in future might further strengthen the understanding of the mechanism of EBN by which it protects the kidney tissues. Similar to EBN, there has been an increase of interest in the consumption of other natural products that serve as antioxidants like seeds of nigella sativa, fruits and vegetables as a strategy to prevent oxidative damage in various health disorders with oxidative stress (Assi *et al*., 2017; Khaki *et al*., 2013). In previous reports, EBN was also praised for its effect of increasing SOD enzyme levels in rats exposed to LA (Albishtue *et al*., 2019b).

5. Conclusion

The present study suggested that pre-treatment of EBN significantly and preventively attenuated LA-induced detrimental effects on the liver and kidney as evidenced by decreased concentrations of toxicity indicators in the sera and maintenance of histomorphological integrity.

Acknowledgement

The authors would like to thank UPM for providing fund for this project (Grant Putra IPS/9641900).

Competing Interests

None

References

Albishtue A A, Yimer N, Zakaria M Z A, Haron A W, Babji A S, Abubakar A A, and Almhanawi B H. 2019a. Effects of EBN on embryo implantation, plasma concentrations of reproductive hormones, and uterine expressions of genes of PCNA, steroids, growth factors and their receptors in rats. *Theriogenology*., **126**: 310-319.

Albishtue A, Yimer N, Zakaria M, Haron A, Babji A, Abubakar A, Almhanna H, Baiee F and Almhanawi, B. 2019 b. Edible bird's nest's role and mechanism in averting lead acetate toxicity effect on rat's uterus. *Vet World*., **12(7):** 1013-1021.

Albishtue A, Yimer N, Zakaria M, Haron A, Yusoff R, Assi M, and Almhanawi B. 2018b. Edible bird's nest impact on rats' uterine histomorphology, expressions of genes of growth factors and proliferating cell nuclear antigen, and oxidative stress level. *Vet World*., **11 (1):** 71-79.

Albishtue AA, Yimer N, Zakaria M ZA, Haron AW, Yusoff R and Almhanawi BH. 2018a. Ameliorating effect of edible bird's nest against lead acetate toxicity on the rat hypothalamic–pituitary–ovarian axis and expressions of epidermal growth factor and vascular endothelial growth factor in ovaries. *Comp Clin Path*., **27**: 1257–1267.

Arii S and Imamura M. 2000. Physiological role of sinusoidal endothelial cells and Kupffer cells and their implication in the pathogenesis of liver injury. *J trauma acute care*., **7(1):** 40-48.

Assi M, Hezmee M, Abba Y, Sabri M, Haron A, Baiee F and Rajion M. 2017a. Effect of Nigella sativa Pre-Treatment on Sub-Chronic Lead Acetate Induced Hematological and Biochemical Alterations. *J Comput Theor Nanosci*., **14(6):** 2752-2758.

Assi, M., Hezmee, M., Abba, Y., Rajion, M., Wahid, H and Yusof, M. 2017b. Assessment of therapeutic effects of Nigella sativa against chronic lead acetate-induced reproductive dysfunction in male Sprague-Dawley rats. *Comp Clin Path*., **26 (1):** 87-97.

ATSDR U. 2005. Toxicological profile for lead.(Draft for public comment). US Department of health and human services. Public Health Service. Agency for Toxic Substances and Disease Registry, Atlanta, USA.

Bussmann UA, Bussmann LE and Barañao JL. 2006. An aryl hydrocarbon receptor agonist amplifies the mitogenic actions of

estradiol in granulosa cells: evidence of involvement of the cognate receptors. *Biol Reprod*., **74(2):** 417-426.

El-Tantawy WH. 2016. Antioxidant effects of Spirulina supplement against lead acetate-induced hepatic injury in rats. *JTCM*., **6(4):** 327-331.

Farrag A.-R. H. 2007. Protective Effect of Nigella sativa Seeds Against Lead-induced Hepatorenal Damage in Male Rats'. *Pak J Biol Sci.*, **10(17):** 2809-2816.

Flora SJS, Pachauri V, Saxena G (2011) Arsenic, cadmium and lead. In: Gupta RC (ed) Reproductive and developmental toxicology. Academic Press, Elsevier Inc, London, 415–438.

Horiguchi H, Oguma E, Sasaki S, Okubo H, Murakami K, Miyamoto K, Hosoi Y , Murata K and Kayama F. 2013. Age-relevant renal effects of cadmium exposure through consumption of home-harvested rice in female Japanese farmers. *Environ. Int*., **56**: 1-9.

Irusta G, Abramovich D, Parborell F and Tesone M. 2010. Direct survival role of vascular endothelial growth factor (VEGF) on rat ovarian follicular cells. *Mol cell endocrinol*., **325(1):** 93-100.

Jin K, Mao X, Batteur S, McEachron E, Leahy A and Greenberg D. 2001. Caspase-3 and the regulation of hypoxic neuronal death by vascular endothelial growth factor. *Neuroscience*., **108(2):** 351-358.

Khaki A., Bayatmakoo R., Nouri M. and Khaki A A.2013. Remedial effect of Cinnamon zeylanicum on serum anti-oxidants levels in male diabetic Rat. *Life Sci. J*., **10(45):**103-107.

Kolios G, Valatas V and Kouroumalis E. 2006. Role of Kupffer cells in the pathogenesis of liver disease. *World J Gastroenterol*., **12(46):** 7413-7420.

Kong Y, Keung W, Yip T, Ko K, Tsao S and Ng M. 1987. Evidence that epidermal growth factor is present in swiftlet's (Collocalia) nest. *Comp Biochem Physiol B Biochem Biol*., **87(2):** 221-226.

Kong Y, Tsao S, Song M, Ng M and Lin Z. 1989. Potentiation of mitogenic response by extracts of the swiftlet's (Apus) nest collected from Huai-ji. *Acta Zool*., **35(4):** 429-435.

Koon, L. Cranbrook Earl of. 2002: Swiftlets of Borneo-Builders of edible nests. Sabah (Malaysia): *Natural History Publication (Borneo) SDN., BHD* : 1-171.

Liu C.-M., Ma J.-Q., and Sun Y.-Z. 2012. Puerarin protects the rat liver against oxidative stress-mediated DNA damage and apoptosis induced by lead. *Exp Toxicol Pathol*., **64(6):** 575-582.

Liu M-Y, Cheng Y-J, Chen C-K, Yang B-C. 2005. Coexposure of lead-and lipopolysaccharide-induced liver injury in rats: involvement of nitric oxide-initiated oxidative stress and TNF-α. *Shock*., **23(4):** 360-364.

Ma F and Liu D. 2012. Extraction and determination of hormones in the edible bird's nest. *ASIAN J CHEM*., **24(1):** 117.

Mujaibel LM, Kilarkaje N. 2015. Mitogen-activated protein kinase signaling and its association with oxidative stress and apoptosis in lead-exposed hepatocytes. *Environ Toxicol Chem*., **30(5):** 513-529.

Ng M, Chan K and Kong Y. 1986. Potentiation of mitogenic response by extracts of the swiftlet's (Collocalia) nest. *Biochem. Int*., **13(3):** 521-531.

Ohkawa H, Ohishi N and Yagi K. 1979. Assay for lipid peroxides in animal tissues by thiobarbituric acid reaction. *Analytical biochemistry*., **95(2):** 351-358.

Omobowale TO, Oyagbemi AA, Akinrinde AS, Saba AB, Daramola OT, Ogunpolu BS and Olopade J O. 2014. Failure of recovery from lead induced hepatoxicity and disruption of erythrocyte antioxidant defence system in Wistar rats. *Environ Toxicol Pharmacol*., **37(3):** 1202-1211.

Oyagbemi AA, Omobowale TO, Akinrinde AS, Saba AB, Ogunpolu BS and Daramola O. 2015. Lack of reversal of oxidative damage in renal tissues of lead acetate treated rats. *Environ Toxicol*., **30(11):** 1235-1243.

Rzymski P, Rzymski P, Tomczyk K, Niedzielski P, Jakubowski K, Poniedziałek B and Opala T. 2014. Metal status in human endometrium: relation to cigarette smoking and histological lesions. *Environ*., **132:** 328-333.

Sharma S and Singh B. 2014. Effects of acute and chronic lead exposure on kidney lipid peroxidation and antioxidant enzyme activities in BALB-C mice (Mus musculus). *Int. J. Sci. Res*., **3:** 1564-1566.

Su GL. 2002. Lipopolysaccharides in liver injury: molecular mechanisms of Kupffer cell activation. *Am J Physiol Gastrointest Liver Physiol*., **283(2):** G256-G265.

Vitale AM, Gonzalez OM, Parborell F, Irusta G, Campo S and Tesone M. 2002. Inhibin a increases apoptosis in early ovarian antral follicles of diethylstilbestrol-treated rats. *Biol Reprod*., **67(6):** 1989-1995.

Winwood P J, and Arthur M J. 1993. Kupffer cells: their activation and role in animal models of liver injury and human liver disease. Paper presented at the Seminars in liver disease.1993 by Thieme Medical Publishers, Inc, **13**, 50-59.

Yida Z., Imam M U, Ismail M., Hou Z, Abdullah M A, Ideris A, and Ismail N. 2015. Edible Bird's Nest attenuates high fat diet-induced oxidative stress and inflammation via regulation of hepatic antioxidant and inflammatory genes. *BMC Complement Altern Med* ., **15 (1):** 310.

Zhiping H, Imam MU, Ismail M, Ismail N, Yida Z, Ideris A, Sarega N and Mahmud R. 2015. Effects of edible bird's nest on hippocampal and cortical neurodegeneration in ovariectomized rats. *Food and Function*., **6(5):** 1701-1711.

JJBS

Volume 13, Number 2, June 2020
ISSN 1995-6673
Pages 219 - 222

Jordan Journal of Biological Sciences

Sexual Restiveness and Colouration between Partial Diallel Cross of Genetically Improved Farmed Tilapia 'GIFT' and UPM red Tilapia.

Oster F. Nwachi[1,2], Yuzine Esa[1*],Annie Christianus[1]and Salleh M. Kamarudin[1]

[1] *Department of Aquaculture, Faculty of Agriculture, Universiti Putra Malaysia;*[2] *Department of Fisheries, Delta State University Abraka, Asaba Campus, Nigeria*

Received July 9, 2019; Revised August 9, 2019; Accepted August 15, 2019

Abstract

The effect of colouration, number of days for reproductive success and female preference for mating between 2 Cichlids: 'Genetically Modified Farm Tilapia' (GIFT) and UPM red tilapia were examined. A total of 24 female and 12 male homozygous stock of each of UPM red tilapia and GIFT were selected, They were paired in one ton tank and labelled as: (T1) at a ratio of 4:2 GIFT female X GIFT male (G x G), T2 UPM red tilapia female X GIFT male (U x G), T3 UPM red tilapia female X UPM red tilapia male (U x U) and T4 GIFT female X UPM red tilapia male (G x U) in triplicates. The experimental units were in triplicates and the trial was conducted at four separate times using the same broodstock. The number of days for reproductive successful varied from 14.2 days for T1 to 14.72 days for T3 with T4 having a longer period at 21.93 days. The mean highest value of swim-up recorded were 154.65 for T2, an indication that female fish shows affinity to the male fish of same colour with a level of preference to male of novel colouration compared to wild type of male.

Keywords: GIFT, Cichlids, restiveness, preference, novel-colouration

1. Introduction

Production of Tilapia seed can be done through many methods, ranging from the more simple ones like pairing of parent stock in pond or hapa and harvesting their eggs after spawning, to high technological based fish ranching (Ramadan *et al.*, 2007;Vilhena *et al.*, 2014; Lu & Takeuchi, 2004). In fish production, understanding assortative mating among strains having colour variations is a way of increasing mating success(Rajaee *et al.*,2010). Generally, expressed phenotype in fish is used as an important trait for species recognition and behaviour in fish culture (Couldridge & Alexander, 2002). Male colouration is reportedly used as a criterion for selecting males for reproduction in some breeds of Cichlids (Selz *et al.*,2014); Couldridge & Alexander. (2002) with the opinion that colour pattern can also be used in understanding speciation based on the rate at which new families of Cichlids emerged.

In the past decade, little or no importance was considered to the variation in colour of Cichlids; however, observation increases the need to study and put the variation into use especially during selection of folk's fish from another region because of the consequences of this variation on breeding. Generally, the colours of Cichlids have a tendency to vary from the colours of Cichlids in other different regions, but the colours maintained by the male Cichlids during breeding in a particular region remain consistent. The implication of this is that interbreeding between Cichlids from two or more different regions will become particularly difficult as the females in a region might not readily mate with males from a different region because of the colour pattern expressed by the male fish. Hence, colour variation has the tendency to influence the pattern of actual sexual selection among closely related Cichlids. A study by Kirkpatrick & Nuismer (2004) expressed this concern, stressing that the development of entirely new species naturally, from the existing parent in the same environment, is difficult particularly for an invading male of different/novel phenotypes to be accepted by females in preference to its type.

Cichlid males' fish display high levels of variable mating behaviours, influenced by high competition among the males for access to mate with the females. The male fish employs varying persuasive, or trait based approaches such as: nest building, beautiful colour display, and even aggression in making sure that they gain the attention of female of interest (Fessehaye*et al.*,2006). Recent studies on fish production aimed at satisfying the fish needs was recommended to increase focus on the production of tilapia, such as *Oreochromis niloticus*, as a 'folks' fish due to its inherent hardy nature and other favourable traits *(Haque et al.*,2016,Lago *et al.*, 2016;Neira*et al.*, 2015).

In general *Oreochromis niloticus* is a typical 'lek' spawning fish. The males build nests to attract females and strongly put up defences against any invader, thus creating

* Corresponding author e-mail: yuzine@upm.edu.my; fish2rod@yahoo.com.

un-even ratio of females to male. Most *O. niloticus* females, like other Cichlid female fish, will select conspecific males of novel colour (Selz *etal.*, 2014); Hence, mating of the females of *O. niloticus* with conspecific males from a different region, even if the male is of novel colouration becomes particularly impossible (Rajaee *et al.*, 2010). Experimental studies byKorzan *et al.*(2008) and Fessehaye *et al.* (2006) to determine time taking for female to accept a male were conducted in monitored water bearing receptacle that made it possible for fertilized eggs to be removed from the mouth of the brooding fish.

This in our opinion could disrupt courtship and breeding process and give results that will not necessarily reflect the actual time at which the female accept the male fish. Therefore,this study aimed to examine the effect of colouration on the number of days of acceptance for a cross between the 'Genetically Modified Farmed Tilapia' also known as GIFT (Hybrid of *O. niloticus*) and an endemic strain of tilapia from Universiti Putra Malaysia (UPM red tilapia), which is a cross between (*Oreochromis niloticus* and *Oreochromis mossambicus*), the female preference for conspecific and novel coloured males, and the reproductive success among the strain.

2. Methodology

2.1. Selection of Brood Stock and Experimental Site

The GIFT strain is greyish/wild-colour while the UPM red tilapia (reddish colour) brood stocks were selected for this study (Figs 1a and 1b). The GIFT broodstock were obtained from the World Fish Center Penang Malaysia and maintained in a designated tank for broodstock at the Universiti Putra Malaysia (UPM) Aquaculture Center. Meanwhile, brood stocks of the UPM red tilapia was produced at the UPM Aquaculture center.

Figure1a: Genetically modified farm tilapia 'GIFT

Figure1b: UPM red tilapia

2.2. Experimental Set Up

A total of 24 females and 12 males' homozygous stocks of each of UPM red tilapia and GIFT were selected for the study. The pairing was carried out in a one ton water holding receptacle. The mouths of the males were clipped to avoid injury while mating and in-tank fighting among the males. The fish were paired in the ratio of 4:2 for the female to male per experimental unit. Tank T1 had 4 GIFT female paired with 2 GIFT male (G x G), T2had 4 GIFT females to 2 UPM red males (G x U) T3 had 4 UPM red tilapia females to 2 UPM red tilapia males (U x U) and T4 had 4 UPM red female to 2 GIFT male (U x G). All the experimental units were in triplicates, the trial was conducted at 4 separate times using the same broodstock.

In all, pairing was initiated to produce hybrid F1 from the stock (GIFT X UPM red tilapia). The males were removed from the spawning tank, allowed to rest for 15 days before re-introducing into the breeding tank, at each time a set of swim-up fry were harvested. The culture water was green by introducing 10 liters of greenish coloured stock water into the culture tank, two 1m length polyvinyl chloride (PVC pipe) was placed in each tank to provide shelter to the fish during mating.

2.3. Spawning and Larvae Collection

The spawning process was certified by looking out for swim-up fries because of the greenish coloured water of the culture tank at 3 to 4 days after hatching out from the eggs. The brood stock was fed with a commercial feed of (40% crude protein) twice daily at 09.00hrs and 05.00hrs. The 'swim up' fries were removed from the tank followed by removal and isolation of the male parent in a well aerated receptacle.

2.4. Water Quality Analysis

The one-ton tank used for the experiment was filled with aerated water and constantly supplied with extra air from a central blower. YSI (Yellow springs Ohio, USA) portable model 556 mps was used to measure the temperature, dissolve oxygen (DO), total dissolve solids and hydrogen ion concentration (pH). The concentration of ammonia was also measured using HACH test kit (HACH Company, USA).

2.5. Statistical Analysis

Data obtained was subjected to two-way analysis of variance (ANOVA) for the number of successful hatching days and the relationship between the strains of the test fish and subjected to SIGMA PLOT software (version 12.0 systat software Inc. California, USA). The means of hatching success and number of swim-up were compared using Turkey test at $p \leq 0.05$ at 95% confidence. Triplicate measures were conducted and mean ± standard error values were reported.

3. Results

3.1. Water Quality Parameters

The recorded mean temperature of the tank containing T1 during the experiment was 26.67^0C, 25.87^0C for T2 as shown in Table 1. The mean dissolved oxygen was 7.86 MgL^{1-} for T1 and 7.32 MgL^{1-} for T2 throughout the duration of this study. The mean observed hydrogen ion concentration (pH) was 6.89, 6.75, 6.76 and 6.88 MgL^{1-} for

T1, T2, T3 and T4 respectively. The highest value of total dissolve solid and ammonia was 0.243 $MgL^{1-}$for T2 and 0.3001 MgL^{1-} for T1. That coincides with Xu & Boyd (2016); Boyd & Lichtkpper (2002) who reported that these parameters contribute significantly to the culture environment of the tested fish. However, authors like Haque *et al.,* (2016) Ekasari & Maryam (2012) recommend a slightly higher value compared to what was obtained in the study.

Table 1. Water quality parameter at culture of UPM Red Tilapia and GIFT

S/N	Parameters	G x G	G x U	U x U	U x G	Standard Error
1	Temperature (^{0}C)	26.67	25.87	26.78	26.25	0.032
2	Ammonia (mgL^{1-})	0.3001	0.3000	0.2999	0.2988	0.079
3	Dissolve Oxygen (mgL^{1-})	7.86	7.32	7.87	7.77	0.004
4	pH	6.89	6.75	6.76	6.88	0.093
5	Total dissolve solids (mgL^{1-})	0.237	0.243	0.236	0.229	0.014

T1 = GIFT female X GIFT male (G x G); T2= GIFT female X UPM red tilapia male (G x U); T3 = UPM red tilapia female X UPM red tilapia male (U x U) T4= UPM red tilapia female X GIFT male (U x G). Data represents the means and 3 replicates (± standard error). Means without superscript on the same raw indicates no statistical difference by the Turkey test $p \leq 0.05$ for the water quality parameter.

3.2. Spawning Variation

A total of four trials with their means (mT1-mT4) were represented in Table 2, and statistical significance was recorded within all the batches. The highest total mean value of swim-up produced was from the cross between the GIFT and UPM red tilapia (G x U) at 154.49. A mean total of 137. 77 swim-up fries was harvested for the 4 batches of mating from the cross between UPM red tilapia and GIFT (U x G). The cross between the pure breed of the test fish yielded mean value of 149.37 and 148.16 for GIFT and UPM red tilapia at a significant difference of ($p \leq 0.05$).

Table 2. The mean number of swim-up in a successful batch mating of test fish.

Batch	G x G	G x U	U x U	U x G
mT1	138.50 ± 1.201^a	142.8 ± 0.577^b	142.41 ± 0.666^b	131.25 ± 1.154^c
mT2	151.5 ± 0.333^a	154.25 ± 0.333^a	147.75 ± 0.577^b	133.75 ± 0.333^c
mT3	154.16 ± 0.577^a	156.83 ± 0.333^a	148.91 ± 0.333^b	141.25 ± 0.333^c
mT4	153.33 ± 0.333^a	164.75 ± 0.333^b	153.48 ± 0.577^a	144.83 ± 0.577^c
Mean Total	149.37	154.65	148.16	137.77

T1 = GIFT female X GIFT male (G x G); T2 = GIFT female X UPM red tilapia male (G x U), T3 = UPM red tilapia female X UPM red tilapia male (U x U) T4= UPM red tilapia female X GIFT male (U x G). Data represents the mean and 3 replicates (± standard error). Different letters within the same raw indicate statistical difference by the Turkey test $p < 0.05$) for the number of swim-up that is harvested.

The highest number of days required for a successful mating was recorded in U x G mating (21.93 days) as seen in table 3 the time spent before successfully production of swim-up in the tank that has their mating pair varies from 14.53, 14.72 and 14.2 days for G x G, G x U and U x U respectively. The pair G x G recorded mean number of 26.58 days at mT1 compared to the mean value of 8.16 days at mT4 this observation could be seen across all the test fish. Similarly, in U x G a mean value of 15.91 days from initial value of 32.25 days at mT4 was obtained.

Table 3. The mean number of days for a successful swim-up harvest fish.

Batch (Days)	G x G	G x U	U x U	U x G
mT1	26.58 ± 0.378^a	26.58 ± 0.312^a	26.25 ± 0.371^a	32.25 ± 0.350^b
mT2	12.58 ± 0.192^a	13.41 ± 0.228^b	12.00 ± 0.213^a	22.50 ± 0.261^c
mT3	10.83 ± 0.270^a	11.00 ± 0.275^a	10.75 ± 0.278^a	17.08 ± 0.259^b
mT4	8.16 ± 0.259^a	7.91 ± 0.259^b	7.83 ± 0.207^b	15.91 ± 0.287^c
Mean Total	14.53	14.72	14.2	21.93

T1 = GIFT female X GIFT male (G x G); T2 = GIFT female X UPM red tilapia male (G x U); T3 = UPM red tilapia female X UPM red tilapia male (U x U) T4= UPM red tilapia female X GIFT male (U x G) Data represents the mean and 3 replicates (± standard error). Different letters within the same raw indicate statistical difference by the Turkey test $p \leq 0.05$) for observed successful days

4. Discussion

4.1. Means of Successful Days

A partial diallel crossing in Table 2 examines the hypothesis of no differences on the reproductive success with the number of days for the pairings of the test fish at ($p \leq 0.05$); however, deductions infer that there was a significant difference between the days that the fish record successful reproduction that is associated with the day fries swim up. The reddish coloured UPM red tilapia female and the wild coloured GIFT female readily accept the male in a shorter number of days compared to the pair of the reddish coloured fish to the wild type (GIFT). However, the pair of the GIFT female to the UPM red tilapia (G x U) produced the highest number of swim-up throughout the study.

Breeding success in a 'lekspawner' is related to individual fish success in fertilizing a batch of egg. Logically, *Oreochromis niloticus* strain is known to prepare breeding space and attract female of choice. Preparing and protecting this space, however, depends on the individual's ability to undergo assortative mating, which is an important features in a fish that readily speciates. In this study, two males of similar morphology were paired with females although the mouth of the males were clipped as a deterrent to aggression during mating because males with the same pattern or colour tend to attack each other but hardly attack males of novel phenotypic traits, in line with Seehausen & Schluter (2004) who reported 'a negatively frequency-dependent fitness advantage' which is an indices that affects the distribution of males of same species in a particular territory. Similarly sound of particular frequency can be a source of attraction to fish (Verzijden *et al.*,2010).

The female's individual mating success in this work skewed towards crossing of female fish with novel colour and or conspecific male. This assertion is observed in the

number of days swim-up was detected in the G x U pair compared to U x G pairing. The G x U pairing reveals great affinity for reddish coloured (UPM red tilapia) female compared to those of wild coloured GIFT strain. In Table 3, the average successful days for the pair between conspecific UPM red tilapia female with UPM red tilapia male (U x U), GIFT female pairing with GIFT male (G x G) were not significant. However, when compared to the heterospecific pair between UPM red tilapia (novel coloured female) with wild coloured GIFT male (U x G) a level of significance is observed.

This assertion is in line with the Karen et al. (2005); Plenderleith et al. (2005); and Couldridge & Alexander (2002)findings on crossing of fishes with different express phenotypic traits. Likewise, Selz *et al.* (2014) and Reichard & Polačik (2010)reported findings on the female fish preference for conspecific males of the same colour and or novel colouration to wild type. Studies by Dijkstra *et al.*(2008) and Plenderleith et al. (2005) infer that in addition to colour, olfactory organ and ability of males to claim and protect territory also increase the chances of being selected by female. In general, the main underling factor is the exhibition of the preferred colour of interest that will attract females because of the urge to choose male of novel coloration

5. Conclusion

This study examined the spawning success from pairing of GIFT and UPM red tilapia. The results show that when fishes of different colouration are paired, the time period for spawning success to be achieved depends on the female affinity to the male, the female fish has the tendency to copulate with male of same colour and male of novel colouration (Reddish) compared to wild type of male.

Acknowledgement

The authors would like to extend their sincere appreciation to Educational Trust Fund (TETFUND) Nigeria. Delta State University Abraka and Universiti Putra Malaysia Aquaculture center.

Declaration

There is no conflict of interest to be declared.

References

Boyd CE and Lichtkpper F. 2002. Water quality management in pond culture. In *Research and Development series* (22nd ed.).

Couldridge VCK and Alexander GJ. 2002. Color patterns and species recognition in four closely related species of Lake Malawi cichlid. *Behav.Ecol.*, **13**: 59-64.

Dijkstra PD, Van Der Zee EM and Groothuis TGG. 2008. Territory quality affects female Preference in a Lake Victoria cichlid fish. *Behavioral Ecology and Sociobiology*, ***62*(5)**, 747–755.

Ekasari J and Maryam S. 2012. Evaluation of Biofloc Technology Application on Water Quality and Production Performance of Red Tilapia *Oreochromis sp*. Cultured at Different Stocking Densities. *HAYATI Journal of Biosciences* ***19*(2)**, 73–80.

Fessehaye Y, El-bialy Z, Rezk MA, Crooijmans R, Bovenhuis H and Komen H. 2006. Mating systems and male reproductive success in Nile tilapia (*Oreochromis niloticus*) in breeding hapas: A microsatellite analysis. *Aquaculture*, ***256*(**1–4), 148–158.

Haque MR, Islam MA, Wahab MA, Hoq ME, Rahman MM and Azim ME. 2016. Evaluation of Production Performance and Profitability of Hybrid Red tilapia and Genetically Improved Farmed tilapia (GIFT) strains in the carbon/nitrogen Controlled Periphyton-based (C/N- CP) on-farm Prawn Culture system in Bangladesh. *Aquaculture Reports*, ***4,*** 101–111.

Karen lC, Juliet WL, Parry JK, Bowmaker DMH and Seehausen O. 2005. Colour vision and speciation in Lake Victoria cichlids of the genus Pundamilia. *Molecular Ecology*, 4341–4353.

Kirkpatrick M and Nuismer SL. 2004. Sexual selection can constrain sympatric speciation. *Proceedings of the Royal Society B: Biological Sciences*, ***27(1***), 687-693.

Korzan WJ, Robison RR, Zhao S and Fernald RD. 2008. Color change as a potential behavioral strategy. *Hormones and Behavior*, ***54*(3)**, 463–470.

Lago A, De A, Rezende TT, Dias MAD, Freitas RTF and Hilsdorf AWS. 2016. The development of genetically improved red tilapia lines through the backcross breeding of two Oreochromis niloticus strains. *Aquaculture*. DOI: 10.1016/j.aquaculture.2016.06.042

Lu J and Takeuchi T. 2004. Spawning and egg quality of the tilapia Oreochromis niloticus fed solely on raw Spirulina throughout three generations. *Aquaculture*, ***234***: 625–640.

Neira R, García X, Lhorente JP, Filp M, Yáñez JM and Cascante AM. 2015. Evaluation of the growth and carcass quality of diallel crosses of four strains of Nile tilapia (Oerochromis niloticus). *Aquaculture*. https://doi.org/10.1016/j.aquaculture.

Plenderleith M, Van Oosterhout C, Robinson RL and Turner GF. 2005. Female preference for conspecific males based on olfactory cues in a Lake Malawi cichlid fish. *Biology Letters*, ***1*(4)**, 411–414.

Rajaee AH, Huntingford FA, Ranson KJ, McAndrew BJ and Penman DJ. 2010. The effect of male colouration on reproductive success in Nile tilapia (Oreochromis niloticus). *Aquaculture*, ***308***, 119–S123.

Ramadan M, Abou-Zied and Ahmed AA. (2007). Evaluation of Nile tilapia commercial hatcheries systems in Fayoum governorate 2 1-. *Egypt. J. Aquat. Boil. & Fish.*,***11***: 230–238.

Reichard M and Polačik, M. 2010. Reproductive isolating barriers between colour-differentiated populations of an African annual killifish, Nothobranchius korthausae (Cyprinodontiformes). *Biological Journal of the Linnean Society*, ***100***: 62–72.

Seehausen O and Schluter D. 2004. Male-male competition and nuptial-colour displacement as a diversifying force in Lake Victoria cichlid fishes. *Proceedings of the Royal Society B: Biological Sciences*, ***271*(1546)**, 1345–1353.

Selz OM, Pierotti MER, Maan ME, Schmid C and Seehausen O. 2014. Female preference for male color is necessary and sufficient for assortative mating in 2 Cichlid sister species. *Behavioral Ecology*, ***25*(3)**, 612–626.

Verzijden MN, Van Heusden J, Bouton, N, Witte F, Ten Cate C and Slabbekoorn H. 2010. Sounds of male Lake Victoria cichlids vary within and between species and affect female mate preferences. *Behavioral Ecology*, ***21*(3)**, 548–555

Vilhena R, Neto R, Antônio C, Oliveira L, De-Ribeiro RP, Tadeu R and Freitas FD. 2014. Genetic parameters and trends of morphometric traits of GIFT tilapia under selection for weight gain. *Scientia Agricola*, ***71*(4)**, 259–265.

Xu Z and Boyd CE. 2016. Reducing the monitoring parameters of fish pond water quality. *Aquaculture*, ***465***, 359–366.

JJBS

Jordan Journal of Biological Sciences

Volume 13, Number 2, June 2020
ISSN 1995-6673
Pages 223 - 229

Micro RNA 192 Gene Expression and Pathogenesis of Nephrotic Syndrome in Egyptian Children

Faten Z. Mohamed [1], Doaa M. Youssef [2], Amal S. El-Shal [3] and Asmaa A. Abdelsalam[1*]

[1]Chemistry Department, Faculty of Science, [2]Pediatrics Department, [3]Biochemistry Department, Faculty of Medicine, Zagazig University, Egypt.

Received June 23, 2019; Revised August 8, 2019; Accepted August 18, 2019

Abstract

Idiopathic Nephrotic syndrome (INS) is a condition in which the glomeruli of the kidney leak protein from the blood into the urine. This leads to hypoproteinaemia and generalized edema. Children with NS have an increased risk of bacterial infection and are often accompanied with malnutrition due to the loss of a large number of plasma proteins. NS pathogenesis and management remain unclear and the need for novel molecular mechanisms is necessary. The recent discovery of microRNAs (miRNAs) and their cellular functions provide an opportunity to fill these critical gaps. Because miRNAs possibly modulate the actions of key factors involved in nephrotic syndrome such as transforming growth factor-ß (TGF-β), they could be novel diagnostic biomarker of NS. This study examined association of serum miRNA-192 as a potential diagnostic biomarker of NS and its correlation with the pathogenesis of nephrotic syndrome including dyslipidemia, proteinuria and potential fibrosis. This study included 50 child NS cases and 50 age-matched healthy children as controls. MiRNA-192 expression levels were measured using quantitative real-time polymerase chain reaction (qRT-PCR) and TGF-ß serum levels were assessed by enzyme-linked immunosorbent assay (ELISA). Correlations among miRNA192, TGF-ß and severity of NS (dyslipidemia and proteinuria) were investigated. Our results revealed significantly lower miRNA-192 expression levels in NS patients than in the control group ($P < 0.001$). Serum TGF-ß levels were significantly increased in NS cases as compared to control group ($P < 0.001$). Furthermore, serum miRNA-192 expression levels were significantly negatively correlated with serum TGF-ß concentrations, dyslipidemia and proteinuria, whereas serum TGF-ß concentrations were significantly positively correlated with proteinuria. Collectively, levels of both serum miRNA-192 and TGF-ß may explain their role in pathogenesis of NS, and they are promising diagnostic biomarkers.

Keywords: Nephrotic syndrome, miRNA-192, TGF- ß, qRT-PCR, ELISA, dyslipidemia, proteinuria.

1. Introduction

Idiopathic Nephrotic syndrome (INS) is the most common chronic kidney disease among children which is characterized by triad of proteinuria, hypoalbuminaemia, and edema (Damien *et al.*, 2018). Its incidence is from 2 to 7 cases/100,000 children/year, and its global prevalence is of 16 cases/100,000 children aged below 16 years (Deschênes and Leclerc, 2010). Typically, the histological classifications corresponding with idiopathic childhood NS are described either as minimal change disease (MCD) or focal segmental glomerulosclerosis (FSGS) the quintessential podocyte diseases (A report of the International Study of Kidney Disease in Children, 1978). Glucocorticoids (GC) are the primary therapy of INS. However, not all children, who initially appear to have similar histological and clinical features of NS, respond to steroid therapy; they are classified into as steroid sensitive (SS) or steroid resistant (SR), and these differences in steroid response can be attributed to genetic factors (Rheault and Gbadegesin. 2016).

MicroRNAs (miRNAs) are endogenous, short non-coding RNA molecules that play a critical role in modulating many cellular and physiological activities (Schena *et al*., 2014). The miRNAs are relatively stable, which makes them ideal diagnostic & prognostic biomarkers for many diseases. Although plenty of miRNAs are widely expressed in many tissues, some miRNAs are found to be highly organ-specific (Liang *et al*., 2007). In the kidney, miRNAs are indispensable to development and homeostasis (Schena *et al*., 2014). Yinfeng et al. suggested possible roles and miRNAs expression in acute kidney injury and disease pathogenesis (Yinfeng *et al*., 2017). Another study was performed by Tesch proposed aberrant miRNAs expression level in renal fibrosis (Tesch, 2010). Additionally, according to their hypotheses, miRNAs lead to renal fibrosis by causing changes in TGF-β, extracellular matrix and epithelial-mesenchymal transition (Conway and Hughes, 2012 and Kato et al., 2012). TGF-β is a fibro genic cytokine that contributes to renal tissue fibrosis (Reeves and Andreoli, 2000). TGF-β causes proliferation in extracellular matrix, stimulating myofibroblastosis (LAN, 2011). The number of TGF-β receptors increases with renal damage, activating

* Corresponding author e-mail: asmaaahmedabdelsalam@gmail.com.

the TGF-β/Smad3 pathway and initiating fibrosis (Meng *et al.*, 2013). Recent studies have shown that miRNA-192 target sites are located within TGF-β mRNA; therefore, miRNA-192 can significantly inhibit the translation process after TGF-β transcription (Kato *et al.*, 2011). Therefore, we aimed to investigate possible role of miRNA-192 expression levels as a novel diagnostic biomarker and its correlation with the serum level of Transforming TGF-ß as a pro-inflammatory fibrotic cytokine and severity of NS.

2. Subject and method

2.1. Subjects

The current study was conducted in the Nephrology Unit Pediatrics Department and Medical Biochemistry Department; Zagazig University. The protocol was approved by the ethics committee of Zagazig University. Written informed consent was obtained from all children parents. Fifty patients with steroid sensitive NS with an age range between 5 and 9 years (28 males and 22 females) were diagnosed clinically and proven by laboratory results. These patients had been followed up at the Nephrology unit of the Department of Pediatrics, Zagazig University Hospital. The control group consisted of 50 age- and sex-matched apparently healthy children selected from the general pediatric outpatient department. All samples were withdrawn during the period from March 2018 to June 2018. Demographic data of the patients were recorded from the medical history and electronic files. The inclusion criteria were both male and female children, age at start of study greater than 5 years, and normal kidney function in the control group. The exclusion criteria were a family history of premature cardiovascular diseases.

2.2. Blood Sampling

A 5 mL blood sample was withdrawn under aseptic conditions from each patient and healthy children and left for 30 min for spontaneous clotting at room temperature before being centrifuged at 3,000 rpm. Serum samples were immediately stored at −70 °C for determination of TGF-ß levels and RNA extraction.

2.3. Measurement of serum TGF-ß level:

Serum samples of all subjects were aliquoted and levels of TGF-ß were measured by an enzyme-linked immunosorbent assay (ELISA) kit provided from R&D Systems, Inc., Minneapolis, USA (Cat No. DB100B) and applied according to manufacturer instructions. The minimum detectable dose (MDD) of TGF-β ranged from 1.7-15.4 pg/mL.

2.4. Extraction of serum miRNA-192:

Serum samples of all subjects were aliquoted and all procedures occurred on ice bar and repeated freeze/thaw cycles were avoided to prevent RNA damage.

Total RNA including miRNAs was extracted using RNA extraction kit (Qiagen Inc., Foster city, California, USA) following the manufacturer's instructions (Cat. No.217004). Briefly, 500 µl QIAzol lysis reagent was added to 100 µl serum samples and the mixture was incubated for 5 min at room temperature. Then, addition of (100 µl) chloroform was performed and tube was vigorously shaken by hands for 15 s and incubated at room temperature for 5 mins. After centrifugation at 12,000 × g for 15 min at 4 °C, the upper aqueous phase of supernatant was transferred to a fresh tube and 700µl of 100% ethanol were added. 700 µl of this mixture was transferred into RNeasy mini spin column and centrifuged at 8000 × g for 1 min at room temperature. After the mixture had completely passed the column, this step was repeated until all of the mixture had completely passed the column to the mini column. Next, the column was washed two times with 500 µl RNA wash buffer (RWT buffer) and centrifuged for 15 s at 8,000× g at room temperature. Then, 500 µl buffer RPE was added to the column and centrifuged at 8000×g at room temperature for 15 s. Another 500 µl buffer RPE was added to the column and centrifuged at 8000×g at room temperature for 2 min. For RNA elution, the column was transferred to a new 1.5 mL collection tube and 40 µl RNase-free water was directly pipetted onto the column and centrifuged for 1 min at 8000 × g. Finally, the quantity and purity of serum RNA were confirmed by the value of optical density (OD) at 260 and 280 nm using a spectrometer, with acceptable RNA purity ranging from 1.8 to 2.1.

2.5. Reverse transcription and quantification of serum miRNA-192:

The miScript II reverse transcription kit (Qiagen Inc., USA, and Cat. No. 218161) was used for polyadenylation and reverse transcription of miRNA to complementary DNA (cDNA). After mixing with template RNA (100 ng), 5X miScript buffer, miScript reverse transcriptase mix and RNase-free water in a final volume of 20 µl, the mixture was centrifuged briefly and incubated for 60 min. at 37°C. To inactivate the reverse transcriptase mix, the samples were incubated for 5 min. at 95°C and then placed on ice for further PCR analysis. The diluted cDNA templates were either stored at –20 °C or used to proceed further to quantitative real-time polymerase chain reaction (qRT-PCR).

2.6. The expression level of serum miRNA-192:

The resultant cDNA was subjected to qRT-PCR to evaluate expression of serum of miRNA-192 using miScript SYBR® Green PCR Kit with miScript Primer assays (Qiagen Inc., USA). This kit includes QuantiTect SYBR Green PCR Master Mix and the Primer (reverse primer used to detect miRNA-192) was provided from miScript Primer Assay kit that specifically recognizes the targeted miRNA-192(Cat. No. MS00003689). The expression levels of miRNA were normalized to RNU6, which was selected as internal control (Cat. No. MS000033740). The PCR conditions were as follows: 95°C for 15 min, followed by 40 cycles at 94 °C for 15 s, 55 °C for 30 s and 70 °C for 34 s. The cycle threshold (CT) is defined as the number of cycles required for the fluorescent signal to cross the threshold in real-time PCR. The expression of miRNAs was reported as the ΔCt value, which was calculated by subtracting the CT values of miRNA U6 from the CT values of the miRNA-192. Because there is an inverse correlation between ΔCt and miRNA expression levels, lower ΔCt values are associated with increased miRNA expression. The relative gene expression was calculated as ΔΔCt. The amplitude of change of the expression miRNA observed in patients in relation to control group was analyzed by the $2^{-\Delta\Delta Ct}$ method (Livak and Schmittgen, 2001).

2.7. Statistical Analysis:

All data were collected, tabulated and statistically analyzed using SPSS 20.0 for windows (SPSS Inc., Chicago, IL). Quantitative data were expressed as the mean ± standard deviation (SD), and percentages when appropriate. Student's t-test was used to compare two groups of normally distributed data. Receiver operating characteristic (ROC) curve analysis was used to identify the optimal sensitivity and specificity of miRNA-192 and TGF-ß. The correlation coefficients were calculated using Spearman correlation. Multiple logistic regression analysis was conducted to test possible association between miRNA-192 and TGF-ß as well as other parameters and to also evaluate whether the biomarker miRNA-192 and TGF-ß could be used as predictors for nephrotic syndrome. P-value < 0.05 was considered statistically significant.

3. Results

3.1. Clinico-demographic

characteristics, biochemical laboratory and miRNA-192 expression profiles among nephrotic patients and healthy controls

Data represented in Table 1 indicated that sex distribution was comparable between the patient and control groups. Body mass index (BMI) and systolic blood pressure (SBP) was significantly greater in the patient group than the control group (Table 1). Serum total cholesterol(TC), serum triglycerides (TGs) and serum low density lipoprotein- cholesterol (LDL-C) were higher significantly in cases of patients than in healthy children (P <0.001) while serum levels of high density lipoprotein-cholesterol were significantly lower in patients than in healthy controls(p<0.001). Urinary protein was significantly higher in the patient group (P < 0.001 for each) while serum total protein was significantly lower among patients' group than the control group (P < 0.001 for each) (Table 1).

In this study, serum miRNA-192 expression was measured using qRT-PCR and normalized to RNU6 as reference control. The expression level of miRNA 192 was significantly lower in nephrotic children in comparison with healthy controls (P < 0.001 for each) (Table 1). Also, serum TGF-ß level was significantly higher among patients' children compared to control group (P <0.001).

Table 1. Clinico-demographic characteristics, biochemical laboratory and miRNA- 192 expression profiles in nephrotic patients and healthy controls

Parameters	Patients (N=50)	Controls(N=50)	P-value
Age (range)	7.4±1.1 (5-9)	7.36±1.0 (5-9)	> 0.9
Gender, n (%)			
Male	28 (56)	28 (56)	> 0.9
Female	22 (44)	22 (44)	
BMI (Kg/m^2)	31.7 ± 4	25.4 ± 1.6	<0.001*
SBP (mmHg)	117.4 ± 4.4	108 ± 12	<0.001*
DBP (mmHg)	75.4 ± 8.4	79.4 ± 4.2	0.003
Total cholesterol (mg/dL)	404±55	126.1±2.3	<0.001*
Triglycerides(mg/dL)	463.4±93	120±17.8	<0.001*
HDL-C(mg/dL)	29.7±5.4	62.6±6.6	<0.001*
LDL-C(mg/dL)	379.4±56	63.5±6.7	<0.001*
Serum Total Protein (g/dL)	4.1 ± 0.9	7.0 ± 0.5	<0.001*
Urinary Protein (g/dL)	1.45 ± 0.2	0.17 ± 0.07	<0.001*
Serum TGF-ß (pg/mL)	167.5 ± 7.9	50.1 ± 4.4	<0.001*
miRNA 192 expression levels (fmol/L)	47.9 ± 1.7	263.5 ± 12.6	<0.001*

BMI: body mass index, SBP: systolic blood pressure, DBP: diastolic blood pressure, TGF-ß: transforming growth factor- beta.

(*) Considered significant statistically (P-value < 0.05).

3.2. ROC curve analysis: receiver operating characteristics (ROC) was used to determine the threshold (cutoff) value for optimal sensitivity and specificity at which the biomarker could be used to differentiate between nephrotic cases and healthy controls.

ROC analysis (Figure.1) revealed that miRNA-192 could differentiate nephrotic patients from healthy controls with an AUC of 0.978 for miRNA-192 (95% CI: 0.940 – 1.016, P < 0.001). The optimal sensitivity and specificity to differentiate nephrotic children from controls were (94.0% and 98.0% at a cutoff expression value <149). This finding suggests that miRNA-192 could be a potential diagnostic biomarker in childhood nephrotic syndrome.

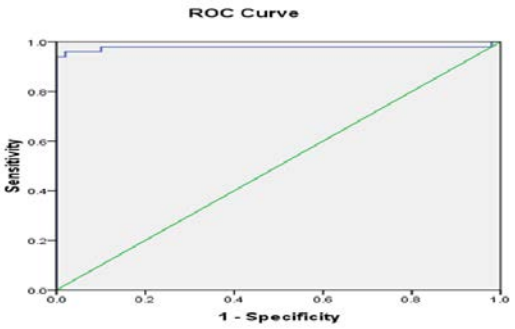

Figure 1. Receiver operating characteristic (ROC) curve analysis for miRNA-192 discriminating between nephrotic patients and healthy controls.

Moreover, ROC analysis (Figure.2) showed that TGF-ß could differentiate nephrotic patients from healthy controls with an AUC of 0.970 (95% CI: 0.940 – 0.999, P < 0.001). At cutoff value >160, TGF-ß provided sensitivity of 80.0% and specificity of 98.0% for acting as a novel diagnostic marker for nephrotic syndrome.

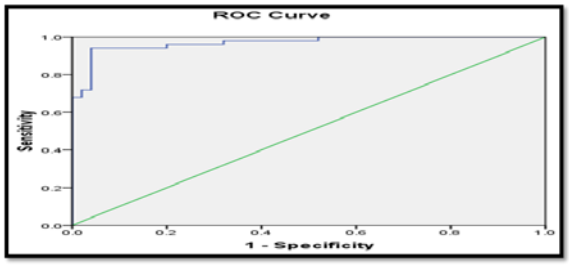

Figure 2. Receiver operating characteristic (ROC) curve analysis for TGF-ß discriminating between nephrotic patients and healthy controls.

3.3. Correlation of miRNA-192 expression level with serum level of TGF-ß and Urinary protein among nephrotic patients:

The relation between the quantitative expression levels of miRNA-192 with serum TGF-ß level and Urinary protein among the nephrotic patients was clarified using Spearman correlation analysis. As shown in Figures (3 and 4), miRNA-192 expression levels were negatively correlated with both TGF-ß (r = - 0.88, P < 0.001) and urinary protein (r=-0.88, P<0.001).

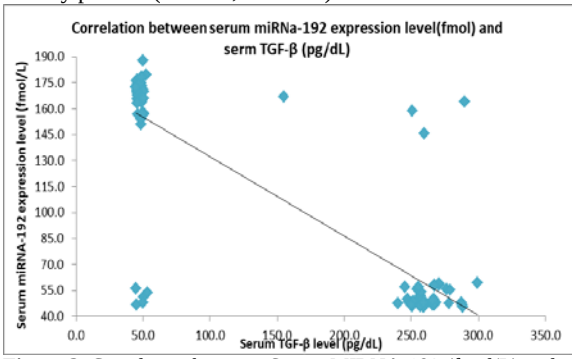

Figure 3. Correlation between Serum MIRNA-192 (fmol/L) and serum levels of TGF-β (pg/mL)

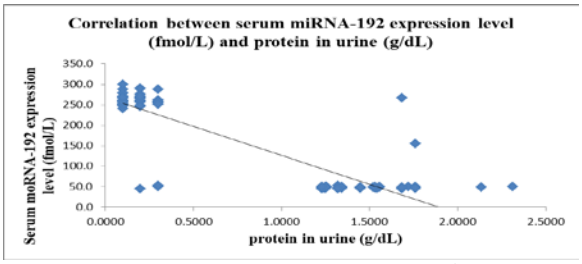

Figure 4. Correlation between Serum miRNA-192 (fmol/L) and Urinary protein (g/dL)

3.4. Correlation of miRNA-192 expression level with serum level of lipid indices among nephrotic patients:

The quantitative expression levels of miRNA-192 showed significant negative correlations with serum LDL-c (r = -0.88, P-value <0.001), TGs (-0.84, P-value <0.001) and TC (-0.87, P-value <0.001) level among the nephrotic patients. As shown in Figure (5, 6and 7)

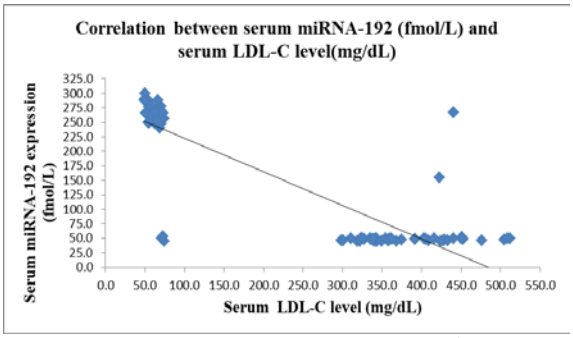

Figure 5. Correlation between Serum MIRNA-192 (fmol/L) and Low density lipoprotein – Cholesterol (LDL-C) (mg/dL)

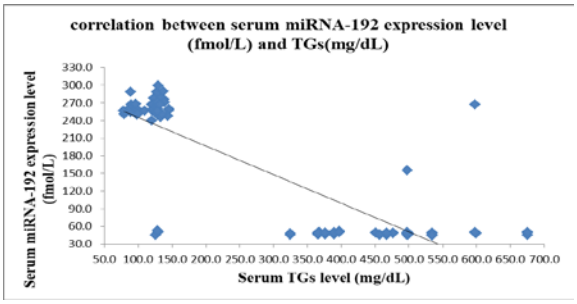

Figure 6. Correlation between Serum MIRNA-192 (fmol/L) and Triglycerides (TGs) (mg/dL)

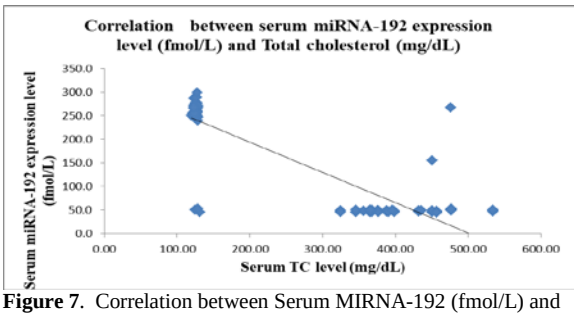

Figure 7. Correlation between Serum MIRNA-192 (fmol/L) and Total Cholesterol (TC) (mg/dL)

3.5. Correlation TGF-ß with urinary level of protein among nephrotic patients:

As shown in Figure (8), the serum level of TGF-ß showed a highly significant positive correlation with urinary protein level among the nephrotic patients (r = 0.86, P<0.001).

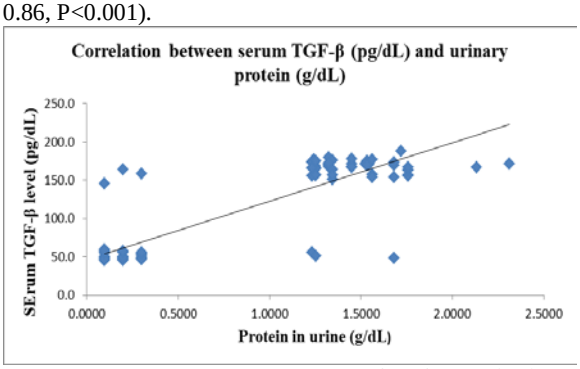

Figure 8. Correlation between Serum TGF-β (pg/mL) and Urinary protein (g/dL)

3.6. Analysis of the power of miRNA-192 and TGF-ß to predict nephrotic syndrome pathogenesis:

Multiple Logistic regression analysis was performed to evaluate whether miRNA-192 & TGF-ß could predict the NS pathogenesis in nephrotic patients. We found that

miRNA-192 was an independent predictor for significant dyslipidemia (-2.88±0.79), P-value <0.001 and TGF-ß serum level (-.051±0.17), P-value<0.001while it did not show any significant regression with the other parameters (P-value >0.05) as shown in Table 2.

Table 2. Multiple logistic regressions Analysis for miRNA- 192 and other parameters among Nephrotic syndrome patients

Parameters	B ± SE	P-value
Age (years)	4.1±4.7	>0.05
BMI(Kg/m^2)	-2.0±1.69	>0.05
Blood Pressure(mmHg)	0.068±0.54	>0.05
Protein in Serum(g/dL)	-4.3±7.0	>0.05
Dyslipidemia(mg/dL)	-2.88±0.79	<0.001*
TGF-β (pg/mL)	-0.51±0.17	<0.001*

(*) Considered significant statistically (P-value < 0.05).

Furthermore, TGF-ß was found to be an independent predictor for significant serum miRNA-192 level (-0.17 ±0.05, P-value <0.001) and proteinuria (34.6±13.7, P-value = 0.01), while it did not show any significance regression to any other parameters as shown in Table 3.

Table 3. Multiple logistic regressions Analysis for TGF-ß and other parameters in Nephrotic syndrome

Parameters	B ± SE	P-value
Age (years)	3.85±2.68	>0.05
BMI(Kg/m^2)	1.03±0.97	>0.05
Blood Pressure(mmHg)	0.15±0.31	>0.05
Protein in Serum (g/dL)	-2.7±4.0	>0.05
Protein in Urine (g/dL)	34.6±13.7	0.01*
Dyslipidemia(mg/dL)	0.6±0.48	>0.05
miRNA-192(fmol/L)	-0.17±0.05	<0.001*

4. Discussion

Despite several advances in INS pathophysiology**,** MCD and FSGS still remain complex diseases for which new therapies are needed. Clinical evolution is still Our study also revealed a significant negative correlation between serum levels of miRNA-192 and dyslipidemia, which reflects the possibility to metabolic syndromes arising from insulin resistance accompanying with abnormal adipose deposition, causing alternation disturbances in biological activities in disease pathology including glucose homeostasis, vascular signaling affecting cardiovascular risks and obesity. Kato and his colleagues matched our hypothesis; their study examined the involvement of miRNA- 192 in the regulation of biological events related to the pathogenesis of diabetes (Kato et al., 2007). Also, another study in mice model explored the role of miRNA-192 during the development of obesity associated with dyslipidemia, glucose intolerance (Castaño et al., 2018). Shah et al., correlated miRNA-192 expression level with waist circumference and visceral fat quantity in humans as well as an increase in TG/HDL ratio (Shah et al., 2017). In line with our findings, Hamdia and her colleagues suggested that miRNA-192 expression levels accompanied with dyslipidemia and obesity are risk factors related to the prevalence of renal, cardiovascular, ocular and nervous system complications among diabetic patients (Hamdia et al., 2013).

We also found a significant negative correlation between miRNA-192 expression level and proteinuria reflecting changes in glomerular protein filtration and/or defects in tubular reabsorption that cause the appearance of proteins in the urine. The presence of proteinuria emphasizes alternation in the intercellular junction and cytoskeletal structure of the foot processes of podocyte, and the cell showed a simplified, effaced phenotype (Kriz et al., 2012). Damage to these cells may manifest vacuolization, fusion of foot processes, and focal detachment of epithelial cells from the underlying basement membrane. These changes appear to be the consequence mainly of persistent abnormalities in intra glomerular capillary hemodynamics (Rennke and Klein, 1989). Another study by Putta et al. found that the suppression of miRNA-192 in diabetic mice attenuated proteinuria and induced renal fibrosis (Putta et al., 2012). In contrast to our results, Xiaoyi et al. found a positive significant correlation between the serum expression level of miRNA-192 and urinary protein level in patients with FSGS and MCD (Xiaoyi et al., 2013). Also, a recent study reported that miRNA-192 was significantly higher in overt proteinuria than in normoalbuminuria and microalbuminuria groups (Hung-Yu et al., 2016). Further studies are needed to highlight this relation and influence the diagnosis and management of nephrotic syndrome.

TGF-β is a potent and versatile cytokine. When activated, it exerts both physiological and pathologic functions including immune functions, inflammation, wound healing and organ fibrosis (Karim et al., 2019). TGF-β is ubiquitously expressed and all cells appear to respond TGF-β (Jenkins, 2008). TGF- β induces trans-differentiation of extracellular matrix components (Humphreys et al., 2010). TGF- β exerts its profibrotic activity through stimulation of fibroblast proliferation, extracellular matrix synthesis (e.g., collagen types I, III, and IV, proteoglycans, laminin, and fibronectin), and epithelial-to-mesenchyme transition (EMT). Induced expression of ECM remodeling genes, increasing in the apoptosis rate, and EMT lead to tubulointerstitial fibrosis and glomerulosclerosis (Lamouille et al., 2014). In our study, there was a significant increase of serum TGF-β levels in nephrotic children as compared to healthy controls. ROC analysis confirmed that TGF- β may be useful as potential diagnostic biomarkers in childhood nephrotic syndrome (sensitivity: 80.0% and specificity 98.0% at a cutoff value > 160). In accordance with our data, Xiaoyi, et al. reported that TGF- β level was significantly increased Diabetic Nephropathy Patients (Xiaoyi, et al., 2016). This result was expected by another study which identified TGF- β as being upregulated during the course of progressive renal injury (Bottinger, 2007). Similarly, inhibition of TGF- β has been shown to ameliorate renal injury (Border and Noble, 1997). Our findings also showed a highly significant positive correlation between serum TGF- β and proteinuria. Goumenos believed that TGF-β was not only involved in ECM accumulation, fibrosis, and progressive renal impairment, but also played a role in changes to the glomerular filtration barrier and induction of proteinuria. There is substantial evidence to support this observation. Urinary TGF- β correlates with the degree of proteinuria (Goumenos et al., 2002).

Also, a previous study demonstrated that activation of TGF-β pathway contributes to the progression, invasion and poor prognosis of renal cancer patients (Kato et al., 2007).

Interestingly, we observed a significant negative correlation between miRNA-192 expression levels and TGF-β in nephrotic children (r =- 0.88 and p <0.001). We hypothesized that the microRNA-192 which expression correlated with TGF-β levels might be linked with progression of NS and may lead to increased fibrosis resulting in disarrangements in renal functional parameters that induce angiotensin, proteinuria, and hypoxia. This theory is in line with another study performed by Wang and his colleagues that demonstrated the potential for enhanced airway renal fibrosis mainly through TGF-ß activity (Wang et al., 2010). In parallel with our findings, Krupa et al. explained the same relation as TGF- β 1 inhibited miR-192 expression in human proximal tubular cells (PTCs) and deficiency of miR-192 associates with renal fibrosis acceleration and GFR reduction in Diabetic Nephropathy. There are two transcription factors namely zinc finger E-box binding homeobox-1 (Zeb1) and Zeb2 that are located downstream of TGF-β signaling pathway can suppress E-cadherin and control renal fibrosis. Overexpression of miRNA-192 could inhibit the TGF-β1 signaling pathway and the expression of Zeb1 and Zeb2 and then prevented the kidney from fibrosis. So, it was reported that TGF-β1 inhibits the expression of miRNA-192 that targeted Zeb1/2 to activate TGF-β1 signaling pathway and accelerate renal fibrosis in DN (Krupa et al., 2010). Similarly, another study by Wang et al. in rat model reported that the expression of miRNA-192in rat PTCs, mesangial cells, and human podocytes was decreased by TGF-β (Wang et al. 2013). Recently, Xiaoyi et al. found that miR-192 was negatively correlated with TGF-β1 and Fibronectin, two parameters which represent the fibrosis extent of the kidney (Xiaoyi et al., 2016). However, there are different studies with opposite conclusions. Kato and colleagues found a significant expression of miRNA-192 increased in mesangial cells due to high glucose level, and it has a vital role in the kidney disease pathogenesis as it amplifies TGF-β1 signaling (Kato et al., 2012). The discrepancy in these studies may be due to the different samples species, cell types differences (including podocyte, renal tube cells, and mesangial cells), and experiment conditions.unpredictable. No cohort study has succeeded in bringing out prognostic factors. The discovery of the genetic role in the pathophysiology of nephrotic syndrome or disease progression is one of the hot spots in pediatric nephrology and has an important clinical impact (Suvanto *et al*., 2016). Several studies revealed the involvement of miRNA as a diagnostic parameter in NS (Wang *et al*., 2013 and Luo *et al*., 2013). Recent studies have shown that miRNA-192 target sites are located within TGF-β mRNA; therefore, miRNA-192 can significantly inhibit the translation process after TGF-β transcription (Kato *et al.*, 2011).

Therefore, we hypothesized that the different expression of miRNA-192 between nephrotic patients and healthy children leads to alterations in its target, Smad-interacting protein 1 located within TGF-β mRNA, in childhood nephrotic syndrome. This disturbance may lead to podocyte alterations with protein expression resulting proteinuria or localization defects, actin cytoskeleton remodeling, or intracellular signaling pathway activation and influencing metabolism leading to Hyperlipidemia. Furthermore, alterations lead to a disturbance of glomerular filtration barrier properties. Besides, miRNA-192 could be a novel diagnostic biomarker of NS patients which helps in rapid assessment of the disease and limiting its progression. Our study revealed that as compared with healthy children, the serum level of miRNA-192 expression level in nephrotic patients showed significance decrease. ROC analysis confirmed that miRNA-192 may be useful as potential diagnostic biomarkers in childhood nephrotic syndrome (sensitivity: 94.0% and specificity 98.0% at a cutoff value <149).

Most investigations have found that miR-192 expression increases in diabetic nephropathy (DN) models and in renal cells, but several other studies have reported that miR-192 expression decreases (Yang *et al.*, 2013). Our results are in accordance with the study that explored the potential diagnostic difference between FSGS and MCD on basis of miR-192 and approved that serum miR-192 had higher expression level in patients with FSGS than those with MCD but lower than healthy controls (Xiaoyi *et al.*, 2013). Similarly, Sayilar and his colleagues revealed that miR-192 expression was 1.5 fold lower in plasma and 1.8 fold higher in urine samples of stage five chronic kidney disease (CKD) patients compared to the control group, while it was much higher in both plasma and urine samples (3.8 and 3.3 fold, respectively) of stage three CKD patients (Sayilar *et al*., 2016). In contrast, Kato et al.'s rat model study showed increased miR-192 expression in diabetic rats (Kato *et al.*, 2007). A recent systematic literature survey found that miRNA-192 is increased in body fluids (including plasma and urine) of patients with diabetic nephropathy (Yang *et al.*, 2013). Similar to this study, further support of miRNA-192 involvement in the pathobiology of the kidney, it has been recently reported that sera of patients with early stages of DN had a higher expression of miR-192 compared to the late stages cases of clinical course of this disease process (Krupa *et al*., 2010). Also, a study established by Barutta et al. found that miRNA 192 expression levels is higher in patients with microalbuminuria DN (Barutta *et al.*, 2013). This discrepancy might be due to the different samples used between our study and others.

5. Conclusions

Our study revealed that serum miRNA-192 has a high predictive pathogenic value in NS prognosis and management as a promising severity biomarker through its negative correlations with proteinuria and TGF-β as well as dyslipidemia.

Although our findings did not match other experimental studies, further studies are needed.

Acknowledgments

The authors acknowledge the kindness of the participating patients and control parents.

Funding

This research did not receive any specific grant from funding agencies in the public, commercial, or profit sectors.

Declarations of interest: None

References

Barutta F, Tricarico M, Corbelli A, et al. 2013. Urinary exosomal microRNAs in incipient diabetic nephropathy. *PLoS One*, **8**: e73798.

Border WA and Noble NA.1997. TGF-beta in kidney fibrosis: a target for gene therapy. *Kidney Int*, **51**:1388–1396.

Bottinger EP. 2007. TGF-beta in renal injury and disease. *Semin Nephrol*, **27**:309–320.

Carlos Castaño, Susana Kalko, Anna Novialis and Mrcelina Párrizas. 2018. Obesity-associated exosomal miRNAs modulate glucose and lipid metabolism in mice. *PNAS*, **115** (48) 12158-12163.

Conway B. and Hughes J. 2012. Cellular orchestrators of renal fibrosis. *QJM*, **105**: 611-615.

Damien G Noone, Kazumoto Iijima and Rulan Parekh. 2018. Idiopathic nephrotic syndrome in children. *Lancet*, **392**: 61-74.

Deschênes G and Leclerc A. 2010. Epidémiologie du syndrome néphro-tique de L'Enfant. *Arch Pediatr*, **17**:622-3.

Goumenos DS, Tsakas S, elNahas AM, Alexandri S, Oldroyd S, Kalliakmani P and Vlachojannis JG. 2002. Transforming growth factor- beta (1) in the kidney and urine of patients with glomerular disease and proteinuria. *Nephrol. Dial. Transplant*, **17**:2145-2152.

Hamdia Ezzat, Abdelwahab M.,Fatma A. Gihan A. et al. 2013. Expression of micro RNA 192 in type 2 diabetes mellitus relation to glycemic control, metabolic abnormalities, renal and ocular complications. *American Journal of biochemistry*, **3**(4):97-106.

Humphreys BD, Lin SL, Kobayashi A, Hudson TE, Nowlin BT, Bonventre JV, Valerius MT, McMahon AP and Duffield JS. 2010. Fate tracing reveals the pericyte and not epithelial origin of myofibroblasts in kidney fibrosis. *Am JPathol*, **176**:85–97, 2010

Hung-Yu Chien, Chang-Yi Chen, Yen-Hui Chiu, Yi-Chun Lin and Wan-Chun Li. 2016. Differential microRNA Profiles Predict Diabetic Nephropathy Progression in Taiwan. *Int. J. Med. Sci.*, **13** (6):457-465.

Jenkins G. 2008. The role of proteases in transforming growth factor- beta activation. *Int J Biochem Cell Biol*, **40**:1068–1078.

Karim Kouzbari, Mahmoud R. Hossan, Jullien H. Arrizabalaga, Rohan Varshney, et al. 2019. Oscillatory shear potentiates latent TGF-β1 activation more than steady shear as demonstrated by a novel force generator. *Nature. SCIENTIFIC REPORTS*, **9**:6065. http://doi.org/10.1038/s41598-019-42302-x

Kato M, Arce L, Wang M, et al. 2011. A microRNA circuit mediates transforming growth factor-beta1 auto regulation in renal glomerular mesangial cells. *Kidney Int*, **80**: 358–368.

Kato M, Park JT and Natarajan R. 2012. MicroRNAs and the glomerulus. *Exp. Cell Res*, **318**:993-1000.

Kato M, Zhang J, Wang M, Lanting L, Yuan H, et al. 2007. MicroRNA-192 in diabetic kidney glomeruli and its function in TGF-beta-induced collagen expression via inhibition of E-box repressors. *Proc Natl Acad Sci. U S A*, **104**: 3432-3437.

Kriz W, Shirato I, Nagata M, et al. 2012. The podocyte's response to stress: the enigma of foot process effacement. *Am J Physiol Renal Physiol*, **304**:F333–F347.

Krupa A, Jenkins R, Luo DD, Lewis A, Phillips A and Fraser D. 2010. Loss of MicroRNA-192 promotes fibrogenesis in diabetic nephropathy. *J of the American Society of Nephrology*, **21**:438-447.

Lamouille S., Xu J., and Derynck R. 2014. Molecular mechanisms of epithelial-mesenchyme transition. *Nature Reviews Molecular Cell Biology*, **15** (3):178-196.

LAN HY. 2011. Diverse roles of TGF-β²/Smads in renal fibrosis and inflammation. *Int J Biol Sci*, **7**: 1056-1067.

Liang Y, Ridzon D, Wong L and Chen C. 2007. Characterization of microRNA expression profiles in normal human tissues. *BMC Genomics*, **8**:166.

Livak, K. J. and Schmittgen, T. D. 2001.Analysis of relative gene expression data using real-time quantitative PCR and the 2 (-delta delta C (T)) method. *Methods*, **25**:402-408.

Luo Y., Wang C., Chen X., et al. 2013. Increased serum and urinary microRNAs in children with idiopathic nephrotic syndrome. *Clin Chem*, **59**:658-66.

Meng XM, Chung AC. and LAN HY. 2013. Role of the TGF-β²/BMP-7/Smad pathways in renal diseases. *Clin Sci (Lond)*, **124**: 243-254.

Nephrotic syndrome in children: prediction of histopathology from clinical and laboratory characteristics at time of diagnosis. 1978. A report of the International Study of Kidney Disease in Children. *Kidney Int*, **13**:159-165.

Putta S, Lanting L, Sun G, Lawson G, Kato M and Natarajan R. 2012. Inhibiting micro RNA-192 ameliorates renal fibrosis in diabetic nephropathy. *J Am Soc Nephrol*, **23**:458-469.

Reeves WB, and Andreoli TE. 2000. Transforming growth factor beta contributes to progressive diabetic nephropathy. *Proc Natl Acad Sci USA*, **97**:7667-7669.

Rennke HG and Klein PS, 1989. Pathogenesis and significance of non primary focal and segmental glomerulosclerosis. *Am J Kidney Dis*, **13**:443–456, 1989.

Rheault MN and Gbadegesin RA. 2016 The genetics of nephrotic syndrome. *J Pediatr Genet*, **5** (1):15-24.

Sayilar EI, Gullulu M, Tuncel E, Peynirci H, Alemdar A, et al. 2016. Biomarker Potential of Urine miR-451 at Different Stages of Diabetic Nephropathy. *J Diabetes Metab*, **7**: 650.

Schena F.P., Serino G. and Sallustio F., 2014. MicroRNAs in kidney diseases: new promising biomarkers for diagnosis and monitoring, *Nephrol. Dial. Transplant*, **29**:755-763.

Shah R et al. 2017. Extracellular RNAs are associated with insulin resistance and metabolic phenotype. *Diabetes care*, **40**:546-553

Suvanto M., Jahnukainen T., Kestilä M. and Jalanko H. 2016. Single nucleotide polymorphisms in pediatric idiopathic nephrotic syndrome. *Int. J. Nephrol*, 1417456.

Tesch GH. 2010. Review: Serum and urine biomarkers of kidney disease: A pathophysiological perspective. *Nephrology (Carlton)*, **15**: 609-616.

Wang B, Herman-Edelstein M, Koh P, Burns W, Jandeleit-Dahm K, Watson A, Saleem M, Goodall GJ, Twigg SM, Cooper ME and Kantharidis P. 2010. E-cadherin expression is regulated by miR-192/215 by a mechanism that is independent of the profibrotic effects of transforming growth factor-β. *Diabetes*, **59** (7):1794-1802.

Wang G., Kwan BC. Lai FM., Chow KM., Li PK. and Szeto CC. 2013. Urinary sediment miRNA levels in adult nephrotic syndrome. *Clin Chim Acta*, **418**:5-11.

Xiaoyi Cai, Zhengkun Xia, Chunni Zhang, Yang Luo, Yuanfu Gao, Zhongmin Fan, Mengyuan Liu and Ying Zhang. 2013. Serum microRNAs levels in primary focal segmental glomerulosclerosis. *Pediatr Nephrol*, **28**:1797-1801.

Xiaoyi Ma, Canlu Lu, Chuan Lv, CanWu, and Qiuyue Wang. 2016. The Expression of miR-192 and Its Significance in Diabetic Nephropathy Patients with Different Urine Albumin Creatinine Ratio. *J Diabetes Research*, 6789402.

Yang Y., Xiao L., Li J., Kanwar Y. S., Liu F., and Sun L. 2013. Urine miRNAs: potential biomarkers for monitoring progression of early stages of diabetic nephropathy. *Medical Hypotheses*, **81** (2):274-278.

Yinfeng Ma, Jun Fu, Le Qian, Tingting Tao. 2017. Serum miRNA expression and correlation with clinical characteristics in acute kidney injury. *Int J Clin Exp Pathol*, **10(**8):8721-8726.

JJBS

Volume 13, Number 2, June 2020
ISSN 1995-6673
Pages 231 - 236

Jordan Journal of Biological Sciences

Temporal Variation of Relative Growth Pattern and Condition of *Glossogobius giuris* (Hamilton, 1822) in the Garai River, SW Bangladesh

Md. Abul Kalam Azad, Md. Yeamin Hossain*, Md. Rabiul Hasan, Zannatul Mawa, Md. Ataur Rahman, Md. Akhtarul Islam, Asma Afroz Chowdhury, Obaidur Rahman, Md. Ashekur Rahman, Dalia Khatun and Most. Farida parvin

Department of Fisheries, Faculty of Agriculture, University of Rajshahi, Rajshahi 6205, Bangladesh

Received May 23, 2019; Revised July 27, 2019; Accepted August 22, 2019

Abstract

The present study designates the length-frequency distributions (LFDs), temporal variations of relative growth pattern and relative condition factor (K_R) of the *Glossogobius giuris*, which are evidently lacking in the literature. Sampling was done in the Garai River, southwestern Bangladesh using traditional fishing gears (*Doar* and Cast net) from March 2016 to February 2017. Total length (TL) was measured by digital slide calipers, while individual body weight (BW) was determined using digital electronic balance. A total of 972 specimens (male = 446, female = 526) ranging from 3.4 to 28.0 cm TL and 0.3 to 212.0 g BW were analyzed in this study. The LFDs showed that the 6.99−9.99 cm TL size group was dominant for both sexes, constituted 46% for males and 41% for females of its population, respectively. The allometric coefficient (*b)* values were 2.89 for males and 2.92 for females, which indicated that the relative growth pattern was negative allometric ($b< 3.00$) in both sexes. The LWRs were significantly different between males and females (ANCOVA, $p < 0.001$). Minimum value of K_R was found in April and maximum value in December for male. For the female, minimum value was found in January and maximum value in December. The K_R were not significantly different between males and females (ANCOVA, p=0.9745). These results will help further studies on the population assessment as well as stock assessment of the *G. giuris*. Furthermore, this research has established a strong base for monitoring the biological changes of this important species due to high fishing pressure, climate changes or other reasons within the Garai River ecosystem or elsewhere.

Keywords: Temporal variations, length-weight relationship, condition factor, *Glossogobius giuris*, Garai River

1. Introduction

The Tank gobi, *Glossogobius giuris* (Hamilton, 1822) (Perciformes: Gobiidae) is broadly distributed in Africa to Oceania, Madagascar to India and the Indian subcontinent to China (Froese and Pauly, 2019). It is commonly known as *Bele, Balia, Bekukor, Bulla, Bakla, Tenk dikkop,* and *Weligouva* in the Bangladesh, India, Malaysia, Nepal, Philippines, South Africa, and Sri Lanka, respectively (Talwar and Jhingran, 1991; Froese and Pauly, 2019). The *G. giuris* is a benthopelagic, amphidromous species, and it inhabits clear to turbid, freshwaters (i.e. rivers streams, canals, ditches and ponds) to estuarine habitats with rock, gravel or sand. This species feeds on small insects, crustaceans and small fishes (Allen, 1991). It is a low fat-high protein fish, and the percentage of moisture, protein, ash, and lipid are about 85%, 15.6%, 2.94% and 1.54%, correspondingly (Islam and Joadder, 2005). The conservation status of this fish has been categorized as least concern (IUCN, 2018).

Size stucture (length-frequency distribution, LFD) represents fundamental information to assess reproductive potential of fish population (Vazzoler, 1996). In riverine fish, the study of the LFD expresses the river health, stock status and fish spawning period (Ranjan *et al.,* 2005) as well as reflects the interaction of the dynamic rate of growth, recruitment and mortality (Neuman and Allen, 2001).

The relationship between length and weight (LWR) − along with condition factors− is useful parameters for the assessment of the well-being of individuals and determines probable variations among different stocks of the same species (King, 2007). Furthermore, condition factor is important for assessing the well-being of the fish and also prediction of future population success by its influence on growth, reproduction, and survival (Richter, 2007).

However, a number of studies have been conducted on different aspects of *G. giuris* including reproduction (Allen, 1991), LWRs, and LLRs in the Ganges River, Bangladesh (Hossain *et al*., 2009a, 2009b), LWRs in the Pampanga River, Philippines, and in the estuaries of South Africa (Harrison, 2001; Garcia, 2010). Therefore, this is the first description on temporal variation of the relative growth pattern and relative condition factor of *G. giuris*

* Corresponding author e-mail: hossainyeamin@gmail.com.

using monthly data over a one year study period in the Garai River, southwestern Bangladesh.

2. Materials and Methods

2.1. Study site and sampling period

The present study was conducted in the Garai River (a distributary of the Padma River), southwestern region of Bangladesh (Latitude: 23° 32' N; Longitude: 89° 31' E). Monthly samples of *G. giuris* were collected from the fisherman catch landed at the several points (*Mohanagar* Track, *Barokhada Ghat*, *Ganga-Kopotakkho Ghat*, *Ghora Ghat*) of Kushtia during March 2016 to February 2017. This fish is usually caught by different types of nets (gill nets, cast nets, stake nets, lift nets, etc) and traps (*Doar*, *Kholson* etc). After catching, the samples were immediately preserved with ice on site and then were fixed with 5 % formalin solution.

2.2. Fish measurement

For each individual, total length (TL) was measured to the nearest 0.01 cm using digital slide calipers and whole body weight (BW) was taken on a digital electronic balance with 0.01 g accuracy. All specimens were sexed by gonad observation under a microscope.

2.3. Population structure

The length frequency distribution for *G. giuris* was constructed using 1.0 cm intervals of TL.

2.4. Growth pattern

The LWR was calculated using the expression: $BW= a*(TL)^b$. Parameters a and b were estimated by linear regression analysis based on natural logarithms: $ln\ (W) = \ln(a) + b\ ln\ (L)$. Additionally, 95% confidence limits of a and b, and the coefficient of determination r^2 were estimated. Based on Froese, (2006), all extreme outliers were excluded from the analyses. A t-test was applied to determine significant differences from the isometric value of $b = 3$ (Sokal and Rohlf, 1987) to characterize the growth patterns to either isometric or (+/-) allometric.

2.5. Condition factor (KR)

The relative condition factor (K_R) for each individual was calculated using the equation of Le Cren (1951): $K_R = W/(a\times L^b)$, where W is the BW, L is the TL, and a and b are the LWR parameters.

2.6. Statistical analyses

Statistical analyses were done using Microsoft® Excel added in solver, Graph Pad Prism 6.5. Tests for normality of each group were confirmed with the Shapiro-Wilk normality test. The homogeneity of variance was also checked. Where test for normality assumption was not met, the nonparametric Mann-Whitney U test was used to compare TL, BW, K_R between sexes. The Spearman rank test was used to correlate TL and BW with K_R. In addition, analysis of covariance (ANCOVA) was applied to justify the significant differences between sexes for the slopes (b) of the regression lines of LWRs. All statistical analyses were considered significant at 5% ($p<0.05$).

3. Results

3.1. Population structure

A total of 972 specimens (male = 446, female = 526) ranging from 3.4 to 28.0 cm TL and 0.3 to 212.0 g BW were analyzed in this study. The minimum and maximum size range of males and females were 3.4 to 28.0 and 3.5 to 27.5 cm in TL, respectively. Additionally, LFDs showed that the 6.99–9.99 cm TL size group was numerically dominant for both sexes, constituted 46% for males and 41% for females of its population (Figure 1). The Mann-Whitney U-test showed no significant differences in the LFDs between sexes (U = 114545, p=0.5280). In addition, BW of females (0.33-210 g; 95% CL = 15.42-19.62 g) was less than males (0.30-212 g; 95% CL=14.88-18.97 g). The differences between the sexes were not statistically significant (Mann-Whitney U=115782, p = 0.7282).

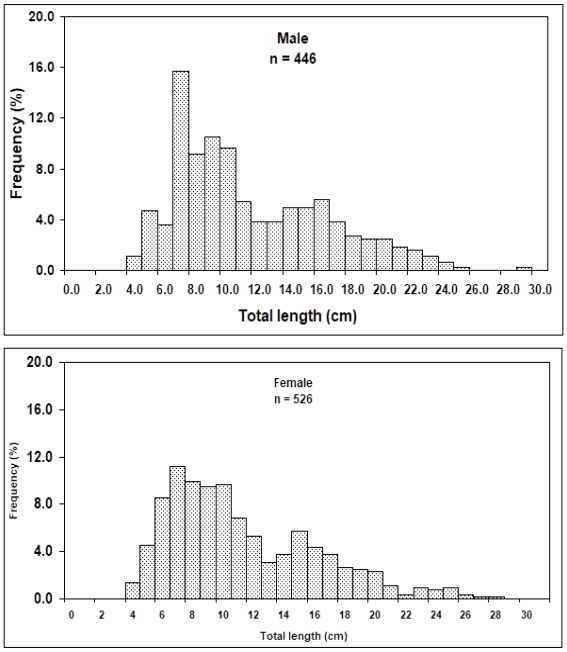

Figure 1.The length-frequency distribution of male and female *Glossogobius giuris* in the Garai (Padma River distributary) River, southwestern Bangladesh

3.2. Relative growth pattern

Monthly length and weight measurements, sample sizes (n), regression parameters and 95% confidence limit for a and b of the LWR, and coefficients of determination (r^2) of *G. giuris* in the Garai River are summarized in Table 1 and 2. The b values for TL-BW relationships (Figure 2) indicate positive allometric growth ($b > 3.00$) in January for male and in November for both male and female. Isometric (b=3.00) for female in January and for males in May and September. The b values of TL-BW relationships indicate negative allometric growth ($b< 3.00$) for both male and female in February, April, June, October and December (Figure 3).

The overall b value for LWR indicates a significantly negative allometric growth (> 3.00) in male (95% CL of b = 2.86-2.92) and female (95% CL of b = 2.89-2.95). All LWRs were significant ($p < 0.01$) with all r^2 value being ≥ 0.986, and analysis of covariance (ANCOVA) reveals significant difference in LWRs between sexes ($p <$ 0.0001).

Table 1. Descriptive statistics on the total length (cm) and body weight (g) measurements of *Glossogobius giuris* (Hamilton, 1822) in the Garai River of southwestern Bangladesh during March 2016 to February 2017

Month	Sex	*n*	TL (cm)				BW (g)			
			Min	Max	Mean ± SD	95% CL	Min	Max	Mean ± SD	95% CI
March	M	33	8.1	28	11.50 ± 4.15	10.03 – 2.98	4.1	212.00	21.39 ± 37.72	8.02–34.77
	F	47	8.1	27.5	12.12 ± 3.82	11.00 – 3.25	4.99	210.00	22.21 ± 32.00	12.82–31.61
April	M	27	7.3	21.1	11.45 ± 3.75	9.97 –12.94	3.90	76.40	17.05± 17.14	10.28–23.84
	F	53	7.9	23.2	11.49 ± 3.35	10.57 – 2.42	4.18	78.32	17.43 ± 15.37	13.20–21.67
May	M	34	4.5	23.8	14.61 ± 5.44	12.71–16.51	0.93	98.71	33.65 ± 26.63	24.36–42.95
	F	46	4.6	24.1	14.41 ± 5.63	12.75–16.09	1.10	140.21	35.13 ± 34.20	24.98–45.29
June	M	40	5.2	19.2	8.29 ± 3.79	7.08–9.50	1.35	59.00	8.55 ± 13.72	4.17–22.95
	F	40	5.1	24.2	7.68 ± 4.39	6.28–9.09	1.16	115.00	9.49 ± 23.63	1.94–17.05
July	M	45	4.7	22.1	11.80± 4.34	10.49–13.10	0.89	1.15	18.57 ± 17.81	13.22-23.92
	F	35	4.9	20.5	10.76 ± 5.21	8.96–12.55	0.91	72.96	18.61 ± 23.57	10.51–26.71
August	M	36	7.1	22.5	14.41 ± 4.00	13.06–15.77	4.57	80.77	27.09 ± 21.01	19.98–34.20
	F	44	7.3	19.8	13.65 ± 3.53	7.30–19.80	3.50	56.40	24.04 ± 16.21	19.09–28.94
September	M	34	12.0	20.0	15.39 ± 1.92	14.80–15.99	12.95	61.04	31.02 ± 11.65	27.43–34.60
	F	37	12.2	19.3	14.94 ± 1.58	14.41–15.46	14.09	60.32	19.63 ± 9.73	26.38–32.87
October	M	39	3.4	20.4	8.17 ± 4.87	6.59–9.75	0.30	23.78	8.23± 12.75	4.09–12.36
	F	41	3.5	17.4	7.03 ± 4.04	5.75–8.30	0.33	34.8	5.39 ± 9.10	2.45–8.26
November	M	32	4.5	9.5	6.93 ± 1.42	6.42–7.44	0.68	6.93	3.26 ± 1.84	2.60–3.93
	F	48	3.7	9.5	6.58 ± 1.30	6.20–6.96	0.40	7.96	2.95 ± 1.70	2.45–3.44
December	M	36	4.6	22.0	8.07 ± 3.97	6.93–9.42	0.63	77.33	8.32 ± 16.62	2.70–13.95
	F	44	4.0	21.5	7.97 ± 3.55	6.89–9.05	1.17	77.45	7.56 ± 14.93	3.02–12.10
January	M	37	6.7	10.9	8.39 ± 1.15	8.00 – 8.78	2.54	12.30	5.77 ± 2.64	4.89–6.65
	F	36	5.8	16.0	9.28 ± 1.90	8.63 – 9.92	1.57	34.84	8.19 ± 6.43	6.02–10.37
February	M	44	4.3	24.7	10.85 ± 5.67	9.13 – 12.58	0.67	115.29	19.04 ± 30.00	9.92–28.17
	F	55	4.6	26.9	12.12 ± 6.30	10.42 –3.83	0.89	146.55	26.80 ± 38.87	16.29–37.31

n, sample size; M, male; F, female; TL, total length (cm) W, body weight (g); min, minimum; max, maximum, SD, standard deviation; CL, confidence limit

Table 2. Descriptive statistics and estimated parameters of the length-weight relationships ($W=a\times TL^{b}$) of *Glossogobius giuris* (Hamilton, 1822) in the Garai River of southwestern Bangladesh during March 2016 to February 2017

Month	Sex	*n*	Regression parameters				r^2	t_s	GT
			a	*B*	95% CL of *a*	95% CL of *b*			
March	M	33	0.0091	3.01	0.0064 – 0.0130	2.86 – 3.16	0.98	-0.11	I^{ns}
	F	47	0.0106	2.95	0.0076 – 0.0147	2.81 – 3.08	0.97	-0.71	I^{ns}
April	M	27	0.0182	2.71	0.0139 – 0.0237	2.60 – 2.82	0.99	-5.80	$-A^{***}$
	F	53	0.0160	2.78	0.0107 – 0.0239	2.62 – 2.95	0.95	-2.75	$-A^{***}$
May	M	34	0.0161	2.75	0.0129 – 0.0201	2.66 – 2.83	0.99	-6.25	$-A^{***}$
	F	46	0.0128	2.83	0.0100 – 0.0165	2.73 – 2.93	0.98	-3.40	$-A^{***}$
June	M	40	0.0108	2.90	0.0084 – 0.0140	2.78 – 3.03	0.98	-1.66	$-A^{***}$
	F	40	0.0095	2.96	0.0076 – 0.0119	2.85 – 3.07	0.98	-0.80	I^{ns}
July	M	45	0.0100	2.93	0.0075 – 0.1340	2.80 – 3.05	0.98	-1.75	$-A^{***}$
	F	35	0.0074	3.04	0.0052 – 0.0107	2.88 – 3.19	0.97	-0.50	I^{ns}
August	M	36	0.0193	2.65	0.0123 – 0.0301	2.48 – 2.80	0.96	-4.37	$-A^{***}$
	F	44	0.0185	2.69	0.0121 – 0.0284	2.52 – 2.85	0.96	-3.87	$-A^{***}$
September	M	34	0.0070	3.05	0.0043 – 0.0115	2.87 – 3.23	0.96	0.55	I^{ns}
	F	37	0.0094	2.97	0.0050 – 0.0177	2.73 – 3.19	0.95	-0.25	I^{ns}
October	M	39	0.0099	2.89	0.0088 – 0.0112	2.79 – 2.91	0.99	-3.66	$-A^{**}$
	F	41	0.0096	2.88	0.0082 – 0.0112	2.79 – 2.96	0.99	-3.00	$-A^{**}$
November	M	32	0.0071	3.10	0.0049 – 0.0103	2.90 – 3.29	0.97	1.11	$+A^{***}$
	F	48	0.0068	3.16	0.0051 – 0.0092	2.99 – 3.31	0.97	2.28	$+A^{***}$
December	M	36	0.0156	2.74	0.0110 – 0.0221	2.56 – 2.91	0.96	-3.25	$-A^{**}$
	F	44	0.0190	2.65	0.0128 – 0.0283	2.45 – 2.84	0.95	-3.88	$-A^{***}$
January	M	37	0.0055	3.25	0.0033 – 0.0086	3.03 – 3.47	0.96	2.27	$+A^{***}$
	F	36	0.0093	2.99	0.0096 – 0.0131	2.83 – 3.15	0.98	-0.14	I^{ns}
February	M	44	0.0090	2.94	0.0083 – 0.0098	2.90 – 2.97	0.99	-0.50	I^{ns}
	F	55	0.0104	2.90	0.0096 – 0.0113	2.87 – 2.94	0.99	-5	$-A^{***}$

n, sample size; M, male; F, female; *b* are length-weight relationships parameter; CL, confidence limit; r^2, co-efficient of determination; GT, growth type; -A, negative allometric growth; I, isometric growth; +A, positive allometric growth

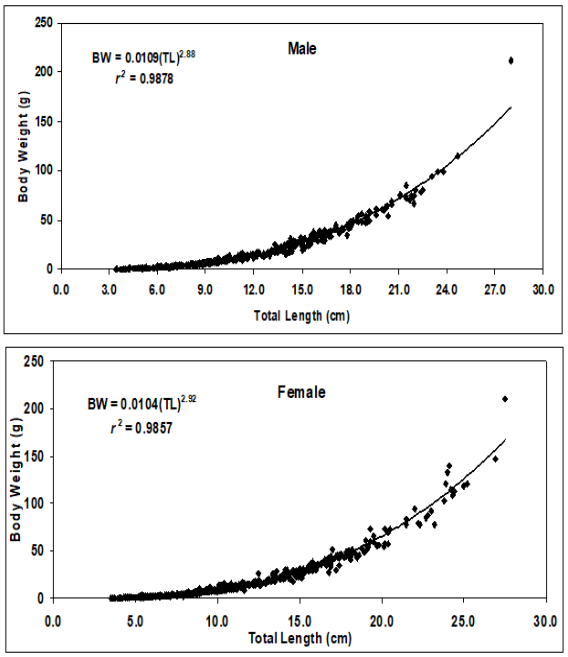

Figure 2. The relationships (BW= aL^b) between body weight (BW) and total length (TL) of the overall male, female of *Glossogobius giuris* in the Garai (Padma River distributary) River, southwestern Bangladesh

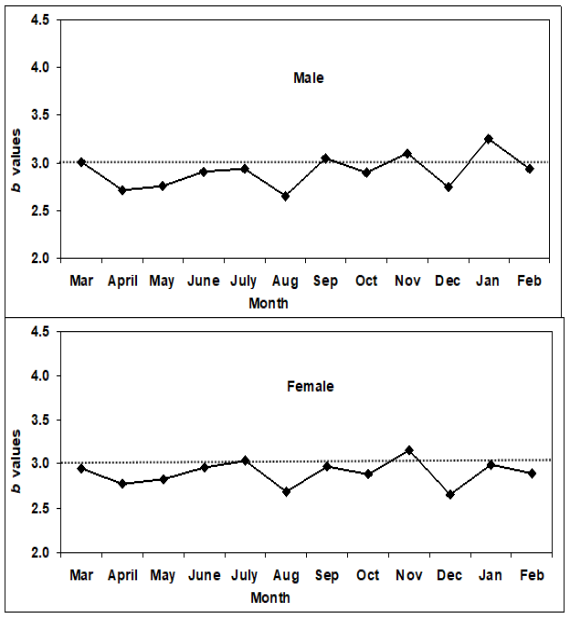

Figure 3. Monthly variations of the *b* values for male and female of *Glossogobius giuris* in the Garai (Padma River distributary) River, southwestern Bangladesh

3.3. Relative condition factor (KR)

The minimum and maximum value of relative condition factor (K_R) for both male and female were 1.00 to 1.01 and 1.00 to 1.03, respectively. The effect of month on the relative condition factor was similar to that of size, where male K_R value decreased from January to the April, and increased from April to the July; then from the July to the October it decreased and increased to the December. For the female K_R, the value increased from January to the April then slightly went down from the April to June and suddenly increased to July then dramatically went down to October then increased to December (Figure 4). The K_R value was almost similar for both male and female which was near about 1 (≤1) in every month. So, the growth rate of *G. giuris* was well balanced throughout the year.

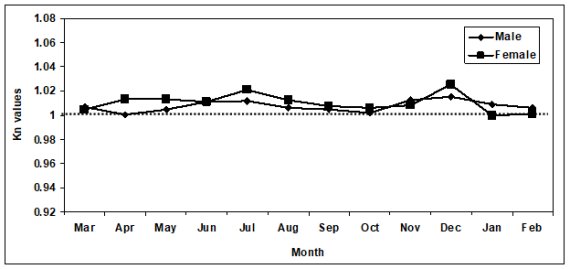

Figure 4. Monthly variations of the Relative condition factor (K_R) for male and female of *Glossogobius giuris* in the Garai (Padma River distributary) River, southwestern Bangladesh

4. Discussion

Information on temporal variation of population structure and growth pattern of *G. giuris* is very limited in literature. In this study, a large number of individuals with different body sizes were collected from the Garai River using traditional fishing gear all over the year to describe the temporal variations in LWRs and condition of this fish

In this study, sampling of individuals smaller than 3.4 cm in TL and 0.3 g in BW was not possible, which can be ascribed to selectivity of fishing gear rather than their absence on the fishing ground or fishermen not fishing where the smaller sizes exist (Azad *et al*., 2018; Hossain *et al*., 2012, 2017a, b; Nawer *et al*., 2017). The LFDs showed that the 6.99–9.99 cm TL size group was numerically dominant for both sexes, constituting 46% and 41% of its population, accordingly, although statistically there were not significantly different. In our works, the maximum TL of *G. giuris* was 28.0 cm, which is much higher than the value of 17.9 cm from the Ganges River, Bangladesh (Hossain *et al*., 2009a); 19.5 cm from Lakes of Agusan Marsh, Philippines (Jumawan and Seronay, 2017) and 17.5 cm from the Hongshui River, Southwest China (Que *et al*., 2015) but lower than the maximum recorded value of 50.0 cm SL reported from the freshwater fishes of Tanzania (Eccles, 1992) and 25.8 cm in the lower part of the Ganges River, Bangladesh (Hossain *et al.*, 2009a).

The allometric coefficient *b* may differ between 2.0-4.0; however, values ranging from 2.5-3.5 are more common (Carlander, 1969; Froese, 2006). In the present study, the *b* values of LWR remained within the range of 2.89–2.93 (*b*= 2.86–2.92 for males and *b*= 2.89–2.95 for females), which is consistent with the expected range for teleost species (Froese, 2006). In the present study, the overall *b* for the relative growth pattern indicated negative allometric growth (< 3.00) in both males and females. Similar growth pattern (*b* value for male = 2.95 and female = 2.29) were reported by Hossain *et al*. (2009b) for *G. giuris* from Ganges River, northwestern Bangladesh. According to Froese (1998), the growth pattern of *G. giuris* was negative allometric (*b*=2.90). Negative growth pattern was also stated by Que *et al*. (2015) and Islam *et al*. (2017) for this fish from the Hongshui River, southwest China and Brahmaputra River, Bangladesh, respectively. Conversely, isometric growth was detected by Hossain *et al*. (2009a) (*b*=3.03); Garica (2010) (*b*=3.06) and Harrison (2001) (*b*=3.06) while positive allometric growth (*b* = 3.16 & *b*=3.29) was recorded by Hossain *et al*. (2009b) for both male and female *G. giuris* from the Ganges River, Bangladesh. In this present study, December month shows highest K_R value for male 1.02 and female 1.03. This

indicates that both males and females are in better condition in the month of December. It is not possible to compare others due to lack of available studies on this aspect. However, the differences in relative growth pattern can be credited due to numerous factors including, habitat availability, seasonal effect and level of stomach fullness (Hossain *et al.*, 2013, 2018), which were not considered in this study.

To sum up, our findings describe the length-frequency distribution, temporal variation of relative growth pattern based on LWR and condition of *G. giuris*. LWRs would be useful in fishery management for both applied and basic use to: (i) estimate weight from length observations; (ii) calculate production and biomass of a fish population; and/or (iii) provide information on stocks or organism condition at the corporal level. The result of this study will provide an important baseline for future studies and would be very effective for stock assessment of *G. giuris* in the Garai River and adjoining ecosystems.

Acknowledgments

The authors would like to extend their sincere appreciation to (i) TWAS for research grants (Ref: RGA No. 14-028 RG/BIO/AS_1; UNESCO FR: 324028574), (ii) BARC, PIU, NATP-2, Sub-project ID: 484 for technical (usage of equipment's) supports. The present study is part of the research for Ph.D degree for the senior author M.A.K. Azad.

Conflicts of Interest

The authors declare that there is no conflict of interest regarding the publication of the present paper.

References

Allen GR. 1991. Field guide to the freshwater fishes of New Guinea. Christensen Research Institute, Madang, Papua New Guinea. 268p.

Azad MAK, Hossain MY, Khatun D, Parvin MF, Nawer F, Rahman O and Hossen MA. 2018. Morphometric Relationships of the Tank goby *Glossogobius giuris* (Hamilton, 1822) in the Gorai River using Multi-linear Dimensions." *Jordan J Biol Sci.,* **11**: 81–85.

Bagenal JB and Tesch FW.1978. Methods for assessment of fish production in freshwaters. Blackwell Scientific publication, Oxford, p. 361.

Carlander KD. 1969. Handbook of freshwater fishery biology. The Iowa State University Press. Ames, IA, **1**:752.

Dall W, Hill BJ, Rothlisberg PC and Staples DJ. 1990. Biology of the Penaeidae. In: Blaxter, J.H.S., Southward, A.J. (Eds.), Advances in Marine Biology. Academic Press, London, UK, 27: 489

Eccles DH. 1992. FAO species identification sheets for fishery purposes. Field guide to the freshwater fishes of Tanzania. Prepared and published with the support of the United Nations Development Programme. FAO, Rome. 145 p.

Froese R and Pauly D. (Eds). 2019. Fish base 2019. World Wide Web electronic publication. Available at: http://www.fishbase.org.

Froese R. 1998. Length-weight relationships for 18 less-studied fish species. *J Appl Ichthyol.,* **14**: 117-118.

Froese R. 2006. Cube law, condition factor and weight-length relationships: History, meta-analysis and recommendations. *J Appl Ichthyol.,* **22**: 241-253.

Garcia LMB. 2010. Species composition and length-weight relationship of fishes in the Candaba wetland on Luzon Island, Philippines. *J Appl Ichthyol.,* **26**: 946-948.

Harrison TD. 2001. Length-weight relationships of fishes from South African estuaries. *J Appl Ichthyol.,* **17**: 46-48.

Hossain MY, Arefin MS, Mohmud MS, Hossain MI, Jewel MAS, Rahman MM, Ahamed F, Ahmed ZF and Ohtomi J. 2013. Length-weight relationships, condition factor, gonadosomatic index-based size at first sexual maturity, spawning season and fecundity of *Aspidoparia morar* (Cyprinidae) in the Jamuna River (Brahmaputra River distributary), northern Bangladesh, *J Appl Ichthyol.,* **29**: 1166-1169

Hossain MY, Hossen MA, Pramanik MNU, Ahmed ZF, Hossain MA and Islam MM. 2016. Length–weight and length–length relationships of three Ambassid fishes from the Ganges River (NW Bangladesh). *J Appl Ichthyol*., **32**: 1279-1281.

Hossain MY, Hossen MA, Khatun D, Nawer F, Parvin MF, Rahman O and Hossain MA. 2017a. Growth, condition, maturity and mortality of the Gangetic Leaffish *Nandus nandus* (Hamilton, 1822) in the Ganges River (Northwestern Bangladesh). *Jordan J Biol Sci.,* **10**: 57–62.

Hossain MY, Hossen MA, Ali MM, Pramanik MNU, Nawer F, Rahman MM, Sharmin S, Khatun D, Bahkali AH, Elgorban AM and Yahya K. 2017b. Life-History traits of the Endangered carp *Botia dario* (Cyprinidae) from the Ganges River in Northwestern Bangladesh. *Pakistan J Zool.,* **49**: 801–809.

Hossain MY, Rahman MM, Bahkali AH, Yahya K, Arefin MS and Hossain MI. 2016. Temporal variations of sex ratio, length-weight relationships and condition factor of *Cabdio morar* (Cyprinidae) in the Jamuna (Brahmaputra River distributary) River, northern Bangladesh. *Pakistan J Zool.,* **48**: 1099–107.

Hossain MY, Pramanik MNU, Hossen MA, Nawer F, Khatun D, Parvin MF, Rahman O, Ahmed ZF and Ahamed F. 2018. "Life-history traits of the Pool barb *Puntius sophore* (Cyprinidae) in different ecosystem of, Bangladesh." *Indian J G Mar Sci.,* **47**: 1446-1454.

Hossain MY, Rahman MM, Miranda R, Leunda PM, Oscoz J, Jewel MAS, Naif A and Ohtomi J. 2012. Size at fist sexual maturity, fecundity, length-weight and length-length relationships of *Puntius sophore* (Cyprinidae) in Bangladeshi waters, *J Appl Ichthyol.,* **28**: 818-822

Hossain MY, Ohtomi J, Ahmed ZF, Ibrahim AHM and Jasmine S. 2009a. Length-weight and morphometric relationships of the tank goby *Glossogobius giuris* (Hamilton, 1822) (Perciformes: Gobiidae) in the Ganges of the northwestern Bangladesh. *Asian Fish Sci.,* **22**: 961-969.

Hossain MY, Jasmine S, Ibrahim AHM, Ahmed ZF, Rahman MM and Ohtomi J. 2009a. Length-weight and length-length relationships of 10 small fish species from the Ganges, Bangladesh. *J Appl Ichthyol.,* **25**:117-119.

Hossen MA, Hossain MY, Ali MM, Pramanik MNU, Nawer F, Islam MA, Hossain MA, Bahkhali AH and Elgorban MA. 2017. Seasonal variations of growth pattern and condition of Paradise threadfin *Polynemus paradiseus* (Polynemidae) from Tetulia River in Southern Bangladesh. *Indian J G Mar Sci.,* **46**: 582–590.

Islam MR, Azom MG, Faridullah M and Mamun M. 2017. Length-weight relationship and condition factor of 13 fish species collected from the Atrai and Brahmaputra rivers, Bangladesh. *J Bio Env Sci.,* **10**: 123-133.

Islam, MN and Joadder MAR. 2005. Seasonal variation of the proximate composition of freshwater Gobi, *Glossogobius giuris* (Hamilton) from the river Padma. *Pakistan J Biol Sci.,* **4**: 532-536.

IUCN. 2018. The IUCN Red List of Threatened Species. Version 2018-2. Downloaded on 19 November 2018.https:// www.iucnredlist.org.

Jumawan JC and Seronay RA. 2017. Length-weight relationships of fishes in eight floodplain lakes of Agusan Marsh, Philippines. *Phil J Sci.,* **146**:95-99.

Nawer F, Hossain MY, Hossen MA, Khatun D, Parvin MF, Ohtomi J and Islam MA. 2017. Morphometric relationships of the endangered Ticto barb *Pethia ticto* (Hamilton, 1822) in the Ganges River (NW Bangladesh) through multi-linear dimensions. *Jordan J Biol Sci.*, **10**: 199–203.

Neuman, RM and Allen MS. 2001. Analysis and Interpretation of Freshwater Fisheries Data. Department of Natural Resources Management and Engineering, University of Connecticut.

Que YF, Pan L, Chen F, Xie S, Liao XL and Zhao N. 2015. Length-weight relationships of thirty-seven fish species from the Hongshui River, Southwest China. *J Appl Ichthyol.*, **31**: 804-806.

Ranjan JB, Herwig W, Subodh S and Michael S. 2005. Study of the length frequency distribution of sucker head, *Garra gotyla* (Gray, 1830) in different Rivers and Seasons in Nepal and its Applications. *Kathmandu Uni J Science Eng Tech.*, **1**:1–14.

Richter TJ. 2007. Development and evaluation of standard weight equations for bridgelip sucker and large scale suckers, N Am J Fish Manage., **27**:936-939

Talwar PK and Jhingran AG. 1991. Inland Fishes of India and Adjacent Countries. A.A Balkema, Rotterdam, p.541.

Tesch FW. 1971. Age and Growth. In Methods for Assessment of Fish Production in Fresh Waters, edited by Ricker, W.E. Oxford: Blackwell Scientific Publications, 98-130 pp.

Vazzoler AEAM. 1996. Reproduction Biology of Teleostean Fishes. Theory and Practice. Maringá, EDUEM, Brazilian Society of Ichthyology, 169p.

JJBS

Volume 13, Number 2,June 2020
ISSN 1995-6673
Pages 237 - 245

Jordan Journal of Biological Sciences

Therapeutic and Prophylactic Efficacy of Garden Cress Seed Oil against Osteoporosis in Rats

Aida I.El makawy[1*], Dalia M. Mabrouk[1], Faten M. Ibrahim[2], Sekena H. Abdel-Aziem[1] and Hafiza A. Sharaf[3]

[1]Cell Biology Department; [2]Medicinal and Aromatic Plants Research Dept., Division of Pharmaceutical and Drug Industries Research;[3]Pathology Department, National Research Center, 33 El Bohouth St., Dokki, Giza, P.O.12622, Egypt

Received July 30, 2019; Revised August 23, 2019; Accepted August 27, 2019

Abstract

The target of this study was to estimate the efficacy of garden cress seed oil in the treatment of osteoporosis in rats. Seventy adult female Sprague-Dawley albino rats were used that were divided into seven groups (n-10/ group). Methotrexate (MTX) was subcutaneously injected (0.65 mg/kg) for two separate 5 days courses (5 days on/9 days off), to induce osteoporotic rat model. Garden cress seed oil was orally gavages with two patterns: the therapeutic pattern in which rats were orally gavages with oil in two doses (200 and 400 mg/ kg b w) after completion of injection of methotrexate. The prophylactic pattern rats were injected with methotrexate in concurrent with the oil at the same doses. The oils injection period for the two treated pattern was four weeks. After the completion of the treatment, animals were anesthetized and blood samples were collected for biochemical analysis. Femoral bones of the treated and control groups were collected to study the expression of genes associated with bone remodeling (Cathapsin K and TNF-αand Osterix). Bones histopathological and morphometric studies were performed. Garden cress oil improved minerals and vitamin D content in osteoporotic animals. The results of the gene expression showed that the oil reduced the gene expression level of Cathapsin K and TNF-α, while increased the level of Ostrix, leading to improving the histological structure and bone thickness of the osteoporotic animals. Garden cress seed oil considerably improved the osteoporosis bone marker through both therapeutic and prophylactic approaches. In addition, data revealed that the therapeutics pattern was more alleviative than prophylactic.

Keywords: Osteoporosis, Minerals, Vitamin D, Bone remodeling genes, Bone morphometric.

1. Introduction

Osteoporosis is a metabolic bone disease resulting in an imbalance of bone remodeling, in which the rate of bone resorption is higher than bone formation (lama *et al*., 2017). In turn, this provides rise to low bone mass, micro-architectural deterioration, and finally an increased risk for fragility fractures (Sucuoglu & Koyuncu, 2017; Poole *et al*., 2017). Methotrexate (MTX) is a folic acid antagonist and it is the most commonly used anti-metabolite agent for different malignancies such as choriocarcinoma and osteogenic sarcoma (Fan *et al*., 2012). MTX is used as first line therapy in treatment of rheumatoid arthritis (RA) and other inflammatory diseases such as psoriasis and dermatomyositis (Minaur *et al*., 2002). MTX was known to cause reduced bone mineral density (BMD), fractures and ingrowths defects (Fischer *et al*., 2005). The current utilize of oral corticosteroids is allied with severe side effects, include osteoporosis (Henneicke *et al*. 2014).

Osteoporosis recent therapies focus on stopping bone resorption and reducing bone remodeling (Wu *et al*., 2017). Parathyroid hormone, and its analogue teriparatide, is the only anabolic therapies obtainable to treat osteoporosis (Reginster *et al*., 2013). The existing drug therapies have been established to improve bone mineral density and moderate fracture risk, but prolonged use has been allied with various side effects (Hough *et al*., 2014). Consequently, the exploration for new drugs is continuing (Fouda *et al*., 2017). The osteoporosis prophylactic agents are restricted to calcium and vitamin D. Epidemiological studies have explored the connotation between fruits and vegetables ingestion and bone health. Most observational studies establish that more intakes of fruits and vegetables are linked with growth in bone mass and reductions in bone loss and fracture risk (Xie *et al*., 2013; Byberg *et al*., 2015; Benetou *et al*., 2016).

Natural products of plant origin as drugs alternative sources are still a main part of traditional medical schemes in developing countries. *L. sativum* (family cruciferae) is cultivated in Egypt by three species: *L. latifolium*, *L. sativum* and *L. aucheri*. The most public one is *L. sativum* and its seeds can be used as functional food (Sakran *et al*., 2014). Garden cress (*Lepidium sativum*) is a high-nutrient plant and has considerable content of vitamins A, C and K and dietary minerals. Garden cress is an excellent source of folic acid, linoleic acid and tocopherols (Datta *et al*., 2011). Seeds, leaves and roots of Garden cress (GC) are commercially vital for their useful pharmaceutical compounds and are utilized in traditional medicine (Pinheiro *et al*., 2011; Mohammad *et al*., 2012; Kashani *et al*., 2013). Garden cress is considered as one of the popular

* Corresponding author e-mail: eaelmakawy@yahoo.com.

medicinal plants used in numerous Arab countries as a good mediator for bone fracture healing (Wadhwa *et al*. 2012). The seeds have carbohydrates, phenolic compounds, flavonoids, proteins, saponins and lipids. Oleic and linolenic acids are the crucial fatty acids in *L. sativum* oil and it has worthy quantity of lignans and antioxidants that can stabilize the n-3 polyunsaturated fatty acids. The plant is recognized to have imidazole, lepidine, semilepidinoside A and B, β-carotenes, ascorbic, palmitic, stearic, sinapic and sinapin acids (Bryan *et al*., 2009).

The objective of the present research was the evaluation the efficacy of Garden cress seed oil as a therapeutic and prophylactic agent in Methotrexate induced osteoporotic rats through biochemical studies to evaluate minerals and vitamin D content and histological as well as morphometric studies. The relationship between the role of plants in improving bone health and expression of genes that regulate bone formation was also studied.

2. Materials and Methods

2.1. Drugs

Methotrexate vial was obtained from EIMC United Pharmaceuticals Company (Cairo-Egypt). Garden cress seed oil (GCSO) was obtained from Haraz Co. Cairo, Egypt.

2.2. Experimental design

Seventy adult female Sprague-Dawley albino rats at the age of 5 weeks, weighing approximately (100-150 g) were obtained from the animal house of National Research Centre, Giza, Egypt. Animals were housed in clear plastic cages with stainless steel wire lids and kept in an animal room with controlled environmental conditions (12-h light/12-h dark cycle, temperature 22 ºC) on closed ventilated shelves. The animals were fed on rat chow pellets and received water *ad libitum.* The Ethics Committee of the National Research Centre (Approval No. 19032) approved the research. Rats were randomly categorized into seven groups of ten animals each. Rats were adapted for one week prior to commencement of the experiment. Irrespective of their allocated treatment groups, all rats received daily subcutaneous injections of MTX as well as oral gavages of GCSO with prophylactic and therapeutic pattern. The MTX group was subcutaneously injected by (0.65 mg/kg/day) for two separate 5 days courses (5 days on/9 days off) according to Fan *et al*. (2012). Garden cress oil groups was administered at 200 and 400 mg/kg once daily according to Yogesh *et al.(*2010) via oral gavages throughout the trial: for 28 days after the final MTX administration (200 and 400 GCSO Ther) and for 28 days concurrently with MTX administration (200 and 400 GCSO Pro). Control groups received oral gavages of saline as negative control and GCSO 400mg/kg.

2.3. Biochemical analyses

At the end of experiment, the rats were fasted overnight, blood samples were collected in tubes, and centrifuged at 3000 rpm under cooling for 15 min to separate the serum that was subjected to different assays. Serum calcium (Ca), phosphorus (P) levels were determined using colorimetric assay kits (BioSystems S.A., Costa Brava, Barcelona, Spain). Serum bone-specific alkaline phosphatase (b-ALP) was estimated by colorimetric assay using specific enzyme kits (Boehringer Mannheim, Germany) according to Nawawi *et al*. (2002). Serum 25(OH) D was analyzed by radioimmunoassays and competitive protein binding assays according to Holick (2005).

2.4. Bone tissue collection

The animals of each treated group were sacrificed by neck vertebra luxation. Femoral bones were isolated and washed with ice-cold saline to carry out the gene expression and histopathology studies. Right femurs were dissected out from all animals and fixed in buffer formol for the histopathological study. The left femur was collected and kept frozen at −80°C for gene expression analysis.

2.5. Real-time quantitative PCR for bone-related gene expression

RNA extraction from the rat right tibias by crushes the bones with liquid nitrogen and homogenized in Easy red total RNA extraction kit (Intronbio, Korea) according to the manufacturer's instructions. The yield and quality of RNA were analyzed using NanoDrop™ 1000 Spectrophotometer (Thermo Fisher Scientific, USA) and gel electrophoresis. RNA (1µg) was treated with RNase-free DNase kit (Promega) to remove any genomic DNA contamination and cDNA was synthesized using HiSenScript ^{TM} cDNA kit (Intronbio, Korea).

2.6. Real-time PCR analysis

Three genes (Cathepsin K, Tumer Necrosis Factor-α (TNFα) and Osterix), related to bone formation and resorption, and glyceraldehyde-3- phosphate dehydrogenase (GAPDH), endogenous control, were used in the present study; see primers properties in Table 2. Real-time polymerase chain reaction (PCR) was performed in Stratagene Mx3005P Real-Time PCR System (Agilent Technologies) in a 20µL reaction. Each 20µL PCR cocktail contained one µL cDNA, 10µl TOPreal^{TM} qPCR 2X PreMIX (SYBR Green with low ROX) (Enzynomics), 0.75µL of forward primer (10 pmol), 0.75µL of reverse primer (10 pmol) and 7.5µL ddH_2O. Amplification conditions included 15 min at 95°C , followed by 40 cycles at 95°C for 15 sec , at 58-63°C for 15sec and 72°C for 30 sec. Melting curve analysis was conducted following each real time PCR. Gene expression data were normalized to GAPDH and analyzed using the $2^{-\Delta\Delta\ Ct}$ method (Livak and Schmittgen, 2001).

Table 1. Primers Property

Gene	Accession no.	Nucleotide sequence 5´–3`	Size of PCR product (bp)
Cathepsin K	NM_007802.4	TGGATGAAATCTCTCGGCGT TCATGTCTCCCAAGTGGTTC	123
TNF	NM_013693.2	CCACCACGCTCTTCTGTCTAC ACCACCAGTTGGTTGTCTTTG	256
Osterix	NM_001348205.1	AGCGACCACTTGAGCAAACAT GCGGCTGATTGGCTTCTTCT	121
GAPDH	NM_001289726.1	AACTTTGGCATTGTGGAAGG ACACATTGGGGGTAGGAACA	223

2.7. Bone histological analysis

Right femurs were dissected out from all animals, fixed in buffer formol for 3 days and decalcified in EDTA solution (10% ethylenediaminetetraacetic acid (in 0.1 M phosphate buffer, pH 7, 8) for approximately 4 to 5 weeks (solution changed once a week). The decalcified specimens were dehydrated processed to form paraffin blocks. Serial sections (5 µm thick) from the femurs were prepared and stained by haematoxylin and eosin (H&E) for microscopic examination (Bancroft, 1994).

2.8. Morphometric study

Morphometric analysis was carried out on routine haematoxylin and eosin stained slides. To measure the mean thickness of the outer cortical bone of the middle shaft of the femur, perpendicular lines were drawn from the periosteum to the endosteum at many sites. The maximum number of osteocytes , mean areas of trabecular concellous bone and the areas of Haversian canal were measured in a ten field/five serial sections for each group at a magnification of ×50 using the image analyzer (a Leica Qwin 500 Image Analyzer (Leica Systems Ltd, Cambridge, UK) in Pathology Department, National Research Center. The results appear automatically on the monitor in the form of the distance measured in µm and area in μm^2 with the mean, SD, the minimum length, and the maximum length and area were measured.

2.9. Statistical Analysis.

Statistical analyses were conducted with SPSS19 software (IBM, New York, NY, USA). Data are expressed as the means ± standard Error (SE). Differences between groups were evaluated by one-way ANOVA followed by Duncan test. A *p*-value ≤ 0.05 was considered to indicate a statistically significant difference.

3. Results

3.1. Biochemical results

Serum calcium content in osteoporotic animals significantly decreased than in control animals. Therapeutic pattern gavages of GCSO significantly ($p\leq$ 0.05) increased the serum calcium level of osteoporotic animals to the control level. Conversely, in the prophylactic pattern GCSO at 200mg/kg significantly decreased the calcium level in MTX treated animals, while gavages of GCSO at 400mg/kg did not affect the calcium level (Figure 1A). In addition, animals administrated with high dose of GCSO alone exhibited no significant increase in calcium content compared to control.

Phosphorous content of osteoporotic animals was significantly less ($p\leq$ 0.05) than control. Garden Cress seed oil gavages with therapeutic pattern at 200mg/kg none significantly affect the phosphorus content of osteoporotic animals, while, GCSO 400mg/kg significantly ($p\leq$ 0.05) elevated the phosphorous content, while the prophylactic pattern of GCSO gavages at two doses has no change in the phosphorous content of MTX treated animals (Figure 1B). Control animals administrated with 400mg/kg GCSO showed significant decrease ($P\leq$ 0.05) in the phosphorus level than control.

Serum bone alkaline phosphatase (b-ALP) content of osteoporotic animals significantly decreased as compared to control animals,whereas GCSO (200 and 400 mg/kg) gavages with both therapeutic and prophylactic pattern induced significant increase ($p\leq$ 0.05) in the b-ALP content of osteoporotic animals. GCSO 400mg/kg gavage with therapeutic pattern was more efficient. Meanwhile, oil gavages alone significantly increased ($p\leq$ 0.05) the b-ALP content than control (Figure 1C).

Vitamin D analysis result demonstrated that osteoporotic animals showed significant reduction in the concentration of 25 OH Vitamin D as compared to control, while both the therapeutic and prophylactic pattern gavages of GCSO 200mg/kg none significantly increased the Vitamin D level in osteoporotic animals. Moreover, the 400mg/kg GCSO gavages with both two patterns significantly increased ($p\leq$0.05) the Vitamin D level of osteoporotic animals. There was no significant change in vitamin D level between the GCSO treated animals and the control (Figure 1D).

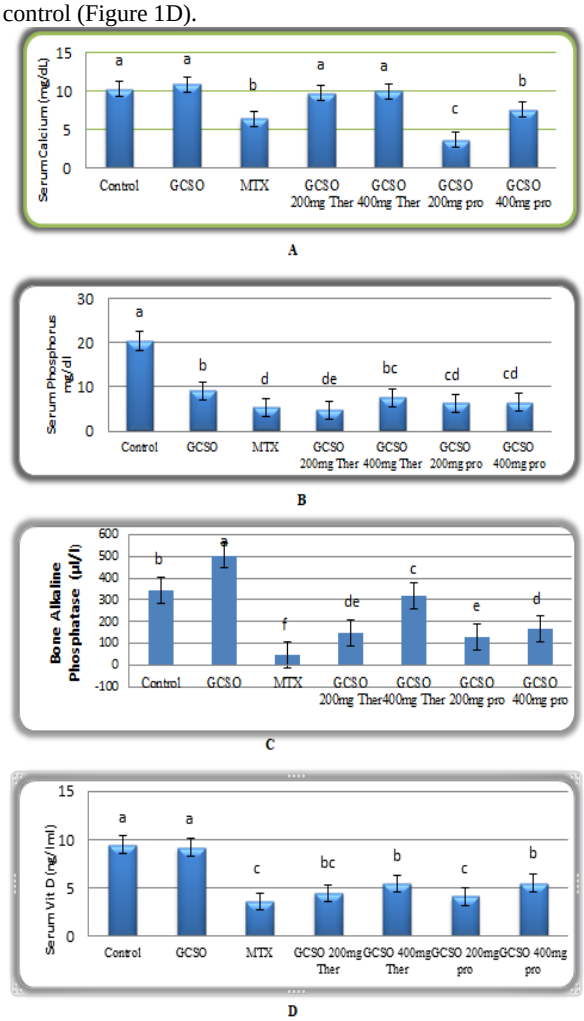

Figure 1. Effects of different doses of garden cress seed oil as therapeutic and protective pattern on serum parameters. A): calcium; B): serum phosphrous; C): bone alkaline phosphatase; D): Vitamin D in MTX osteoporotic rats. Data is presented as mean ± SE (n=5). Mean values with unlike superscript letters were significantly different ($p\leq$ 0.05).

3.2. Gene expression

The gene expression levels of Cat k and TNF-α genes involved in bone resorption and Osterix which involved in bone formation were evaluated to investigate the GCSO therapeutic and prophylactic role against the methotrexate-induced osteoporosis in female rats. Results demonstrate that osteoporotic rats had a significant increase ($p\leq$0.05) in

both Cat k and TNF-α mRNA levels when compared with the control rats. These elevations in gene expressions were significantly ameliorated by either therapeutic or prophylactic treatment with GCSO ($p \leq 0.05$) at 200 or 400 mg/kg b.w. (Figure 2A and B). On the other hand, MTX-induced osteoporotic rats showed significant decrease ($p \leq 0.05$) in Osterix mRNA levels when compared with the control rats. Garden Cress therapeutic (400 mg/kg) treated rats showed a significant mRNA levels increase ($p \leq 0.05$) when compared with the osteoporotic rats, whereas Garden Cress therapeutic (200 mg/kg) and prophylactic treated rats showed non-significant increase in mRNA levels when compared with the MTX-injected rats (figure 2C). In addition, the mRNA expression levels of Cat K, TNF-α and Osterix in rats received only Garden Cress seed oil 400mg/kg was not significantly different from their levels in the control group.

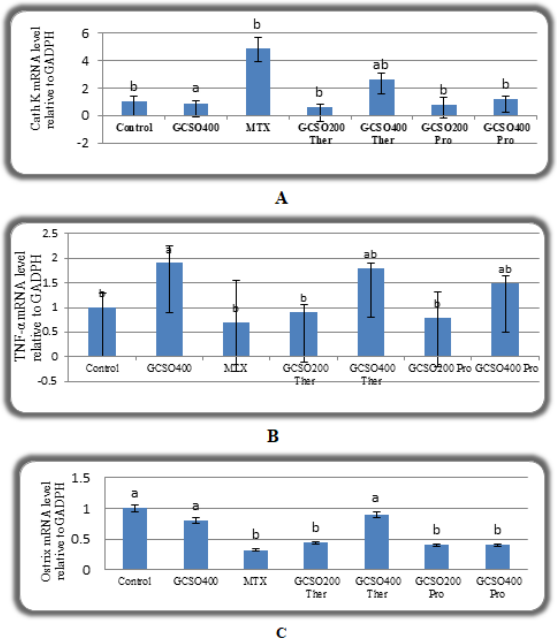

Figure 2. Representative mRNA levels for A: Cathepsin K (Cath K), B:Tumor necrosis factor-alpha (TNF-α) and C:Osterix in rats received normal saline (Control), Garden Cress seed oil at 400 mg/kg (GC400), Methoterxiate (MTX), Garden Cress seed oil as therapeutic pattern at 200 and 400 mg/kg (GCSO 200 and GCSO 400 Ther), Garden Cress seed oil as prophylactic pattern at 200 and 400 mg/kg (GCSO 200 and GCSO400 Pro). Data is presented as mean ± SE (n=5). One−way analysis of variance was used for data analysis (n=5), mean values with unlike superscript letters were significantly different ($p \leq 0.05$).

3.3. Histological and morphometric results

The stained sections of control group showed that the middle shaft of femur bone tissue was of the compact type, covered by two layers, the periosteum located externally, which is a dense connective tissue, and the endosteum, a thin cell-rich connective tissue, lining the internal surface of the bone facing the bone marrow cavity. Histologically, within the bone matrix, osteocytes in their lacunae were detected (Figure 3 A). Compact bone forms a shell around cancellous bone and is the primary component of the long bones. The cancelluos bone trabeculae was formed of a network of bones, consisted of bone lamellae in between which osteocytes stay in their lacunae and bone marrow spaces were present between trabeculae (Figure 3B) .

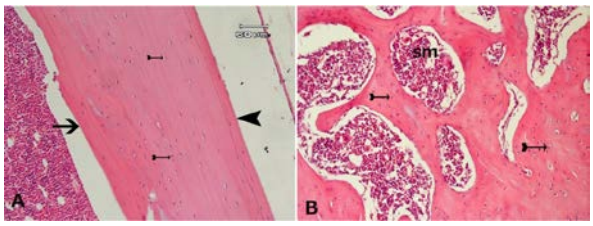

Figure 3. Photograph of femur bone of control rat A) Femur bone shaft showing normal architecture of cortical bone of middle shaft with osteocyte in lacunae (small arrow), surrounded by layer of dense connective tissue periosteum (head arrow) and endosteum an inner layer facing the marrow cavity (arrow); B): Femur head showing normal structure of trabecular concellous bone , osteocyte in their lacunea and bone marrow space (Hx &E x200).

The GCSO 400mg/kg administration revealed no histological alterations in structure of bone tissue, (Fig 4 A). While there was significant increase in shaft of femur cortical thickness as compared to control, no significant difference in Haversian canal areas and the osteocytes number was less than control (195 vs 210) (Table 2). The cancellous bone trabeculae showed no obvious difference in mean areas of trabecular bone compared to control with widening in bone marrow spaces (Figure 4 B & Table 2).

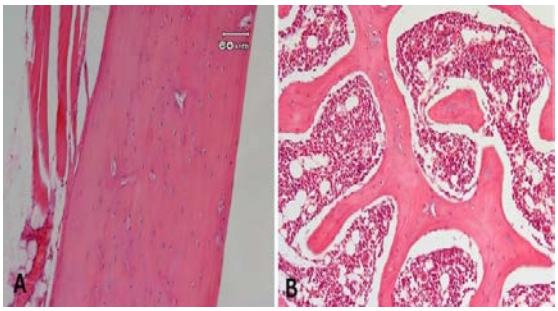

Figure 4: Photograph of bone tissue of rat treated with GCSO 400mg/kg A) The of femur middle shaft with normal structure of bone, significant increase in thickness ,reduction in Haversian canal and osteocytes number ; B) Head femur Trabecular concellous bone showing significant increase in thickness of trabecular bone and widening in bone marrow cavities (H&E x200).

Osteoporotic rat revealed significant decrease in bone thickness of shaft, significant increase in Haversian canal areas and reduction in osteocytes number than control (102 vs 210). Meanwhile, irregularity of the general architecture of bone tissue, gaps, osteoporotic and erosion cavities were observed (Figure 5 A & Table 2). The cancellous bone of osteoporotic animals showed loss of architectures of trabecular bone, with significant reduction of areas of trabecular bone compared to control with widening of bone marrow spaces (Figure 5 B & Table 2).

The microscopic examination of femur shaft of osteoporotic rats treated with GCSO at dose (200 and 400 mg/kg) showed obvious improvement of structure of cortical bone, manifested by significant increase in thickness of compact bone, significant decrease in mean areas of Haversian canal than MTX treated animals (Table 2), and marked increase in osteocyte number (n = 315 and 350, respectively) against MTX group (n=102) indicating recovery of bone tissue. The erosion cavity in endosteal surface of 200mg GCSO treated animals was still found**,** while, no erosion or resorption cavities were noticed in those of 400mg/kg GCSO (Figures 6 A & 7A). Meanwhile, the both two doses of GCSO significantly

increased the mean area of trabecular of cancellous bone than in MTX group (Table 2). The architecture of trabecular bone of 400mg/kg gavages animals appeared nearly normal and in those of both doses narrowing in bone marrow cavities were observed (Figures 6 B & 7 B).

Table 2: Mean area of cortical bone thickness (shaft), mean Haversian canals area, trabecular thickness and number of osteocytes of control and treated groups

Groups	Cortical bone thickness (µm)	Haversian canal area (µm2)	Trabecular mean area (µm2)	Number of Osteocytes
Control	336.62±5.91 [c]	3058.172 ± 535.6 [b]	71109.43 ±10957.0 [a]	210
GCSO (400mg)	372.74± 4.18 [a]	2498.727 ± 434.3 [b]	48873.64 ±7891.7 [a]	195
MTX	90.35 ± 4.45 [e]	45016.49 ± 11453[a]	8669.799 ± 2751.4 [b]	102
GCSO 200mg ther.	272.77 ± 3.75 [d]	5545.00 ±1433.4 [b]	55986.19.±12240.9 [a]	315
GCSO 400mg ther.	365.39 ±2.54 [a]	1557.77± 329.5 [b]	62482.19 ± 14177.7 [a]	350
GCSO 200mg pro	348.82 ± 3.33 [b]	3704.599 ± 786.4 [b]	48815.74 ± 7556.2 [a]	167
GCSO 400mg pro	373.98 ± 3.32 [a]	1087.955 ± 119.5 [b]	71078.5± 11754.4 [a]	189

Note: Values are expressed as the mean ± SEM. Different superscripts within the same column designate significant differences ($p \leq 0.05$)

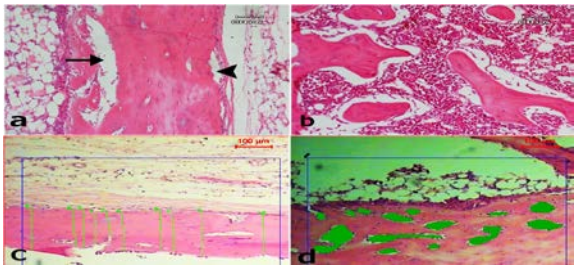

Figure 5. Photograph of MTX treated rat femur bone A) Section of the middle shaft showing significant decrease in bone thickness of cortical bone, irregularity of the general architecture of the tissue, gaps (arrow head),osteoporotic and erosion cavities (arrow) are observed.; A) Section of trabecular of concellous bone showing significant decrease in areas of trabecular bone and widen bone marrow spaces ; C) Section of cortical bone thickness of the same group, the number shown in the figure are the number of measuring lines used by image analyzer system; D) Section of the same group showing sever widen of Haversian canal in cortical bone (H&E x200) (C&d Binary images morphometric measurement).

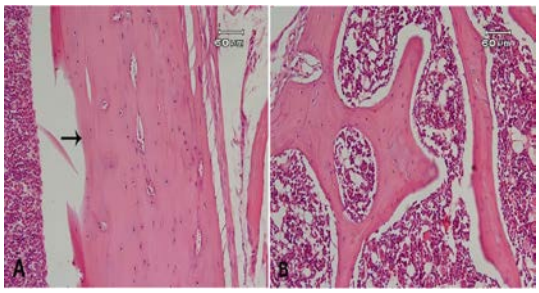

Figure 6. Photograph of femur bone sections of osteoporotic rat treated with 200mg/Kg GCSO A) The middle shaft showing some improvement of structure of cortical bone manifested by significant increase in thickness of shaft reduction in mean areas of Haversian canal and increase in osteocyte count, while, crack (arrow) and the erosion cavity in endosteal surface still found; B) Trabecular bone showing noticeable increase in trabecular area compared with MTX group with increase in the number of osteocytes (H&E x200).

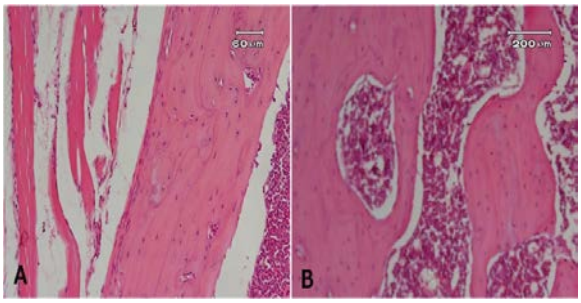

Figure7. Photograph of femur bone sections of osteoporotic rat treated with 400mg/Kg GCSO A) The middle shaft showing highly amelioration in bone tissue represented in significant increase in cortical bone thickness, marked reduction in Haversian canal areas and marked increase in number of osteocytes; B) Trabecular bone showing arked increase in thickness of cortical bone with increase in number of osteocyte and narrowing in bone marrow space (H &E x200).

Examination of shaft cortical bone of rat treated with MTX along with 200 and 400mg/kg GCSO revealed marked protection in architecture of bone tissue represented in significant increase in thickness of cortical bone, significant decrease in Haversian canals compared to MTX treated animal (Figure 8 A & 9 A) and increase in osteocyte number (167 &189 respectively) comparing to MTX (n=102) (Table 2). While, the osteoporotic cavity and erosion in endosteal surface still present in 200mg/kg GCSO treated animals (Figure 8 A). Meanwhile, the trabeculae of cancellous of two dose treated animals showed significant increase in areas of inner cancellous bone trabecular as compared to MTX group (Table 2). Also, calcified cartilage, and dilation of bone marrow space were observed in 200mg/kg treated animals (Figure 8 B). In addition, 400mg/kg GCSO administration revealed normalization of bone trabeculae reach near to control, but increase in osteocytes and narrow in bone marrow spaces (Figure 9 B).

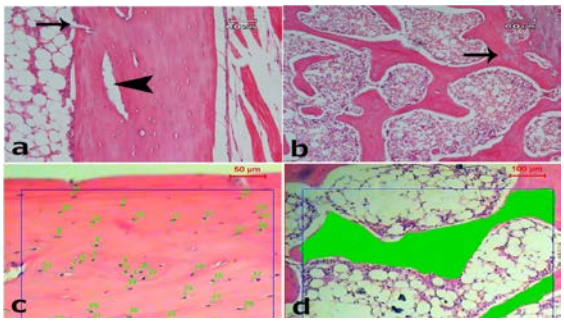

Figure 8: Photograph of femur bone sections of rat treated with MTX along with 200mg/Kg GCSO showing A) Shaft of bone showing significant increase in thickness, marked reduction of Haversian canal area and increase osteocyte count. while osteoporotic (arrow head) and erosion cavity (arrow) in endosteal surface still found; B) Trabecular bone showing significant increase in thickness, calcified cartilage (arrow) and widened in marrow spaces; C): Cortical bone showing count of osteocyte number; D): Concellous bone trabeculae showing area of inner concellous bone (H&E x200) . (C&D: binary of image morphometric measurements).

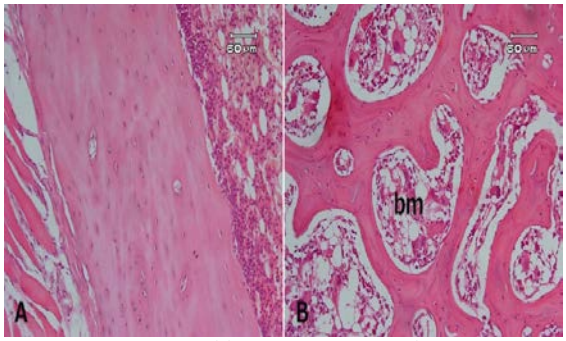

Figure 9. Photograph of femur bone sections of rat treated with MTX along with 400mg/Kg GCSO showing A) Middle shaft bone showing marked protection in structure of bone tissue represented in significant increase in bone thickness, increase in osteocyte number and significant decrease in Haversion canal areas, while some cavity still present.; B) Trabecular of cancelloue bone showing normalization of bone trabeulae, significant increase in thickness of trabecular bone with increase in osteocytes and narrowing of marrow space (bm) (H&E x200).

4. Discussions

In the present study, the methotrexate osteoporotic rat model showed a decline in the levels of serum minerals, including (calcium, phosphorous), bone alkaline phospatase and vitamin D. Corticosteroid-induced osteoporosis was shown to diminish bone mineral density associated with enhanced the fracture risks in animal models (Leonard, 2007). Goralczyk *et al*. (2015) reported that patients treated with MTX verified lower levels of serum 25(OH) D, calcium (Ca), phosphorus (P), and total alkaline phosphatase (ALP). The turn down in the serum levels of Ca and P could be due to enhanced renal excretion and alteration in their transport across the brush border membrane (Banji *et al*., 2014). Extra glucocorticoid declines intestinal calcium absorption and hypercalciuria due to defective vitamin D metabolism. These result in increased bone resorption, declined osteoblast proliferation and biosynthetic activity.

Bone alkaline phosphatase marker (b-ALP) reveals the bone destruction in conditions that affect bone metabolism. ALP, a non-specific bone formation marker, is existing in all tissues of the body, but is particularly intense in liver, bile duct, kidney, bone, intestinal mucosa and the placenta (Iqbal, 2011). The b-ALP values in the current study were significantly reduced in the osteoporosis rats showing an alteration in the bone formation and bone mineralization. Our findings were consistent with Cavalcanti *et al*. (2014); they confirmed that alkaline phosphatase levels decreased after MTX treatment. In addition, several studies indicated a marked decrease in ALP level of glucocorticoid-induced osteoporotic rats, a marker of osteoblast differentiation in primary rat osteoblasts (Elshal *et al*., 2013; Chen *et al*., 2016; Lucinda *et al*., 2017).

Conversely, the administration of GCSO with both therapeutic and prophylactic pattern attenuates the levels of Ca, P, b-ALP and Vitamin D of osteoporotic rats, the therapeutic pattern was efficient more the prophylactic. These findings were in agreement with Elshal *et al*. (2013); they noticed that osteoporotic animals treatment with *Lepidium sativum* recovers the concentration of serum b-ALP to levels higher than that in control. These findings are in harmony with mentioned benefits of *Lepidium sativum* seeds that brought a marked impact on rabbits fracture healing (Juma, 2007). In addition, Gabr *et al*. (2017) reported that *L. sativum* extract is effective in protection against PA-induced osteoporotic hypocalcemia in male and female rats. In this connection, *L. sativum* extract is a worthy source of linolenic acid, which was shown to prevent bone reabsorption, bone remodeling markers and decrease the elimination of Ca.

Cathepsin K is highly expressed in osteoclasts secreted into the osteoclast–bone cell interface leads to efficient degradation of type I collagen. Cathepsin deficiency in humans causes pycnodysostosis that is categorized by enlarged bone mineral density (Drake, 2017). The cytokine tumor necrosis factor α (TNF-α) plays an important role in modulation of bone cell function, regulation and differentiation (Osta *et al*., 2014; Kotrych *et al*., 2016; Mortezazadeh *et al*., 2018). The gene expression data revealed high levels of Cathepsin k and TNF-α mRNA in MTX- induced osteoporotic rats. Song *et al*. (2018) confirmed that the gene expression of Cat K was significantly higher in osteoporotic mice. Various clinical cases revealed TNF-α level up regulation in patients undertaking chemotherapy, recommending its prospective role in chemotherapy-induced osteoclastogenesis. According to the osteoblasts and osteoclasts role in bone regeneration, it is evident that the degree of new osteoblasts and osteoclasts formation has critical impact on bone degradation (Tremollieres and Ribot, 2010). Sex steroids deficiency up-regulates the formation of osteoclasts and osteoblasts by up-regulating the creation of cytokines, including IL-6, TNF, IL-1, which mediate osteoclastogenesis and osteoblastogenesis (Gallagher, 2008).

Epidemiological indication advises that ingesting of vegetables and fruits rich diet that comprises major quantities of bioactive phytochemicals has positive effects for health (Pandey and Rizvi, 2009). In the present study administration of GCSO revealed down regulated the expression of both the Cat K and TNF-α in osteoporotic animals. This finding was in simultaneous with Bu *et al*. (2008) who informed that dried plum polyphenols inhibit the activity of TNF-α and down regulate the transcription factor-T cell nuclear factor (NFATc1) during

osteoclastogenesis. In addition, a study on p-coumaric acid, a polyphenol existing in many vegetables and fruits, established its effective immunosuppressive property for it significantly down regulated the TNF-α expression of in adjuvant arthritic rats (Pragasam *et al*., 2013).

Concerning the osteoblastic differentiation, our data showed a significant down-regulation in the mRNA expression level of osterix which was observed in the MTX-stimulated osteoblasts. Osterix is a major transcription factor that plays a vital character in bone formation and the osteoblast genes expression (Sinha & Zhou, 2013). Lu *et al*. (2006) found that TNF control the Osx expression by suppressing the transcriptional action of its promoter and the inhibition mechanism was mediated *via* a mitogen-activated protein kinase (MAPK) signal. In our results, however, we establish that GCSO promoted osteoblast differentiation and elevated the expression levels of Osterix, the master gene of osteoblast differentiation. This was supported with the study of Choi *et al*. (2016)who found that a novel osteogenic plant showed an capacity to induce osteoblast differentiation. It enhanced osteogenic activity via increased the level of ALP besides the Runx2 transcriptional activity and Osterix.

The ameliorated role of vegetables and fruits against bone osteoporosis or in maintaining bone health turn back to vitamin C, vitamin K, and phytochemicals highly enriched in fruits and vegetables that participate in bone matrix synthesis. Vitamin C has potency to affect bone mass in the hydroxylation of lysine and proline that are required for the construction of stable collagen triple helixes. Vitamin K may show a protecting character against bone loss related age through vitamin K dependent γ-carboxylation of osteocalcin (Ahmadieh and Arabi, 2011). Fruits and vegetables, as a worthy source of alkaline precursors (e.g., K, Ca, Mg), can neutralize the calciuric action of acids diet as confirmed in a modern meta-analysis (Lambert *et al*., 2015).

Regarding the histological examination of our study, osteoporotic rats revealed decrease in bone thickness of shaft, increase in Haversian canal areas, reduction of trabecular bone areas and bone marrow spaces widening and reduction in osteocytes number. The results of the current work are compatible with those of Elsaid and Sadek (2017) who found that MTX caused marked thinning of the periosteum specially the fibrous layer and seeming lessen in the osteocytes number. In addition, the cancellous bone of MTX treated animals revealed thin, commonly detached bone trabeculae with bone marrow spaces widening. Previous animal study revealed that while long term low-dose MTX treatment caused no damage to the growth plate, two cycles of high-dose MTX caused a significant decrease in growth plate height (Fan *et al*., 2009), that was for the diminished of chondrocyte proliferation and collagen-II production, in addition to the stimulation of chondrocyte apoptosis probably through the Fas/FasL death receptor pathway (Xian *et al*., 2007). Due to the growth plate dysfunction, a significant reduction in the thickness of newly formed primary spongiosa bone was originated in the adjacent metaphyseal bone, mirroring the thinning of the growth plate (Xian et al., 2007; 2008). El-Morsi *et al*. (2011) supposed that osteoporosis could be demonstrated as thinning of bone trabeculae or as deletion of some bone trabeculae with remaining trabeculae of normal thickness .

Histological examination showed that administration of GCSO to osteoporotic induced obvious improvement of structure of cortical bone. The architecture of trabecular bone of high dose appeared nearly normal and in those of both two doses narrowing in bone marrow cavities were observed. This data was in line with Elshal *et al*. (2013) who evaluated the role of *Lepidium Sativum* supplementation on histological appearance of tibia trabecular bone in glucocorticoid-induced osteoporosis (GIO) rats, where the trabeculae of inner cancellous bone missing their normal architecture and seemed as irregular bony ossicles disjointed by widened bone marrow spaces. *Lepidium Sativum*-nourished rats revealed marked improvement as compared to those of the GIO-rats, where the cortical bone thickness was exactly like the control and the cancellous bone trabeculae partially recovered near normal structure and looked extra continuous with fewer enlarged bone marrow spaces. Diwakar *et al*. (2008) attributed the constructive effect on bone density *of Lepidium Sativum* to its rich content of calcium, and to its capability to rise serum and liver alpha linolenic acid (ALA), docosahexaenoic acid (DHA) and eicosapentaenoic acid (EPA) that have beneficial effects on bone. In addition, numerous epidemiological studies have inspected the link among fruits and vegetables intake and bone health. Most observational studies have reported that more intakes of fruits and vegetables are concomitant with an upturn in bone mass and declines in bone loss and fracture risk (Xie *et al*., 2013; Byberg *et al*., 2015; Benetou *et al*., 2016).

5. Conclusion

We prove that garden cress seed oil oral gavages considerably improved the osteoporosis bone markers through both therapeutic and prophylactic approaches. In addition, data of the tested parameters revealed that the therapeutics pattern was more alleviative than prophylactic. The present article highlights the prospective mechanism of action of garden cress seeds against osteoporosis and recommends further studies for evolving novel therapeutic tools in osteoporosis treatment.

Acknowledgement

This research was financially supported by the National Research Centre grant for applied research grant No: AR 111107.

References

Ahmadieh H and Arabi A. 2011. Vitamins and bone health: beyond calcium and vitamin D. Nut Rev, **69(10):** 584–598.

Banji D, Banji O J, Chiluka VL and Abbagoni S. 2014. Role of *Triticum aestivum* aqueous extract in glucocorticoid induced osteoporosis in rats. Indian J Exp Biol, **52:**153-158.

Bancroft D, Williams L D, Rich A and Egli M. 1994. The low-temperature crystal structure of the pure-spermine form of Z-DNA reveals binding of a spermine molecule in the minor groove. Biochem, **33:**51073-1086.

Benetou V, Orfanos P, Feskanich D, Michaelsson K, Pettersson-Kymmer U, Eriksson S, Grodstein F, Wolk A, Bellavia A, Ahmed L A, Boffeta P and Trichopoulou A. 2016. Fruit and vegetable intake and hip fracture incidence in older men and women: The CHANCES project. J Bone Mineral Res, **31:** 1743–1752.

Bryan R M, Shailesh N S, Jill K W, Steven F V and Roque L E.2009. Composition and physical properties of cress (*Lepidium sativum* L.) and field pennycress (*Thlaspi arvense* L.) oils. Indust Crops Prod, **30:** 199-205.

Bu S Y, Lerner M, Stoecker B J, Boldrin E, Brackett D J, Lucas E A and Smith B J 2008. Dried plum polyphenols inhibit osteoclastogenesis by down regulating NFATc1 and inflammatory mediators. Calcified Tissue Int, **82(6):** 475–488.

Byberg L, Bellavia A, Orsini N, Wolk A and Michaelsson K. 2015.Fruit and vegetable intake and risk of hip fracture: a cohort study of Swedish men and women. J Bone Mineral Res, **30:** 976–984.

Cavalcanti SC, Correa L, Mello S B and Luz J G. 2014. The effect of methotrexate on the bone healing of mandibular condylar process fracture: an experimental study in rats. J CranioMaxillofacial Surg, **42(7):**1133-1139.

Chen Z, Xue J, Shen T, Mu S and Fu Q. 2016. Curcumin alleviates glucocort icoid- induced osteoporosis through the regulation of the Wnt signaling pathway. Int J Mol Med, **37:** 329-338. Choi Y H, Kim GS, Choi JH, Jin SW, Kim HG, Han Y and Jeong HG. 2016. Ethanol extract of *Lithospermum erythrorhizon* Sieb. et Zucc. promotes osteoblastogenesis through the regulation of Runx2 and Osterix. Int J Mol Med, **38:** 610-618.

Datta P K, Diwakar BK, Viswanatha S, Murthy KN and Naidu K A. 2011. Safety evaluation studies on Garden cress (*Lepidium sativum* L.) seeds in Wistar rats. Int J Appl Res Nat Prod, **4(1):**37-42.

Diwakar B T, Datta P K, Lokesh B R and Naidu KA. 2008. Bio-availability and metabolism of n-3 fatty acid rich garden cress (*Lepidium sativum*) seed oil in albino rats. Prostaglandins, Leukotrienes and Fatty Acids, **78:** 123-130.

Drake M T, Clarke B L, Oursler M J and Khosla S. 2017. Cathepsin K Inhibitors for Osteoporosis: Biology, Potential Clinical Utility, and Lessons Learned. Endocr Rev, **38 (4):** 325–350.

El-Morsi, A.S., Beshir, S.R., Farag, K., Saber, M. and Hamam, G. (2011)Comparative study on the effect of Vitamin K versus combined Ca and vitamin D administration on the prevention of experimentally induced osteoporosis in adult male albino rats. Egypt J Histol, 34:5 -14.

Elsaid G A and Sadek S A. 2017. The Protective Role of Simvastatin on Meth otrexate -Induced Bone Injury in Adult Albino Rat. Egypt J Histol , **40(1):** 105-115.

Elshal F M, Almalki L A, Hussein KH and Khan A J. 2013. Synergistic anti-osteoporotic effect of *lepidium sativum* and Alendronate in glucocorticoid-induced osteoporosis in wistar rats. Afr J Tradit Complement Altern Med, **10(5):** 267-273.

Fan C, Cool JC, Scherer MA, Foster BK, Shandala T, Tapp H and Xian CJ. 2009. Damaging effects of chronic low dose methotrexate usage on primary bone formation in young rats and potential protective effects of folinic acid supplementary treatment. Bone, **44(1):**61–70.

Fan C, Foster B, Hui S and Xian C. 2012. Prevention of bone growth defects, increased born resorption and marrow adiposity with folinic acid in rats receiving long-term methotrexate. Plos One, **7(10):** 1 -11.

Fischer GS, Neira L L, Ferreiro M M, Torres CMT, Giadrosich R V, Milinarsky T A, Arriagada M M and Arinoviche S R**.** 2005. Bone mineral density in leukemic children after completing one month of chemotherapy. Revista Medica De Chile, **133:** 71 -76.

Fouda A M and Youssef A R. 2017. Antiosteoporotic activity of salvadora persica sticks extract in an estrogen deficient model of osteoporosis. Osteoporosis and Sarcopenia, **3:** 132–137.

Gabr G A, Soliman GA, Abdul Samad, Al-Tamimi N. A and Abdel-Kader M. S. 2017. The potential protective effects of vigna radiate and lepidium sativum against bone loss induced by prednisolone acetate in male and female rats. Indo Am J Pharma Sci, **4(05):** 1085-1094.

Gallagher C J. 2008 . Advances in bone biology and new treatments for bone loss. Maturitas, **60 (1):** 65–69.

Goralczyk A, Konstantynowicz J, Abramowicz P, Dobrenko E and Babinska-Malec E. 2015. Deficits of vitamin D are strongly associated with methotrexate treatment in patients with juvenile idiopathic arthritis. Bone Abs, **4:** 183

Henneicke H, Gasparini S, Brennan-Speranza T, Zhou H and Seibel M. 2014. Glucocorti -coids and bone: local effects and systemic implications. Trends in Endocr and Metab, **25:** 197–211.

Holick M F. 2005. 25-OH-vitamin D assays. J Clin Endocr Metab, **90:** 3128**-** 3129.

Hough, F.S., Brown, S.L., Cassim, B., Davey, M.R., de Lange, W., de Villiers, T.J., Elli GC, Lipschitz S, Lukhele M and Pettifor J M. 2014 . The safety of osteoporosis medication. South Afr Med J, **104:** 279–282.

Iqbal J. 2011. An enzyme immobilized microassay in capillary electrophoresis for characterization and inhibition studies of alkaline phosphatases. J Anal Biochem, **414:** 226-231. Juma AH. 2007. The effects of Lepidium sativum seeds on fracture-induced healing in rabbits. Medscape General Med, 9:23.

Kashani HH, Moshkdanian G, Atlasi MA, Taherian A A, Naderian H and Nikzad H. 2013. Expression of galectin-3 as a testis inflammatory marker in vasectomised mice. Cell J, **15(1):** 11-18.

Kotrych D, Dziedziejko V, Safranow K, Sroczynski T, Staniszewska M, Juzyszyn Z and Pawlik A. 2016. TNF-α and IL10 gene polymorphisms in women with post -menopausal osteoporosis. Eur J Obst Gynecol Reprod Biolo, **199:** 92-95.

Lama A, Santoro A, Corrado B, Pirozzi C, Paciello O, Pagano TB, Russo S, Calignano A, Mattace R G and Meli R. 2017. Extracorporeal shock waves alone or combined with raloxifene promote bone formation and suppress resorption in ovariectomized rats. PLoS ONE, **12:** e0171276.

Lambert H, Frassetto L, Moore JB, Torgerson D, Gannon R, Burckhardt P and Lanham-New S. 2015.The effect of supplementation with alkaline potassium salts on bone metabolism: a meta-analysis. Osteoporosis Int, **26:** 1311-1318.

Leonard M B. 2007. Glucocorticoid-induced osteoporosis in children: impact of the underlying disease. Pediatrics, **119 (2):** S166–S174.

Livak KJ and Schmittgen TD. 2001. Analysis of relative gene expression data using real-time quantitative PCR and the 2(-Delta Delta C (T)) method. Methods, **25(4):** 402–408.

Lu X, Gilbert L, He X, Rubin J and Nanes MS. 2006.Transcriptional Regulation of the Osterix (Osx, Sp7) Promoter by Tumor Necrosis Factor Identifies Disparate Effects of Mitogen-activated Protein Kinase and NF-α Pathways. J Biol Chem, **281(10):** 6297–6306.

Lucinda L M F, Aarestrup B J V, Reboredo M M, Pain TD A, Chaves R Z, Reis JEP, Louzada M JQ and Guerra M O. 2017. Evaluation of the anti-osteoporotic effect of *Ginkgo biloba* L. in Wistar rats with glucocorticoid-induced-osteoporosis by bone densitometry using dual-energy x-ray absorptiometry

(DEXA) and mechanical testing**.** An Academia Brasileira de Ciencias, 89 (4):2833-2841.

Minaur N J, Jefferiss C, Bhalla A K and Beresford J N. 2002. Methotrexate in the treatment of rheumatoid arthritis. I. In vitro effects on cells of the osteoblast lineage. Rheumatol, **41:** 735-740.

Mohammad SM, Kashani HH and Azarbad Z. 2012. Capparis spinosa L. Propagation and medicinal uses. Life Sci J, **9 (4):** 684-6.

Mortezazadeh F, Fathabady F F, Norouzian M, Nematollahi-Mahani SN, Amini A, Jafarinejad-Farsangi S, Rouholamini S E Y, Babaee A and Basiri M. 2018. Investigating the effect of tumor necrosis factor alpha on placenta and gene related bone formation of newborn mice. J Res Med Dental Sci, **6 (5):** 133-138.

Nawawi H and Girgis S I. 2002. Serum levels of bone-specific alkaline phosphatase and procollagen type I carboxyterminal peptide in vitamin D deficiency. Southeast Asian J Trop Medi Public Health, **33:** 124-130.

Osta B, Benedetti G and Miossec P. 2014. Classical and paradoxical effects of TNF-α on bone Homeostasis. Fronties Immun, **5 (48):** 1-9.

Pandey KB and Rizvi S I. 2009. Plant polyphenols as dietary antioxidants in human health and disease. **Oxid Mede Cell Longev, 2(5):** 270–278.

Pinheiro L S, de Melo AD, Andreazzi AE, Caires-Junior L C, Costa M and Garcia R M G. 2011. Protocol of insulin therapy for streptozotocin-diabetic rats based on a study of food ingestion and glycemic variation. Scandinavian Jo Lab Animal Sci, **38(2):** 117-27.

Poole K E S, Skingle L, Gee A H, Turmezei T D, Johannesdottir F, Blesic K, Rose C, Vindlacheruvu M, Donell S, Vaculik J, Dungl P, Horak M, Stepan J J, Reeve J and Treece GM. 2017. Focal osteoporosis defects play a key role in hip fracture. Bone, **94:**124–134.

Pragasam S J, Venkatesan V and Rasool M. 2013. Immunomodulatory and anti-inflammatory effect of p-coumaric acid, a common dietary polyphenol on experimental inflammation in rats. Inflammation, **36(1):** 169–176.

Reginster J Y, Pelousse F and Bruyere O. 2013. Safety concerns with the long-term management of osteoporosis. Expert Opinion Drug Safety, **12:** 507–522.

Sakran M, Selim Y and Zidan N. 2014. A new isoflavonoid from seeds of *lepidium sativum* l. and its protective effect on hepatotoxicity induced by paracetamol in male rats. Molecules, **19:** 15440-15451.

Sinha K M and Zhou X. 2013. Genetic and molecular control of osterix in skeletal formation. J cell biochem, **114:** 975-984.

Song Z, Xie W, Zhu S, Pan J, Zhou L and He C. 2018. Effects of PEMFs on Osx, Ocn, TRAP, and CTSK gene expression in postmenopausal osteoporosis model mice. Int J Clin Exper Pathol, **11(3):**1784-1790

Sucuoglu H and Koyuncu H . 2017. Distribution of male osteoporosis patients according to age, classification, and fracture. Istanbol Med J, **18:**13–17.

Tremollieres F and Ribot C.2010. Bone mineral density and prediction of non-osteoporotic disease, Maturitas, **65 (4):** 348–351.

Wadhwa S, Panwar M S, Agrawal A, Saini N and Patidar L N. 2012. A review on pharmacognostical study of *Lepidium sativum*. Adv Rese Pharma Biol**, 2(4):** 316–323.

Wu L, Ling Z, Feng X, Mao C and Xu Z. 2017. Herb medicines against osteoporosis: Active compounds & relevant biological mechanisms. Curr topics med chem, **17:**1670–1691.

Xian C J, Cool J C, Scherer M A, Macsai C E, Fan C, Covino M and Foster B K. 2007. Cellular mechanisms for methotrexate chemotherapy-induced bone growth defects. Bone, **41(5):**842–850.

Xian C J, Cool J C, Scherer M A, Fan C and Foster B K. 2008. Folinic acid attenuates methotrexate chemotherapy-induced damages on bone growth mechanisms and pools of bone marrow stromal cells. J Cell Physiol, **214(3):** 777-785.

Xie H L, Wu B H, Xue W Q, He M G, Fan F, Ouyang W F, Tu S L, Zhu H L, Chen YM. 2013. Greater intake of fruit and vegetables is associated with a lower risk of osteoporotic hip fractures in elderly Chinese: a 1:1 matched case control study. Osteoporosis Int, **24:** 2827-2836.

Yogesh C Y, Srivastav DN, Seth AK. 2010. In vivo antioxidant potential of *Lepidium sativum* L. seeds in albino rats using cisplatin induced nephrotoxicity. Inter J Phytomed, **2:** 292-298.

JJBS

Volume 13, Number 2, June 2020
ISSN 1995-6673
Pages 247 - 252

Jordan Journal of Biological Sciences

Study of *MTHFR* C677T Polymorphism and Associated Oxidative Stress Biomarkers among Autism Spectrum Disorder Patients in Jordan

Laila M. Al-Omari [1], Abdelrahim A. Hunaiti [2], Mohammad A. Beirat[3] and Yasser K. Bustanji [4,5*]

[1]Department of Biological Sciences,[2]Department of Clinical Laboratory Sciences, Faculty of Sciences, The University of Jordan,[3] Department of Special Education, Faculty of Educational Sciences, King AL-Hussien Bin Talal University, Ma'an, [4] Hamdi Mango Center for Scientific Research, [5]Department of Biopharmaceutics and Clinical Pharmacy, School of Pharmacy, The University of Jordan, Amman 11942.

Received July 3, 2019; Revised August 22, 2019; Accepted August 29, 2019

Abstract

Autism spectrum disorder (ASD) is a neurodevelopmental disorder caused by both genetic and environmental factors. The impact of the environmental triggers is associated with increases in oxidative stress. The aim of this study was to test the serum levels of oxidant/antioxidant status along with analysis of *MTHFR* C677T polymorphism (rs1801133) in autistic children. Twenty five patients (20 males and 5 females) diagnosed with ASD and twenty five healthy sex-matched and age-matched control participants were included in this study. *MTHFR* C677T polymorphism was analyzed by using polymerase chain reaction-restriction fragment length polymorphism (PCR-RFLP) method. The serum levels of reduced (GSH), total antioxidant capacity (TAC), cysteine, folate and vitamin B_{12} contents in autistic patients were significantly lower than control group. In addition, high levels of serum oxidized glutathione (GSSG), malondialdehyde (MDA), homocysteine, total oxidant status (TOS) and carbonylate proteins were found in children with autism compared to control group. The *MTHFR* C677T frequency was significantly higher in autistic as compared to non-autistic children. The homozygous genotype CC of the *MTHFR* C677T was lower in patients with autism than the control group (28% vs 52%), while heterozygous CT genotype of the *MTHFR* C677T and the homozygous TT genotype were higher in patients with autism compared to control group (52%, 44%) and (20%, 4%), respectively. The *MTHFR* C677T polymorphism and reduction in cysteine, folate and vitamin B12 levels as well as increase in oxidative stress could contribute to ASD risk in Jordan. Further studies are needed on a larger scale to explore other genes polymorphisms and other risk factors that may be associated with ASD in Jordan.

Keywords: Autism, oxidative stress, glutathione, PCR-RFLP, MTHFR gene.

1. Introduction

Autism spectrum disorder (ASD) is a neurodevelopmental disorder characterized by deficits in social communication, repetitive and restrictive behavior. Autism is most likely caused by multiple factors interacting in complex ways genetic, biological, environmental, and developmental. Therefore, ASD is not etiologically homogenous (Kroncke *et al*., 2016, Boucher, 2017). Autism is becoming a major public health issue in the world due to its yearly exponential increase in the numbers of individuals diagnosed with Autism (Boucher, 2017, Baio *et al*., 2018). The Center for Disease Control and Prevention (CDC) in the United States released a new report on the prevalence of ASD with an increase from 1 in 68 children from the previous report in 2016 to 1 in 59 children in the 2018 report (Baio *et al*., 2018). In the Arab world, there is a growing interest in autistic disorders due to global prevalence increases as reported by prevalence studies from different parts of the world over the past few years which come up with a more conservative median estimate of prevalence of 62 in 10,000 children (Elsabbagh *et al*., 2012). ASD is considered as a new field in the Arab world (Hussein and Taha 2013). The number of confirmed cases of ASD is unknown, and available reports suggest that the prevalence of ASD is 1.4, 29, and 59 per 10,000 children, respectively, in Oman (Al-Farsi *et al*., 2011), the United Arab Emirates (Eapen *et al*., 2007), and Saudi Arabia (Aljarallah *et al*., 2006). In a neighboring country to Jordan, a prevalence of 1 in 66 children was reported in Lebanon (Chaaya *et al*., 2016). In Jordan, a previous study was conducted between 2006 and 2007 reported that 5.2% of sample consist of 229 children with global developmental disorder (GDD) were diagnosed as autistic (Masri *et al*., 2011).

* Corresponding author e-mail: bustanji@ju.edu.jo.

* **Abbreviation list** : ASD: Autism Spectrum Disorder; MTHFR: Methylenetetrahydrofolate reductase; GSH: Reduced Glutathione; GSSG: Oxidized Glutathione; Cys: Cysteine; Hcy: Homocysteine; PCR-RFLP: Polymerase Chain Reaction– Restriction Fragment Length Polymorphism; MDA: Malondialdehyde; TOS: Total Oxidant status; TAC: Total Antioxidant Capacity; ELISA: Enzyme linked Immunosorbent Assay; SNPs: Nucleotide Polymorphisms

A recent study assessed the correlation between vitamin-D deficiency and autism spectrum disorder (ASD) in Jordan. Their results showed that Vitamin D levels in ASD patients were significantly lower, suggesting a possible role for vitamin D deficiency in the pathophysiology of ASD (Alzghoul *et al*., 2019a). Another related study aimed at identifying a possible association between levels of inflammatory markers among Jordanian children by comparing the plasma levels of selected cytokines in autistic children with those of their unaffected siblings and unrelated healthy controls. It was found that Interleukin-8 and TNF- α were exclusively elevated in autistic Jordanian children, while interlekin-6 was elevated in both autistic children and their siblings, potentially dismissing its significance. These results may be used for early testing and diagnosis of ASD as the researchers suggested (Alzghoul *et al*., 2019b).

Genetic bases have been shown to play a strong role in the development of ASD; 65-90% of twin studies can be explained by genetic factors and most of the genetic data for ASDs depends on protein products (Bralten *et al*., 2018). Some evidence for a genetic risk comes from having specific Single Nucleotide Polymorphisms (SNPs) associated with ASD (Wu *et al.*, 2017, Mohmuda *et al*., 2016). Many studies found that autism is associated with C677T polymorphism in the methylenetetrahydrofolate reductase (MTHFR) gene, which regulates folate/homocystine pathway (Boris *et al*., 2004, Guo *et al*., 2012, Divyakolu *et al*., 2013, Shawky *et al*., 2014, Sener *et al*., 2014, and Rai, 2016). The location of *MTHFR* gene is on chromosome 1, and the C667T polymorphism is located at exon 4 which causes the conversion of alanine to valine at codon 222 (Liew and Gupta, 2015). Several investigators reported that individuals with ASDs have a deficiency in serum level of B_{12} and folate (Kałużna-Czaplińska, 2013, Zou *et al.*, 2019).

On the other hand, individuals with ASD have been found to have lower GSH/GSSG ratio compared to normal individuals as well as significantly lower levels of serum cysteine, the limiting substrate in GSH synthesis (Main *et al*., 2012, Han *et al*., 2015). There is overwhelming evidence that the dysregulation of GSH homeostasis is implicated in the etiology and progression of several diseases such as neurodegenerative diseases (Johnson *et al.*, 2012). Moreover, a decrease in the glutathione redox ratio has been reported in individuals with autistic disorder and a possible role of oxidative stress and mitochondrial dysfunction in the pathophysiology of this disease (Main *et al*., 2012, González-Fraguela, 2013, Ozturk *et al*., 2016, and Ugur *et al*., 2018). It was suggested that abnormalities in glutathione metabolism and imbalance in GSH concentration may lead to neuro-developmental problems in Autism (Rossignol and Frye, 2014, Kern *et al*., 2011, Main *et al*., 2012, and Hodgson *et al*., 2014). In Jordan, few studies have been reported to identify some biomarkers which can be measured to predict early diagnosis and possible causes of autism in children. The present study aims to investigate *MTHFR* C677T polymorphism and the possible association between oxidative stress biomarkers among Autism spectrum disorder Jordanians by comparing the plasma levels of selected biomarkers in autistic patients with healthy sex-matched and age-matched controls.

2. Materials and Methods

2.1. Participants

A total of 25 individuals (with age range from 7 to 18 years) from both sexes with autistic spectrum disorder (ASD) were recruited from the Autism Academy of Jordan, Amman, Jordan for this case-control study, and 25 age and sex matched normal children from Med labs medical laboratory, Amman, Jordan participated as controls. For ASD group, exclusion criteria were the presence of neurological diseases (such as cerebral palsy, bipolar disorder and epilepsy) or metabolic disorders (e.g. phenylketonuria). Exclusion criteria for control group were language disability, autoimmune disorders or genetic disorder. At the time of blood draw, children in both groups were in good health and not taking any vitamin supplementation.

The autistic individuals were diagnosed previously by other psychiatrist, psychologist, and developmental pediatrician. A written consent was provided by parents of the children for the participation of their respective children in this study. The study was conducted in accordance with Declaration of Helsinki, and the protocol was approved by the Ethics committee of Graduate Studies School in The University of Jordan, Amman, Jordan **(**Project code: 4/ 2018/2017/3/137).

2.2. Blood Sample collection

About five milliliters of blood were withdrawn from each subject using plane tubes. Serum was extracted and stored at -20 ºC for a maximum of a week or stored at -70 ºC for longer period unless the test required freshly prepared samples. For DNA extraction, 2 ml blood was collected using heparin tubes.

2.3. Study measurements

2.3.1. Genotyping

Genomic DNA was extracted from blood sample using the Promega Wizard™ DNA Purification System (Promega). The quality of DNA was verified using NanoDrop 2000 spectrophotometer (Thermo Fisher Scientific, Waltham, MA, USA), and its concentrations was determined at 260/280 nm (should be around 1.8) and then it was examined using a 2% agarose gel. C677T (rs1801133) polymorphism of *MTHFR* gene was studied in both autistic and normal age matched control individuals using polymerase chain reaction– Restriction Fragment Length Polymorphism (PCR-RFLP) assay with the following primers to amplify a 497-bp region from genomic DNA:

5'-TGGGGTCAGAAGCATATCAGTCA-3' (forward)
5'-CTGGGAAGAACTCAGCGAAC-3' (reverse).

PCR conditions were done as in (Delshadpour *et al*., 2017). PCR reactions were prepared in 25 µl reaction volume containing: 1 µl from each primer (100 pmol/µl), 12.5 µl master mix (New England $BioLabs_{Inc}$), and 4 µl genomic DNA (80 ng/µl) and 6.5 µl deionized water. PCR cycle condition was as follows: initial denaturation step of 94 °C for 5 min, and 35 cycles at 94 °C for 45 s, 62 °C for 45 s, and 72 °C for 45 s followed by final extension step at 72 °C for 5 min. Then, 5 µl of the PCR product was run on 2% Agarose gel and 1% TBE (Tris-Borate-EDTA) buffer. For genotyping, restriction enzyme digestion was carried

out following the PCR using Taq *I* restriction enzyme (20,000 units/ml, New England BioLabs$_{Inc}$). For 2 h at 65 °C, the digestion enzyme mixture (50 µl volume) was: 1µl restriction enzyme, 5 µl NEBuffer, 10 µl DNA PCR product (about 1 µg) and 34 µl free nuclease water. Then 10 µl of the mixture was checked with 2% agarose gel electrophoresis (at 100 volt for 2 hr).

2.3.2. Biochemical assays

2.3.2.1. Determination of Folate, B12, Cysteine and Homocysteine.

In our study, the serum levels of folate, $B_{12,}$ Cysteine and homocysteine were measured by a quantitative sandwich enzyme linked immunoassay technique (ELISA) using commercial kits (Mybiosource, USA) and the ELISA reader (AccuReader version1.10).

2.3.2.2. Determination of Oxidative stress indicators.

Reduced glutathione (GSH), Oxidized Glutathione (GSSG), Glutathione redox (GSH/GSSG), Malondialdehyde level (MDA), Total Oxidant Status (TOS), Total Anti-oxidant Capacity (TAC) and Carbonylated protein concentration were measured using a commercially available assay kit for each test and the ELISA reader (AccuReader version1.10).

2.3.2.2.1. Reduced glutathione (GSH)

This Quantitative Sandwich ELISA kit is to be used for determination the level of GSH in fresh undiluted human serum (Mybiosource, USA).

2.3.2.2.2. Oxidized Glutathione (GSSG)

This ELISA kit applies the competitive enzyme immunoassay technique to determine GSSG in fresh human serum (samples were diluted with sample diluents as recommended by the Kit) (Mybiosource, USA).

2.3.2.2.3. Glutathione redox (GSH/GSSG)

In this part, the ratio between GSH and GSSG for each sample was measured.

2.3.2.2.4. Malondialdehyde level (MDA)

This experiment used double-sandwich ELISA technique; the pre-coated antibody is human MDA monoclonal antibody. If samples are not timely detected, they should be divided according to single usage amount and frozen reserved at -20 ºC (Mybiosource, USA).

2.3.2.2.5. Total Oxidant Status (TOS)

In this kit, the TOS was measured in fresh prepared undiluted human serum sample. The absorbance was read in three interval times (after 30 sec, after 5 min and after 10 min.) then delta absorbance (Δ Abs) was measured (Mybiosource, USA).

2.3.2.2.6. Total Antioxidant Capacity (TAC)

This assay measures total antioxidant capacity in fresh prepared human serum (detect directly). The sample was diluted with the sample diluents immediately before the test as recommended in the kit (Mybiosource, USA).

2.3.2.2.7. Carbonylated protein concentration

It is colorimetric assay that utilizes the DNPH reaction to measure the protein carbonyl content in the serum. If the sample could not test at the same day, it could be stable for 1 month at -70 ºC.

2.4. Statistical analysis

For the biomedical results, unpaired Student's t-test was used to compare between two groups and the level of statistical significance was set at $P < 0.05$. To compare the differences in allele and genotype frequencies between cases and controls Chi-square (χ^2) test were applied. The strength of association was assessed by calculating odd ratio (OR) and 95% confidence interval. A p value < 0.05 was considered statistically significant. Hardy-Weinberg Equilibrium was assessed for genotype and allele type. All the statistical analyses were performed using GraphPad Prism (7) statistical package.

3. Results

3.1. MTHFR genotyping

Genotyping of *MTHFR* C677T was done by PCR-RFLP method (Figs. 1 and 2). The *MTHFR* C677T genotypes frequencies in the ASD children are shown in Table 1. The homozygous TT genotype was present in (20%) of the ASD children and in (4%) of the controls (<0.05). The heterozygous CT genotype occurred in 52% of children in the ASD group and in 44% the control group (0.285). The T allele frequency in the ASD children was 46% compared to an allele frequency of 26% among the controls (<0.05). These results indicate that *MTHFR* C677T polymorphism (rs1801133) was associated with autism in this population sample from Jordan.

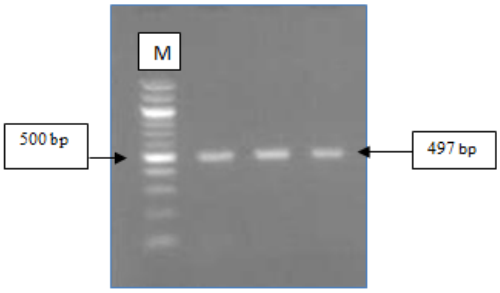

Figure 1. The products of MTHFR gene PCR amplification, an agarose gel electrophoresis.
Fragments of 497 bp are for the MTHFR gene.
M- marker 100 bp DNA ladder. 2% Agarose gel

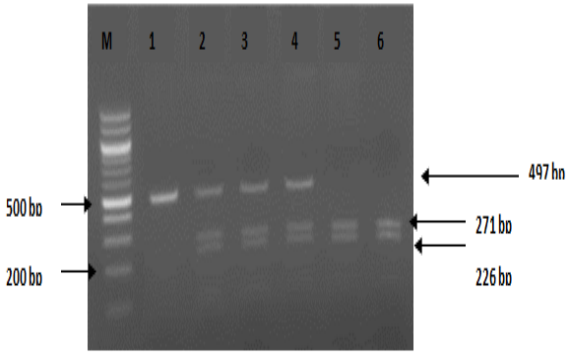

Figure 2. The products of MTHFR gene PCR-RFLP amplification on 2% Agarose gel electrophoresis.
CC homozygote had a single band (1) of 497 bp. TC heterozygote had three bands of 497, 271 and 226 bp (2,3,4) and TT homozygote had a two fragment of 271 and 226 bp (5,6). M-marker 100 bp DNA ladder.

Table 1: Genotype and the distribution of alleles of MTHFR C677T SNP in people with and without autism

Genotype	Autism n (%)	Control n (%)	*P* value	OR (95% CI)
CC	7 (28%)	13 (52%)	0.0416 *	0.359 (0.11-1.179)
CT	13 (52%)	11 (44%)	0.286	1.379 (0.4489-4.449)
TT	5 (20%)	1 (4%)	0.0409*	6 (0.6683-73.17)
At least one C model	20 (80%)	24 (96%)	0.0409	0.167 (0.0137-1.49)
CC and CT				
TT	5 (20%)	1 (4%)		
At least one T model	18 (72%)	12 (48%)	0.0416*	2.786 (0.848-9.091)
TT and CT				
CC	7 (28%)	13 (52%)		
Allele C	27 (54%)	37 (74%)	0.0186*	0.413 (0.1855-0.9369)
Allele T	23 (46%)	13 (26%)		
Expected genotypes (H.W. Freq.)	Autism n (%)	Control n (%)	*P* value for Autism	*P* value for control
CC	7.29 (29.16%)	13.69 (54.76%)	0.055	0.515
CT	12.42 (49.68%)	9.62 (38.48%)		
TT	5.29 (21.16%)	1.69 (6.76%)		

*Significant level $p<0.05$, *p* value calculated by Chi-square. CC: homozygous wild type, CT: heterozygous, TT: homozygous mutant. OR: odd ratio; CI 95% confidence interval; H.W freq: Hardy-Weinberg frequencies.

3.2. Serum levels of vitamin B12, cysteine, Homocysteine and folate

The mean serum levels of B_{12}, Cystiene, homocysteine and folate were evaluated for both autistic and control subjects in this study. The results were summerized as mean±SD in table 2.

The levels of cysteine, folate and vitamin B_{12} were significantly lower in the ASD group compared to the control group, while significantly higher level of homocysteine was found in the ASD patients compared to the control group (Table 2).

Table 2: The level of vitamin B_{12}, cysteine, Hcy and folate in serum between autistic and control, Amman, Jordan, results are mean±SD (n=25).

Metabolite	**Autism**	**Control**	***P*-value**
Vitamin B_{12} (ng/ml)	335.64 ± 86.63	461.16 ± 8.25	<0.05
Cysteine (Cys) µmol/l	192.35 ± 22.15	247.112 ± 44.012	<0.05
Homocysteine (Hcy) µmol/l	15.27 ± 3.517	8.984 ± 2.04	<0.05
Folate ng/ml	4.464 ± 1.30	8.604 ± 1.25	<0.05

3.3. Serum oxidative stress biomarkers in autistic and control groups

The levels of GSH, TAC and Glutathione were statistically significant lower in the ASD group than in the control group, while the levels of GSSG, TOS and carbonylated protein values were statistically significant higher in the ASD group than in the control group ($p<0.05$). The results are given as mean ± SD for each measured parameters as shown in table 3.

Table 3: Oxidative stress biomarkers in serum of autistic and control children, Results are expressed as mean ±SD.

	Autistic	Normal	*P* value
MDA (µmol/l)	2.094 ± 0.44	0.82 ± 0.20	<0.05
GSH (µmol/l)	2.84 ± 0.86	8.69 ± 1.48	<0.05
GSSG (µmol/l)	0.56 ± 0.08	0.25 ±0.058	<0.05
TAC (mmol/l)	0.49 ± 0.09	1.36 ± 0.25	<0.05
TOS (µmol H2O2 Equiv./L)	47.48 ± 1.46	42.80± 3.14	<0.05
Glutathione redox (GSH/GSSG) (µmol/l)	5.23 ± 1.77	29.51 ± 3.98	<0.05
Carbonylated protein concentration (µmol/l)	1.25 ± 0.17	0.83± 0.097	<0.05

MDA-Malondialdehyde, GSH-Reduced glutathione, GSSG-Oxidized glutathione, TAC-Total antioxidant capacity, TOS-Total oxidant status.

4. Discussion

This is the first study to examine several parameters that were found to be associated with autism in Jordan. Several investigators studied oxidative stress in autism by measuring products of lipid peroxidation and antioxidants such as glutathione (Main *et al*., 2012, Han *et al*., 2015, Johnson *et al*., 2012, González-Fraguela *et al*., 2013, Hodgson *et al*., 2014). Lipid peroxidation biomarkers such as MDA are usually increased in autism along with altered glutathione levels as well as the homocysteine/methionine metabolism, which indicates that oxidative stress in this disease is elevated. The results indicated that the ASD group had significantly higher levels of GSSG, TOS, Hcy, MDA and carbonylated protein concentrations as well as low levels of Cys, GSH, GSH/GSSG, TAC, folate and $B_{12,}$ which suggested that antioxidant capacity and redox homeostasis were significantly decreased in children with ASD. The present findings are in agreement with a previous study that reported that children with ASD have weakness in glutathione (GSH) redox metabolism and chronic oxidative stress (Rose *et al.*, 2012). Several studies showed that decreased (GSH) and increased (GSSG) in plasma of children with ASD indicate that oxidative stress may play a central role in the pathogenesis of ASD due to accumulation of toxic materials, which can promote neuronal damage in genetically predisposed individuals (González-Fraguela *et al*., 2013, Rose *et al*., 2012). Moreover, Al-Gadani *et al*., 2009 reported significantly lower GSH in plasma of Saudi autistic children as compared to age matching controls. Weak antioxidant response and increase in total oxidants as measured by the blood level of TOS can cause neuronal cell damage (Ozturk *et al.*, 2016, Ugur *et al*., 2018). In agreement with this notion, the present study reported a significant elevation in TOS level in children with autism. Previously reported data are in line with our results that suggested significantly higher levels of serum Hcy in autistic children, compared to non-autistic children (Zou *et al*., 2019, Ali *et al*., 2011). Methionine synthase enzyme remethylates Hcy to methionione by using 5-methyltetrahydrofolate as a methyl donor and vitamin B_{12} as cofactor. So, deficiency in vitamin B_{12} leads to metabolic disturbances of Hcy, and an elevation of Hcy levels in serum. In addition, the enzyme methylenetetrahydrofolate reductase (MTHFR) regulates folate availability and acts at the cross road between

methyl group transfer and biosynthesis of nucleotides (Boris *et al*., 2004, Divyakolu *et al*., 2013).

The low TAC and high Hcy levels shown in our study in ASD children indicate that Hcy can cause oxidative stress by affecting the redox signaling pathways of neuronal cells causing imbalance in the antioxidant/oxidant system. Our findings are in agreement with those reported by Zou *et al*., 2019.

Another significant outcome of the present investigation is the association between the polymorphism of Methylenetetrahydrofolate reductase (*MTHFR*) gene and autism. 5,10-Methylenetetrahydrofolate reductase - a key enzyme in methionine-homocysteine metabolism - maintains the folate pool between the methylation pathways and DNA synthesis. To our knowledge, there is no previous study in our population that investigated the polymorphism of the *MTHFR* gene and autism. There is statistically significant correlation between autism and the C677T polymorphic genotypes of *MTHFR* gene among autistic individuals in several studies (Boris *et al*., 2004, Rai, 2016, Liu *et al*, 2011). *MTHFR* C677T (rs1801133) is a risk factor for ASD especially in the homozygous state. Many studies have reported that autism could be associated with metabolic abnormalities in the folate/homocysteine pathway, which is contributed in DNA methylation, thus altering gene expression (Pasca *et al*., 2009, Divyakolu *et al*., 2013, Pu *et al*., 2013). These polymorphism at position C677T of *MTHFR* gene and the disturbances of the folate metabolic pathway in autism have been reported in many populations such as Egypt (Meguid *et al*., 2015, Shawky *et al*., 2014), Saudia Arabia (Elhawary et al., 2016) , Turkey (Sener *et al*., 2014), Iran (Delshadpour *et al*., 2017) and China (Guo *et al*., 2012). *MTHFR* gene C677T polymorphism could predict higher levels of Hcy concentrations in populations with mild folate deficiency (Han *et al*., 2015).

Our results are in agreement with the result reported by Boris *et al*., 2004 and Shawky *et al*., 2014. There is more prevalence of the homozygous 677TT allele of the MTHFR gene in the typical autism group (Boris *et al*., 2004, Guo *et al*., 2012, Shawky *et al*., 2014). It was found that the individuals with homozygous (TT) have an approximately 50% decrease in the activity of MTHFR enzyme, and a 30% decrease in enzyme activity of individuals with the heterozygous (CT) (Guo *et al*., 2012). However, Delshadpour *et al*., 2017 reported that there was no significant correlation between *MTHFR* 677T gene polymorphism and autism and that MTHFR role in folate metabolism may participate in epigenetic mechanisms that modify complex gene expression which can cause autism. The mechanisms of *MTHFR* C677T polymorphisms as a risk factor of autism are still unclear and need more investigation.

5. Conclusion

In conclusion, oxidative stress in combination with the C677T polymorphism of *MTHFR* gene might play a crucial role in the etiology and wide spread of ASD in Jordan. However, we cannot exclude other risk factors; and more research is still needed with larger sample size to fully characterize the potential causes of ASD in Jordan.

Declarations of interest:

none

Acknowledgements

We thank The Autism Academy of Jordan and Hamdi Mango for Scientific Research for their assistance in conducting this research.

Funding

This work was supported by the University of Jordan/ School of Graduate Studies (Grant number 94/2017-2018)**; (Project** code: 4/ 2018/2017/3/137).

References

Al-Farsi YM, Al-Sharbati MM, Al-Farsi OA, Al-Shafaee MS, Brooks DR and Waly MI. 2011. Brief report: Prevalence of autistic spectrum disorders in the Sultanate of Oman. *J Autism develop dis.* **1 (6)**:821-825.

Al-Gadani Y, El-Ansary A, Attas O and Al-Ayadhi L. 2009. Metabolic biomarkers related to oxidative stress and antioxidant status in Saudi autistic children. *Clin Biochem*, **42**:10-11, 1032-1040.

Ali A, Waly M I, Al-Farsi Y M, Essa M M, Al-Sharbati M M and Deth, R C. 2011. Hyperhomocysteinemia among Omani autistic children: a case-control study. *Acta Biochimica Polonica*, **58**(4): 547-551.

Aljarallah A, Alwaznah T, Alnasari S, and Alhazmi M. 2006. A study of autism and developmental disorders in Saudi children. Riyadh: Report, King Abdulaziz City for Science and Technology http:// www.kacst.edu.sa. Accessed 13 June 2014.

Alzghoul L, Abdelhamid S S, Yanis A H, Qwaider Y Z, Aldahabi M, and Albdour S A. 2019. The association between levels of inflammatory markers in autistic children compared to their unaffected siblings and unrelated healthy controls. *Turkish J Medical Scie*. **49**(4):1047-1053

Alzghoul L, AL-Eitan LN, Aladawi M, Odeh M, and Hantash OA. 2019. The Association Between Serum Vitamin D3 Levels and Autism Among Jordanian Boys. *J Autism develop dis.* **16**:1-6.

Baio J, Wiggins L, Christensen D L, Maenner M J, Daniels J, Warren Z and Durkin,M S. 2018. Prevalence of autism spectrum disorder among children aged 8 years—autism and developmental disabilities monitoring network, 11 sites, United States, 2014. *MMWR Surveillance Summaries*, **67**:1-23

Boris M, Goldblatt A, Galanko J and James S J. 2004. Association of MTHFR gene variants with autism. *J Ame Phy Sur*, **9**: 106-8.

Boucher J M .2017. Autism spectrum disorder: Characteristics, causes and practical issues. *SAGE*.

Bralten J, Van Hulzen K J, Martens M B Galesloot T E, Vasquez A A, Kiemeney L A & Poelmans G. 2018. Autism spectrum disorders and autistic traits share genetics and biology. *Mol psych*, **23**: 1205-1212.

Chaaya M, Saab D, Maalouf F T and Boustany R M. 2016. Prevalence of autism spectrum disorder in nurseries in Lebanon: a cross sectional study. *J Autism Dev dis*, **46**: 514-522.

Delshadpour M, Mashayekhi F, Bidabadi E, Shahangian S & Salehi Z. 2017. MTHFR rs1801133 Gene polymorphism and autism susceptibility. *Cas J Neu Sci*, **3**: 39-45.

Divyakolu S, Tejaswini Y, Thomas W, Thumoju S, Sreekanth V R, Vasavi M and Ahuja Y. R. 2013. Evaluation of C677T polymorphism of the methylenetetrahydrofolate reductase (MTHFR) gene in various neurological disorders. *J Neu Dis.* http://dx.doi.org/10.4172/2329-6895.1000142

Eapen V, Mabrouk AA, Zoubeidi T, and Yunis F. 2007. Prevalence of pervasive developmental disorders in preschool children in the UAE. *J Tropical Pediatrics*. **53(3)**:202-205.

Elhawary N, Tayeb M, Bogari N and Qotb N. 2016. Vulnerability of genetic variants to the risk of autism among Saudi children. *Hum Geno*, **10**: 236.

Elsabbagh M, Divan G, Koh YJ, Kim YS, Kauchali S, Marcín C, Montiel-Nava C, Patel V, Paula CS, Wang C and Yasamy MT. 2012. Global prevalence of autism and other pervasive developmental disorders. *Autism Res*. **5(3)**:160-79.

González-Fraguela M E, Hung M L D, Vera H, Maragoto C, Noris E, Blanco L and Robinson M. 2013. Oxidative stress markers in children with autism spectrum disorders. *J Adv Med Medi Res*, 307-317.

Guo T, Chen H, Liu B, Ji W and Yang C. 2012. Methylenetetrahydrofolate reductase polymorphisms C677T and risk of autism in the Chinese Han population. *Gen Tes Mol Biom*, **16**: 968-973.

Han Y, Xi Q Q, Dai W, Yang S H, Gao L, Su Y Y and Zhang X. 2015. Abnormal transsulfuration metabolism and reduced antioxidant capacity in Chinese children with autism spectrum disorders. *Inter J Develop Neuro*, **46**: 27-32.

Hodgson N W, Waly M I, Al-Farsi Y M, Al-Sharbati M M, Al-Farsi O, Ali A and Deth R C. 2014. Decreased glutathione and elevated hair mercury levels are associated with nutritional deficiency-based autism in Oman. *Exper Bio Med*, **239**: 697-706.

Hussein H and Taha G R. 2013. Autism spectrum disorders: A review of the literature from Arab countries. *Midd East Cur Psychi*, **20**: 106-116.

Johnson W M, Wilson-Delfosse A L and Mieyal J. 2012. Dysregulation of glutathione homeostasis in neurodegenerative diseases. *Nutri*, **4**: 1399-1440.

Kałużna-Czaplińska J, Żurawicz E, Michalska M and Rynkowski J. 2013. A focus on homocysteine in autism. *Acta Biochimica Polonica*, **60 (2):**137-142.

Kern J K, Geier D A, Adams J B, Garver C R, Audhya T and Geier M R. 2011. A clinical trial of glutathione supplementation in autism spectrum disorders. *Medical science monitor: International Med J Experi Clini Res*, **17**: CR677.

Kroncke A P, Willard M and Huckabee H. 2016. The Causes of Autism. In *Assess Autism Spec Dis*,11-21. Springer, Cham.

Liew SC and Gupta ED. 2015. Methylenetetrahydrofolate reductase (MTHFR) C677T polymorphism: epidemiology, metabolism and the associated diseases. *Eur J Med Gen*. **58(1)**:1-0.

Liu X, Solehdin F, Cohen I L, Gonzalez M G, Jenkins E C, Lewis M S and Holden J J. 2011. Population-and family-based studies associate the MTHFR gene with idiopathic autism in simplex families. *J Autism Develop Dis*, **41**: 938-944.

Mahmuda N, Yokoyama S, Huang J J, Liu L, Munesue T, Nakatani H and Higashida H. 2016. A study of single nucleotide polymorphisms of the SLC19A1/RFC1 gene in subjects with autism spectrum disorder. *Inter J Mole Scie*, **17**: 772.

Main P A, Angley M T, O'Doherty C E, Thomas P and Fenech M. 2012. The potential role of the antioxidant and detoxification properties of glutathione in autism spectrum disorders: a systematic review and meta-analysis. *Nutr Meta*, **9**: 35-37.

Masri A, Hamamy H, and Khreisat A. 2011. Profile of developmental delay in children under five years of age in a highly consanguineous community: a hospital-based study–Jordan. *Brain and Develop*. **1(10):**810-5.

Meguid N, Khalil R, Gebril O and El-Fishawy P. 2015. Evaluation of MTHFR Genetic Polymorphism as a Risk Factor in Egyptian Autistic Children and Mothers. *J Psych*, **18**: 1-4.

Ozturk O, Basay O, Basay B K, Alacam H, Buber A, Kaptanoglu B and Kardesler A C. 2016. Oxidative imbalance in children and adolescents with autism spectrum disorder. *Klinik Psikofarmakoloji Bülteni-Bulletin Clini Psychopharma*, **26**: 257-264.

Paşca S P, Dronca E, Kaucsár T, Crăciun E C, Endreffy E, Ferencz B K and Dronca M. 2009. One carbon metabolism disturbances and the C677T MTHFR gene polymorphism in children with autism spectrum disorders. *J Cel Mol Med*, **13**: 4229-4238.

Pu D, Shen Y and Wu J. 2013. Association between MTHFR Gene Polymorphisms and the Risk of Autism Spectrum Disorders: AM eta-Analysis. *Autism Res*, **6**: 384-392.

Rai V. 2016. Association of methylenetetrahydrofolate reductase (MTHFR) gene C677T polymorphism with autism: evidence of genetic susceptibility. *Meta Brain Dis.*, **31**: 727-735.

Rose S, Melnyk S, Pavliv O, Bai S, Nick T G, Frye R E and James S J. 2012. Evidence of oxidative damage and inflammation associated with low glutathione redox status in the autism brain. *Trans Psych*, **2**: e134.

Rossignol, D A and Frye R E. 2014. Evidence linking oxidative stress, mitochondrial dysfunction, and inflammation in the brain of individuals with autism. *Front Physi*, **5**: 150.

Sener E F, Oztop D B and Ozkul Y. 2014. MTHFR gene C677T polymorphism in autism spectrum disorders. *Gene Res Inter*. http://dx.doi.org/10.1155/2014/698574

Shawky R M, El-baz F, Kamal T M, Elhossiny R M, Ahmed M A and El Nady G H. 2014. Study of genotype–phenotype correlation of methylene tetrahydrofolate reductase (MTHFR) gene polymorphisms in a sample of Egyptian autistic children. *Egyp J Med Hum Gene*, **15**: 335-341.

Uğur Ç, Tunca H, Sekmen E, Üneri ÖŞ, Alişik M, Erel Ö and Solmaz E. 2018. A comparative study of the oxidative stress indices of children with autism and healthy children. *Anatolian J Psych*, **19**:314-22.

Wu Z, Qin J, You Y, Ma Y, Jia M, Wang L and Li J. 2017. Genetic variants in the transcription regulatory region of MEGF10 are associated with autism in Chinese Han population. *Scie Rep*, **7**: 2292.

Zou M, Sun C, Liang S, Sun Y, Li D, Li L and Xia W. 2019. Fisher discriminant analysis for classification of autism spectrum disorders based on folate-related metabolism markers. *J Nutr Bioch*, **64**:25-31.

JJBS

Volume 13, Number 2, June 2020
ISSN 1995-6673
Pages 253 - 256

Jordan Journal of Biological Sciences

Short Communication

Chemical components and insecticidal effects of *Lavandula angustifolia* and *Origanum vulgare* essential oils on the growth different stages of *Habrobracon hebetor* Say (Hymenoptera: Braconidae)

Samira Molapour[1], Robab Shabkhiz[1], Omid Askari[1], Homeyra Shiri[1], Akbar Keramati[1] and Vahid Mahdavi[2]

**Corresponding authors: vahidmahdavi@live.com*

[1] Agricultural Jihad Organization of Zanjan Province, Zanjan; [2] Department of Plant Protection, Faculty of Agriculture and Natural Resources, University of Mohaghegh Ardabili, P.O.Box 179, Ardabil, Iran.

Received May 27, 2019; Revised July 24, 2019; Accepted July 27, 2019

Abstract

Habrobracon hebetor Say is an ectoparasitoid of larval stage of various lepidopteran pests. In this study, fumigant toxicity of *Lavandula angustifolia* and *Origanum vulgare* essential oils on the different growth stages of *H. hebetor* were assessed at 26 ± 2 °C, 60 ± 5% RH, and a photoperiod of 16:8 (L:D) h. Essential oils were extracted from the plant samples using a Clevenger-type apparatus where the plant material is subjected to hydrodistillation. The chemical constituents of essential oils were detected by Gas Chromatography-Mass spectrometry (GC-MS). Glass vials containing 250 ml were used for the experiments. Chemical analysis by GCMS displayed 1,8-Cineol (45.31%) and Camphor (15.78%) for *L. angustifolia* and Pulegone (37.83%) and 1,8-Cineol (17.02%) for *O. vulgare* as major constituents. LC_{50} values of *L. angustifolia* and *O. vulgare* essential oils were 0.06 and 0.08 µl for larval stage, 0.29 and 1.39 µl for pupal stage, 0.23 and 0.91 µl for female adults, and 0.17 and 0.23 µl for male adults, respectively. Fumigant bioassays revealed that *L. angustifolia* oils were more toxic than *O. vulgare* oils against all stages of *H. hebetor*. This research indicates that *O. vulgare* essential oils have less toxicity on *H. hebetor* and recommends as a compatible botanical compound with this biocontrol agent in integrated pest management programs.

Keywords: Habrobracon hebetor, bioassay, GC-MS, essential oils, Lavandula angustifolia, Origanum vulgare.

1. Introduction

The repeated and intense use of synthetic insecticides for several decades has raised long-term human health and environmental concerns, mainly due to their slow degradation in the environment and toxic residues in the products, and the evolution of resistance to pesticides in pest populations (Isman, 2006). These effects have increased the need for effective and biodegradable pesticides and created a significant market opportunity for alternative products (Isman, 2000; Isman *et al.,* 2011). Botanical insecticides have the advantages of reducing risk to non-target organisms due to their rapid degradation in the environment and providing novel and multiple mode of actions that reduce the probability of developing resistance in pest populations (Isman, 2006; Rajendran and Sriranjini, 2008).

Essential oils (EO) are volatile mono- and sesquiterpenoids that interfere with basic metabolic, biochemical, physiological, and behavioral functions in insects and have been demonstrated to possess contact, fumigant, inhalation and ingestion toxicity. They also have antifeedant activity, capacity to delay development, adult emergence and fertility, deterrent effects on oviposition and arresting and repellent action (Tripathi *et al.,* 2009). Also, the biological and insecticidal activities of essential oils are influenced by their chemical composition that needs to be identified.

Biological control using natural enemies is receiving greater attention as an environmentally friendly management option for controlling pests in crops (Scholler *et al.,* 2006). *Habrobracon hebetor* Say (Hymenoptera: Braconidae) is a gregarious larval ectoparasitoid of several species of pyralid and nuctoid moths (Dweck *et al.,* 2008). In Iran, mass rearing of *H. hebetor* is performed on Mediterranean flour moth, *Anagasta kuehniella* (Zeller). For the success of the IPM, contemporaneous use of biological control agents and chemical compounds are recommended (Hull and Beers, 1985). Therefore, the effects of compounds on biological control agents should also be evaluated.

The available information about the effects of plant essential oils on the ectoparasitoid wasp, *H. hebetor* is very limited. Asadi *et al.,* (2018a) evaluated the effects of *Rosmarinus officinalis* L. and *Salvia officinalis* L. (Lamiaceae) essential oils on *Habrobracon hebetor* Say (Hymenoptera: Braconidae) in *Ephestia kuehniella* Zeller (Lep.: Pyralidae) larvae and their bioassay results showed that LC_{50} values for *R. officinalis* and S. *officinalis*

essential oils are 4.15 and 18.36 µl/l air, respectively. *R. officinalis* essential oils showed high acute toxicity on the female wasps of *H. hebetor* compared with *S. officinalis* essential oils.

The objective of the current study is to evaluate the effects of the *Lavandula angustifolia* and *Origanum vulgare* essential oils on the different growth stages of *H. hebetor* to enable selection of soft pesticides to protect beneficial insects and thereby improve the IPM.

2. Materials and methods

2.1. Rearing of insects

Colony of *H. hebetor* parasitoid wasps was obtained from the Department of Plant Protection, University of Mohaghegh Ardabili, Iran. Then, the parasitoid wasps were reared under laboratory conditions in growth chamber that was set at 26 ± 2 ℃, 60 ± 5% RH and a photoperiod of 16:8 (L:D) h, on fifth-instar larvae of flour moth (*A. kuehniella*), that was reared on flour in a growth chamber at above mentioned environmental conditions. Moreover, a honey solution (10%) was applied as food source for feeding of the adult parasitoids (Mahdavi *et al.*, 2011).

2.2. Plant material and extraction of essential oils

L. angustifolia and *O. vulgare* were collected from Zanjan province, Iran. The essential oils were obtained by hydro-distillation in a Clevenger type apparatus. The extraction condition was as follows: 50 g of dry plant (in powder form); 500 ml of distilled water, and 3 h distillation. The obtained oils were dried over anhydrous sodium sulphate to extract the oils. Extracted oils were stored in a refrigerator at 4 ^{o}C for required studies.

2.3. Chromatographic analysis

Gas Chromatography-Mass Spectrometry (GC-MS) was used to analyze the essential oils of *L. angustifolia* and *O. vulgare*. GC-MS analysis was carried out on a GC 6890 N (Agilent, USA) equipped with a split injector and MS 5973 N mass selective detector system. Chromatographic separation was carried out in an HP5ms capillary column (30 m × 0.25 mm, 0.25 µm in film thickness). Helium (99.99%) was used as the carrier gas with a flow rate of 1 ml min^{-1}. The injector temperature was set at 150℃, the column temperature program started at 10 ℃ for 3 min, increased by 10℃ min^{-1} to 120 ℃, by 10℃ min^{-1} to 150℃, and by 7℃ min^{-1} to 240℃, and was maintained for 5 min. Identification of spectra was carried out by studying their fragmentation and comparing with standard spectra present in the library of the instrument (Adams 2001).

2.4. Fumigant toxicity of essential oils

Acute toxicity bioassay test on the immature (larval and pupal) and mature (male and female) stages were carried out by using the fumigant method (Mahdavi *et al.*, 2018). Preliminary dose-setting experiments were carried out to determine 20 and 80% mortality ranges. Glass containers (250 ml) were used as a fumigation chamber. Twenty individuals of selected developmental stages of insects were placed in the glass vials. Distilled water was used in control treatments. Each concentration of the essential oils was bioassayed in four replications. Different growth stages were exposed to the treatments for 24 h. Mortality was recorded 24 h after treatment in all stages, except pupal stage. Mortality were recorded in the pupal stage after the pupal period.

2.5. Data analysis

Experiments were tested for lack of fit by using PROC GENMOD (Robertson *et al.*, 2007; SAS Institute, 2002), and data were analyzed using PROC PROBIT to compute (Lethal Concentration) LC_{10}, LC_{50} and LC_{90} values on a standard and log scale with associated 95% fiducial limit by SAS program (SAS Institute, 2002).

3. Results

3.1. Chemical components of essential oils

The GC-MS analysis results of isolated essential oils are shown in Tables 1 and 2. Twelve major compounds from *L. angustifolia* essential oils and eleven compounds from *O. vulgare* essential oils were detected. The constituents 1,8-Cineol (45.31%), Camphor (15.78) and Borneol (14.46%) from *L. angustifolia* and Pulegone (37.83%), 1,8-Cineol (17.02%) and Menthofuran (12.14%) from *O. vulgare* were detected as major constituents of each mentioned essential oils.

Table 1. Chemical analysis of essential oils of *L. angustifolia* by GC-MS

Components	**Retention time (min)**	**Rate (%)**
α- Pinene	10.86	1.48
o-Cymene	16.33	2.93
Limonene	16.79	1.51
1,8-Cineol	16.99	45.31
Linalool	20.67	1.07
Camphor	23.14	15.78
Borneol	24.59	14.46
Crypton	25.24	2.11
Isobornyl formate	26.99	1.42
Cumin aldehyde	27.91	1.91
Thymol	30.06	7.71
Carvacrol	33.43	0.81
Total		96.5

Table 2. Chemical analysis of essential oils of *O. vulgare* by GC-MS

Components	Retention time (min)	Rate (%)
α- Pinene	10.86	2.02
2-β-Pinene	12.95	2.99
1,8-Cineol	16.98	17.02
Menthofuran	22.43	12.14
Cis-iso-pulegone	23.01	9.38
Borneol	24.60	1.23
Neo-iso-dihydro carveol	25.18	2.24
Pulegone	26.33	37.83
2-Cyclohexane-1-van-1-decene	30.77	4.01
Caryophellene oxide	40.17	1.94
Total		90.8

3.2. Fumigant bioassay

The LC_{10}, LC_{50} and LC_{90} values for *L. angustifolia* and *O. vulgare* essential oils against the larvae, pupae,

males and females of *H. hebetor* are shown in table 3. LC_{50} values of *L. angustifolia* and *O. vulgare* essential oils at the larval stage of the *H. hebetor* were 0.06 and 0.08 µl, respectively. The LC_{50} values of *L. angustifolia* and *O. vulgare* essential oil at the pupal stage were 0.29 and 1.39 µl, respectively. For the female adult stage, these values were 0.23 and 0.91 µl, respectively. Moreover, the LC_{50} values of *L. angustifolia* and *O. vulgare* essential oils at the male adult stage were 0.17 and 0.23 µl, respectively (table 3). A statistically significant difference in the toxicity of *L. angustifolia* and *O. vulgare* essential oil treatments was found at the pupa and female adult growth stages of *H. hebetor*, as inferred by the lack of overlap in the LC_{50} confidence intervals (table 3).

Table 3. Toxicity of essential oils to different growth stages of the ectoparasitoid *Habrabracon hebetor*

Essential oil plants	Growth stages	Number	Slope ± SE	Lethal concentrations (µl)		
				LC10 (95% FL)	LC50 (95% FL)	LC90 (95% FL)
Lavandula angustifolia	Male adults	360	2.88 ± 0.4	0.06	0.17	0.46
				(0.04-0.08)	(0.14-0.19)	(0.36-0.71)
	Female adults	360	2.36 ± 0.34	0.07	0.23	0.79
				(0.04-0.09)	(0.19-0.27)	(0.58-1.33)
	Pupae	360	2.13 ± 0.3	0.07	0.29	1.16
				(0.04-0.1)	(0.24-0.35)	(0.82-2.05)
	Larvae	360	5.59 ± 0.79	0.005	0.06	0.77
				(0.002-0.009)	(0.04-0.08)	(0.41-2.26)
Origanum vulgare	Male adults	360	1.42 ± 0.2	0.03	0.23	1.86
				(0.01-0.05)	(0.18-0.31)	(1.11-4.4)
	Female adults	360	4.99 ± 0.75	0.5	0.91	1.64
				(0.39-0.58)	(0.84-0.98)	(1.41-2.12)
	Pupae	360	1.17 ± 0.17	0.82	1.39	2.35
				(0.66-0.93)	(1.30-1.49)	(2.06-2.95)
	Larvae	360	1.92 ± 0.28	0.02	0.08	0.35
				(0.008-0.024)	(0.06-0.09)	(0.24-0.68)

Lethal concentrations and 95% fiducial limits (FL) were estimated using logistic regression (SAS Institute 2002)

4. Discussion

The essential oils of plants could be alternative sources for pest control because of their innate biodegradability, minimal effects on non-target organisms and on environment (Feldlaufer and Ulrich, 2015), and their different pesticide mode of action (El-Wakeil, 2013). In this study, the fumigant toxicity of *L. angustifolia* and *O. vulgare* essential oils on different growth stages (larvae, pupae, female adults and male adults) of *Habrobracon hebetor* was evaluated.

The results of the effects of plant essential oils on different growth stages of the parasitoid wasp showed that the male parasitoids are more susceptible than female insects. This difference in sensitivity may be due to differences in terms of size (weight) and the amount of fat in the body (Weaver *et al.,* 1995; Papachristos and Stamopoulos, 2002). Based on the values of LC_{50}, the larval and pupal stages were the most sensitive (with the least value of LC_{50}) and the most resistant (with the highest value of LC_{50} to the essential oils, respectively. Also, the results of our studies showed that lavender essential oils has a higher toxicity to growth stages of the parasitoid wasp compared to the *O. vulgare* essential oil. Asadi *et al.,* (2018b) investigated effects of *Allium sativum* L., *Rosmarinus officinalis* L., *Piper nigrum* L., *Salvia officinalis* L. and *Glycyrrhiza glabra* L. essential oils on *H. hebetor* Say (Hymenoptera: Braconidae) in its host. Their results showed that the acute toxicity of *R. officinalis* essential oils on the female wasps of *H. hebetor* was higher than the others. Also, *G. glabra* essential oils showed the lowest acute toxicity suggesting that *G. glabra* essential oils can be recommended with *H. hebetor* in integrated pest management. Other studies have also been conducted by researchers regarding the insecticidal effects of essential oils on different insect pests and natural enemies (González *et al.,* 2013; Hashemi *et al.,* 2014; Naghizadeh *et al.,* 2016; Mahdavi *et al.,* 2017).

Several studies have shown that the insecticidal effects of essential oils are associated with some chemical constituents existing in essential oils (Regnault-Roger *et al.,* 1993). The insecticidal constituents of many plant extracts and essential oils are monoterpenoids. Due to their high volatility they have fumigant activity that might be of importance for controlling stored-product insects (Coats *et al.,* 1991; Konstantopoulou *et al.,* 1992; RegnaultRoger and Hamraoui, 1995; Ahn *et al.,* 1998). It is possible to understand the structure of essential oil constituents with the help of gas chromatography/mass spectrometry (GC/MS). GC/MS analysis showed that 1,8-Cineol (45.31%) and Camphor (15.78) in *L. angustifolia* and Pulegone (37.83%) and 1,8-Cineol (17.02%) in *O. vulgare* were detected as major constituents. These results are consistent with the results of Yazdani *et al.,* 2013 where the major constituents of the essential oils of *L. angustifolia* Mill were identified as Borneoll (8.57%)). The toxic effects of *L. angustifolia* and *O. vulgare* could be attributed to major constituents such as Camphor and 1,8-cineol.

Based on these laboratory results, it seems that *O. vulgare* essential oils are potentially more compatible with a chosen IPM approach. After laboratory studies, more attention should be devoted on storage environment experiments to obtain more applicable results under storage conditions.

References

Adams RP. 2001. **Identification of essential oil components by gas chromatography/ mass spectroscopy.** Carol Stream: Allured Publishing Co.

Ahn YJ, Lee SB, Lee HS and Kim GH. 1998. Insecticidal and acaricidal activity of carvacrol and b-thujaplicine derived from *Thujopsis dolabrata* var. *hondai* sawdust. *J. Chem. Ecol.* **24:** 1–90.

Asadi M, Nouri-Ganbalani G, Rafiee-Dastjerdi H, Hassanpour M and Naseri B. 2018a. The effects of *Rosmarinus officinalis* L. and *Salvia officinalis* L. (Lamiaceae) essential oils on demographic parameters of *Habrobracon hebetor* Say (Hym.: Braconidae) on *Ephestia kuehniella* Zeller (Lep.: Pyralidae) larvae. *J. Essent. Oil Bear. Pl.*, **21(3):** 713-731.

Asadi M, Rafiee-Dastjerdi H, Nouri-Ganbalani G, Naseri B and Hassanpour M. 2018b. The effects of plant essential oils on the functional response of *Habrobracon hebetor* Say (Hymenoptera: Braconidae) to its host. *Invertebrate Surviv. J.*, 169-182.

Coats JR, Karr LL and Drewes CD. 1991. Toxicity and neurotoxic effects of monoterpenoids in insects and earthworms. In: Hedin, P.A. (Ed.), **Naturally Occurring Pest Bioregulators**. ACS Symposium Series No. 449. American Chemical Society, Washington DC, pp. 305–316.

Dweck HKM, Gadallah NS and Darwish E. 2008. Structure and sensory equipment of the ovipositor of *Habrobracon hebetor* (Say) (Hymenoptera: Braconidae). *Micron.*, **39(8):** 125–126.

El-Wakeil NE. 2013. Botanical pesticides and their mode of action.*Gesunde Pflanz.*, **65:**125–149.

Feldlaufer MF and Ulrich KR. 2015. Essential oils as fumigants for bed bugs (Hemiptera: Cimicidae) . *J. Entomol. Sci.*, **50:** 129-137.

González JOW, Laumann RA, da Silveira S, Miguel M, Borges MCB and Ferrero AA. 2013. Lethal and sublethal effects of four essential oils on the egg parasitoids *Trissolcus basalis*. *Chemosphere.*, **92:** 608-615.

Hashemi Z, Goldansaz SH and Hosseini Naveh V. 2014. Effects of *Ferula assafoetida* essential oil on biological characteristics of *Habrobracon hebetor (*Hym.: Braconidae) in vitro. **21th Congress of Plant Protection.** Orumiyeh, Iran.

Hull LA and Beers EH. 1985. Ecological sensitivity modifying chemical control practices to preserve natural enemies. In: Hoy MA, Herzog DC, editors. **Biological pest control in agricultural ecosystem.** Orlando (FL): Academic Press. pp. 103–121.

Konstantopoulou LL, Vassilopoulou L, Mavragani-Tsipidou P and Scouras ZG. 1992. Insecticidal effects of essential oils. A study of the effects of essential oils extracted from eleven Greek aromatic plants on Drosophila auraria. *Experientia.*, **48:** 616–619.

Isman MB. 2000. Plant essential oils for pest and disease management. *Crop Prot*., **19:** 603-608.

Isman MB. 2006. Botanical insecticides, deterrents, and repellents in modern agriculture and an increasingly regulated world. *Ann. Rev. Entomol.*, **51:** 45-66.

Isman MB, Miresmailli S and Machial C. 2011. Commercial opportunities for pesticides based on plant essential oils in agriculture, industry and consumer products. *Phytochem. Rev.*, **10:** 197-204.

Mahdavi V**,** Rafiee-Dastjerdi H, Asadi A, Razmjou J and Fathi Achachlouei B. 2018. Synthesis of *Zingiber officinale* essential oil-loaded nanofiber and its evaluation on the potato tuber moth, *Phthorimaea operculella* (Lepidoptera: Gelechiidae). *J. Crop Prot.*, **7(1):** 39-49.

Mahdavi V, Rafiee-Dastjerdi H, Asadi A, Razmjou J, Fathi Achachlouei B and Kamita ShJ. 2017. Effective management of the *Phthorimaea operculella* (Zeller) using PVA nanofibers loaded with *Cinnamomum zeylanicum* essential oil. *Am. J. Potato Res.*, **94(6):** 647-657.

Mahdavi V, Saber M, Rafiee-Dastjerdi H and Mehrvar A. 2011. Comparative study of the population level effects of carbaryl and abamectin on larval ectoparasitoid *Habrobracon hebetor* Say (Hymenoptera: Braconidae). *BioControl.*, **56(6):** 823–830.

Naghizadeh S, Rafiee-Dastjerdi H, Golizadeh A, Esmaielpour B and Mahdavi V. 2016. The effects of essential oils of *Artemisia absinthium* L., *Achillea millefolium* L. and *Artemisia dracunculus* L. against potato tuber moth, *Phthorimaea operculella* Zeller (Lepidoptera: Gelechiidae). *Jordan J. Agric. Sci.*, **12(4):** 1115-1123.

Papachristos DP and Stamopoulos DC. 2002. Repellent, toxic and reproduction inhibitory effect of essential oil vapours on Acanthoscelides obtectus (Say) (Coleoptera: Bruchidae). *J. Stored Prod. Res.*, **38:** 117-128.

Rajendran S and Sriranjini V. 2008. Plant products as fumigants for stored product insect control. *J. Stored Prod. Res.*, **44:** 126-135.

Regnault-Roger C and Hamraoui A. 1995. Fumigant toxic activity and reproductive inhibition induced by monoterpenes on *Acanthoscelides obtectus* (Say) (Coleoptera), a bruchid of kidney bean (*Phaseolus vulgaris* L.). *J. Stored Prod. Res.*, **31:** 291–299.

Regnault-Roger C, Hamraoui A, Holeman M, Theron E and Pinel R. 1993. Insecticidal effect of essential oils from Mediterranean plants upon *Acanthoscelides obtetus* (Say) (Coleoptera: Bruchidae), a pest of kidney bean (*Phaseolus vulgaris* L.). *J. Chem. Ecol.*, **14:** 1965-1975.

Robertson JL, Russell RM, Preisler HK and Savin NE. 2007. **Bioassays with Arthropods.** 2nd ed, 224. Boca Raton: CRC Press.

SAS Institute. 2002. **The SAS system for windows.** Cary: SAS Institute.

Scholler M, Flinn PW, Grieshop MJ and Zdarkova E. 2006. Biological control of stored-product pests. In: Heaps JW, editor. **Insect management for food storage and processing**, 2nd ed. St. Paul (MN): AACC International. pp. 67–87.

Tripathi KA, Upadhyay S, Bhuiyan M and Bhattacharya PR. 2009. A review on prospects of essential oils as biopesticide in insect-pest management. *J. Pharmacogn. Phytother.*, **1:** 52-63.

Weaver DK, Phillips TW, Dunkle FV, Weaver T, Grubb RT and Nance EL. 1995. Dried leaves from Rocky Mountain plants decrease infestation by stored-product beetles. *J. Chem. Ecol.*, **21:** 127–142.

Yazdani E, Jalali Sendi L, Aliakbar A and Senthil-Nathan S. 2013. Effect of *Lavandula angustifolia* essential oil against lesser mulberry pyralid *Glyphodes pyloalis* Walker (Lep: Pyralidae) and identification of its major derivatives. *Pest. Biochem. Physiol.*, **107(2):** 250-257.

Subscription

Jordan Journal of Biological Sciences

An International Peer – Reviewed Research Journal

Published by the Deanship of Scientific Research, The Hashemite University, Zarqa, Jordan

Name: ..... الاسم:

Specialty: ..... التخصص:

Address: ..... العنوان:

P.O. Box: ..... صندوق البريد:

City &Postal Code:..... المدينة: الرمز البريدي:

Country: ..... الدولة:

Phone: ..... رقم الهاتف

Fax No.: ..... رقم الفاكس:

E-mail: ..... البريد الإلكتروني:

Method of payment: ..... طريقة الدفع:

Amount Enclosed: ..... المبلغ المرفق:

Signature: ..... التوقيع:

Cheque should be paid to Deanship of Research and Graduate Studies – The Hashemite University.

I would like to subscribe to the Journal

For

- ☐ One year
- ☐ Two years
- ☐ Three years

One Year Subscription Rates

	Inside Jordan	Outside Jordan
Individuals	JD10	$70
Students	JD5	$35
Institutions	JD 20	$90

Correspondence

Subscriptions and sales:

The Hashemite University
P.O. Box 330127-Zarqa 13115 – Jordan
Telephone: 00 962 5 3903333
Fax no. : 0096253903349
E. mail: jjbs@hu.edu.jo

المجلة الأردنية للعلوم الحياتية
Jordan Journal of Biological Sciences (JJBS)

http://jjbs.hu.edu.jo

المجلة الأردنية للعلوم الحياتية: مجلة علمية عالمية محكمة ومفهرسة ومصنفة، تصدرعن الجامعة الهاشمية وبدعم من صندوق دعم البحث العلمي والإبتكار – وزراة التعليم العالي والبحث العلمي.

ترسل البحوث الى العنوان التالي:

رئيس تحرير المجلة الأردنية للعلوم الحياتية

الجامعة الهاشمية

ص.ب , 330127 , الزرقاء, 13115 , الأردن

هاتف: 0096253903333

E-mail: jjbs@hu.edu.jo, Website: www.jjbs.hu.edu.jo

المملكة الأردنية الهاشمية

المجلة الأردنية

للعلوم الحياتية

مجلة علمية عالمية محكمة

تصدر بدعم من صندوق دعم البحث العلمي و الابتكار

http://jjbs.hu.edu.jo/